Study on the role of Cofilin 2 in the brain

Dissertation

zur

Erlangung des Doktorgrades (Dr. rer. nat.)

der

Mathematisch-Naturwissenschaftlichen Fakultät

der

Rheinischen Friedrich-Wilhelms Universität Bonn

Vorgelegt von

Kathrin Bläsius

aus

Ensch

Bonn, im Juni 2016

Angefertigt mit Genehmigung der Mathematischen-Naturwissenschaftlichen-Fakultät der Rheinischen Friedrich-Wilhelms-Universität Bonn.

Gutachter:

1. Gutachter: Prof. Dr. Walter Witke
2. Gutachter: Prof. Dr. Bradke

Erscheinungsjahr: 2016

Danksagung

Ein besonderer Dank gilt meinem Doktorvater Prof. Dr. Walter Witke für die Überlassung des sehr interessanten Themas und die wertvollen Ratschläge und Anregungen. Auch wenn wir manchmal sehr chaotisch waren, hoffe ich dass er mit einem Lächeln auf die gemeinsame Zeit zurück blickt. Weiterhin möchte ich ihm für die Begutachtung dieser Arbeit und die freundliche Aufnahme in seine Arbeitsgruppe danken.

Herrn Prof. Dr. Frank Bradke danke ich für die Übernahme des Koreferats, sowie Herrn Prof. Dr. Höhfeld und Herrn Prof. Dr. Hullin für Ihre Teilnahme an der Prüfungskommission als fachnaher und fachangrenzender Gutachter.

Besonders herzlich möchte ich mich bei meiner Betreuerin Dr. Christine Gurniak bedanken, die sich eine Menge Zeit zum Korrigieren dieser Arbeit genommen hat und mir mit vielen konstruktiven Anmerkungen zur Seite stand.

Des Weiteren möchte ich mich bei Dr. Andreas Husch bedanken, ohne den die Elektrophysiologie nicht möglich gewesen wäre. Danke das du auch nach monatelangen Fehlschlägen mit adulten Tieren die Hoffnung nicht aufgegeben hast und nebenbei meinem musikalischen Horizont erweitert hast.

Ein großer Dank geht auch an die gesamte Arbeitsgruppe für die gemeinsame Zeit, das angenehme Arbeitsklima und die vielen wertvollen Ratschläge und Aufmunterungen. Besonders bedanken möchte ich mich bei Dr. Pietro Pilo Boyl für die Hilfe während den Verhaltensexperimenten. Ein besonderer Dank gilt auch Gabriele Matern für die jahrelange Genotypisierung der Mäuse. Des Weiteren möchte ich mich bei Andree Salz, Nina Roy, Julia Hecker, Melanie Jokwitz, Gerda Hertig, Ola Hauck, Steffi Stöcker, Stefan Klein, Christian Liemersdorf und Gertrud Dienst und allen Bacheloren (insbesondere meinem persönlichen Küken) bedanken.

Ein großer Dank gilt auch meinem Freund der mich während dieser sehr anstrengenden Zeit unterstützt und ausgehalten hat. Ich entschuldige mich hiermit in aller Form bei dir, aber jetzt steht wenigstens bald „Doktor“ auf unserem Klingelschild. Danke das du mit mir nach Berlin gezogen bist damit ich meinen beruflichen Horizont erweitern kann. Jetzt da die Wochenenden wieder frei sind machen wir hoffentlich endlich die Hauptstadt unsicher.

Mein größter Dank gilt meiner Familie und ganz besonders meinen Eltern die mich immer unterstützt und an mich geglaubt haben. Ich habe so viel von euch gelernt und ohne eure Hilfe wäre ich nicht derselbe Mensch. Danke das Ihr den weiten Weg mit mir gegangen seid und ich mich immer auf euch verlassen konnte.

Summary

Three actin depolymerization factors are expressed in the brain, named Cofilin 1 (non-muscle Cofilin), ADF and Cofilin 2, which was long declared as muscle-specific isoform. All three members share similar biochemical properties, but distinct knockout mouse models with a deletion of only one or two members of this family revealed isoform-specific functions, as well as functional redundancy in defined neuronal subcellular localizations.

So far, only little attention was given to Cofilin 2 in the brain since the complete knockout displays a muscle-specific phenotype, while no changes in neuromuscular junctions were detected. The complete knockout of Cofilin 2 is postnatal lethal around P7. In this thesis the expression pattern of Cofilin 2 was studied during developmental time points of the brain starting from P0 until adulthood. A ubiquitous expression of Cofilin 2 was detected in all analyzed brain areas (olfactory bulb, cortex, hippocampus, striatum, cerebellum, hypothalamus and midbrain). Interestingly, the highest expression of Cofilin 2 was detected around P7, when the complete knockout was starting to become lethal. Colocalization studies revealed the expression of Cofilin 2 in neuronal subpopulations like dopaminergic, serotonergic, cholinergic, glutamatergic and GABAergic neurons. No expression of Cofilin 2 was detected *in vivo* in glial cells (astrocytes and microglia). Additionally an upregulation of Cofilin 1 and ADF was detected in the cortex, hippocampus and midbrain of P7 knockout animals, indicating a compensatory upregulation upon the loss of Cofilin 2.

To study the exact role of Cofilin 2 in the brain, a mouse-line with a brain-specific deletion of Cofilin 2 using Nestin-Cre recombinase was analyzed. Cofilin $2^{fl/fl}$ Nestin-Cre animals were viable, but displayed a reduced body size and weight compared to control animals. Histological analysis revealed no gross brain malformations, or alterations in cortical migration. A Golgi staining indicated a reduced dendritic arborization and changes in dendritic spine morphology, although the number of spines was not altered. A pre- and postsynaptic localization of Cofilin 2 was detected in synaptosomes. Electrophysiological studies revealed no changes in the frequency of spontaneous glutamatergic vesicle release or AMPA receptor number in Cofilin $2^{fl/fl}$ Nestin-Cre animals. Further studies on inhibitory postsynaptic currents indicated an increased frequency of inhibitory vesicle release, while the amplitude was not significantly altered. As a next step behavioral tests were performed, but no changes upon the single loss of Cofilin 2 were detected. The dual loss of ADF and Cofilin 2 leads to a reduced anxiety-related behavior and impairments in working memory, indicating a functional redundancy for ADF and Cofilin 2 in these circuits.

The obtained results indicate that ADF and Cofilin 1 are not able to compensate the complete loss of Cofilin 2 and highlight the contribution of Cofilin 2 in neuronal development, synaptic functionality and spine morphogenesis. Further the functional redundancy of ADF/Cofilin family members for specific brain functions was proven once more.

Table of Content

Abbreviation

°C	Degrees Celsius
µg	Microgram
µm	Micrometer
ABP	Actin binding proteins
ACC mice	ADF Cofilin 1 CamKII-Cre
Ach	Acetylcholine
AD	Alzheimer Disease
ADF	Actin depolymerizing factor
ADP	Adenosine diphosphate
AMPA	A-amino-3-hydroxy-5-methyl-4-isoxazolepropionic acid
AP	Action potential
AP	Alkaline phosphatase
APS	Ammonium persulfate
ATP	Adenosine triphosphate
BDNF	Brain-derived neurotrophic factor
Bp	Base pair
BrdU	Bromdesoxyuridin
bs	Brainstem
BSA	Bovine serum albumin
Ca	Calcium
CaMKII	Calcium-Calmodulin dependent protein kinase II
CASK	calcium/calmodulin-dependent serine protein kinase
cb	Cerebellum
ChAT	Choline acetyltransferase
Cl	Chloride
CNS	Central nervous system
CP	Cortical plate
CRH	Corticotrophin-releasing hormone
cx	Cortex
CytoD	Cytochalasin D
DAPI	4',6-diamidino-2-phenylindole
dg	Dentate gyrus
DMEM	Dulbecco's modified Eagle's medium
DMSO	Dimethyl sulfoxide
DNA	Deoxyribonucleic acid
dNTP	Deoxynucleotide triphosphate
e.g.	exempli gratia = for example
ECL	Enhanced chemiluminescence
ECM	Extracellular matrix
EDTA	Ethylenediaminetetraacetic acid
EGF	Epidermal growth factor
EGTA	Ethylene glycol tetraacetic acid
ELISA	Enzyme Linked Immunosorbent Assay
EM	Electron microscopy
Emx	Reffering to Emx cre recombinase
EPM	Elevated plus maze
ERK	extracellular-signal regulated kinases
et al.	et alii = and others
EtBr	Ethidiumbromide
EtOH	Ethanol
Ex	Embryonic day x
EZ	Endocytic zone
F-actin	Filamentous actin

FCS	Fetal calf serum
Fig	Figure
FSI	Fast-spiking interneurons
G	Gram
GABA	γ-aminobutyric acid
G-actin	Globular actin, monomeric actin
GAD67	Glutamic acid decarboxylase 67
GAPDH	Glyceraldehyde 3-phosphate dehydrogenase
GEF	Guanine nucleotid exchange factor
GFAP	Glial fibrillary acidic protein
GFP	Green fluorescent protein
GH	Growth hormone
GHIH	Growth hormone inhibiting hormones
GHRH	Growth hormone releasing hormone
GSK3ß	Glycogen synthase kinase 3ß
H	Hour
H_20	Chemical formula for water
hc	Hippocampus
HEPES	Hydroxyethyl-piperazinyl-ethanesulfonic
HPLC	High liquid chromatography
HRP	Horseradish peroxidase
ht	Hypothalamus
IEI	Inter-event interval
IF	Immunofluorescence
IZ	Intermediate zone
kbp	Kilobase pair
kDa	Kilodalton
ko	Knockout
LatA	Latrunculin A
LGE	Lateral ganglionic eminescence
LGE	Lateral ganglionic eminescence
LIMK	Lin-11Isl-1/Mec-3 kinases
Lis1	Lissencephaly type 1 gene
LSF	Low frequency stimulation
LTD	Long term depression
LTP	Long term potentiation
M	Molar
MACS	Magnetic Activated *Cell Sorting*
MAPK	Mitogen-activated protein kinase
MBP	Myelin-basic protein
mEPSCs	Miniature excitatory postsynaptic currents
mg	Milligram
Mg	Magnesium
mg	Milligram
MGE	Medial ganglionic eminescence
MGE	Medial ganglionic eminence
MilliQ	Highly purified and deionized water
min	Minutes
mIPSCs	Miniature inhibitory postsynaptic currents
ml	Milliliter
mM	Millimolar
mRNA	Messenger ribonucleic acid
ms	Mouse
MSN	Medium spiny neurons
Mt	Mutant
MT	microtubule

MZ	Marginal zone
NA	Nucleus accumbens
NBQX	2,3-Dihydroxy-6-nitro-7-sulfamoyl-benzo[f]chinoxalin-2,3-dion
Neo	Neomycin
Nes	Reffering to Nestin cre recombinase
Nex	Reffering to Nex cre recombinase
NGF	Neural growth factor
NMDA	N-methyl-D-aspartic acid
NPCs	Neural progenitor cells
NR1	NMDA receptor subunit
NSCs	Neural stem cells
NTS	Nuclear translocation signal
o.n.	Over night
ob	Olfactory bulb
OPC	Oligodendrocyte progenitor cells
pA	Pico-ampere
PAGE	Polyacrylamide gel electrophoresis
Pak1	P21 Protein (Cdc42/Rac)-Activated Kinase 1
PBS	Phosphate buffered saline
PC	Purkinje cells
PCR	Polymerase chain reaction
PFA	Paraformaldehyde
PFC	Prefrontal cortex
pH	The negative logarithm (base 10) of the molar concentration of dissolved hydronium ions
P_i	Anorganic phosphate
PI3K	Phosphoinositide-3 kinase
PIP	Phosphatidylinositol phosphate
PIP_2	phosphatidylinositol 4,5-bisphosphate
PKC	Protein kinase C
PP	Preplate
PS	Pial surface
PSD	Postsynaptic density
rb	Rabbit
RNA	Ribonucleid acid
ROCK	Rho-associated coiled-coil-forming protein kinase
rpm	Rounds per minute
RRP	Readily releasable pool
RT	Room temperature
sec	Seconds
SDS	Sodium dodecyl sulphate
Sem3A	Semaphorin 3A
SER	Smooth endoplasmatic reticulum
Ser3	Serine 3
SNc	Substanita nigra pars compacta
SP	Subplate
SSH	Slingshot phosphatase
str	Striatum
SVZ	Subventricular zone
TAE	Tris-acetate-EDTA-buffer
Taq	DNA polymerase
TC	Tissue culture
TCM	Trichlormethazide
TESK	Testicular protein kinase
tha	Thalamus
TPH	Trypthophan hydroxylase

Tris	Tris(hydroxymethyl)-aminomethane
TrkA	receptor tyrosine kinase
TSH	Thyroid-stimulating hormone
TTX	Tetrodotoxin
U	Enzyme unit
UV	Ultraviolet
V	Volt
v/v	Volume per volume
vGLUT	Vesicular glutamate transporter
vs.	Versus
VTA	Ventral tegmental area
VZ	Ventricular zone
w/v	Weight per volume
Wt	Wildtype
αPKC	Atypical protein kinase C

List of figures

Tables

1. Introduction

1.1. The actin cytoskeleton

The cytoskeleton is involved in many cellular functions and displays a major impact on essential events like cell division, vesicle transport or migration. To obtain these different functions cells exhibit three different cytoskeletal proteins: microtubules, intermediate filaments and the actin cytoskeleton. The cytoskeletal polymers share general features, but are involved in different cellular tasks depending on their characteristic properties.

Actin is involved in cellular processes like cell growth, differentiation, cell polarization, cytokinesis, membrane organization, vesicle trafficking and cell motility (Pollard and Earnshaw 2008).

Depending on its important functions it is not surprising that actin is one of the most abundant highly conserved proteins among eukaryotes. Therefore, actin must be highly dynamic and tightly regulated both spatially and temporally according to intra- and extracellular cues. This could be achieved by up to 162 different actin-binding proteins, which have the ability to regulate actin dynamics, the shape and rapid turnover of filamentous actin *in vivo*. In vertebrates three isoforms of actin exist, which differ in their function and localization: the α-isoform is expressed in muscle cells, whereas the β- and γ-isoforms are localized to non-muscle cells (Khaitlina 2001).

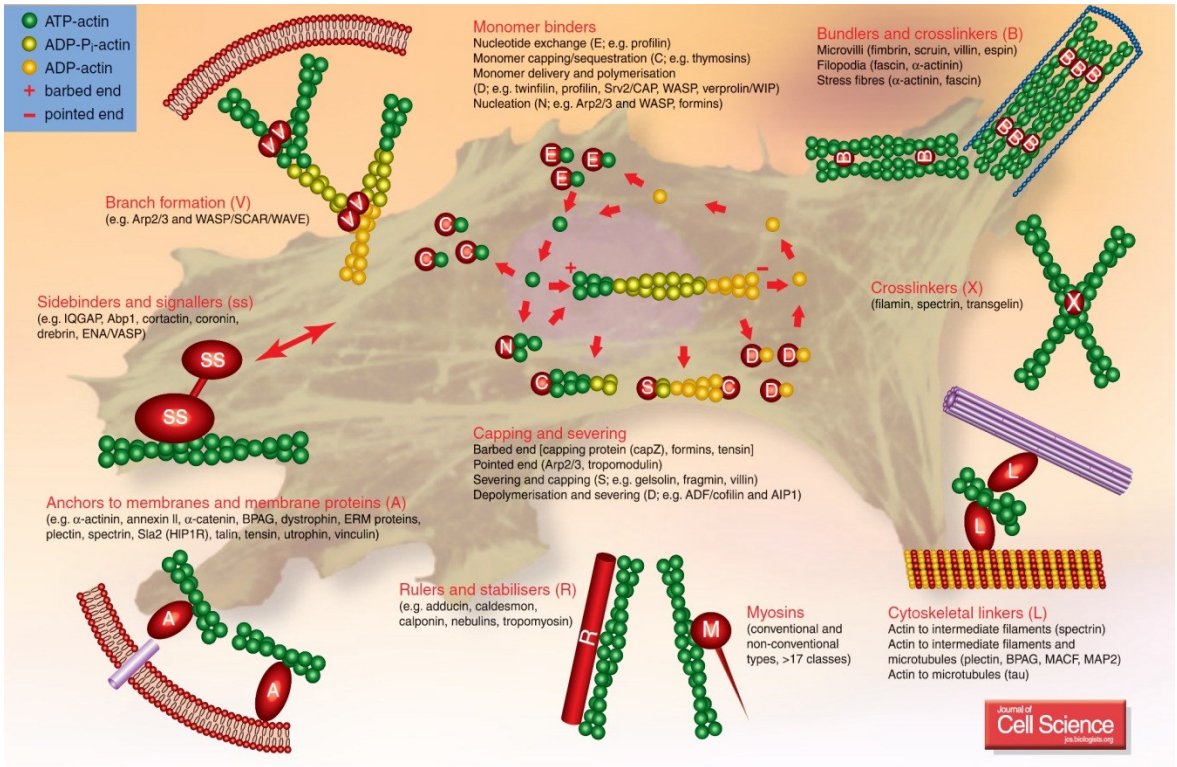

Fig. 1: Schematic overview of actin-binding proteins, which differ in their functionality to obtain the high dynamic of the actin cytoskeleton (Winder and Ayscough 2005).

In the cell actin exists in two different forms, as a globular monomer (G-actin) and as a filamentous polymer (F-actin). Actin filaments form double-stranded right-handed helices. This process is reversible, which generates a high dynamic of the actin cytoskeleton. Within a filament, an individual actin subunit is connected to four neighboring subunits, strengthening the actin filament and avoiding shearing. The actin monomer is a 42 kDa molecule consisting of four subdomains (figure 2), which form a furrow between subdomains 2 and 4 for the reversible binding of nucleotides (ATP or ADP) and divalent cations (Mg^{2+} or Ca^{2+}) (Otterbein et al., 2001). Thereby, actin binds ATP more tightly than ADP.

Fig. 2: Ribbon structure of uncomplexed actin in the ADP state. The four subdomains of actin are represented in different colors: subdomain 1 in (purple), 2 (green), 3 (yellow) and 4 (red). Subdomain 2 and 4 mark the pointed end of filaments, while subdomain 1 and 3 display the barbed end. ADP is bound at the center, where the four subdomains meet. Additionally, four Ca^{2+} ions (red dots) are bound to the actin monomer, with one Ca^{2+} ion localized in close proximity to the nucleotide and termed therefore catalytic. The other three Ca^{2+} ions are bound to subdomains 1, 2 and 4 (Otterbein et al., 2001).

The polymerization process is reversible and monomers are constantly being added to and dissociated from the ends of filaments. This process of assembly and disassembly is the driving force for actin-based cellular processes, like cell motility. The actin filament is a structurally polarized polymer and monomers assemble in a “head-to-tail” fashion, which enables all subunits to be orientated in the same direction. The filament ends differ in their associating-rate for actin monomers. The barbed end (“+”-end) is the fast-growing end with a rapid monomer elongation rate, and is always exposed to membranes for a dynamic membrane ruffling and the formation of filopodia and lamellipodia, which are essential for cell migration. In contrast, the pointed end (“-“-end) shows a minor monomer elongation and is located to the cell soma. This polarity is important for directional transport and a polarized cell shape (Pollard and Borisy 2003).

The actin polymerization process can be divided into four steps: 1. Activation of the monomer by substitution of a Ca^{2+} for Mg^{2+} leading to a conformational change; 2. Nucleation via the formation of a trimeric ATP-actin-nucleus to increase the probability of filament growth; 3. Elongation by the extension of the polymers; 4. Annealing by joining of two filaments at the ends (Pollard and Cooper 1986). After polymerization the actin subunit hydrolyzes ATP, which is an irreversible step and is responsible for the fact that actin

polymerization is a non-equilibrium process (Kuhn and Pollard 2005). ADP and Pi stay non-covalently bound to actin, followed by a slow release of Pi, whereas ADP remains tightly bound as long as the actin subunit is incorporated into the filament. After dissociation of ADP-actin from the pointed end, a replacement of the bound nucleotide must occur to enable a new incorporation at the barbed end, which has a higher affinity for ATP-actin. This process is driven by the actin binding protein profilin, which catalyzes an exchange from ADP to ATP. This process of polymerization and depolymerization generates a constant flux of subunits through the filament without changing the overall concentration of actin and is called treadmilling. During this process the actin polymer reaches a steady state level, which is indicated by the fact that a net elongation of actin at the barbed end occurs, while coincidentally a net depolymerization at the pointed end appears, which leads to a constant length of actin filaments.

1.2. Actin binding proteins

In order to promote cytoskeletal based functions, cells are obligated to regulate the polymerization and depolymerization process, to facilitate a rapid remodeling of the actin cytoskeleton in response to environmental cues. Therefore, regulatory mechanisms must exist which control the length of filaments, elongate pre-existing filaments, nucleate new actin filaments or inhibit the spontaneous polymerization of the monomeric actin pool. To ensure these processes different actin-binding proteins are expressed in the cell, which compete for the actin binding sites and facilitate the high dynamic in response to different functions of the cell (figure 1) (Pollard and Cooper 1986). To modulate the actin cytoskeleton monomer binding proteins exists (thymosin ß4 or profilin) that help to maintain a pool of unpolymerized monomers for spontaneous polymerization. Nucleating proteins (Arp2/3 or formin), which regulate the polymerization step by compromising the rate limiting nucleation step and are also important for the branching of filaments. To regulate the length and mechanical properties of actin filaments capping proteins bind to either the barbed or pointed end and inhibit the elongation (gelsolin) or depolymerization (tropomodulin) of the filament. Crosslinking proteins (fimbrin, spectrin or fascin) are necessary for the organization of actin into higher order structures like bundles and networks. Two important examples are the formation of lamellipodia and filopodia, which display either an arrangement of filaments into a criss-cross organized meshwork, or into bundles of parallel packed filaments.

This study will focus on the ADF/Cofilin family, which is necessary for the recycling and severing of actin filaments. Actin filaments must disassemble to maintain a soluble pool of actin monomers that allows a rapid rearrangement into filaments due to extracellular signals. Additionally a depolymerization of older filaments is necessary to guarantee the forward protrusion of motile structures. The severing of filaments increases the number of filament

ends available for assembly or disassembly and is an important step for the branching of filaments.

1.2.1. The ADF/Cofilin family

The family of actin-depolymerizing factors, including ADF, Cofilin 1 and 2, are essential in regulating actin filament turnover. ADF/Cofilins can bind to actin-monomers and filaments (Bamburg 1999) and are localized to regions of rapid actin dynamics, like neuronal growth cones, the leading edge and ruffling membranes of motile cells (Bamburg and Bray 1987). The ADF/Cofilin family also belongs to the minimal set of proteins required for motility of the *Listeria* actin tail (Loisel et al., 1999). The activities of ADF/Cofilins are fundamental for the cell, because the inactivation of Cofilin 1 is embryonic lethal (Gunsalus et al., 1995; Gurniak et al., 2005; McKim et al., 1994; Moon et al., 1993). In strong contrast to that the complete knockout of ADF displays no obvious changes and animals are also viable (Bellenchi et al., 2007; Gurniak et al., 2005). A complete knockout of Cofilin 2 displays a muscle-specific phenotype with a postnatal lethality around P7. Due to their high affinity to actin only a very low concentration of ADF/Cofilins is needed in the cell, which makes up circa 0, 44% of total protein (Bamburg and Bray 1987).
The ADF/Cofilin family is ubiquitously expressed among eukaryotic organisms (Bamburg 1999). In mouse and most likely in all other mammalian species exist three ADF/Cofilins with different biochemical properties and localizations to fulfill specific requirements for actin filament dynamics in different cell types. The three highly conserved genes are termed Cofilin 1 (n-Cofilin) for non-muscle cofilin, Cofilin 2 (m-Cofilin) for muscle cofilin and ADF, which stands for actin depolymerizing factor or destrin: destroys F-actin.

1.2.2. Structure of ADF/Cofilins

ADF/Cofilins consists of 165 - 168 amino acids with a molecular mass of 18 – 20kDa. DNA analyses suggest an 80% identical sequence between Cofilin 1 and Cofilin 2, and of 70% between both Cofilins and ADF. The ADF/Cofilin fold is formed by a central, mixed β-sheet flanked by two α-helices on each side. The putative actin-binding sites include the N-terminus and residues located on and preceding helices 3 and 4 (Bowman et al., 2000). For an efficient binding of actin the conserved structural “kink” or disruption of α-helical hydrogen bonding in the middle of α-helix 3 is needed, as well as the highly conserved tyrosines at positions 67 and 103. Additionally, the “kink” is surrounded by a conserved region at position 104-106, which consists of amino acids with small side chains like alanine, serine and threonine. The elimination of the hydroxyl group at Serine 106 leads to a significantly attenuation in actin binding, suggesting that this region contacts actin directly. Further is the

binding to actin achieved by a hydrophobic and charged surface character, an electrostatically conserved region consisting of the three acidic residues at position 93, 125 and 128 and a lysine at position 100.

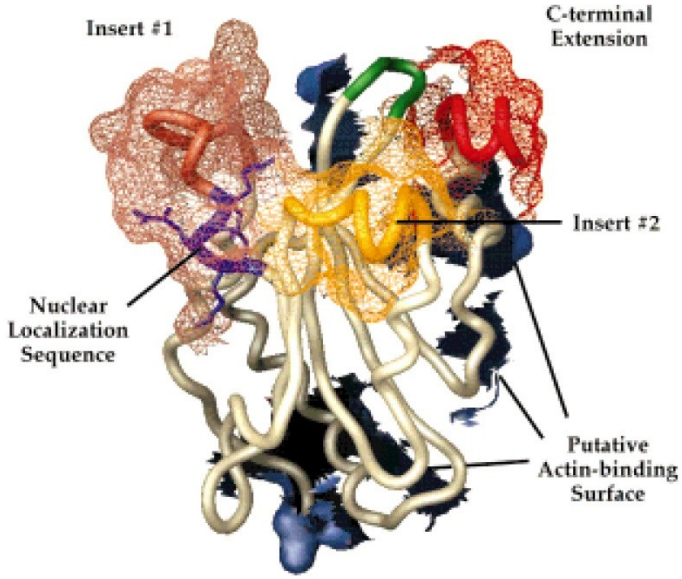

Fig. 3: A molecular surface rendering of human destrin, highlighting the vertebrate specific inserts and C-terminal extension (mesh surfaces). Additionally, the putative actin-binding surface is indicated, as well as the nuclear localization sequence (purple) (Bowman et al., 2000).

1.2.3. Function of ADF/Cofilins

One important function of the ADF/Cofilin family is the regulation of the turnover and reorganization of F-actin *in vivo* (Bamburg 1999);(Svitkina and Borisy 1999). ADF/Cofilins bind co-operatively to F-actin (Hayden et al., 1993) and display a higher affinity for the ADP-actin subunits. Through the binding of F-actin ADF/Cofilins stabilize a twisted form of F-actin, which changes the thermodynamic stability of filaments (McGough and Chiu 1999). This conformational change promotes the cooperative binding of other ADF/Cofilins. Additionally, this twist of filaments exerts a physical strain that advances the dissociation of subunits from the pointed end and severs filaments by disrupting longitudinal and lateral contacts among actin subunits.

The creation of more barbed- and pointed-ends on F-actin via their severing activity allows a faster F-actin turnover. ADF/Cofilins alone are sufficient for a high treadmilling-rate *in vivo*, due to the fact that they increase the off-rate at the pointed end by about 30%. The preferential binding of ADF/Cofilins to ADP-actin leads to a selective severing and depolymerization of “older” ADP bound filaments. In contrast to that is the affinity for ADP-Pi-actin quite weak, which ensures that newly built filaments are not directly depolymerized again. A depolymerization of actin filaments occurs only when the filaments are capped at the barbed ends through specific proteins like Cap1 (figure 3).

Although all three members share between 70-80% amino acid similarity murine Cofilin 2 binds ATP-actin monomers with a 5-10 fold higher affinity than ADF or Cofilin 1, suggesting

differences in their physiological functions. Cofilin 2 also displays a smaller difference between the affinity for ADP- and ATP-actin monomers (Vartiainen et al., 2002).

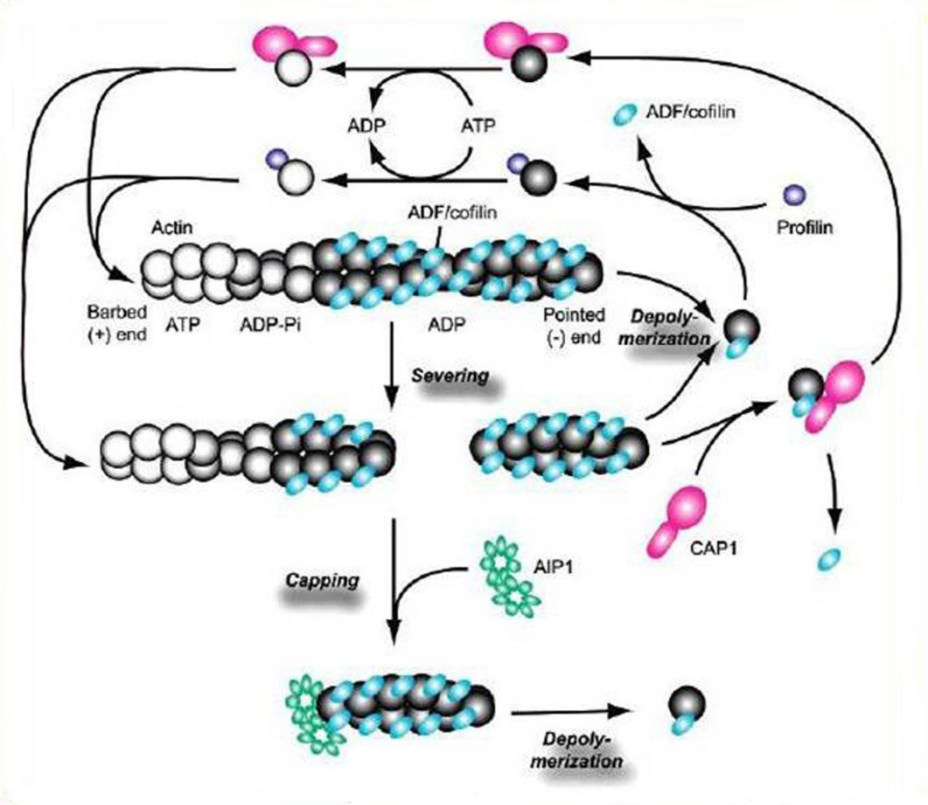

Fig. 4: Function of ADF/Cofilins on the actin cytoskeleton and their interaction with capping proteins. ADF/Cofilins display higher affinity for ADP-bound actin and are therefore bound to the pointed ends. The activity of ADF/Cofilins leads to the depolymerization of filaments from the pointed ends and the severing of filaments, generating more free barbed ends for a rapid elongation. This elongation process could be prevented through the capping protein AIP1 at the barbed ends. AIP1 specifically caps ends of ADF/Cofilin-bound filaments and enhances fragmentation. Additionally, ADF/Cofilins inhibit the exchange of actin-bound nucleotides, controlling the recycling of the monomer pool and act as a competitors for the actin-binding proteins profilin and CAP1 (Ono 2003).
AIP1: actin-interacting protein 1; CAP1: cyclase associated protein 1

Additionally, ADF/Cofilins stay bound to ADP-actin monomers and inhibit the nucleotide exchange, which regulates the recycling of the monomeric actin pool for the generation of ATP-actin. The disassembly of actin filaments is important to maintain a soluble pool of actin monomers, so that the rapid elongation of filaments can occur in response to extracellular signals.

All three mammalian ADF/Cofilins contain a nuclear-translocation sequence (NTS) and are therefore implicated in the targeting of actin to the nucleus (Iida et al., 1992). Actin is known to have no nuclear translocation signal (Rando et al., 2000), but upon cellular stress, actin gets indirectly transported to the nucleus, where it binds to a component of the BAF helicase, a chromatin-remodeling-complex. Actin is supposed to have a function in chromatin remodeling and gene transcription and ADF/Cofilins might act as chaperones for the translocation of actin to the nucleus. As a result the concentration of ADF/Cofilins in the

cytoplasm is reduced, which could affect the turnover of actin or the interaction with actin binding proteins, leading to a different cell response to a given stimulus.

1.2.4. Regulation of ADF/Cofilin family members

The regulation of ADF/Cofilins can occur by different mechanisms in addition to a competitive binding of other actin binding proteins to the ADF/Cofilin binding site on actin.
The ADF/Cofilin family can be inactivated through phosphorylation of serine 3 via the kinases LIM kinase 1 and 2, as well as TES kinase 1 and 2 (Moriyama et al., 1996). All four kinases have a high specificity towards this serine residue, but vary in their cellular localization and affiliation to different signaling-pathways. LIMK1 is predominantly expressed in the nervous system, whereas LIMK2 shows a more ubiquitous expression. An activation of LIMKs occurs upon phosphorylation via the Rac- and Cdc42-activated kinase PAK, or by the Rho A kinase ROCK. Thus, LIMKs are involved in the stimulus-induced remodeling of the actin cytoskeleton (figure 4), which links the signals from Rho family GTPases to a change in ADF/Cofilin activity. TES kinases are also produced in various tissues and are activated downstream of Rho, independently of ROCK.

The reactivation of ADF/Cofilins is regulated by the activity of the phosphatase slinghshot (SSH), which is known to dephosphorylate ADF/Cofilins (Huang et al., 2006). Thereby, the dephosphorylation can be regulated by the availability of ADF/Cofilins Ser3-Phosphate to the phosphatase, which is under the control of protein 14-3-3ζ, an isoform of a family of phosphoserine- and phosphothreonine-binding proteins (Fu et al., 2000). Sequestering of the phosphorylated ADF/Cofilins by 14-3-3ζ can restrict their dephosphorylation or subcellular localization. A further phosphatase implicated in the activity regulation of ADF/Cofilins is chronophin, which increases the ADF/Cofilin activity after stimulation with EGF in a PI3-kinase- and Rac1-dependent manner (Delorme-Walker et al., 2015; Gohla et al., 2005).
Phosphoinositides block the actin-ADF/Cofilin interaction through a competition for the actin binding site on the loop preceding α-helix 3 on ADF/Cofilins (Kusano et al., 1999). This suggests that the membrane lipids phosphatidylinositol 4-phosphate (PIP) and phosphatidylinositol 4,5-bisphosphate (PIP_2) and actin bind to overlapping sites and that ADF/Cofilins are regulated by transmembrane signaling through PIP_2 (Yonezawa et al., 1990). The binding of PIP_2 to ADF/Cofilins inhibits actin depolymerization and nucleotide exchange (Tirion et al., 1995). This influences, together with the activity of ADF/Cofilins, the elongation of filaments at membranes and plays a central role for migration and membrane protrusion.

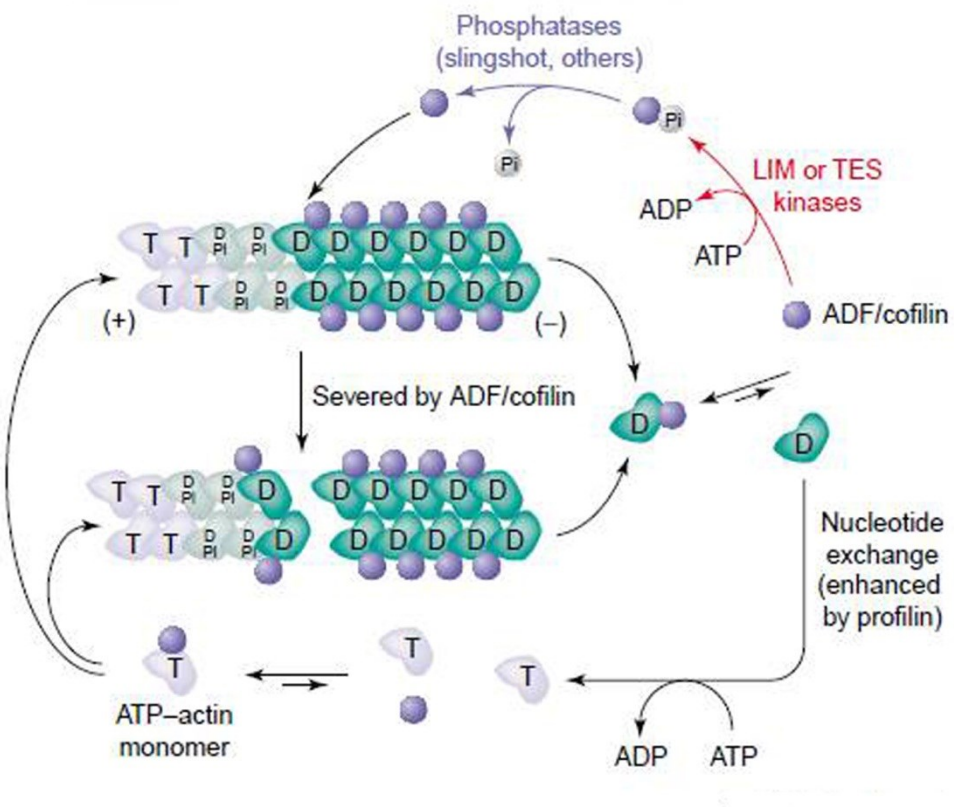

Fig. 5: Regulation of ADF/Cofilin activity in a cycle of phosphorylation and dephosphorylation. The inactivation of ADF/Cofilins is regulated by phosphorylation of Ser3 via the LIM (Lin-11Isl-1/Mec-3) kinases or TESK (testicular protein kinases). Due to the phosphorylation of ADF/Cofilins charge repulsion occurrs that changes the character of the actin-binding surface and inhibits actin-binding. Activation depends on the activity of the phosphatases slingshot and chronophin, which allow ADF/Cofilins to exert their function in the actin cytoskeleton (Bamburg and Wiggan 2002).
D: ADP-actin; T: ATP-actin; Pi: inorganic phosphate

The ability of ADF/Cofilins to assemble or disassemble F-actin is pH dependent *in vitro* (Bernstein et al., 2000). Acidic conditions (pH below 6.8) enhance the ability of ADF/Cofilins to stabilize F-actin, while at a more alkaline pH above 7.3 ADF/Cofilins can rapidly depolymerize F-actin (dos Remedios 2003). Also the critical concentration of the Cofilin-actin-complex is pH-dependent, being lower at pH 6.5 and significantly higher at pH 8.2. Thus an elevated pH level induced through activated signaling pathways increases the depolymerization of filaments. The different isoforms also differ in their pH-sensitivity, with Cofilin 1 and 2 being less responsive to altered pH than ADF.

ADF/Cofilins show structural homologies with gelsolin and profilin suggesting a binding to the same region of G-actin (subdomain 1 and 3) (Pollard and Borisy 2003). Profilin is the antagonist of ADF/Cofilins, catalyzing the exchange of bound nucleotides from monomers, which promotes elongation exclusively at the barbed end (figure 4). Therefore, a reciprocal regulation is necessary to maintain a balance between elongation and dissociation of filaments. Gelsolin is a barbed end capping protein, which inhibits the elongation of filaments. Only when filaments are capped depolymerization by ADF/Cofilins can occur. Thus, both

gelsolin and ADF/Cofilins regulate the length of filaments and therefore the size of specific actin structures (Mazur et al., 2010), as well as the mechanical properties of actin filaments, with shorter filaments being stiffer than longer ones. ADF/Cofilins also compete with spectrin, which stabilizes short-actin oligomers and tropomodulin, which caps the pointed ends and inhibits the disassembly from the pointed end.

1.2.5. Expression of the ADF/Cofilin family members in mouse

Although all members of the ADF/Cofilin family share similar biochemical properties, they vary in their depolymerization efficiency and expression patterns in different cell types. For example ADF is the most efficient family member for the actin filament turnover, through an improved ability to disassemble actin filaments (Vartiainen et al., 2002). Additionally ADF displays a stronger pH-dependent activity than both Cofilins, with an increased disassembly activity at a pH of 8.5. In contrast, Cofilin 2 is less efficient in actin disassembly and shows an increased severing activity. This heterogeneity in function is due to specific requirements in the actin filament dynamics of different cell types and results in different expression pattern of the family members (Vartiainen et al., 2002).

The expression levels of the three isoforms vary in the course of embryonic development, with Cofilin 1 being expressed at a constant level during development, whereas ADF and Cofilin 2 are expressed at lower levels (Vartiainen et al., 2002). Cofilin 1 is uniformly expressed in embryonic day 9.5 (E9.5) (Vartiainen et al., 2002). At this time point no ADF or Cofilin 2 expression could be detected. In E14 embryos, Cofilin 1 is intensively expressed in all cell types and ADF is expressed in the brain and epithelial tissues such as intestines and skin, whereas Cofilin 2 is detectable in developing muscles (Ono et al., 1994).

In adult mice Cofilin 1 is highly expressed in brain and liver; moderately in heart, spleen, lung, kidneys and testes and completely absent from muscles (Bellenchi et al., 2007; Gurniak et al., 2005). Cofilin 2 expression is found in skeletal muscles and the brain and at lower amounts also in the heart, liver and testes (Obinata et al., 1997). The expression of ADF is restricted to endothelial and epithelial tissues, but also found in the brain.

Although the isoforms are coexpressed in many organs, they are localized into different compartments and cell types (Vartiainen et al., 2002). It is conspicuous that ADF and Cofilin 1 are coexpressed in several cell tissues (Meberg et al., 1998), but the expression of ADF and Cofilin 2 is not generally found in the same tissues, except for the brain. In this study a closer look on the expression of the ADF/Cofilin family members in different brain regions starting from P0 to adulthood and the possible compensation by other family members upon the loss of Cofilin 2 were examined. Therefore a first overview over the function of different

brain regions, their neuronal circuits, as well as neuronal subtypes, which are localized in these regions are discussed. During this study the expression of Cofilin 2 in distinct brain regions was analyzed via Western Blot and the specific localization of Cofilin 2 to distinct neuronal subtypes in these regions was examined by immunofluorescence colocalization studies.

1.3. Brain areas and neuronal subtype localization

The mouse brain can be divided into three anatomical categories: the hindbrain, midbrain and forebrain. The hindbrain (rhombencephalon), which is responsible for the connection between the brain and the spinal cord, consists of the medulla, pons and cerebellum. The midbrain (mesencephalon) forms a major part of the brainstem and all information that is passed between the higher brain and brainstem has to traverse the midbrain. The last one is the forebrain (prosencephalon) which consists of the cerebrum (telencephalon) and the thalamus and hypothalamus (diencephalon). The cerebrum is instrumental in conscious behavior, learning and sensory perception.

To study the detailed expression of Cofilin 2 in the brain, lysates of the following brain areas were prepared and biochemical analyses were performed: cortex, hippocampus, striatum, olfactory bulb, hypothalamus, midbrain (containing the thalamus) and cerebellum.

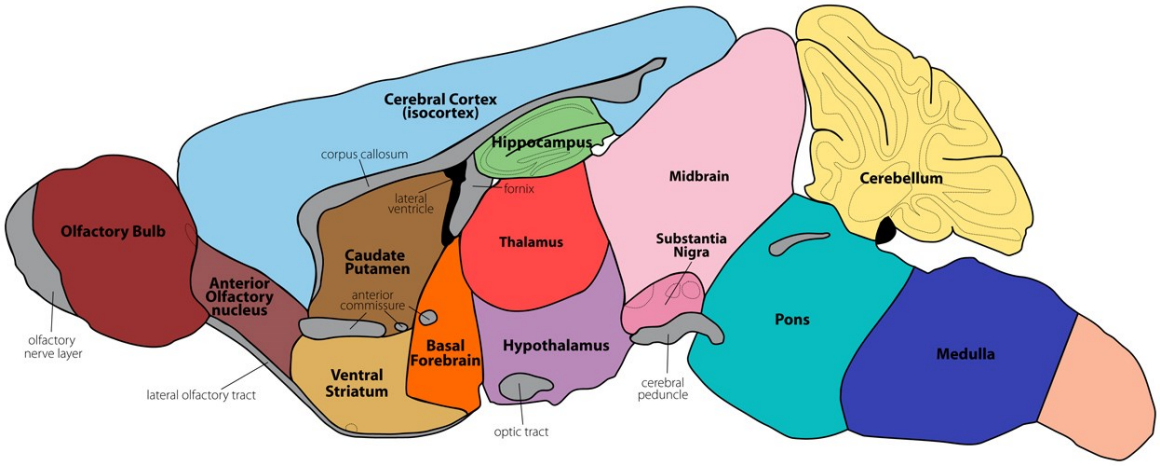

Fig. 6: Sagittal section of a mouse brain from the Allen Brain Atlas.

1.3.1. Striatal circuits regulate the behavioral outcome

The striatum is part of the basal ganglial system and the major input station. It exerts an inhibitory influence on the motor system and the working memory. Therefore the striatum receives information from cortico-striatale projections, especially from the motoric, sensory and prefrontal cortex, as well as nigro-striatale projections from the substantia nigra pars compacta. The initiation and performance of movement depends on the release of

neurotransmitters in the basal ganglia, which consists mainly from interplay between GABA, glutamate, dopamine and acetylcholine (Smeets et al., 2000). The striatum consists of the nucleus caudatus and the putamen, which are connected ventrally by the nucleus accumbens that is built by the amygdala and nucleus basalis. 90% of neurons in the nucleus caudatus and putamen are medium spiny neurons, which release mainly GABA and are therefore inhibitory (Pollack 2001). These neurons can be classified by the expression of the antibody calbindin. Second classes of striatal neurons are cholinergic interneurons that release acetylcholine and respond to salient environmental stimuli (Lim et al., 2014). Additionally minor groups are fast-spiking GABAergic interneurons that participate in feed-forward inhibition of principal neurons and can be characterized by the expression of the antibody parvalbumin. Excitation of cortical neurons leads to the release of glutamate in the putamen, which results in the activation of GABAergic neurons. These interneurons transmit the information to the output regions of the striatum, which are the globus pallidus and the substantia nigra, which regulate the information influx into the thalamus (Bolam et al., 2000). For the regulation and modulation of these excitatory and inhibitory neuronal circuits, dopaminergic projections from the substantia nigra to the striatum exist. Mice lacking ADF and Cofilin 1 show an increased glutamate release in the striatum, which results in behavioral abnormalities like hyper-locomotion (Zimmermann et al., 2015).

1.3.2. Dopaminergic neurons fulfill modulatory functions

Various clusters of dopaminergic neurons have different anatomical positions and project to different brain areas (Chinta and Andersen 2005). They play an important role in voluntary movement and behavioral processes and a loss of domapinergic neurons is associated with Parkinson. Dopaminergic neurons are found in the substantia nigra pars compacta, where they only make up 3 – 5% of the total neurons. This nigrostriatal system originates in the zona compacta of the substantia nigra and extends its fibers into the putamen of the striatum (figure 7). The phasic dopamine release on dopaminergic terminals in the putamen leads to the excitation of GABAergic neurons via D1-receptors, while an inhibitory influence on these neurons is executed via D2-receptors (Nishi et al., 2011). Additionally dopamine inhibits cholinergic interneurons, which would activate GABAergic neurons via the release of acetylcholine. Glutamatergic cortico-striatale projections stimulate the dopamine release from dopaminergic terminals via the activation of NMDA-receptors on dopaminergic neurons (Krebs et al., 1991). The interplay between these striatal neurotransmitters is important to fulfill a coordinated movement. A dopamine deficit leads to an increased GABAergic inhibition of the thalamus, which results in a lack of information processing in the thalamus. At the same time, the balance between dopaminergic and cholinergic transmission is shifted towards acetylcholine, which results in an increased activation of GABAergic neurons leading

to a disappearance of inhibition and the motoric over-activation, which is reflected in the occurrence of tremor and rigor in Parkinson's disease (Mallet et al., 2006). Zimmermann et al (2015) found a hyperlocomotion, impulsivity and impaired working memory in mice deficient for ADF and Cofilin 1. These double mutants show a disturbed morphology of striatal excitatory synapses, which leads to an increased glutamate release. Thereby the deregulation of actin results in an enhanced glutamate release, which alters the dopamine release. The application of the psychostimulant methylphenidate, which blocks dopamine transmission results in normal locomotion. This result links the disturbance of the actin cytoskeleton to a deregulation of dopamine release (Zimmermann et al., 2015). A second mesolimbic and mesocortical system arises from dopaminergic cells in the ventral tegmental area (VTA), which project into the nucleus accumbens (NA), olfactory tubercle, septum, amygdala and the hippocampus and is involved in emotion-based behavior. A colocalization between Cofilin 2 and dopaminergic neurons was analyzed with the antibody Tyrosine hydroxylase, an enzyme which builds the precursor for dopamine and is therefore localized to dopaminergic neurons (Daubner et al., 2011).

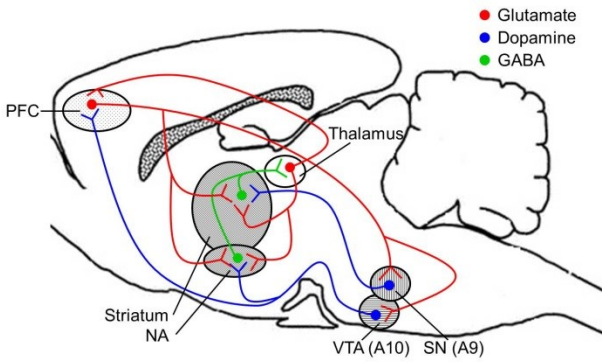

Fig. 7: Dopaminergic neuronal circuits and their modulatory effect on different brain regions. Dopaminergic neurons (blue) in the substantia nigra (SN) project to the dorsal striatum and are known as the nigrostriatal pathway. Additionally are some dopaminergic neurons localized to the ventral tegmental area (VTA), which project to the prefrontal cortex (PFC) that compromise the mesocortical system and the nucleus accumbens (NA) of the striatum. From the striatum inhibitory neurons extend to the thalamus and regulate the glutamatergic signaling to the cortex in response to environmental stimuli. Therefore the interplay between dopaminergic, inhibitory and glutamatergic neurons is important to fulfill a coordinated movement. (Miller et al., 2013)

1.3.3. The hippocampus is important for learning and memory processes

The hippocampus belongs to the limbic system and plays important roles in the consolidation of information from short-term memory to long-term memory and spatial navigation. Many neurons in the hippocampus respond as so called place cells and O´Keefe and Nadel developed the theory that the hippocampus might act as a cognitive map (O´Keefe and Nadel 1978). In the hippocampus dorsal, intermediate and ventral regions can be classified, which serve different functions. The dorsal region plays a role in spatial memory and learning

(Pothuizen et al., 2004) and contains the highest number of place cells, while the ventral region is associated with fear conditioning and affective processes (Anagnostaras et al., 2002; Cenquizca and Swanson 2007). During learning and memory processes synaptic plasticity plays an important role, with two regulatory events: long-term potentiation (LTP) showing a persistent increase in synaptic strength, and long-term depression (LTD) with an activity-dependent reduction in synaptic strength (Fukazawa et al., 2003). Both processes are mediated via actin rearrangements and will be further discussed in chapter 1.4.

The hippocampus has a defined laminar structure with arranged layers of pyramidal cells. Connections within the hippocampus follow this laminar format and are unidirectional, so that closed loops are formed, with defined routes for the information flow (figure 8). Thereby the perforant path is the major input to the hippocampus and axons arises mainly from the enthorinal cortex and project to granule cells of the dentate gyrus (dg) (van Groen et al., 2003). The mossy fiber pathway comprised axons of the dg granule cells to the Ca3 pyramidal cells. Ca3 neurons then project to the Ca1 region of the hippocampus in the Schaffer Collateral pathway. From their Ca1 pyramidal neurons project to the subiculum and from there back to the entorhinal cortex, the principal output station. Additional pathways go to the prefrontal cortex, lateral septum and the hypothalamus. The hippocampus also receives modulatory input from serotonin, norepinephrine and dopamine systems, as well as cholinergic and GABAergic fibers from the medial septum.

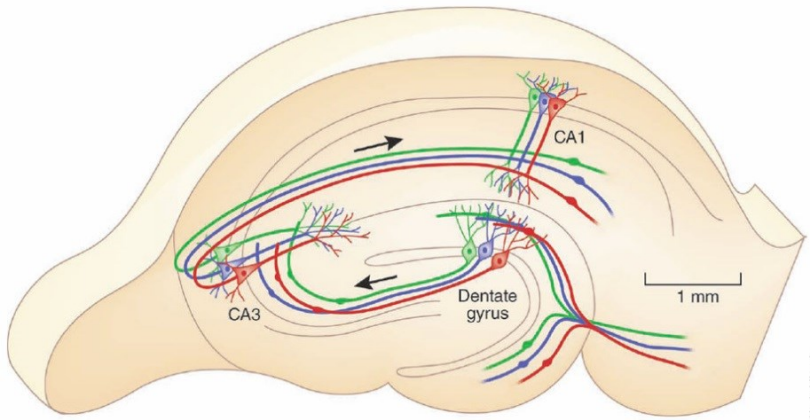

Fig.8: The unidirectional hippocampal network. The entorhinal cortex (EC) projects to granule cells in the dentate gyrus (dg) and reflects the main input station into the hippocampus (hc). Axons from granule cells in the dg pass the information forward to apical dendrites of Ca3 pyramidal neurons in the mossy fiber pathway. From there the information is processed in the Schaffer Collateral pathway from the Ca3 region to pyramidal neurons in the Ca1 layer. Ca1 neurons send axons back to the entorhinal cortex. The EC is connected to many other parts of the cerebral cortex, as well as the thalamus and hypothalamus. The dorsal region of the hc is implicated in spatial memory and learning, while the ventral part is associated with fear conditioning. The uniform organization of pyramidal cells in the hc is often used in electrophysiology studies to analyze synaptic parameters like LTD and LTP. (Moser 2011).

1.3.4. Migrational waves from the SVZ built up the cortex

The cerebral cortex plays a key role in memory, attention, perception and awareness and is mainly composed of two types of neuronal cells: first projection (pyramidal) neurons which are glutamatergic and excitatory and second interneurons which are GABAergic and inhibitory. Cortical neurons arise from progenitor cells in the ventricular zone (Kriegstein and Noctor 2004). The first postmitotic cortical neurons that migrate out of the ventricular zone at E11 form a transient layer, the preplate. This preplate is split through subsequent waves of migrating cortical neurons at E13 into a superficial layer, called marginal zone and a deeper layer, the subplate. Both layers form the cortical plate. As additional waves of migrating neurons arrive in the cortical plate, they bypass the existing layers and migrate to the surface, where they form the cortical layers in an inside-out-fashion (Nadarajah and Parnavelas 2002). This means early-generated neurons are localized in deeper cortical layers (V-VI), while late-born-neurons migrate through the existing layers and form the more superficial layers (II, III and IV) (Ayala et al., 2007). A brain specific knockout of Cofilin 1 leads to the loss of cortical layers II, III and IV and a translucent appearance of the cortex (Bellenchi et al., 2007).

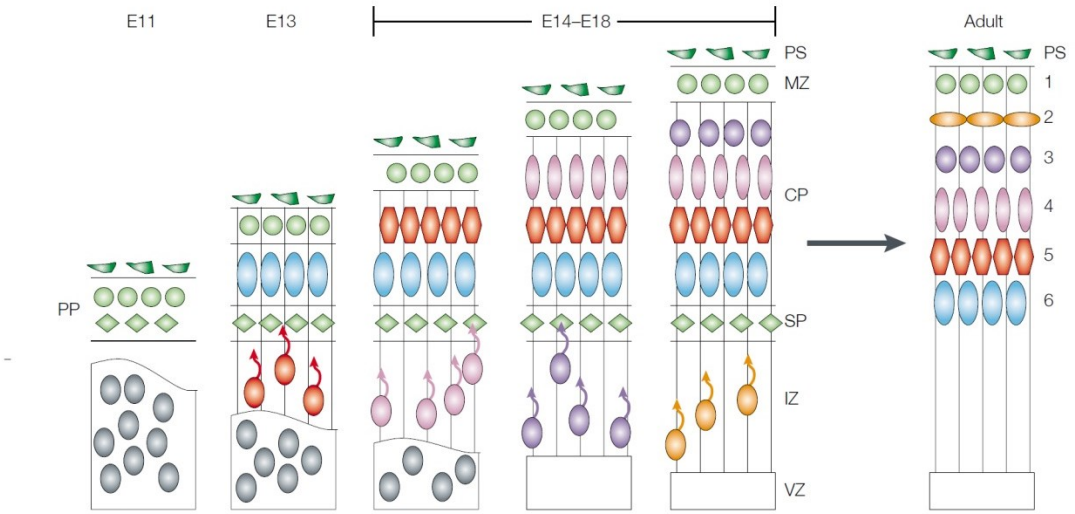

Fig. 9: Formation of the cortical layers during embryonic development. The cerebral neocortex is organized into 6 distinct neuronal layers. At E11 the preplate (PP) is established through the postmitotic migration of neurons from the ventricular zone (VZ) to the pial surface (PS). A second postmitotic wave migrates through the intermediate zone (IZ) and splits the preplate into the marginal zone (MZ) and the more superficial subplate (SP), which generates the cortical plate (CP) at E13. During E14- E18 a subsequent wave of neurons from the subventricular zone (SVZ) reaches the cortical plate and expands it in an insight-out-fashion, which means that later born neurons migrate through the existing layers to the pial surface. In the adulthood the subplate degenerates and leaves behind a six-layered cortex (Gupta et al., 2002).

In the adult stage the cortical plate contains six cortical layers. Each layer contains a characteristic distribution of neuronal cell types and connections with other cortical and subcortical regions, like the thalamus and the basal ganglia. Vertically connections of neurons in various layers form small microcircuits, called cortical columns. Thereby the cortex can be classified into three areas: sensory, motor and association. The sensory area receives and processes information about senses and receives sensory input from the thalamus. Control of voluntary movements are regulated by the motor areas, while the integration of sensory information with stored memory, as well as planning actions and movement is performed by the association area. To reach their position in the cortical plate neurons must be capable of sensing local microenvironmental cues, which establish layer fate. These microenvironmental cues change over time leading to different positions in the cortical plate. Important receptors to sense these guidance cues are localized in the membrane of a specific structure called growth cone, which will be explained further in the next chapter.

1.3.4.1. Actin assembly in the growth cone

The establishment of highly ordered neuronal networks depends on the precise control of axon guidance during development. Growth cones at the distal tips of growing neurites sense a variety of attractive (BDNF) or repulsive (semaphoring 3A) cues from the environment, which induce changes in cell shape and motility (Pak et al., 2008). These changes are accompanied by alterations in the actin filament dynamics and reorganization, guiding the axon to its target. The axonal growth cone is composed of a central region filled with organelles and microtubules and a peripheral highly dynamic actin-rich region (Ishikawa and Kohama 2007; Tahirovic and Bradke 2009). At the periphery highly dynamic actin-based structures like filopodia and lamellipodia are located (figure 10). Both actin-rich structures vary in their actin arrangement. Lamellipodia are broad veil-like cellular protrusions with a branched actin network and can be further characterized by the absence of tropomyosins and the presence of Cofilin (Ishikawa and Kohama 2007). In contrast filopodia are thin protrusions containing unbranched and parallel F-actin bundles (Dickson 2002). The barbed ends of filaments are located to the ruffling membranes, whereas the pointed ends are located to the center of the growth cone. This guarantees a continuous in-cooperation of ATP-actin at the barbed ends, which drives the membrane further on and leads to the elongation towards the source of a guidance cue, and the dissociation of ADP-actin at the pointed end for the recycling of actin monomers.

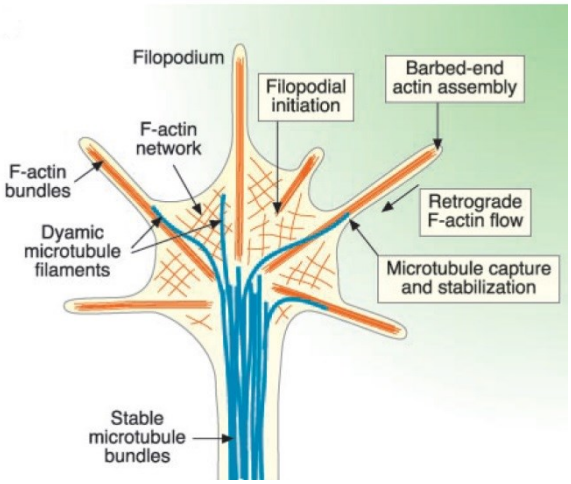

Fig. 10: Assembly of the growth cone. The growth cone at the tips of neurites is composed of a central domain, which contains microtubules and a peripheral domain, which consists of the actin cytoskeleton and shows the typical migrational protrusions at the ruffling membrane. Lamellipodia display a meshwork of actin filaments, while filopodia can be characterized through a parallel alignment of actin filaments. The assembly of actin filaments at the barbed ends is necessary for the outgrowth of growth cones, which drives the membrane further on. Based on this the barbed ends of filaments are always localized to the membrane , while the pointed end is directed to the transition zone, where microtubule- and actin-filaments meet (Dickson 2002). Blue: microtubule; orange: actin

Additionally the rearrangements of the actin cytoskeleton and microtubules are crucial for the initial establishment of polarity. The future axon is characterized by an enhanced growth cone dynamic (Bradke and Dotti 1999), whereas dendrites show very static growth cones. The local exposure of extracellular signals to one neurite leads to the activation of signaling pathways, which alter the activity of actin-binding proteins and therefore promote actin remodeling. Extracellular signals are propagated by the Rho family of GTPases (Rac1, Cdc42 and RhoA), which induce the activation of ROCK that regulates the activation state of LIMK, controlling ADF/Cofilin activity (Endo et al., 2003). In this one neurite the actin cytoskeleton is more permissive for microtubule protrusion from the core, which drives the center of the growth cone further on (Bradke and Dotti 1999). This suggests that actin filaments in dendritic growth cones form a barrier for the protrusion of microtubules and therefore the growth cone remains static. Studies have shown that Cofilin 1 is highly active in the axonal growth cones compared to non-growing dendritic growth cones (Garvalov et al., 2007). The severing activity of the ADF/Cofilin family generates more available barbed ends, which is important for the branching of filaments in lamellipodia and leads to an increase in motility (Krause et al., 2004). The loss of filopodia and lamellipodia from growth cones, by application of cytochalasin to disrupt actin filaments, decreases axon growth rates and leads to a complete loss of guidance (Bentley and Toroian-Raymond 1986).

An impact on the polarization process could also affect the branching and dendritic arborization of cortical pyramidal neurons resulting in a reduced neurite length or dendritic arborization (Li et al., 2000). The role of actin during dendritic development will be further discussed in the next chapter.

1.3.4.2. Actin is involved in dendritic arborization

During development the nervous system must progress from `disconnected` neurons to a network of neuronal circuits that is able to dynamically process information and generate an appropriate output. Proper dendritic arborization is a critical process for accurate development of neuronal circuits and for activity-dependent plasticity of mature neurons (Scott and Luo 2001). Dendrites are the site of 90% of all excitatory synaptic contacts and dendritic development determines the number and pattern of synapses (Hume and Purves 1981). Therefore dendritic abnormalities are the most common pathological correlation for mental retardation. Extension, retraction and branching of dendritic processes are complex functions that are regulated by an interaction between intrinsic developmental programs and local environmental cues, and additionally the level of neuronal activity. Dendritic growth is dependent on the stabilization of a subset of highly motile and protrusive dendritic structures. Real-time imaging has demonstrated that dendritic elaboration occurs through a net growth of highly dynamic filopodia that are actin-based structures (Dailey and Smith 1996). The Rho family of small GTPases (Rho, Rac and Cdc42) is known to be a regulator of signaling pathways to the actin cytoskeleton (Luo 2000). A blockade of Rac or Cdc42 reduces the number of primary dendrites, while an increase in RhoA activity causes a retraction of dendrites (Li et al., 2000). Actin binding proteins, like ADF/Cofilins are known regulators of actin depolymerization, which are controlled by RhoA. Additionally RhoA mediates the increase in dendritic growth caused by NMDA receptor activation (Nimchinsky et al., 2002). Therefore neuronal activity has a major effect on dendritic arborization, as shown by the fact that a decrease in activity results in reduced dendritic outgrowth (McAllister 2000). Repetitive depolarization activates ERK and CaMKII, which promote dendritic outgrowth by enhancing transcription of Wnt. Wnt in turn stimulates the Rac pathway that modulates the actin cytoskeleton (Rosso and Inestrosa 2013). Additionally neuronal activity also regulates the number of dendritic filopodia, which may be a substrate for new branches. Kossel et al (1997) showed that cultured hippocampal neurons form dendritic branches only in the presence of afferent innervations, showing that new dendritic branches are stabilized by synapses (Kossel et al., 1997). It was proposed that the formation of synaptic contacts may guide dendritic growth (Vaughn 1989). The loss of Cofilin 1 alters spine density and influences receptor motility to dendritic spines and could therefore contribute to alterations in dendritic arborization (Rust et al., 2010). A direct link between the ADF/Cofilin family and dendritic branching was made by Bläsius (2012), who showed that the ablation of Cofilin 1 leads to a reduced dendritic branching of cortical neurons in culture (Bläsius 2012).

1.4. Actin in synapses

Synapses are specialized morphological structures, which reside between two synaptic cells to enable the communication through the release of neurotransmitters from the presynaptic neuron, which bind to receptors on the postsynaptic cell. During development and throughout life, synapses are highly dynamic structures which are modulated by activity to alter the synaptic strength and morphological plasticity, which build the basis for learning and memory processes (Holtmaat and Svoboda 2009). In the human brain a number of 10^{16} neurons are estimated, which exhibit a pattern of synaptic connectivity (Munno and Syed 2003). Actin is the most abundant cytoskeletal protein in presynaptic terminals as well as in postsynaptic dendritic spines (Fifkova and Delay 1982). The contribution of actin to the establishment of a functional synapse, as well as its important role in the assembly and functionality of the pre- and postsynaptic site will be discussed in the next chapters.

1.4.1. The role of actin in postsynaptic dendritic spines

At the postsynaptic site actin is the only cytoskeletal protein in dendritic spines, which are specified protrusions on dendrites that receive more than 90% of excitatory synaptic input (Nimchinsky et al., 2002). The human brain contains more than 10^{13} dendritic spines. They undergo constant changes in shape, which are the basis of learning and memory processes (Segal 2005). Early in development also larger movements in the order of microns over minutes and hours are possible in hippocampal neurons (Engert and Bonhoeffer 1999). After maturation of spines the motility decreases again. Additionally spines can be classified into three morphological types: thin, stubby and mushroom. Whereas the thin spines are found during early developmental steps, the number of mushroom-shaped spines increases upon maturation or learning processes (Nimchinsky et al., 2001). Thereby the mushroom-shaped spines are known to be the strongest spines, based on the increased accumulation of the postsynaptic density (PSD), which is responsible for the organization of glutamatergic neurotransmitter receptors. PSD-95 is known to regulate the mobility of actin during synaptic plasticity (Zheng et al., 2010) and actin is known to anchor glutamatergic receptors in the membrane. AMPA receptors are linked to actin via several PDZ domain containing proteins including Grip, Pick1, SAP97 and Stargazin (Xia et al., 1999). In addition actin is also involved in the lateral diffusion of receptors to the postsynaptic membrane. The number of receptors on the surface at the PSD can be modulated upon LTP, due to an increased lateral diffusion of receptors to the membrane (Morales et al., 2000; Sankaranarayanan et al., 2003). In general the actin depolymerization leads to an increased diffusion of a subset of glycine receptors, whereas excitatory AMPA and NMDA receptors are differentially sensitive

to actin depolymerization (Allison et al., 1998; Kirsch and Betz 1995). This indicates that actin contributes to the differential organization of distinct pools of postsynaptic receptors to obtain a postsynaptic specialization. Studies with GFP-tagged actin revealed two distinct actin pools in dendritic spines (Honkura et al., 2008). On the one hand stable longitudinal filaments that are present along the core of spines are involved in the exo - endocytic trafficking of receptors and regulate synaptic receptor abundance and synaptic strength, as well as the overall stability of the spine. On the other hand the dynamic sub-plasmalemmal actin network at the postsynaptic scaffold is responsible for the anchoring and organization of receptor pools and thereby for the morphological remodeling of the spine head. Differences in the turnover rates and structures of these filaments are important for different postsynaptic mechanisms. For example the stabilization of F-actin by jasplakinolide results in a reduced endocytosis of AMPA receptors, while actin depolymerization via latrunculin accelerates AMPA receptor internalization into the PSD (Zhou et al., 2001).

Learning and memory processes lead to morphological changes in dendritic spines by strengthening or weakening a synapse in an activity-dependent manner. Upon a high frequency stimulation of a synapse a persistent increase in synaptic strength, which is known as long term potentiation (LTP), is induced. These LTP is associated with a reorganization of the spine actin cytoskeleton and induces a shift in the G- to F-actin ratio towards F-actin, which leads to an increase in spine volume (Fukazawa et al., 2003). However actin-depolymerizing agents block the induction of LTP (Kim and Lisman 1999; Krucker et al., 2000). Actin polymerization is thereby necessary to enable the stable expansion of the spine head to increase the number of receptors in a stable scaffold. On the other hand the weakening of synapses upon synaptic depression induces a shrinkage of the spine accompanied with a shift to an increased G-actin level. ADF/ Cofilin is specifically required for spine shrinkage, but is not necessary for LTD (Zhou et al., 2004). Synaptic activity regulates the actin cytoskeleton through multiple signaling pathways, which will be further explained in the next chapter.

The deregulation of the ADF/Cofilin family pathway in LIMK1-deficient animals has been linked to Williams Syndrome and autism spectrum disorders through alterations in dendritic spine morphology (Frangiskakis et al., 1996; Meng et al., 2002). Rust et al showed an increased density and enlargement of dendritic spines upon the deletion of Cofilin 1 with a CaMKII-Cre, together with impairments in associative learning and AMPA receptor mobility (Rust et al., 2010).

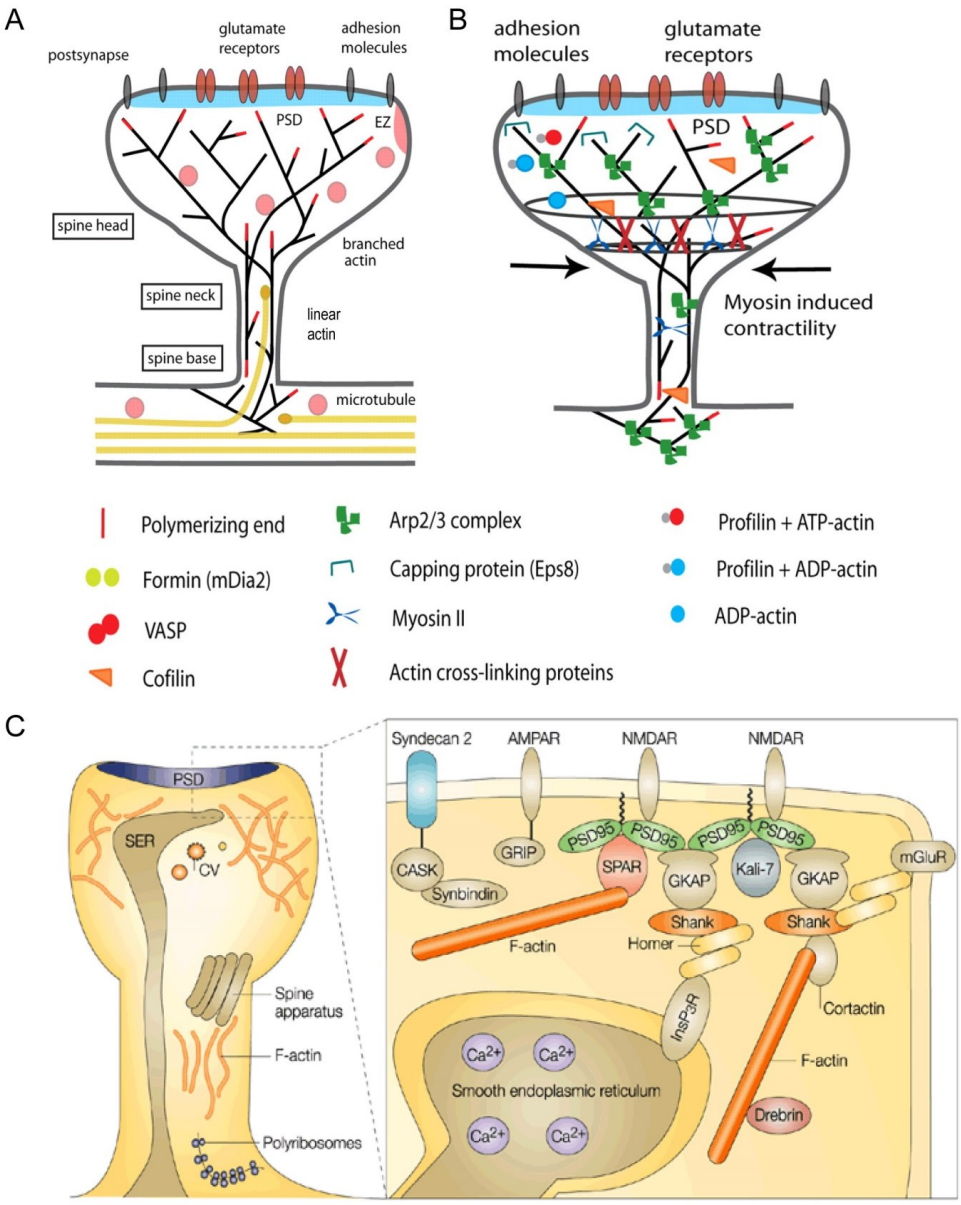

Fig. 11: Overview of the structure and arrangement of actin filaments in dendritic spines. A Actin is the major cytoskeletal protein in dendritic spines. Two different pools of actin filaments are localized in postsynaptic spines, which fulfill different functions and are selectively blocked by drugs which impact on actin. Linear actin filaments in the spine neck are responsible for the endo - exotrafficking of neurotransmitter receptors, while the branched network in the spine head is necessary for the anchoring of receptors. **B** Many different actin binding proteins are localized to the spine to guarantee a remodeling of actin filaments according to synaptic activity. Members of the ADF/Cofilin family are localized to the base of spines as well as in the spine head to fulfill a permanent rearrangement of the actin network (Hotulainen and Hoogenraad; 2010). **C** A closer look to the spine head showing the interaction between actin and PSD95 for the anchoring of different neurotransmitter receptors via different anchoring proteins, like SPAR and Grip (Hering and Sheng 2001).
PSD: postsynaptic density, EZ: endocytic zone, SER: smooth endoplasmatic reticulum

1.4.2. Actin signaling in dendritic spines

Actin is highly enriched in dendritic spines and regulates morphological changes (Dailey and Smith 1996). These changes are important for synaptic plasticity, which is the cellular basis

of learning and memory. A persistence or repetition of neuronal activity tends to induce cellular changes that increase synapse stability and result in an enhanced signal transmission between neurons, a process known as long term potentiation (LTP). Synaptic activity induces multiple signaling pathways which impact on the actin cytoskeleton in postsynaptic spines (Cingolani and Goda 2008). Key regulators of the actin polymerization are Rho GTPases and serine/threonine kinases, which target different actin-binding proteins (Spiering and Hodgson 2011). In dendritic spines the opening of Ca^{2+}-permeable NMDA receptors results in an elevated intracellular Ca^{2+} concentration. This increase in Ca^{2+} activates the Ca^{2+} and calmodulin-dependent protein kinase II (CaMKII) and leads to its translocation to the postsynaptic density (figure 12) (Cingolani and Goda 2008). In turn CaMKII activates multiple downstream signaling targets. One of them is the calmodulin-dependent kinase kinase CaMKK, which activates the guanine-nucleotide exchange factor (GEF) ßPIX, by accelerating its GEF activity. This leads to the activation of the small GTPase Rac1 and p21-activated kinase 1 (PAK1). The phosphorylation and thereby activation of Pak1 mediates the activation of the Lim kinase (LIMK). The ADF/Cofilin family is the main target of the LIMK and its members are inactivated upon phosphorylation by LIMK (Sarmiere and Bamburg 2004). The activation of LIMK can also be promoted by the small GTPase RhoA, which interacts with NMDA receptors. The actin filament stabilization accelerates the transport and incorporation of AMPA receptors into the postsynaptic membrane (Fischer et al., 2000; Matus 2000). Additionally the activation of CaMKII and PKC results in phosphorylation of existing AMPA receptors to increase their activity. By increasing the efficiency and number of AMPA receptors at the synapse, future excitatory stimuli will generate a larger postsynaptic response. During the late phase of LTP gene transcription activation leads to an increased protein synthesis in the postsynaptic cell, which regulates the traffick and reorganization of synaptic scaffolding proteins (Davis and Squire 1984; Nguyen et al., 1994). This results in an increase in dendritic spine number and surface area. The maintenance of LTP is selectively blocked when actin dynamics are disrupted, but normal synaptic transmission is unaffected (Kim and Lisman 1999; Krucker et al., 2000). Dynamic actin filaments play also an essential role in the growth of new synaptic connections or the conversion of silent synapses to active ones (Yao et al., 2006). The activation of CaMKII leads to the synthesis of yet unknown retrograde messenger that travels across the synaptic cleft to the presynaptic terminal (Regehr et al., 2009). There it facilitates the presynaptic response, by increasing synaptic vesicle release and vesicle number, all functions which are known to be accompanied by actin dynamics.

A different effect on the ADF/Cofilin family is induced upon the induction of LTD. Strong synaptic stimulation or persistent weak stimulation induce the activity-dependent reduction in the efficiency of synapses (Mulkey and Malenka 1992). In this case the phosphatase

calcineurin is activated, which dephosphorylates the ADF/Cofilin family members leading to their activation to destabilize actin filaments in the spine head, accompanied with shrinkage of the spine upon synaptic depression (Mulkey et al., 1994). Additionally the internalization of AMPA receptors is elevated upon actin destabilization resulting in reduced receptor efficiency. Stabilization of actin filaments via Jasplaklonide prevents the spine collapse (Halpain et al., 1998). These results indicate that actin depolymerization is necessary to induce LTD. Therefore actin-binding proteins have moved into the focus as regulators for postsynaptic plasticity, as well as learning and memory processes. Changes in actin dynamics in dendritic spines contribute to various neurological disorders, like dementia and schizophrenia, which are caused by alterations in the activity of actin binding proteins (Bardoni and Mandel 2002).

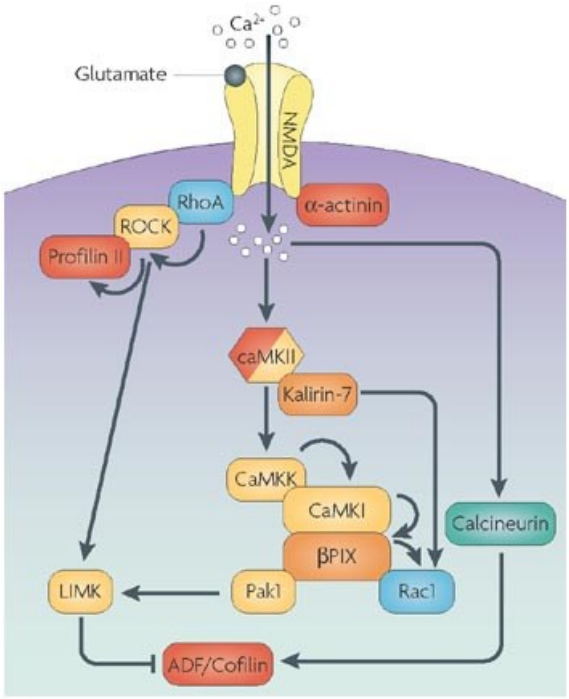

Fig. 12: Signaling pathways in dendritic spines which get activated during LTP or LTD impact on the actin cytoskeleton. The activation of the NMDA receptor leads to the activation of the RhoA GTPAse, which in turn activates the kinase ROCK. One target of ROCK is the LIMK which upon activation phosphorylates the ADF/Cofilin family, leading to inactivation of these proteins and stabilization of the actin network in spines. Additionally, LIMK can be activated upon the CaMKII, which gets activated upon the elevated Ca^{2+} level in the cell. A spine shrinkage or synaptic depression needs a destabilization of the actin network. In this case the phosphatase calcineurin is activated upon low frequency stimuli and dephosphorylates ADF/Cofilin family members. Upon this activation of ADF/Cofilins, actin filaments are depolymerized and the spine shrinks (Cingolani and Goda 2008)

1.4.3. Actin in presynaptic terminals

Presynaptic terminals are subcellular axonal compartments dedicated to release synaptic vesicles filled with neurotransmitters. A release of synaptic vesicles at the active zone is supported by the synaptic vesicle cycle with the major steps of docking, priming, fusion and recycling via endocytosis. Thereby synaptic vesicles are organized into three functionally distinct pools: the readily releasable pool, the recycling pool and the reserve pool (figure 13) (Rizzoli and Betz 2005). The readily releasable pool represents primed vesicles, which are docked to the active zone. In contrast the reserve pool consists of vesicles which are located in the core region of the presynaptic bouton. Actin is highly enriched in presynaptic terminals,

with up to 2% of the total synaptosomal protein content (Wilhelm et al., 2014). It functions in the maintenance and regulation of vesicle pools, by serving as a scaffold to restrict vesicle mobility and on the other hand by providing a track to direct the transfer of vesicles between the pools. Vesicles are linked to the actin cytoskeleton via short filaments of synapsin at the core of the presynaptic bouton (Hirokawa et al., 1989), where the reserve pool is surrounded by actin filaments. Upon increased neuronal activity phosphorylation of synapsin releases the reserve vesicles from actin leading to an increased vesicle exocytosis (Greengard et al., 1993). Additionally long actin filaments exists that extent from the bouton to the active zone and actin is a major constituent of the active zone where it fulfills a dual function (Landis et al., 1988). During the synaptic vesicle cycle vesicles are transported along actin filaments from the reserve pool to the active zone. Actin might guide the arriving vesicles to facilitate their docking and thereby regulate the size of the readily releasable pool. Secondly, actin could form a physical barrier restricting the priming reaction and therefore serves as a brake to prevent vesicle fusion with the active zone. The role of actin might depend on the synapse type, with large, high release probability boutons being more dependent on actin for recruiting vesicles, while small, low release probability boutons need actin to function as a physical barrier (Morales et al., 2000; Sakaba and Neher 2003). This means that different types of boutons rely on actin to a different extent and are more sensitive to alterations in the actin cytoskeleton upon the loss of actin-binding proteins. In addition actin guides the fine-positioning of synaptic vesicles, due to the fact that a stabilization of actin by jasplakinolide abolishes the distribution of recycled vesicles towards the active zone (Marra et al., 2012). The increase in membrane area upon exocytosis must be counterbalanced by endocytosis to keep the presynaptic architecture intact. Additionally endocytosis retrieves vesicle proteins form the release site and allows the generation of new vesicles. Actin is thereby implicated in the clathrin-mediated endocytosis, due to the fact that actin polymerization provides additional force to complete membrane bending. Under high frequency stimulation (40Hz) membrane retrieval was slowed down by latrunculin A, which blocks actin polymerization (Kononenko et al., 2014). A role for the ADF/Cofilin family in the regulation of actin in presynaptic terminals was implicated in ADF$^{-/-}$ Cofilin 1$^{fl/fl}$ CaMKII-Cre animals. The loss of ADF and Cofilin 1 impaired synaptic actin dynamics and affected the distribution, recruitment and exocytosis of synaptic vesicles by enhanced synaptosomal F-actin levels (Wolf et al., 2015). Zimmermann et al also found an increased glutamate release in the striatum of double knockout animals (Zimmermann et al., 2015).

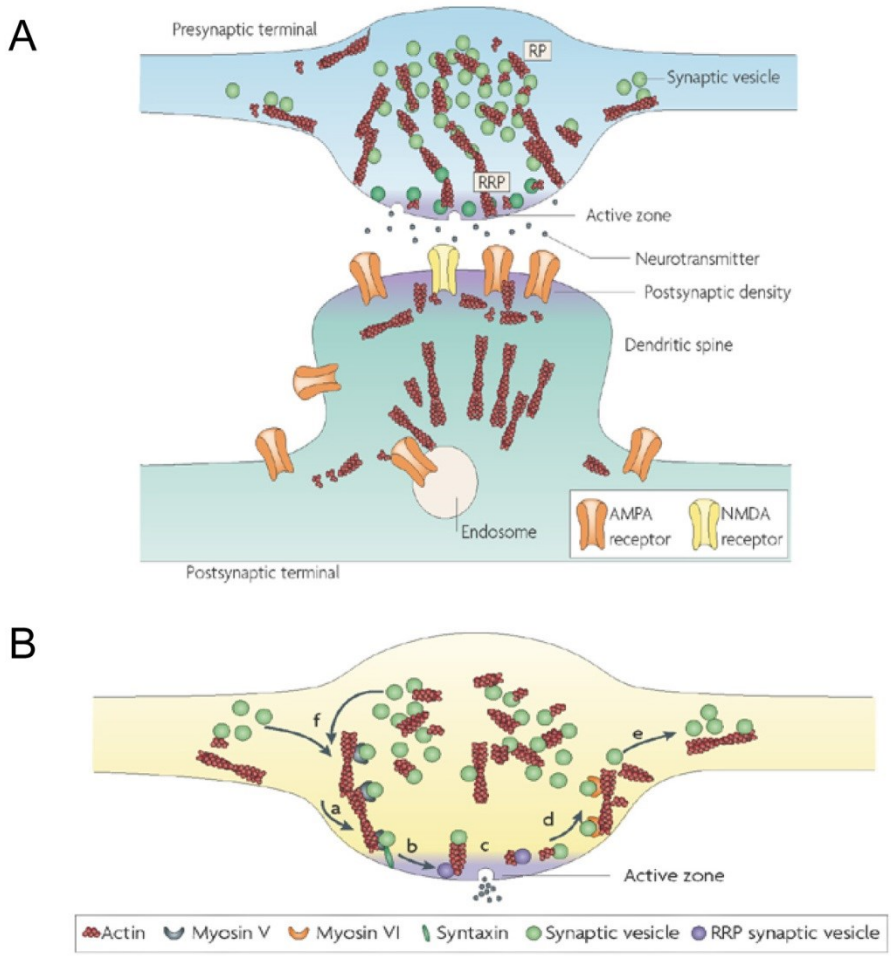

Fig. 13: Overview of the organization of actin at the presynaptic terminal and the role of actin in the synaptic vesicle cycle. A Two pools of actin can be found in the presynaptic terminal: first shorter actin filaments which surround the reserve pool (RP) in the core region of the bouton and interlink different vesicle clusters and second longer filaments which connect the reserve pool with the active zone. At the active zone actin is also a major component and has a dual function on the readily releasable pool (RRP). Actin functions either as track to mobilize vesicles from the reserve pool to the active zone, or as a physical barrier reducing the transport of vesicles. **B** Vesicles are transported along actin filaments to the active zone were upon an elevation of intracellular Ca^{2+} myosin V binds to syntaxin to facilitate the docking and replenishment of the readily releasable vesicle pool (RRP). Upon priming vesicles enter the RRP and can fuse with the active zone to release their neurotransmitter content. Actin regulates the priming and fusion process and thereby affects neurotransmitter release. To maintain the presynaptic terminal size vesicle recycling via endocytosis must occur. Myosin VI transports recycled vesicles along actin filaments back to the center of the bouton (Cingolani and Goda 2008).

1.4.4. Actin in synaptogenesis

The establishment of a functional neuronal network starts with the outgrowth of neurites and the polarization into functional units of dendrites and axons. The fast outgrowth of an axon upon the depolymerization of actin networks for the protrusion of microtubule is the first step in synaptogenesis (Dent et al., 2011). To find the presynaptic binding partner the axon has to migrate upon guiding cues and establish a contact with a dendrite to start the interaction

which leads to the generation of a synapse. All of these processes are based on the remodeling of the actin cytoskeleton (Benson et al., 2001).

Synaptogenesis in the mouse starts postnatally around day P6 and reaches a peak at P15 (Li et al., 2010). Between P15 and P21 a decline in the number of synapses is detected, which marks the formation from immature to mature synapses. Only synapses with a continuous signal propagation are persistent and synapses with minor synaptic activity are depleted during synaptogenesis (Chechik et al., 1999). During adulthood a constant rearrangement of synapses occurs, which leads to the strengthening of synapses and also an increase in the number of synapses during learning processes is observed. To establish contacts with synaptic partners' axonal and dendritic neurites are guided by a specialized structure called growth cone (Mueller 1999; Tessier-Lavigne and Goodman 1996). Thereby actin polymerization produces the protrusive force required for extension of the growth cone (Dent et al., 2011). In the growth cone membrane, receptors are anchored for the recognition of guidance cues during migrational processes, which influence the rearrangement of the actin cytoskeleton over different signaling pathways. Thereby migrating neurons are directed via cadherins and integrins to specific regions or layers of tissue, rather than to specific cells (Graus-Porta et al., 2001). In the specific regions neurons are then guided by diffusible chemotrophic factors, which can be either attractive or repulsive. At the target site, the growth cone slows down and makes a physical contact, during which the ending transforms itself into a presynaptic terminal. From the presynaptic ending diffuse signaling molecules and together with the interaction of cell adhesion molecules on the pre- and postsynaptic site induce a clustering of postsynaptic receptors. Thereby the postsynaptic neuron is not passive and dendritic filopodia rearrange around the synaptic partner. These rearrangements of dendritic filopodia depend on a highly dynamic actin cytoskeleton, which gets remodeled (Cingolani and Goda 2008). Studies in C. elegans have linked extracellular signaling and adhesion events with F-actin organization (Stavoe and Colon-Ramos 2012). Netrin signals through immunoglobulin receptor UNC40/DCC induces local clustering of F-actin and synaptic vesicles. Additionally cadherin-mediated adhesion leads to the presynaptic actin polymerization and synaptic vesicle trapping through Rac GEFßPix and plays also a role in synapse maturation (Sun and Bamji 2011). During the process of identifying and attracting their respective synaptic partner, both the pre- and postsynaptic neuron plays an active role and components of the synaptic machinery appear to be `ready-made´ prior to the assembled contact site. This means that the presynaptic growth cone is able to secret transmitter, while the postsynaptic site possesses functional receptors in the membrane. Thereby both the postsynaptic anchoring of receptors, as well as the presynaptic transport and priming of synaptic vesicles depend on actin rearrangements. The clustering of vesicles at contact sites can be diminished upon the treatment with latrunculin, which indicates that

actin polymerization is required downstream from neuronal adhesion for the clustering of vesicles (Lucido et al., 2009).

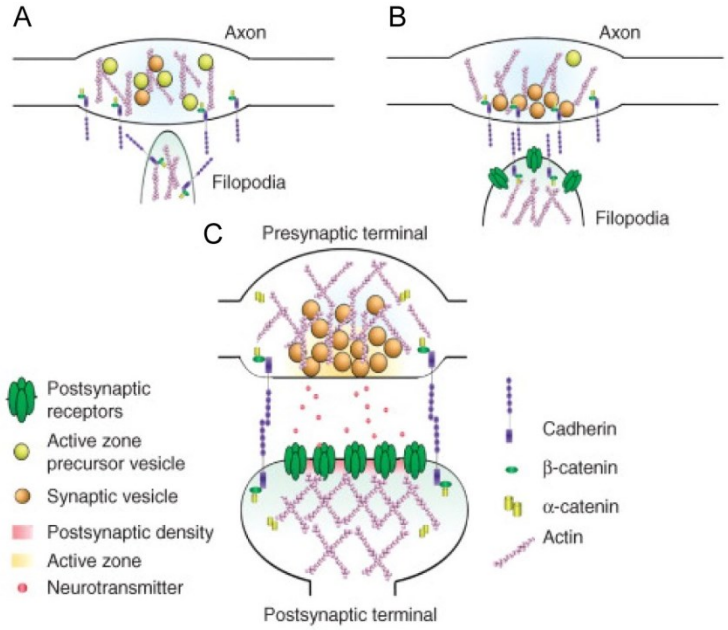

Fig.14: The role of the actin cytoskeleton during synaptogenesis. A The pre- and postsynaptic neurons play an active role in identifying and attracting their potential synaptic partner. Components of the synaptic machinery are ´ready-made´ prior to the establishment of the contact site and are involved in synapse formation. Thereby the adhesion between the pre- and postsynaptic site is accompanied by cadherins, which trigger presynaptic actin polymerization and synaptic vesicle trapping. **B** Actin is involved in the anchoring of receptors at the postsynaptic site and the clustering of vesicles at the presynaptic site. **C** The mainentance of a synapse needs constant synaptic activity, which leads to the strengthening and maturation of the synapse with an elevation in the number of postsynaptic receptors and an enlargement of the dendritic spine. Note that receptors are anchored via PSD-95 and actin. During development and throughout lifetime, synapses are continuously reconfigured both structurally and functionally. (Arikkath and Reichardt 2008)

Pre-assembled components of the synaptic machinery may serve as a beacon for attracting synaptic partners or to assist in target cell selection. Additionally, transmitter-receptor interactions regulate the timing of synapse formation and are important for neuronal viability, survival and final patterns of connectivity. A block of transmitter release leads to a normal establishment of synaptic connectivity, but electrical properties, like the expression of voltage-gated potassium- and sodium-channels, excitability and action potential parameters are perturbed. Responsible for the contact between the pre- and postsynaptic site and the activation of signaling pathways is the neurexin-neuroligin interaction (Craig and Kang 2007). Neurexins are presynaptic transmembrane proteins, their extracellular domains bind to postsynaptic neuroligins. Thereby neuroligin on the postsynaptic site bind to a PSD-95 (postsynaptic density protein 95) to form a complex that attracts postsynaptic proteins to build a postsynaptic terminal. Thereby PSD-95 and actin form a framework for the transport and anchoring of transmitter receptors at the postsynaptic site (El-Husseini et al., 2000; O'Brien et al., 1998). On the presynaptic site the cytoplasmic tail of neurexin is associated

with CASK (Calcium/Calmodulin-Dependent Serine Protein kinase), which is involved in multiple downstream signaling cascades. Thereby CASK builds a complex with Mint1 and Velis, while Mint1 binds to the vesicle trafficking protein Munc 18-1 (Butz et al., 1998). Munc 18-1 binds to syntaxin, which is associated with the actin cytoskeleton for synaptic vesicle exocytosis (de Wit et al., 2006). Treatment of neurons with actin polymerization inhibitors results in the dispersal of synaptic vesicles and presynaptic components, which links actin as a major scaffolding protein for the organization of the presynaptic compartment (Morales et al., 2000). CASK also binds to protein 4.1, which is directly connected to actin and to calmodulin for the entry of Ca^{2+} into the cell. The activity of CASK is required immediately following establishment of the contact to enable the assembly of vesicle release capability at the contact site. Perturbation of the Ca^{2+} signal during early synapse formation blocks synaptogenesis (Saneyoshi et al., 2008). Additionally actin is implicated in the transport mechanism that supports synaptic arborization by providing a track for a local transport in association with motor proteins (Nelson et al., 2013). Thereby immature and mature synapse depend differently on actin and react therefore differently to the application of drugs (Dillon and Goda 2005; Yao et al., 2006). Immature synapses are disassembled by actin-depolymerization drugs like latrunculin, while mature synapses are resistant. In the early synapse actin serves as a temporary scaffold for maintaining synaptic structural integrity and recruits and stabilizes adhesion molecules and synaptic components.

1.5. Conditional knockout mouse lines for the ADF/Cofilin family

Actin is the most abundant cytoskeletal protein in synapses and fulfills important functions in presynaptic terminals, as well as postsynaptic dendritic spines. To fulfill synaptic functions, the actin cytoskeleton needs to be highly dynamic and implicates a role of actin depolymerization factors for ongoing remodeling processes. Actin dynamics crucially depend on LIM kinases, which phosphorylate and inactivate the ADF/Cofilin family (Sumi et al., 1999). An abnormal expression of the neuronal isoform LIMK1 is associated with Williams syndrome, a mental disorder with profound deficits in visuospatial cognition (Hoogenraad et al., 2004). The complete deletion of LIMK1 leads to abnormalities in spine morphology including enhanced hippocampal LTP and altered fear response and spatial learning (Meng et al., 2002). In LIMK knockout animals abnormal clusters of actin and Cofilin were observed. These results indicate that altered actin dynamics can play a role in the development of neurological symptoms.

Several different working groups were investigating the downstream target of LIMK1, which links this kinase to regulatory changes in the actin cytoskeleton. The focus was on the

ADF/Cofilin family which depolymerizes actin filaments and is essential for actin dynamics. All three members of this family are expressed in the brain, but show distinct brain-specific phenotypes. The expression of Cofilin 1 in the brain starts around E8.5 with the highest expression in the neural fold and persists in the developing nervous system (Gurniak et al., 2005). Also postnatally Cofilin 1 expression is maintained in the CNS and displays a ubiquitous expression pattern (Bellenchi et al., 2007). The complete deletion of Cofilin 1 is embryonic lethal around E9.5, due to a neural tube closure defect (Gurniak et al., 2005). To characterize the role of Cofilin 1 in the brain a conditional knockout mouse line was generated using Nestin-Cre mediated deletion. The loss of Cofilin 1 impairs radial migration, which results in the loss of cortical layers II – IV, which is accompanied by an increased cell cycle exit of neuronal progenitors in the ventricular zone (Bellenchi et al., 2007). To study the role of Cofilin 1 in synapses Rust et al analyzed a further conditional mouse line with a CaMKII-Cre-specific deletion of Cofilin 1 in the forebrain starting around postnatal day 18 (Rust et al., 2010). Inactivation of the actin depolymerization factor Cofilin 1 using CaMKII-Cre, leads to significant defects in learning and memory processes. Cofilin $1^{fl/fl}$ CaMKII-Cre mutant mice displayed impairments in associative learning, LTP and LTD, as well as an increased density and head volume of dendritic spines (Rust et al., 2010). Animals were tested for associative learning, aversive learning processes and short-term working memory. Results lead to the conclusion that synaptic plasticity is impaired in all circuits required for associative learning, but short term working memory is independent of Cofilin 1 activity. Further behavioral tasks on this mouse line were performed by Goodson et al, who detected a decreased anxiety in Cofilin 1 mutant mice (Goodson et al., 2012). The deletion of Cofilin 1 led to an increased synaptic F-actin content in the cortex and hippocampus, which indicates a reduced actin filament turnover in neurons of these animals. This could impact postsynaptic mechanisms which rely on actin, like LTP or LTD. Spine shrinkage for example requires active ADF/Cofilin (Zhou et al., 2004). Upon Cofilin 1 deletion in the forebrain, the phenotype is restricted to the postsynaptic site, since no alterations in presynaptic responses, like basal synaptic transmission or Paired-pulse facilitation could be observed. Hippocampal protein lysates showed an increased ADF expression in Cofilin 1 mutant mice; however the upregulation of a second ADF/Cofilin family member was not sufficient to compensate for the loss of Cofilin 1. In these studies the expression of Cofilin 2 was not examined.

Western Blot analyses of brain regions displayed a comparable expression pattern for Cofilin 1 and ADF in the adult brain (Bellenchi et al., 2007; Gorlich et al., 2011). The upregulation of ADF in the brain of Cofilin $1^{fl/fl}$ CaMKII-Cre animals indicates that Cofilin 1 and ADF could have overlapping functions (Rust et al., 2010). Also during embryonic brain development ADF and Cofilin 1 are coexpressed, however knockout mouse models showed distinct

phenotypes for both proteins. The complete deletion of ADF is viable and ADF$^{-/-}$ mice only show a mild hyperplasia of the cornea, while no alterations in brain morphology or behavior could be observed (Bellenchi et al., 2007; Ikeda et al., 2003). Bellenchi et al could not detect a compensatory upregulation of Cofilin 1 in ADF mutant brain lysates. Gorlich et al further analyzed the ADF$^{-/-}$ animals and detected expression of ADF in excitatory synapses, with enrichment in presynaptic terminals (Gorlich et al., 2011). Ablation of ADF had no effect on synapse structure or density and also presynaptic recruitment and exocytosis was not affected. The lack of synaptic defects could be explained by an elevated Cofilin 1 level in synaptosomes of ADF$^{-/-}$ mice, which could compensate for the loss of ADF. Interestingly, the F-actin levels in synaptosomes were further increased in ADF$^{-/-}$ Cofilin 1$^{fl/fl}$ CaMKII-Cre double knockout animals compared to the single Cofilin 1$^{fl/fl}$ CaMKII-Cre knockout, suggesting additive effects of ADF and Cofilin 1. Zimmermann et al further analyzed ADF$^{-/-}$ Cofilin 1$^{fl/fl}$ CaMKII-Cre double knockout animals and found that the dual deletion of ADF and Cofilin 1 resulted in a presynaptic phenotype with a reduced synaptic vesicle mobilization and a strongly increased glutamate release in the striatum (Zimmermann et al., 2015). These ADF$^{-/-}$ Cofilin 1$^{fl/fl}$ CamKII-Cre mutants display also a behavioral phenotype showing a hyperlocomotion, linking presynaptic actin dynamics to mouse behavior and showing that the dysfunction of presynaptic actin turnover has behavioral consequences. This indicates that changes in the regulation of neurotransmitter release could contribute to an altered behavior. Cofilin 1 was known to have a postsynaptic phenotype, while the knockout of ADF had no effect on synapses. Instead, the simultaneous deletion of ADF and Cofilin 1 leads to a presynaptic phenotype, showing that proteins of the ADF/cofilin family do have overlapping functions.

Little attention was given to Cofilin 2 since it was known as the muscle-specific isoform, but Gurniak et al and Vartiainen et al also found an expression of Cofilin 2 in brain (Gurniak et al., 2014; Vartiainen et al., 2002). The complete deletion of Cofilin 2 is lethal around postnatal day 7, due to a muscle-specific phenotype, which leads to a malformation of the diaphragm and consequently respiratory and circulation problems in these newborn animals (Gurniak et al., 2014). Analysis of neuromuscular junctions in Cofilin 2 knockout animals did not reveal anomalies, so the role of Cofilin 2 in neurons and the brain still needed to be unraveled. To answer the question if Cofilin 2 also has an important function in brain development, we analyzed Cofilin 2$^{fl/fl}$ Nestin-Cre animals. In this mouse model a Cre recombinase under the Nestin promotor was used, which is an intermediate filament protein expressed in dividing cells during the early stages of development in the central nervous system (CNS). In this line Cofilin 2 is deleted in neuronal and glial cell precursors of the forebrain (Tronche et al., 1999). Cre expression starts around E10.5 at the onset of neurulation and marks neuronal progenitor cells in the SVZ, which can also give rise to glia

cells. Thus, the Nestin-Cre recombinase would delete Cofilin 2 also in glia cells, which could lead to secondary side effects. To achieve the deletion of Cofilin 2 the exons 2 – 4 are flanked by loxP sites, which are target-sites for the enzyme Cre recombinase. This mouse line was used to study a brain-specific function of Cofilin 2 in neurodevelopmental processes, as well as synapse function.

Since Zimmermann et al showed that the dual deletion of ADF and Cofilin 1 has additive effects, indicating that proteins of the ADF/Cofilin family do have overlapping functions; a further mouse line was analyzed in this study to answer the question whether the dual deletion of ADF and Cofilin 2 in the brain would show a stronger phenotype then the single brain-specific deletion of Cofilin 2. This ADF$^{-/-}$ Cofilin 2$^{fl/fl}$ Nestin-Cre mouse line was studied to see whether Cofilin 1 as the only remaining depolymerization factor would be able to maintain neurodevelopmental processes and synaptic function. Since Cofilin 1 displays the strongest brain phenotype it is interesting to analyze if the loss of Cofilin 2 and ADF leads to malformations in brain and synapse formation, which could give insight into specific roles of single ADF/Cofilin family members and overlapping functions of all three depolymerization factors.

1.6. Aim of this thesis

In previous studies it was shown that actin depolymerization factors play crucial roles in different neurodevelopmental processes. Several neurodegenerative diseases are linked to alterations in the organization and dynamics of the actin cytoskeleton, like Williams syndrome and lissencephaly.

The family of actin depolymerization factors in the mouse includes ADF, Cofilin 1 and Cofilin 2. On DNA level all isoforms share a high degree of homology, leading to the hypothesis that the loss of one ADF/Cofilin family member can be compensated by an upregulation of a second family member. This observation was made in several mouse lines studying the function of ADF/Cofilins in the brain. On the other hand, all three isoforms display biochemically slightly different activities, suggesting differences in their physiological functions.

Most studies were performed on Cofilin 1, since it shows the highest expression of ADF/Cofilin family members in the brain and therefore displays the strongest brain-phenotype. Overlapping functions for ADF and Cofilin 1 were suggested, since additive effects of ADF were found in ADF$^{-/-}$ Cofilin 1$^{fl/fl}$ CaMKII-Cre double knockout animals. Further, the study of double knockout animals also revealed synapse compartment specific functions for ADF and Cofilin 1. The study of double knockout animals was necessary since compensatory effects of ADF/Cofilin family members were observed.

Originally Cofilin 2 was known to be the muscle-specific isoform of the ADF/Cofilin family, until Cofilin 2 was shown to be also expressed in the brain. The first focus of this thesis was to establish an expression profile of Cofilin 2 in the brain. Biochemical analyses were performed on different brain areas throughout different developmental time points. The expression profile was completed by immunofluorescence studies analyzing the localization of Cofilin 2 in distinct neuronal subtypes.

The next aim of this study was to gain insight into the neuronal function of Cofilin 2, using a conditional mouse line with a brain-specific deletion of Cofilin 2. Histology, morphological analyses, as well as electrophysiology and behavioral studies were performed on these mutants. Double knockout animals for ADF and Cofilin 2 were generated to examine a possible additive effect of ADF reflected in a stronger phenotype.

The analysis of these mutants would reveal whether Cofilin 2 would have a specific and unique function that cannot be compensated by Cofilin 1 or ADF in the brain, or if the ADF/Cofilin family members fulfill similar roles in the brain.

2. Material

2.1. Mouse lines

Name	Description	Reference
Cofilin $2^{-/-}$	Transgenic mouse line which shows a complete deletion of Cofilin 2	Christine Gurniak
Cofilin 2 flox	Transgenic mouse line to obtain a conditional deletion of Cofilin 2 in the brain	Christine Gurniak
ADF	Transgenic mouse line with a lacZ Knock-In into the ADF gene loci	Christine Gurniak
Nestin-Cre	Transgenic mouse line with the Cre recombinase under the Nestin-Promotor	Francois Tronche

The Cofilin 2 locus spans 4.063kbp on chromosome 12 and comprises 4 exons, which generate different sized mRNAs. Cofilin 2 belongs to the ADF/Cofilin family, which consists out of three members. All members have the function to depolymerize and sever older actin filaments. Thereby all members show a tissue specific expression, with Cofilin 2 being the muscle-specific isoform. To analyze the role of Cofilin 2 in the muscle development a complete deletion of Cofilin 2 was generated. Thereby a targeting construct was generated with two lox-P sites flanking the exons 2 – 4 and a Neomycin cassette behind exon 4 for the selection process in ES cells. The targeting construct was introduced into ES cells via homologous recombination and heterozygous animals with one wildtype and one targeted allele were generated. To obtain a homozygous deletion, heterozygous animals were crossed. The obtained Cofilin 2 deficient animals were smaller than their littermates and died around postnatal day P7 – P10, due to a misalignment of the diaphragm. In these animals an autosomal dominant form of nemaline myopathy could be observed. Western Blot analysis revealed that Cofilin 2 is also expressed in the CNS, but studies on neuromuscular junctions indicated that the pathology in knockout animals was restricted to skeletal muscles. So the question why Cofilin 2 is also expressed in the brain and what specific function apart from Cofilin 1 and ADF it could have there remained still open. Therefore a brain-specific deletion of Cofilin 2 was introduced by crossing animals with floxed Cofilin 2 alleles with Nestin-Cre mice. The Nestin-Cre mice express the enzyme Cre-recombinase under the Nestin-promotor which leads to the specific deletion of Cofilin 2 in neuronal and glial cell precursors of the forebrain. The expression starts around embryonic day 10.5 at the onset of neurulation. Knockout animals were viable but also displayed a growth retardation compared to their littermates. This obtained Cofilin 2 Nestin-Cre mouse line was used to analyze the specific function of Cofilin 2 in the brain. Due to the fact that all three family members are expressed in the brain, we wanted to know whether a double knockout of ADF and Cofilin 2 results in a

more severe phenotype. Further it was also observed that upon deletion of one member of the family, a second one gets upregulated to compensate the loss. To analyze whether the mild phenotype upon the deletion of Cofilin 2 is due to an upregulation of ADF or Cofilin 1, double knockout animals were obtained for Cofilin 2 and ADF. In a double knockout of $ADF^{-/-}$ and Cofilin $1^{fl/fl}$ CaMKII-Cre a presynaptic phenotype was observed, although the single deletion of either ADF or Cofilin 1 did not lead to alterations in presynaptic mechanisms, showing that a deletion of two members of the same family leads to a different and intensified phenotype. We wanted to address the question whether Cofilin 1 as only ADF/Cofilin family member is sufficient enough to depolymerize and sever the actin network and compensate the loss of Cofilin 2 and ADF to maintain brain physiology. Therefore $ADF^{-/-}$ Cofilin $2^{fl/fl}$ animals were crossed with Nestin-Cre animals to obtain a complete deletion of ADF in combination with a brain-specific deletion of Cofilin 2 (ADF Cofilin 2 Nes-Cre mouse line).

2.2. General stock solutions, buffers and media

2.2.1. General solutions

Solution	**Composition**
PBS^- (no Ca^{2+}, no Mg^{2+}) (1x)	9.6g Dubelcco's PBS → add Milli-Q to 1 liter → autoclave
PBS^- (no Ca^{2+}, no Mg^{2+}) (10x)	96g Dubelcco's PBS → add Milli-Q to 1 liter → autoclave
4% paraformaldehyde (PFA) (pH 7.2, 200ml)	8g PFA In 180ml MilliQ → add 1 M NaOH dropwise until solution clears → stir at 60°C → cool down, add 20ml 10xPBS → sterile filter and store aliquots at –20°C

2.2.2. Solutions for the analysis of nucleic acids

Solution	Composition
TENT buffer (stock) 20mM Tris, pH 8.3	0.1mM EDTA 1% Tween® 20 0.2% Triton®X-100 → autoclave
Proteinase K solution (stock)	10µg/µl Proteinase K in Milli-Q → store at -20°C
Genomic DNA extraction buffer	10ml TENT buffer (stock) 160µl Proteinase K solution →200µl aliquots →store at -20°C
TE buffer	100mM Tris-HCl, pH 8.0 1mM EDTA → autoclave
TAE (50x)	242g Tris base 57.1ml acidic acid 100ml 0.5M EDTA, pH 8.0 → add Milli-Q to 1 liter
DNA loading buffer (100ml)	40% (w/v) Saccharose 0.5% (w/v) SDS 0.25% (w/v) Bromphenol blue → add TE buffer to 100ml
DNA ladder PhiX 174 (HaeIII) 100µl marker	100µl Fermentas loading buffer (1:6) 400µl Milli-Q → store aliquots at 4°C

2.2.3. Solutions and media for the tissue culture

Solution	Composition
N2 media	400ml destilled water 50ml 10x MEM 20ml 5,5% NaHCO3 15ml 20% glucose 5ml Neuropan2 5ml sodium pyruvate Adjust pH to 7.3 with NaOH Fill up to 500ml and filter sterilize
Borate Buffer	1.24g Boric Acid 1.9g Borax Adjust pH to 8.5 and fill up to 500ml Store at 4°C
DNase	1:10 dilution of DNase in HCl to a final concentration of 1mg/ml →Make 500µl aliquots and store them at -20°C →Add 500µl aliquot to 100ml HBSS
MEM-FCS	300ml distilled water 50ml 10x MEM 50ml FCS (heat inactivated) 20ml 5.5% NaHCO3 15ml 20% glucose 5ml Glutamine 10ml 50x MEM essential amino acids 10ml 100x MEM non-essential amino acids →adjust pH to 7.3 with 1M NaOH and fill up to 500ml with distilled water →Filter sterilize

HBSS/HEPES	500ml HBSS + 3.5ml 1M HEPES (pH 7.25) →store at 4°C
Trypsin/HEPES	100ml 0.05% Trypsin + 700µl 1M HEPES →Make 5ml aliquots and store at -20°C
1M HEPES stock solution	20ml distilled water 5.96g HEPES → adjust pH to 7.25 and fill up to 25ml → store at 4°C

2.2.3.1. Solutions and media for cultivating and analyzing neuronal cultures

Solution	**Composition**
2% PFA + 2% sucrose	2% (w/v) PFA 2% (w/v) sucrose in PBS^- →store 10 ml aliquots at -20°C
Antibody solution	1x PBS^- 3% goat serum 1% (w/v) BSA
Permeabilizing solution	1x PBS^- 0,1% Triton X-100
Blocking solution	1x PBS^- 5% goat serum 1% BSA
Nuclear staining	1x PBS^- 1:1000 DAPI
20% Moviol + NPG	20 % (w/v) Moviol 2.5 mg/ml NPG →stir Moviol in MilliQ in the dark until completely dissolved

	→ add NPG
	→ stir
	→ store aliquots at -20°C
PBT	PBS pH 7.5 – 8.0
	0.05% Tween 20
PBT-Block	PBT
	2% BSA
	0.05% gelatine
	50mM glycine
	→ Filter sterilize and store at -20°C

2.2.4. Solutions for protein analysis

Solution	**Composition**
SDS running puffer (10x)	250mM Tris
	1.9M glycine
	1% (w/v) SDS
	in Milli-Q
SDS-PAGE separation gel	25ml 30% Acrylamide
(15%; for 7 gels)	9.4ml 2M Tris-HCl, pH 8.8
	0.5ml 10% SDS
	15ml Milli-Q
	240µl 10% APS
	45µl TEMED
SDS-PAGE stacking gel	4.8ml 30% Acrylamide
(4%; for 7 gels)	0.3ml 10% SDS
	17.4ml H_2O
	7.5ml 0.5M Tris-HCl, pH 6.8
	150µl 10% APS
	30µl TEMED
Coomassie Brilliant Blue staining solution	0.1% Coomassie Brilliant Blue

	50% Methanol
	10% acetic acid
	in Milli-Q
	→stir o.n.
	→filter
Rapid destain	30% Isopropanol
	6% Acetic acid
	in Milli-Q
SDS sample buffer (5x)	110mM Tris, pH6.8
	20% (v/v) Glycerol
	3.8% (w/v) SDS
	8% (v/v) ß-Mercaptoethanol
	Bromphenol blue ad libidum
	in Milli-Q
PEB	20mM Tris, pH 8.0
	100mM NaCl
	5mM EGTA
	2mM EDTA
	0.5% (v/v)Triton®X-100
	1 tablet Protease-Inhibitor in 10ml
	→store at 4°C
Towbin transfer buffer, semi dry (1x)	25mM Tris/HCl, pH8.5
	190mM Glycine
	20% (v/v) Methanol
NCP – azide , pH 8.0 (10x)	100mM Tris/HCl
	1.5M NaCl
	0.5% (v/v)Tween® 20
	→add Milli-Q to 1 liter
NCP + azide, pH 8.0 (10x)	100mM Tris/HCl
	1.5M NaCl

	0.5% (v/v) Tween® 20
	2g Sodium azide
	→add Milli-Q to 1 liter
Western blot blocking solution	5% (w/v) milk powder
	in 1x NCP + azide
Primary antibody solution	1:x diluted antibody
(Western blot)	in Western blot blocking solution
Secondary antibody solution	1:x diluted antibody
(Western blot)	in 1x NCP- azide
	5% Milk powder
Luminol stock solution	0.44g luminol in 10 ml DMSO
	→store at -20°C
p-hydroxy-coumarin stock	150mg in 1 ml DMSO
	→store at -20°C
ECL	Solution A:
	200ml 0.1M Tris-HCl, pH 8.6
	4ml luminol stock
	0.1ml p-hydroxy-coumarin stock
	→store solution in the dark at 4°C
	Solution B:
	200ml 0.1M Tris-HCl, pH 8.6
	0.2ml H_2O_2 (from 30-35% stock solution)
	→store solution in the dark at 4°C
IF permeabilizing solution	1x PBS^-
	0.1% (v/v)Triton®X-100
IF blocking solution	1x PBS^-
	5% (v/v) goat serum
	1% BSA
IF antibody solution	1:x diluted antibody

(primary and secondary antibody)	1x PBS^-
	1% BSA
PHEM (10x, pH 7.0)	600mM PIPES
	200mM HEPES
	100mM EGTA
	20mM $MgCl_2$
	→ store at 4°C
G/ F-actin separation buffer	1% (v/v) Triton®X-100
	in 1x PHEM

2.2.4.1. Solutions for the preparation of synaptosomes

solutions	**Composition**
Homogenizing buffer	0.32M sucrose
	1mM EDTA
	1mg/ml BSA
	5mM HEPES pH 7.4
	→ store at 4°C
Krebs Ringer buffer	140mM NaCl
	5mM KCl
	5mM glucose
	1mM EDTA
	10mM HEPES pH 7.4
	→store at 4°C
SDS loading buffer 5x	110mM Tris pH 6.8
	20% glycerol
	3.8% SDS
	8% ß-mercaptoethanol
	Bromphenol blue ad libitum
Solubilisation solution 2x	40mM Tris
	2% Triton X-100

	➔ adjust to pH 6.0
Washing buffer	20mM Tris
	1% Triton X-100
	➔ Adjust pH to 6.0
Separation buffer	20mM Tris
	1% Triton X-100
	➔ Adjust to pH 8.0

2.2.5. Solutions and kits for histology

solutions	**Composition**
TBS (10x)	1.47M NaCl
	0.4 M Tris/HCl pH 8.0
TBS-T	1x TBS
	0,2% TritonX100
Blocking solution	TBS-T
	2% NGS
	2% BSA
	1% DMSO
Primary antibody solution	Blocking solution
	1:x diluted antibody
Secondary antibody solution	Blocking solution
	1:1000 secondary antibody
Draq5 staining solution	TBS-T
	1:1000 Draq-5
DAPI staining solution	TBS-T
	1:1000 DAPI
Golgi Staining Kit	FD Neurotechnologies

2.2.6. Solutions for electrophysiology studies

solutions	Composition
High chloride internal solution for IPSCs	90mM CsCl
	20mM Cs-Gluconate
	8mM NaCl
	10mM HEPES
	2mM MgCl2
	1mM EGTA
	2mM QX-314
	Adjust pH to 7.2 with CsOH
Internal solution	150mM Cs-Gluconate
	10mM HEPES
	2mM MgCl2
	4mM Na-ATP
	0.2mM EGTA
	5mM QX-314
	8mM NaCl
	Adjust pH to 7.2 CsOH
aCSF	130mM NaCl
	2.8mM KCl
	1.1mM NaH2PO4
	11mM D-Glucose
	28.8mM NaHCO3
	1.4mM MgSO4*7 H2O
	2.5mM CaCl2
	Adjust pH to 7.3 with HCl

Sucrose aCSF	75mM Sucrose
	2mM KCl
	7mM MgCl2
	1.3mM NaH2PO4
	25mM D-Glucose
	26mM NaHCO3
	0.5mM CaCl2
	Adjust pH to 7.3 with HCl
Blocking solution to record mIPSCs	aCSF with 10µM NBQX
	0.2µM TTX
Blocking solution to record mEPSCs	aCSF with 0.2µM TTX
	100µM Picrotoxin
	250µM TCM

2.3. Nucleic acid

2.3.1. Oligonucleotides for PCR

Name	**Sequence (5´ to 3´)**	**Binding site**	**PCR**
589 cof2-INT-3´	GCAGCCGTGGCTAAGACG	1.Intron	Cofilin 2
587 cof2-3´UTR-5`	GCCTACTCCCCGCCTTAGTTT	3'UTR	Cofilin 2
588 cof2-INT2-5`	CATACTGCTCATTCATCCTTC	2.Intron	Cofilin 2
145 Lac-3´	GATTAAGTTGGGTAACGCC	lacZ gene	ADF
106 ADF-150-3´	GAAGAAGGCAAAGAGATCTT	Coding region of exon 2	ADF
403 ADF-INT2-5´	CTACCTAAAGGGCATCCTTTC	Intron sequence between exon 2 and 3	ADF
355 NesPr1	CGCTTCCGCTGGGTCACTGTCG	5`upstream sequence	Nestin
356 Cre3	TCGTTGCATCGACCGGTAATGCAGGC	Cre gene	Nestin

617 NesPr2	TGCAGGCCGCCTCCTCGATGG	exon 1	Nestin

2.4. Antibodies

2.4.1. Primary Antibodies

antibody	**host**	**dilution**	**marker**	**company**
KG60	Rb polyclonal	1:500	Cofilin 1	Witke lab
7D10	Ms monoclonal	1:5	ADF	Witke lab
FHU-I	Rb polyclonal	1:500	Cofilin 2	Witke lab
Calbindin	Ms monoclonal	IF 1:400	Subpopulation of inhibitory neurons	Sigma
Parvalbumin	Ms	IF 1:1000	Subpopulation of inhibitory neurons	SYSY
Tyrosine-hydroxylase	Gp	IF 1:500	Dopaminergic neurons	SYSY
Tryptophan-hydroxylase	Ms	IF 1.250	Serotonergic neurons	Sigma
Choline-acetyltransferase	Ms	IF 1:500	Cholinergic neurons	Abcam
vGLUT1	Gp	IF 1:500	Cortical terminals of glutamatergic neurons	Millipore
vGLUT2	Gp	IF 1:500	Glutamatergic neurons of the thalamus	SYSY
FHU-I	rabbit	IF 1:100	Cofilin 2	Monoclonal self-made
PSD95	Ms	IF 1:500 WB: 1:1000	Postsynaptic marker for excitatory neurons	Millipore
Gephyrin	Ms	IF 1:250	Postsynaptic marker for inhibitory neurons	SYSY
BetaIII Tubulin	Monoclonal Ms	IF 1:500	BetaIII-Tubulin	Promega
C4	Monoclonal Ms	WB: 1:5000	Actin	MPBiomedicals
GAPDH	Monoclonal Ms	WB: 1:10.000	GAPDH	Calbiochem

GFAP	Monoclonal Ms	IF: 1:500 WB: 1:1000	GFAP	Millipore
Syntaxin I	chicken	WB: 1.5000	Presynaptic marker	Abcam
Synaptophysin	rb	WB: 1:2000	Extrasynaptic proteins	Sigma

2.4.2. Secondary antibodies

Antigen	**Clone**	**Species**	**Labeling**	**Dilution**	**Source**
Mouse	Polyclonal	Goat	Horseradish peroxidase	WB 1:1000	Pierce
Rabbit	Polyclonal	Goat	Horseradish peroxidase	WB 1:1000	Pierce
chicken	Polyclonal	Goat	Horseradish peroxidase	WB 1:1000	Pierce
Mouse	Polyclonal	Goat	A594	IF 1:1000	Molecular probes Invitrogen
Mouse	Polyclonal	Goat	A488	IF 1:1000	Molecular Probes Invitrogen
Rabbit	Polyclonal	Goat	A594	IF 1:1000	Molecular Probes Invitrogen
Rabbit	Polyclonal	Goat	A488	IF 1:1000	Molecular Probes Invitrogen
Guinea pig	Polyclonal		A594	IF 1:1000	Molecular Probes Invitrogen

2.4.3. Staining reagents

Name	**Dilution**	**Supplier**
Phalloidin Alexa-488	1:200	Merck
DAPI	1:1000	Sigma
Draq5	1:1000	Abcam

2.5. Marker

2.5.1. DNA Marker

DNA marker PhiX-174-HaeIII

from Fermentas

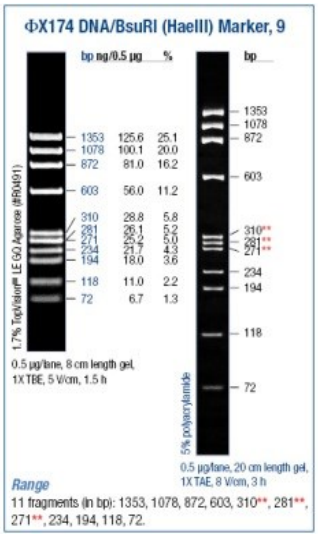

2.5.2. Protein Marker

SeeBlue Plus2 Prestained Standard

Invitrogen

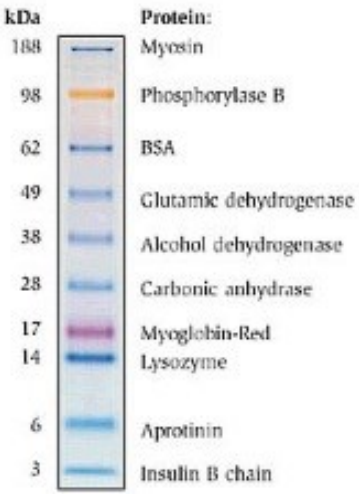

Broad Range Standard

BIO-RAD

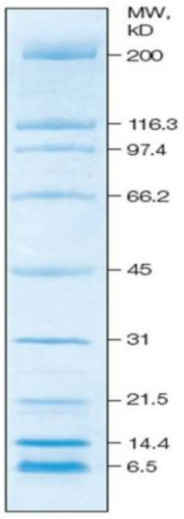

2.6. Commercial solutions

2.6.1. Commercial solutions for nucleic acid analysis

Name	Supplier
dNTPs	Promega
$MgCl_2$	Promega
PCR-flexi-buffer (5x)	Promega
Taq-Polymerase	Promega

2.6.2. Commercial solutions for tissue culture

Name	Supplier
DNase grade II	Roche
10x MEM	Gibco
$NaHCO_3$	Merck
Glucose	Sigma
Neuropan2	PAN
Sodium pyruvate 100x	Gibco
Boric acid	Merck
Borax	Sigma
HBSS	Gibco
Poly-L-Lysine	Sigma
Trypsin-EDTA 0.05%	Gibco
HEPES	Biomol
FCS	PAA
BSA	Roche
L-Glutamine 100x	Gibco

50x MEM essential amino acids	Gibco
100x MEM non-essential amino acids	Gibco
T25 flask	Nunc
PBS^- tissue culture grade	Gibco
Penicillin/Streptomycin antibiotics 100x	Gibco

2.6.3. Commercial solutions for protein analysis

Name	**Supplier**
Bradford 5x solution	BIO-RAD
Broad Range Standard	BIO-RAD
SeeBlue Plus2 Prestained Standard	Invitrogen

2.6.4. Commercial chemicals and reagents for electrophysiology

Name	**Supplier**
Carbogen (95% O_2 and 5% CO_2)	Air Liquide
Borosilicate glass capillary	Science Products GB150-8P 0.86x1.50x80mm
$MgSO_4$	AppliChem
Picrotoxin	Sigma
Trichlormethiazide	Sigma
Cesium hydroxide solution	Aldrich Chemistry
Cesium chloride	Sigma
QX-314 bromide	Tocris bioscience
D-Gluconic acid solution	Aldrich Chemistry
Guanosine 5`triphosphate sodium salt hydrate	Sigma
Adenosine 5`triphosphate sodium salt hydrate	Sigma

Adenosine 5`triphosphate dipotassium salt dihydrate	Sigma
50ml syringe	Injectomat
Filter papers 90mm	Whatman
D+ Saccharose/Sucrose	VWR Chemicals
Potassium chloride	Sigma-Aldrich
$MgCl_2$	AppliChem Pancreac
NaH_2PO_4	AppliChem Pancreac
HEPES	Sigma
D-Glucose	Sigma
$NaHCO_3$	AppliChem
$CaCl_2$	Sigma
NaCl	Chem solute
Tetrodotoxin TTX	Biotrend
NBQX	Tocris
0,2µm pore filters	Millex GP
Micro loader tips	Sarstedt

2.6.5. Equipment for behavioral studies

Open field	Ugo Basile, Italy 46cm x 46cm per chamber divided into: Central square 27cm x 27cm Periphery 46cm long and 9.5cm wide
EPM	Ugo Basile, Italy Two open arms 35cm length x 5cm width Two enclosed arms 35cm length x 5cm width x 15cm high dark walls Middle area 5cm x 5cm Apparatus is lifted 60cm above ground
Y-maze	Ugo Basile, Italy

	Three identical closed arms (35cm length x 5cm width x 10cm height) placed at 120° angle
Video camera system	Samsung sc8-3000
software	Stoelting ANY-maze software, Illinois USA

2.7. General laboratory and tissue culture materials

2.7.1. Plastic ware

Name	Supplier
Eppendorf tubes (1.5 ml/ 2ml)	Eppendorf
Falcons (15 ml, 50 ml)	Sarstedt
PCR tubes	Bioplastics
Pipettes (5 ml, 10 ml, 25 ml, 50 ml)	BD Falcon
Pipette tips (plugged)	Molecular Bio Products
Pipette tips (20µl, 200µl, 1000µl)	Sarstedt
Snap-cap	Sarstedt
Syringe	BD
21G needle	BD

2.7.2. Glass ware

Name	Supplier
Glass bottles	Schott
(50 ml, 100 ml, 250 ml, 500 ml, 1000 ml)	
Glass pipettes	Brandt
Microscope slides	VWR
Glass pasteur pipettes	Volcan
Glass pasteur pipettes (plugged)	Volcan

2.7.3. General tissue culture materials

Name	Supplier
Accu-jet (electronic Pipetteboy)	Brandt
Filter (for medium filtration; 0,2 µm)	Millipore
Plastic pipettes	BD Falcon
(1 ml, 2 ml, 5 ml, 10ml, 25 ml, 50 ml)	
Plastic tubes (15 ml, 50 ml)	Sarstedt
Cell culture flasks (75 cm2, 175 cm2)	Nunc
Petridishes (diameter 3 cm, 6 cm)	Nunc
Well plates (24 well)	Corning
Coverslips (diameter 13 mm)	Marienfeld
Porcelain racks	Thomas-Scientific
15ml falcons	Corning

2.7.4. Further material

Name	Supplier
Transfer membrane Immobilon-P	Millipore

2.8. Commercial chemicals and reagents

2.8.1. Liquids

Name	Supplier
Acidic acid	Merck
Acrylamide (30%)	BIO-RAD
β-Mercaptoethanol	Sigma
Bovine serum albumin (BSA), (10mg/ml)	New England Biolabs
Dimethyl sulfoxide (DMSO)	Merck
Ethanol (technical)	Merck
Ethanol for analysis	Merck

Ethidiumbromide (1%)	BIO-RAD
Glycerol	Sigma
Hydrochloric acid (HCl)	Merck
Isopropanol	Merck
Methanol	VWR
Nitrogen (liquid)	German-Cryo
TEMED	Sigma
Triton X-100	Roche
Tween-20	Sigma
Nitric acid (HNO3)	AppliChem
Percoll	Amersham Bioscience

2.8.2. Solids

Name	**Supplier**
$CaCl_2$	Sigma
APS	Fischer Scientific
Bovine serum albumin (BSA)	Merck
Bromphenol blue	BIO-RAD
Coomassie Brilliant Blue	BIO-RAD
EDTA	Sigma
Glucose	Merck
Glycine	Grüssing
Luminol	Sigma
Milk powder (non-fat)	Roth
PBS-	Sigma
Potassium chloride	Sigma
Potassium hydrogen phosphate trihydrate	Merck
Protease inhibitor cocktail tablets,Complete Mini, EGTA free	Roche
Proteinase K	Sigma

SDS	Merck
Sodium chloride	Roth
Sodium chloride (NaCl)	Merck
Sodium hydrogen carbonate	Merck
Sodium phosphate dibasic dihydrate	Sigma-Aldrich
Sucrose	Roth
Tris Base Ultra Quality	Roth

2.9. Technical equipment

Description	**Manufacturer**
Accu-jet® (electronic Pipette-Boy)	Brandt
Binocular MS 5 +camera ConProgRes C10 plus + light source KL 1500 LCD	Leica JENOPTIK Germany
BioChem VacuuCenter BVC 21 +	BioChem
Biorevo BZ-9000	Keyence
Centrifuge 5415 D	Eppendorf
Centrifuge 5417 R	Eppendorf
Centrifuge tissue culture	Beckmann
CTR 5500 +camera DFC 420 C	Leica
Freezer (-80 °C)	Thermo Scientific
Agarose-gel-electrophoresis running chamber	European Molecular Biology Laboratory
Glass-Teflon tissue grinders	Co
Heating block	Grant/QBT
Homogenizer apparatus	Bosch
Hoods MD14-2G10	Camfil farr
Incubator for tissue culture	Heraeus
LAS Imager Image Quant LAS 4000 mini	GE Healthcare
Leica DM 5500B	Leica
Magnetic stir plate	Heidolph
Microscope tissue culture	Leitz

PCR machine PTC-200 Peltier thermal cycler	MJ Research
pH-meter, ph Level 2	InoLab
Pipettes	Gilson
Power supply (for agarose gels)	Pharmacia
Power supply Power PAC 200	BIO-RAD
Rocker	Heidolph
SDS gel apparatus SE250	Pharmacia Biotech
Semi-dry blotting chamber	BIO-RAD
Shaker New Brunswick	Scientific
Spectrophotometer UV-DU 640	Beckmann
UV-Table	Bachofer
VacuuHandConrol VHC	BioChem
Vortex-Genie 2	Scientific Industries
Water purifier	Millipore
Water bath (cell culture)	GFL
Vibratome	Leica Vibratome VT 1200S
BZ-900 Biorevo microscope	Keyence
LSM	Zeiss
Binocular MS 5 +camera ConProgRes C10 plus +light source KL 1500 LCD	Leica JENOPTIK Germany

2.9.1. Technical Equipment for electrophysiology

Description	**Manufacturer**
Anti-vibration table	Newport
Faraday cage	Custom built
Microscope	Zeiss Axioskop
amplifier	Axon Instruments Axopatch 200
Capillary holder	LN mini 23xy
Pressure control system	Custom buil
Headstage	Axon Instruments

Stimulus Isolator	WPI Stimulus isolation A360
Data interface	Axon Instruments Digidata 1320A
Computer	IBM personal computer
Recording software	Clampex
Analyzing software	Clampfit
Camera	Bosch Dinion B&W camera
Perfusion pump	Gilson Minipuls 3
Glass capillary puller	Narishige Japan model PR-830
Carbogen input	KAYSER Oxy Class 3 EN ISO 2503
Microscope table	LN combi 25
Water bath	GFL
Micromanipulator control panel	LN SMI
Two channel oscilloscope	Tektronix TDS210
Cooling	Julabo F10 UC
Vibratome	Leica

3. Methods

3.1. Molecular Biology

3.1.1. Genotyping by PCR

The polymerase chain reaction is used to amplify a gene sequence of interest. Every PCR cycle consist of three steps, which allow the exponential amplification of a DNA fragment. Necessary for the reaction is the thermoresistant enzyme *Taq* polymerase, which was isolated from *Thermus aquaticus*, and specific primers, which flank the gene of interest. These primers are short oligonucleotides (18-30 bases), which are complementary to a specific part of the gene of interest. The first step is the denaturation of the DNA template at 94°C, followed by the annealing of the primers to the sense and antisense strand of the gene. The annealing temperature depends thereby on the composition of the primers, e.g. their length and G-C content, and ranges from 55-72°C. These primers are used as a starting point for the enzyme *Taq* polymerase, which starts to elongate the primers in the 5`-3` direction in the last phase of the cycle at a temperature of 72°C. The use of primers as a starting point for the elongation is necessary, because the *Taq* polymerase is unable to start elongation *de novo*. For the elongation an addition of the complementary dNTP (desoxyribonucleoside-triphosphate) based on the template DNA strand is used to elongate the hybridized primers. Also important for the reaction is the addition of Mg^{2+}, which is needed as cofactor for the *Taq* polymerase. After the first cycle the amount of the DNA template is multiplied by two. Depending on the number of cycles, which range from 30 – 50 cycles, the gene is amplified by a factor of 2^n (n= number of cycles).

3.1.2. Genotyping of mice by PCR

To determine the genotype of transgenic mice a 2–4 mm tail-biopsy was taken from every animal. Probes were transferred into an Eppendorf tube with 200 µl of genomic DNA extraction buffer with proteinase K and digested overnight at 55°C in a heating block. On the next day, the probes were vortexed vigorously and heated up to 95°C for 10 min to inactivate the proteinase K. Afterwards the tubes were centrifuged at 13,200 rpm for 15 min and 1 µl of the supernatant was used as DNA template in the PCR reaction. The tail probes were stored at RT.

3.1.2.1. Cofilin 2 PCR

To knockout the Cofilin 2 gene a gene targeting construct was created, with lox-P sites that flank the exons 2 – 4 and additionally introduce a Neomycin cassette behind exon 4 for the selection process in ES cells. After the expression of the enzyme Cre-recombinase the

flanked region is deleted, leaving behind only exon 1 to generate the knockout Cofilin $2^{-/-}$ allele. The genotyping of mice was performed in a three primer PCR. Therefore tail biopsies of mice were taken and 1µl of extracted DNA was used as a template in the PCR reaction. A combination of three primers was used to study the allelic composition of the Cofilin 2 gene loci. The wildtype allele generates a 250bp PCR product between the primers cof2-INT2-3´ and cof2-INT2-5´. A PCR product between primers cof2-INT-3` and cof2-3`UTR 5` is not possible, due to the fact that the amplified PCR product would be too blong for an amplification with the Taq polymerase activity in the given elongation time. After the Nestin-Cre deletion of exons 2–4 these two primers come in closer proximity and can know generate a 550bp PCR product. Thereby the primer cof2-INT2-5´ is complementary to exon 2, and therefore cannot bind in the knockout allele. The identification of the floxed allele is possible with the primer combination cof2-INT-3´ and cof2-INT2-5´, which results in a 330bp fragment, due to the addition of the lox-P sites in front of exon 2. For experiments littermates with a $Cof2^{fl/fl}$ genotype were taken as control, while $Cof2^{fl/fl}$ Nestin-Cre animals served as knockout.

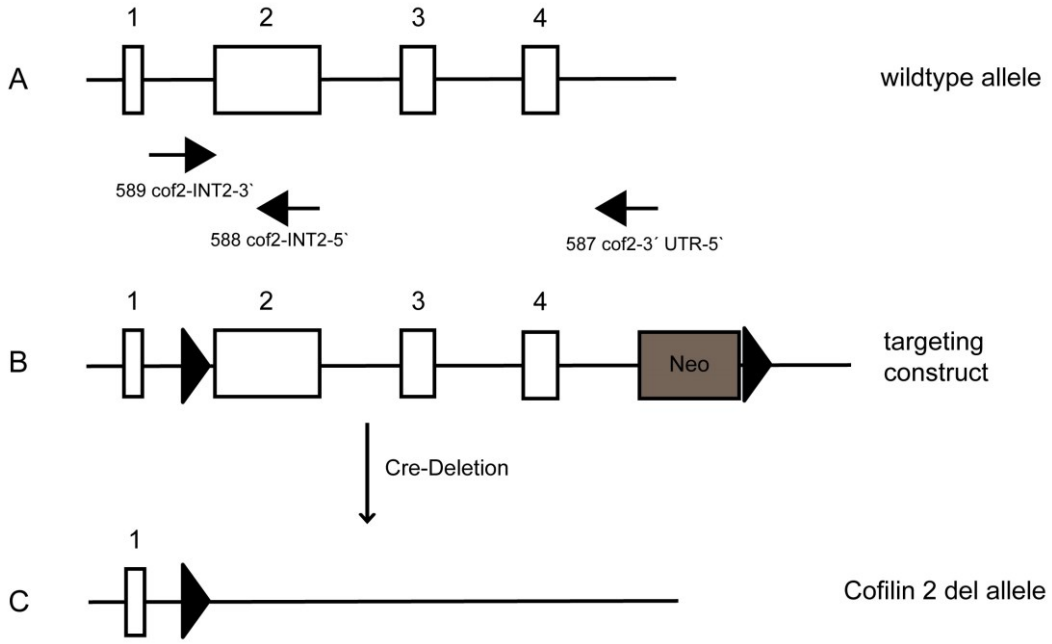

Fig. 15: Gene Targeting of the Cofilin 2 locus. A The wt allele consist of 4 exons, which span 4.063kbp on chromosome 12 (and generates mRNA transcripts of various sizes). The positions and orientations of primers used for genotyping are shown. The wt allele generates a 250bp product from the primer combination 589 and 588. A PCR product between the primers 589 and 587 is not possible due to the fact that the used Taq polymerase activity is not sufficient to build a longer PCR product in the given amplification time. **B** The introduced targeting construct is displayed, with the location of the lox-P sites in front of exon 2 as well as after the Neo cassette. Due to the addition of the lox-P site before exon 2 the amplified PCR product between the primers 589 and 588 is increased to 330bp. **C** The expression of the enzyme Cre-recombinase leads to the deletion of exon 2–4, generating the knock-out allele (del-allele). After deletion the primers 589 and 587 are in closer proximity and can now lead to the generation of a 550bp product. A PCR product between primer 589 and 588 is no longer generated, since the binding site for the primer 588 on exon 2 was deleted.

Mastermix (19µl per probe)	**PCR Programme "3x"**	
9.37µl Milli-Q	94°C 2min	
4µl 5x Puffer	94°C 30sec	35x
1.5µl MgCl2	58°C 30sec	
1.5µl dNTPs (2.5mM)	68°C 40sec	
1.5µl Primer 589 (5pmol)	68°C 5min	
0.5µl Primer 587 (5pmol)	Wt 250bp	
0.5µl Primer 588 (5pmol)	Floxed 330bp Deleted 550bp	
0.13µl Taq Polymerase		

3.1.2.1.1. Nestin-Cre PCR

A three primer reaction was used to detect the insertion of the enzyme Cre-recombinase into the Nestin-locus in the Nestin-Cre mouse line, which was used to generate a conditional Cofilin 2 deletion in the brain. Thereby, the primer Cre3 is complementary to the Cre-recombinase gene and can only hybridize to the DNA template, when the targeting construct is integrated into the allele. An insertion of the Cre-recombinase is confirmed by the amplification of a 300 bp PCR product between the primers 355 NesPr1 and Cre3. The insertion of the targeting construct leads to the deletion of exon 1, which contains the binding site for the third primer 617 NesPr2. In the wildtype allele a 450 bp fragment is generated from the primer combination 355 NesPr1 and 617 NesPr2, which can only hybridize when the targeting construct is not integrated.

Mastermix (19µl per probe)	**PCR Programm "Cre-P"**	
8.1µl Milli-Q	98°C 2min	
4µl 5x Puffer	98°C 30sec	30x
1.2µl MgCl2	58°C 30sec	
1.5µl dNTPs (2.5mM)	72°C 40sec	
2µl Primer 355 (5pmol)	72°C 40sec	
1µl Primer 356 (5pmol)	72°C 5min	
1µl Primer NesPr2 (5pmol)		
0.2µl Taq Polymerase		

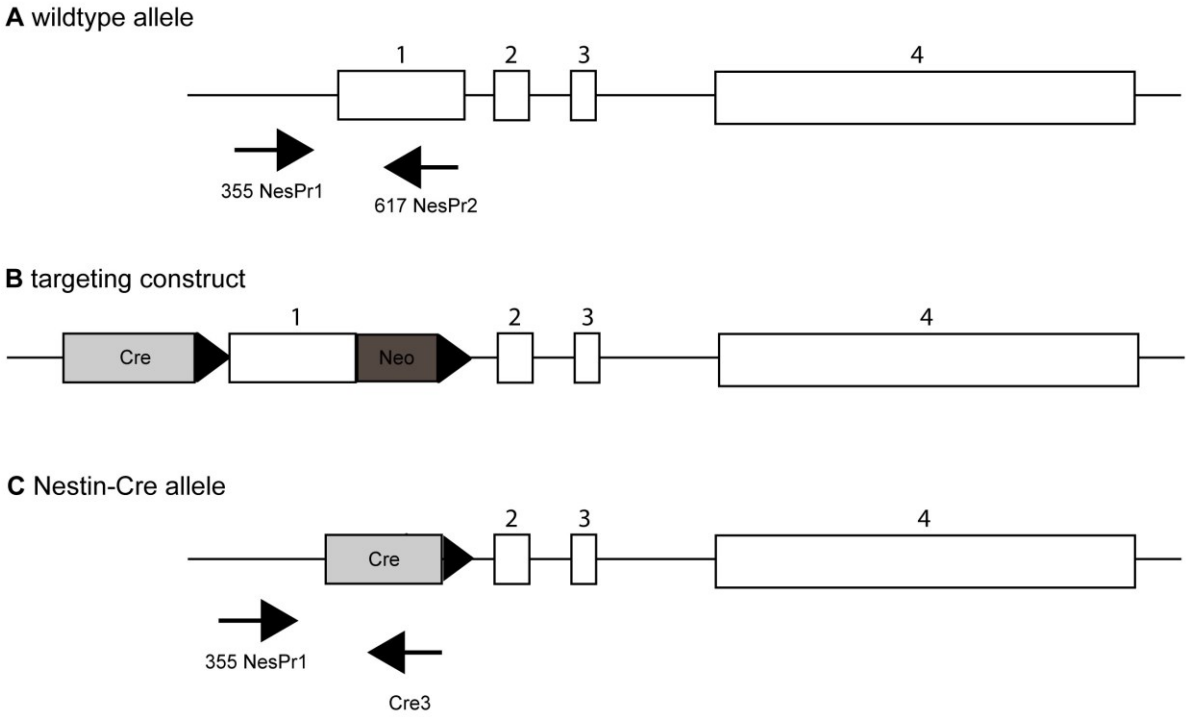

Fig. 16: Insertion of the Cre-recombinase into the Nestin-locus. A The Nestin gene locus on chromosome 3 contains 4 exons that leads to an mRNA construct of 6126bp. With the primer combination 355 NesPr1, which is localized in the 5´sequence and the primer 617 NesPr2 that binds to exon 1, a 300bp PCR fragment is generated and identifys the wildtype allele. **B** The targeting construct for the insertion of the enzyme Cre-recombinase into the Nestin gene-locus is shown. Exon1 and the Neomycin-cassette are flanked by lox-P sites. **C** After insertion the internal exon 1 of the Nestin-locus is replaced by the Cre-recombinase mRNA, which restricts the binding of the primer 617 NesPr2 to its target site. The primer combination 355 NesPr1 and Cre3, which binds in the Cre-gene, generates a 450bp fragment that marks the Nestin-Cre allele.

3.1.2.1.2. ADF PCR

To identify animals with a wildtype and a lacZ knock-in allele a three primer PCR was prepared. Thereby 1µl of extracted DNA from tail biopsy was inserted into the PCR reaction. A wildtype allele leads to a PCR product of 420bp between the primers ADF-150-3´ and ADF-INT2-5´. Due to the fact that the lac3´ primer anneals in the lacZ gene this primer is not able to bind in the wildtype allele. When the lacZ gene was inserted into the ADF gene loci an amplification between the primer pair ADF-150-3´ and ADF-INT2-5´ is not possible, since the lacZ gene spans 2.3kbp and the PCR product is thereby too long to be amplified in these conditions. The third primer lac3´ can bind now to the lacZ gene and synthesizes together with the primer ADF-150-3´ an 180bp PCR product. The insertion of the lacZ gene leads to a misfolding and a degradation of the ADF-lacZ fusion protein For experiments with double knockout animals only mice with an ADF knock-in were used. As a control served $ADF^{-/-}$ Cofilin $2^{fl/fl}$ animals, while $ADF^{-/-}$ Cofilin $2^{fl/fl}$ Nestin-Cre animals were used as double knockout.

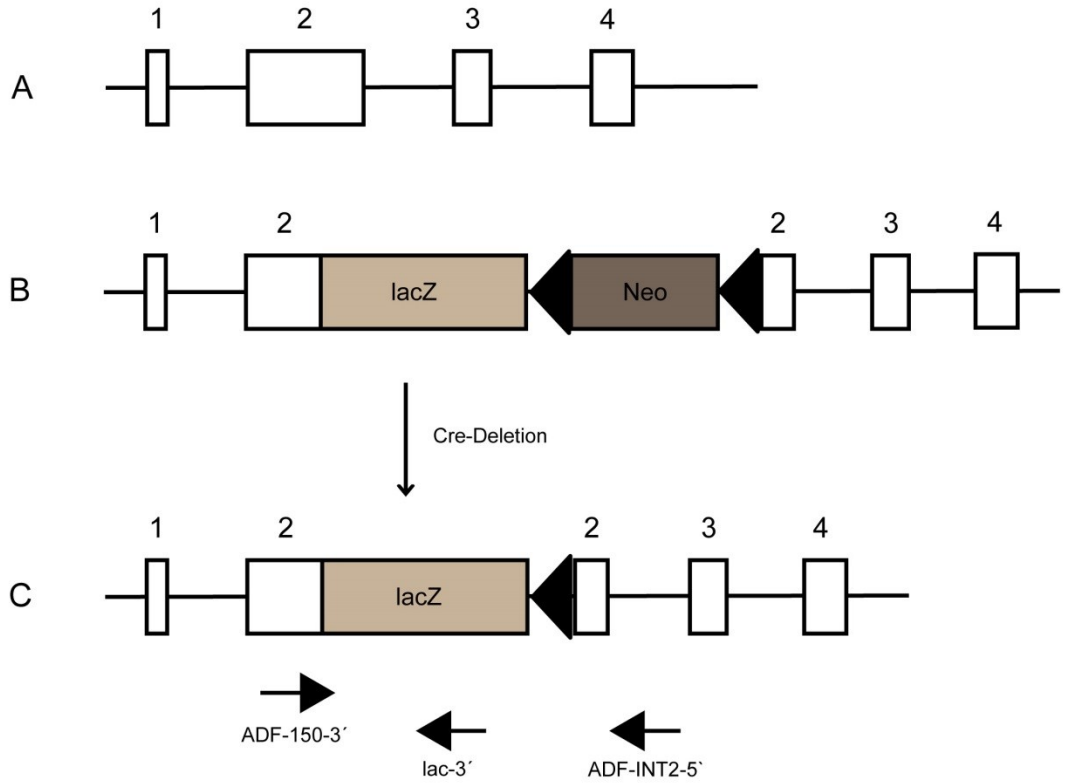

Fig.17: Gene targeting of the ADF locus. A The wildtype allele compromises 4 exons with 27.993bp on chromosome 2. **B** A lacZ gene and a floxed Neomycin cassette was integrated into exon 2 to generate a targeting construct. The insertion of the lacZ gene leads to a misfolding of the protein, which results in degradation of the ADF protein. **C** After Cre-Deletion the Neomycin cassette is removed. The locations of primers used for the genotyping PCR are shown. The wildtype allele generates a PCR product of 420bp between primers ADF-150-3´ and ADF-INT2-5´, which are in close proximity. After the insertion of the lacZ gene, which spans 2.3kbp an amplification between the primers ADF-150-3´ and ADF-INT2-5´ is not possible. Due to the addition of the lacZ gene the primer lac-3` can bind to its target site and generates a PCR product of 180bp with primer ADF-150-3´

Mastermix (19µl per probe)	**PCR-Programme "ADF"**	
9.17µl Milli-Q	94°C 2min	
4µl 5x Puffer	94°C 30sec	33x
1.2µl MgCl2	58°C 30sec	
1.5µl dNTPs (2.5mM)	68°C 40sec	
1.5µl Primer 106 (5pmol/ul)	68°C 5min	
0.5µl Primer 145 (5pmol)		
1µl Primer 403 (5pmol)		
0.13µl Taq Polymerase		

3.1.3. Agarose gel electrophoresis

The amplified DNA fragment was visualized and separated on an agarose gel via a gel electrophoresis. This method separates DNA fragments by size in an electric field. Based on their phosphate backbone DNA molecules display a negative charge and migrate in an electrical field to the anode. The separation upon the size of fragments is achieved through the selected agarose concentration, which forms a network with a defined pore size. Major fragments are more impaired in their migration through this network and migrate with a slower velocity over a shorter distance. Smaller molecules can migrate faster through the network and move over a longer distance. The fragment size can be analysed by comparison with a marker, which displays a mixture of different DNA fragments with a defined size. Based on the expected fragment sizes of the PCR products a 1,5% (w/v) agarose gel was prepared. Therefore, 1,5 g agarose were boiled in 100 ml TAE-puffer until the agarose was completely dissolved. For the visualization of the DNA 3 µl ethidium bromide were added to 100 ml dissolved agarose. The gel was poured into a running chamber and combs were inserted depending on the number of probes. After cooling the gel was covered with 1x TAE-puffer and 15 µl of the PCR samples were loaded onto the gel. Gels were run at a constant voltage of 65 V for 30 – 45 min. Afterwards the results were visualized with a UV light based imager-system.

3.2. Biochemistry

3.2.1. Protein isolation

3.2.1.1. Preparation of protein lysates from mouse tissues

To analyze the expression profile of Cofilin 2 in the brain protein lysates of the following brain areas were prepared from wt animals: cortex, hippocampus, striatum, olfactory bulb, cerebellum, hypothalamus and midbrain. The brain was dissected and tissue was shock frozen in liquid nitrogen. A 2ml glass douncer was filled with 500µl ice cooled PEB puffer for bigger tissue pieces and with 300µl for smaller pieces, like the hippocampus and olfactory bulb. The frozen tissue was transferred into the douncer and homogenizates with 10 strokes on ice at 300rpm until no tissue pieces were left. The lysate was transferred into a 1.5ml tube and centrifuged for 25min at 4°C and 10.000rpm. Afterwards the supernatant was transferred into a ultrazentrifuge tube and centrifuged for 30min at 100.000rpm and 4°C. The obtained cytoplasmic total-lysate was transferred into 1.5ml tubes and stored at -80°C for long term storage. 80µl of the Total lysate was mixed with 20µl 5xSDS and incubated for 10min at 95C.

Afterwards probes were centrifuged for 15min at 13.000rpm. To analyze the protein concentration 5µl of the Total-lysate was mixed with 45µl Milli-Q and 12.5µl of this solution was used for a Bradford assay (X.Y.).

3.2.1.2. Preparation of protein lysates from cultured cells

3.2.1.2.1. Astrocytic lysates

To analyze the expression of Cofilin 2 in astrocytes protein lysates of cultured astrocytes were prepared. Additionally astrocytic cultures were plated onto glass coverslips and fixed for immunofluorescence analysis. Therefore the obtained cultures were grown to confluency in T25 flasks. Cells were trypsinized with 3ml trypsin for 10min in the hood and the trypsin was stopped by adding 6ml of MEM-FCS medium. A single cell suspension was prepared by pipetting the cell suspension up and down against the flask. 4ml of the obtained cell suspension was added into a T75 flask for re-culturing; 1ml was used to fill a 24well plate containing 13mm glass coverslips. To every well 100µl of cell suspension was added and cultivated until cells attached and spread onto the coverslips. The remaining 4ml were used to prepare protein lysates. The cell suspension was centrifuged for 5min at 1000rpm and the pellet was washed with 3ml PBS. After a second centrifugation step the pellet was resuspended in 40µl PBS and 10µl 5xSDS was added. The protein concentration was measured with a Bradford reagent and 10µg were loaded onto a 15% gel. The blot was incubated with the following antibodies: KG60 for Cofilin 1, 7D10 for ADF, FHU-I for Cofilin 2 and GFAP as marker for astrocytes.

3.2.1.2.2. Microglia lysates

To analyze the expression of ADF/Cofilin family members in microglia we obtained microglia cell pellets from Dr. Fuhrmann. 20µl of MACSed microglia from a wt brain were supported to analyze the *in vivo* expression of actin depolymerization factors. A further probe of 20µl from cultured microglia was given to us to check the *in vitro* expression. Both probes were further diluted by the application of 30µl Milli-Q and mixed by flipping against the tube. To obtain a lysate (final 1xSDS) 50µl of 3xSDS were added and the probes were directly vortexed. Afterwards the probes were incubated for 10min at 95C with repeated vortexing steps. 3µl of the lysate was mixed with 27µl Milli-Q and 10µl of this solution were added to 900µl Bradford Reagent to obtain protein concentration. For the blank probe 3µl 3xSDS were diluted with 27µl Milli-Q. To determine the expression of ADF/Cofilin family members different concentrations of the defined recombinant protein were also loaded on the same gel. Thereby the following concentrations of recombinant protein were prepared: 20ng, 40ng,

80ng, 160ng, 320ng and 500ng. From every microglia probe 10µg were loaded onto a 15% gel, together with the different concentrations of the recombinant protein. For every ADF/Cofilin family member a defined blot was prepared and incubated with the appropriate antibody: KG60 for Cofilin 1, 7D10 for ADF and FHU-I for Cofilin 2.

3.2.2. Protein Quantification

In order to determine the protein concentration of lysates two different forms of a Bradford assay were performed. The Bradford assay reflects a spectroscopic analytical procedure to measure the concentration of proteins. Thereby the dye Coomassie Brilliant Blue G-250 is used, which binds to the alkaline side chains of proteins. Upon the binding to proteins a shift in the absorption maximum of the dye could be observed from 465 nm to 595 nm (Bradford 1976). The increase in absorption at 595 nm reflects the protein concentration in a solution. For the calculation of the protein concentration a standard curve with different BSA concentrations was prepared. The straight line exhibited a gradient of 0,048. Based on this standard curve the protein concentration could be analyzed with the following formula:

(Absorption / straight calibration line) / inserted µl of the probes = x µg/µl

3.2.2.1. Quantification of tissue lysates

Before the protein concentrations of the total lysates were quantified, the probes were centrifuged for 10 min at 10.000 rpm and 4°C. In the meantime the Bradford dilution (1:5 dilution in Milli-Q) was prepared. For the quantification 3 µl of the total protein lysates were diluted in 97 µl Milli-Q and mixed well, 900 µl of the Bradford reagent was added to the diluted probes and the absorption at 595 nm was measured. For the baseline setting of the spectrophotometer 3µl of PEB puffer were diluted in 97µl Milli-Q.

3.2.2.2. Quantification of cultured cell lysates

The lysates of cultured cells that contained already 1xSDS reagent, were analyzed with a second protocol for the Bradford assay. Therefore, 5 µl of the lysates were diluted in 45 µl Milli-Q. To 12,5 µl of the diluted probes 1000 µl of the Bradford reagent (1:5 dilution in Milli-Q) was added. Subsequently, the protein concentration was measured at 595nm. For the blank 5µl of SDS sample buffer instead of lysate was used.

3.2.2.3. Coomassie staining of protein gels

To ensure that the same amount of every lysate was loaded onto the western blot gel, 10µg of every probe was loaded onto a gel and stained afterwards with Coomassie. This method is commonly used to stain proteins in analytical biochemistry and allows an optical quantification of the protein concentration. Therefore, the gel was incubated for 30 minutes in Coomassie Brilliant Blue staining solution at room temperature on a rocker. Afterwards the gel was destained in rapid destain solution for 60 minutes at room temperature. Gels were stored in H_2O upon documentation. This procedure was also used after the transfer of the proteins onto a membrane, to ensure that the transfer was successful.

3.2.3. Discontinous SDS-Polyacrylamide gel electrophoresis

Proteins can be composed out of 21 amino acids with different characteristics and electrical charges. Based on this every protein can be distinguished depending on its mass and isoelectric point. For the separation of proteins in a gel, it is necessary to provide a consistent charge. This can be achieved by the detergent sodium dodecyl sulphate (SDS), which is an anionic detergent that denatures proteins. Additionally, it reduces proteins to their primary structure by breaking up hydrogen bonds, which leads to the denaturation of secondary, tertiary and quaternary structures and linearizes the proteins. Negative charges are applied to the proteins according to their mass, which leads to the same charge/mass ratio in all protein-SDS-complexes. Consequently, the running behavior of proteins in the gel depends only on their molecular weight. The SDS sample buffer (Laemmli buffer) also contains Bromphenol Blue and β-mercaptoethanol. The bromphenol blue marks the running front, while β-mercaptoethanol reduces inter- and intra-molecular disulfide bonds. Depending on the molecular weight of the protein of interest, a gel with a defined percentage of polyacrylamide is prepared for the proper separation of the protein-mixture. For the analysis of the ADF/Cofilin family with a molecular weight of 18-20 kDa a 15% acrylamide gel was used. A discontinuous sodium dodecyl sulphate polyacrylamide gel electrophoresis, short SDS-PAGE, consists of two different gels which differ in their pH and pore size. First proteins were loaded into a stacking gel, which has the function to assemble all proteins at the border between the stacking and separating gel, so that all proteins start to migrate into the running gel at the same time. Therefore the stacking gel displays an pH of 6,8 which is near the isoelectric point of glycine. This leads to a very slow running of glycine in the gel, which has the function to locate the glycine above the proteins, which generates a “pushing down” of all proteins to the border. Additionally contains the gel highly mobile chloride ions that migrate

faster than proteins, which causes all proteins to be located in one band between the glycine and chloride ions. The running gel has a pH of 8,8, which leads to a change of the electric charge of glycine. Glycine displays now a negative charge and based on the small size starts to migrate very fast in the running gel and passes all proteins. Therefore a discontinuous SDS-PAGE allows a higher resolution of proteins according to their electrophoretic mobility (Laemmli 1970).

The SDS running chamber was filled with 1x SDS running buffer. Protein lysates were centrifuged for 10 min at 10.000 rpm and 4°C and from every sample 15 µg were loaded on a Western blot. For the determination of protein sizes on the Western blot 5 µl of Sea Blue Plus 2 Prestained marker was loaded into the first lane. To control the efficiency of the Western blot afterwards also 10 µg of a positive control was loaded onto the gel (wt brain control for Cofilin 1; muscle control for Cofilin 2 and a uterus control for ADF). The electrophoretic separation was accomplished at 60 V for the stacking gel for circa 30 min, followed by the separation of proteins at 100 V. Gels were run until the 16 kDA lysozyme marker band reached the bottom of the gel.

3.2.4. Western blot analysis

The Western blot analysis allows the detection of specific proteins in a mixture of a protein lysate obtained from a tissue or cultured cells. Therefore, proteins were separated according to their molecular weight in a SDS-PAGE. Afterwards the separated proteins were transferred onto an “Immobilon (polyvinylidene difluoride, PVDF) membrane. The detection of the protein of interest on the membrane is possible by the use of a specific primary antibody. Visualization occurs upon the use of a secondary antibody, which is directed against the primary antibody and conjugated with the enzyme horseradish peroxidase that starts a chemo-luminescence reaction. Thereby the enzyme catalyzes the oxidation of the substrate luminol, which is accompanied by emission of light at 428nm.

3.2.4.1. Semi dry blotting procedure

Electroblotting is used to transfer proteins from a gel onto a membrane for the detection via specific antibodies. Depending on the size of the protein a wet blot or a semi dry blot is used. Proteins above a molecular weight of 60kDA are better transferred in a wet blot. Smaller proteins, like the ADF/Cofilin family can be transferred onto a membrane in a semi dry blot. Generally in both methods an electric current is used to transfer the proteins from the gel to the membrane. Proteins bind thereby to the membrane based on charged as well as hydrophobic interactions. For the transfer four Whatman paper sheets and one “Immobilon”

membrane were cut to the size of the gel. The membrane needs to be activated in methanol for several minutes and was then equilibrated in Towbin transfer buffer. Also the Whatman papers and the gel were equilibrated in Towbin transfer buffer. The semi dry blot was built up in the following arrangement: Cathode (-): 2 Whatmann papers, gel, immobilon membrane, 2 Whatmann papers: Anode (+).

The transfer was progressed at 20 V for 60 min at room temperature. Afterwards the gel was stained with Coomassie, to check the efficiency of the transfer. The membrane was directly transferred into Western blot blocking solution for one hour at room temperature or overnight at 4°C.

3.2.4.2. Wet Blot

To transfer proteins with a higher molecular weight a wet blot was prepared. Thereby the SDS gel was incubated in Towbin transfer puffer after the run. On a wet blot chamber two Whatman papers were aligned on the black side of the transfer chamber. The activated membrane was placed above the Whatman paper. The gel was placed on top of the membrane and covered by two Whatman papers. Bubbles were removed by putting slight pressure with a rolling pipette on the system. The chamber was closed and inserted in the Wet Blot chamber by turning the black chamber to the red colored anode. The wet blot chamber was filled with ice cooled Towbin transfer puffer after addition of a cooling pack. The chamber was transferred to the cold room and the transfer was progressed overnight at 20mV. On the next day the membrane was transferred into Western blot blocking solution, while the gel was placed in a Coomassie filled chamber to check the efficiency of the transfer.

3.2.4.3. Western Blot analysis using chemo luminescence

The detection of the protein of interest is accompanied by a specific primary antibody which specifically binds to the protein. Afterwards a secondary antibody is used, which is directed against the first antibody, depending on the species from which the first antibody was generated. Additionally, the secondary antibody is conjugated with the enzyme horseradish peroxidase (HRP), which has the ability to oxidated the substrate luminol to a reactive molecule that is able to generate chemiluminescence proportional to the amount of protein. The chemiluminescence was detected in a LAS Imager.

After blocking of the membrane, to avoid unspecific binding sites for the antibodies, the membrane was incubated with the primary antibody diluted in the Western blot blocking solution. The used antibody dilutions are depending on the efficiency of the different

antibodies and the amount of the analyzed protein. Primary antibodies were incubated overnight at 4°C or for 3 hours at room temperature. Afterwards the membrane was washed five times for 10 minutes in 1x NCP (-azide). In the next step, the membrane was incubated with the secondary antibody diluted to a concentration of 1:1000 in Western blot blocking solution for one hour at room temperature. The membrane was washed five times for 10 minutes in 1x NCP-azide. After rinsing the membrane in water, the membrane was incubated for several minutes in ECL reagent. The 1:1 mixture of the ECL reagent was freshly prepared and directly applied onto the membrane. During the incubation in ECL, the membrane was turned several times and the chemiluminescence was analyzed with the LAS imager software. The exposure time was adjusted depending on the strength of the signal.

3.2.4.4. Densitometric analysis of Western Blots

To compare the intensity of bands on a Western blot and prepare a densitometric analysis the Adobe Photoshop software was used. In a first step the color information was discarded and the image was transformed into a grayscale. Under Image and Adjustments the image was inverted, so that the dark Western Blot bands of the image were light, and the light image background became dark. This step is useful since the Western blot bands will get high numerical values when they are measured (dark points have values near zero, while light points have values with a maximum of 255). With the lasso tool from the tool palette a line was drawn around the edges of the first band. The histogram window was opened under “Window” and used in the expanded view to show the values for the analyzed bands. Thereby the histogram information about the “Mean” value and the “Pixels” value was recorded and inserted into an excel sheet. The Mean value is the average gray value (from 0 to 255) for the area inside the selection and the Pixels value is the number of pixels contained in the selection area. The lasso tool was used to record all Mean and Pixel values for the obtained bands on a blot. In an excel sheet the absolute intensity was calculated by multiplying the Mean value by the Pixel value for each band. This allowed an integrated measurement of the intensity and size of the bands. In a next step the relative intensity was calculated by normalization of the GAPDH standard band for each sample. The difference for each sample band to the strongest standard band was calculated and the absolute intensity of the sample band was multiplied by this factor. The relative intensity was generated by addition of the original absolute intensity of the sample band to this calculated difference.

3.2.5. Analysis of the G- and F-actin content in Cofilin 2 deficient animals (acc. to Mc Robbie)

To address the question whether the loss of Cofilin 2 or the dual loss of ADF and Cofilin 2 had an impact on the G- and F-actin ratios in the brain a Mc Robbie assay was prepared on the cortex of wt and mt animals of the Cofilin 2 Nestin and ADF Cofilin 2 Nestin mouse lines. Therefore 500µl of ice cold PHEM buffer with 1% Triton was transferred into a glass beaker. The cortex of wt or mt animals was dissected and transferred into the PHEM buffer. The tissue was dounced with 10 strokes at 600rpm and incubated for 15minutes on ice. The PHEM buffer has pH 7.0, due to the fact that a higher pH would facilitate the depolymerization process. After the incubation step, the probes were spun in a swing-out rotor for 10minutes at 13000rpm and 4°C. The supernatant contained the G-actin and 80% were transferred into a new 1.5ml tube and mixed with 5xSDS to a final concentration of 1xSDS (320µl supernatant + 80µl 5xSDS). The obtained lysate was boiled for 10min. The remaining 20% of the supernatant were discarded and the pellet was washed two times with 1xPHEM and 1% Triton. During the washing steps the pellet was dried with the help of kim wipe papers to remove all parts of the supernatant. The pellet was dissolved in 500µl of 1xPHEM buffer with 1% Triton and mixed with 125µl 5xSDS. After boiling the probes for 10min at 95C° the concentration was measured in a Bradford assay. As a control served PHEM buffer mixed with 5xSDS. On a 10% gel equal volumes of the supernatant and pellet fractions were loaded; to be able to load 1µg onto the gels all probes were diluted 1:10 to avoid the saturation of the membrane. The blots were incubated with an antibody against actin (C4) and GAPDH; due to the fact that GAPDH is a cytoplasmic protein it should only give a signal in the G-actin supernatant fraction. Thereby a contamination of the pellet fraction with G-actin was examined. To be able to compare the G- and F-actin ratio in wt and mt animals of the Cofilin 2 Nestin or ADF Cofilin 2 Nestin mouse lines the obtained Western blot bands for the supernatant fraction were normalized to the GAPDH signal with the Multi Gauge software. Therefore not fully saturated Western blot signals were used and the band intensity (QL-BG) of the C4 and GAPDH signals were measured with the Quant tool. The highest QL-BG value of the blot for GAPDH was determined as 100% and the differences was calculated for every signal to normalize the actin value based on the GAPDH signal. Then the normalized F-actin value was divided with the G-actin value to obtain the ratio between the G- and F-actin signals. The ratio between the wt and mt animals for the Cofilin 2 Nestin and the ADF Cofilin 2 Nestin mouse lines were compared to determine the impact of the Cofilin 2 loss or even the loss of two members of the ADF/Cofilin family on the actin cytoskeleton.

3.2.6. Synaptosomal preparation

Synaptosomes were prepared to analyze the pre- and postsynaptic localization of Cofilin 2. For this purpose an adult wt brain was dissected on ice and the cortices were transferred in 12ml of ice cold homogenizing buffer in a 14ml glass teflon douncer to homogenize the tissue on ice with 10 strokes at 250rpm. The solution was transferred into a snap-cap and centrifuged for 10minutes at 5000g and 4°C in the Beckman centrifuge to remove nuclei and cell debris. The supernatant contained cytoplasmic proteins and the synaptosomes and was poured into a new snap-cap tube. The supernatant was centrifuged for 12min at 14000g and 4°C to pellet synaptosomes. The pellet was resuspended carefully in 500µl ice cold Krebs-Ringer buffer to avoid air bubbles. The dissolved pellet was transferred into a new Eppendorf tube containing 500µl of ice cold Percoll (final 45% v/v). The solution was mixed by gently inverting of the tube. After a 2 minute spun at 14000rpm and 4°C the synaptosomes were enriched on the surface of the flotation gradient and recovered by aspiration of the underlying solution with a 5ml syringe armed with a 21G needle. Therefore the needle was carefully slid along the wall of the tube down to the bottom and the solution was slowly aspirated. The enriched synaptosomes were resuspended in 1ml of ice cold Krebs Ringer buffer. After that the solution was spun for 30 seconds at 14000rpm and the supernatant was discarded. The pellet was carefully resuspended in 150µl ice cold Krebs Ringer buffer and kept on ice. For the quantification of the synaptosomal preparation 4µl of the obtained synaptosomes were transferred into a new 1.5ml tube after invertion of the tube, due to the fact that synaptosomes are heavy and deposit quickly to the bottom of the tube. 1µl of 5xSDS was added to the 4µl synaptosomal preparation to obtain a lysate. As a control for the Bradford assay, also 4µl of the Krebs Ringer buffer were diluted with 1µl of 5xSDS. After the preparation of a total synaptosomal lysate the rest of the synaptosomes were diluted 10x their volume by adding 4.5ml ice cold 0.1mM $CaCl_2$. In addition also 5ml of a solubilisation solution with a pH of 6.0 was added and the probe was incubated for 30minutes on ice with mild agitation. Afterwards the probe was centrifuged for 30min at 40000g in the ultracentrifuge to obtain a supernatant, which contained the extra synaptic proteins and a pellet with the synaptic junctions. The extra-synaptic proteins were transferred into a snap-cap tube and 80µl were mixed with 20µl 5xSDS to obtain an extra-synaptic lysate. The pellet was washed with washing puffer of pH 6.0 and the pellet was afterwards resuspended in 250µl Tris buffer with pH 8.0 to separate the pre- and postsynaptic sites. After an incubation of 30 minutes on ice the probe was centrifuged again at 40000g for 30 minutes and 4°C. The obtained supernatant contains the presynaptic proteins and was mixed with 5xSDS. The pellet was incubated two more times for 30minutes after addition of Tris buffer, followed by the centrifugation step to guarantee a clean separation between pre- and postsynaptic sites.

The obtained postsynaptic proteins in the pellet were resuspended in 500µl 1x SDS sample buffer. All probes were denatured for 5minutes at 95°C and 5µl were transferred into a new tube and diluted with 45µl water. For the analysis of the protein concentration via Bradford 12.5µl of every solution was mixed with 1ml Bradford reagent and the protein concentration was calculated through the increase in the absorption at 595nm. Corresponding volumes of every probe were loaded onto a 15% gel and separated via SDS-PAGE. The Blot was incubated with antibodies against Cofilin 2 (FHU-I), ADF (7D10; GV13) and Cofilin 1 (KG60) to obtain insight into the expression of ADF/Cofilin family members at the pre- and postsynaptic sites. To further prove the extraction of synaptosomes another 10% gel was loaded with the obtained probes and incubated with a marker for extrasynaptic proteins (synaptophysin), a marker for the presynaptic site (syntaxin) and a marker for the postsynaptic site (PSD95).

3.3. Cell biology

3.3.1. General arrangements for the culture of cells

3.3.1.1. Preparation of cover slips

Glass coverslips were cleaned before they were used for the preparation of primary neuronal cultures. Therefore glass coverslips with a diameter of 13mm were placed in a zig-zag pattern into porcelain staining racks to enable a minimum contact area between single coverslips. This guarantees that the acid had free access onto the surface of the coverslips and the coverslips were cleaned thoroughly. The filled porcelain racks were placed into glass beakers under the hood and filled with nitric acid (HNO_3) to incubate them overnight. On the next day the porcelain racks were taken out of the acid and washed two times in Milli-Q by dipping them into Milli-Q filled glass beakers. After the washing steps the porcelain racks were placed into dry glass beakers and covered with aluminum foil. The coverslips were sterilized for 6hours at 220°C with dry heat. Under the cell culture hood the coverslips were placed into 10cm dishes until used.

3.3.1.2. Dotting of coverslips

For the dotting process 8 coverslips were placed with a forcep into a 6cm dish. In the meantime paraffin was melted in a water filled glass beaker on a heating block for several hours. When the paraffin was melted, the glass bleaker was placed under the hood and three dots of paraffin were applied to every coverslip. The dots were dried out over night before usage. The dotted 6cm dishes were stored for up to 3 weeks.

3.3.1.3. Coating of coverslips

At least two days before the hippocampal culture was prepared, the coverslips were coated with Poly-L-Lysine. Therefore the Poly-L-Lysine was dissolved in borate buffer to a final concentration of 1mg/ml and filter sterilized. On every coverslip was placed 150µl of Poly-L-Lysine solution and incubated overnight at room temperature in a humid chamber. The spilling of Poly-L-Lysine over the edge of the coverslip was avoided, due to the fact that dried Poly-L-Lysine is toxic for neurons and cannot be washed away anymore. On the next day the Poly-L-Lysine was removed and the dishes were immediately washed with 5ml sterile water. The washing step was repeated and the sterile water was removed to place 5ml of MEM-FCS in every dish. Coated dishes were transferred into the incubator and equilibrated before use. They were stored in the incubator for 1 week before usage.

3.3.2. Preparation of primary neuronal cultures

3.3.2.1. Astrocyte culture as feeder layer for hippocampal neurons

Astrocytic cultures were prepared from embryos at day 17.5 or later, due to the fact that the development of astrocytes starts around E17.5 and rises postnatally. Therefore the pregnant female was sacrificed and the litter was dissected out of the uterus. The embryos were freed from the placenta and the heads were cut off. With a small scissor and forceps the scalp was opened up and the brain was transferred into a 6cm dish filled with 1xHBSS. Under a microscope the meninges were removed and the cortex was separated from the rest of the brain and placed into a 3cm dish filled with 1xHBSS. All prepared cortices were collected in a 3cm dish. Under the hood the cortices were transferred with a BSA-coated glass pipette into a 15ml falcon tube to fulfill a first rough dissociation of the tissue pieces. The tissue settled down on the bottom of the tube and the 1xHBSS was removed. 3ml Trypsin-EDTA/HEPES was added to the tissue and incubated for 10 minutes at 37°C in the water bath. During the incubation step a glass pipette was fire-polished to reduce the diameter and coated with 5% BSA in PBS. After 10 minutes the Trypsin was removed with a pipette and 5ml prepared HBSS/DNase solution was added to remove the trypsin. The falcon was softly agitated by hand to guarantee the access of the DNase to all parts of the tissue. The washing step with HBSS/DNase solution was repeated and afterwards 5ml HBSS/HEPES was added to remove residual DNase. Again the washing solution was removed and 5ml MEM-FCS was added. The tissue was dissociated with a glass pipette with a standard diameter until all bigger tissue pieces were gone. Afterwards the cells were further dissociated by taken up the

cell solution with the plugged fire polished pipette until all tissue pieces disappeared and a single cell suspension was generated. The cell solution was transferred into a T25 flask and incubated for three days. After three days the medium was changed to remove cell debris and dead cells, which were not able to adhere to the plastic surface. When the T25 flask was grown to confluence, the culture was split by washing the flask with 5ml HBSS, followed by the incubation with 3ml Trypsin/HEPES for 10 minutes in the incubator. The detachment of cells was controlled under the microscope and the flask was shaken until all cells were detached from the surface. Under the hood 7ml MEM-FCS were added to inactivate the trypsin. With a 10ml pipette the cells were dissociated by pipetting them up and down against the flask wall. The generation of a single cell suspension was controlled under the microscope. 1ml of the cell suspension was added to a 6cm dish filled with MEM-FCS. Astrocytic feeder layers with a confluence of 50% were used to grow hippocampal cultures to guarantee a supply of nutrients by the astrocytes and avoid the depletion of media ingredients.

3.3.2.2. Culturing of primary hippocampal neurons

Pregnant females of the Cofilin $2^{-/-}$ mouse line were sacrificed on embryonic day 17.5 and the litter was dissected out of the uterus and placed into a 10cm dish. The embryos were freed from the placenta and a piece of the tail was transferred into an Eppendorf tube with TENT puffer to obtain the genotype. The head was cut off and the scalp and head bones were opened up with a small scissor. The exposed brain was placed in a 3cm dish filled with HBSS. Under a microscope the meninges were removed from the brain to avoid a fibroblast contamination in the cultures. The cortex was opened up from the mid line with forceps and removed from the rest of the brain. Remaining meninges were removed and the hippocampus was dissected out of the cortex and placed into an Eppendorf tube filled with 1ml HBSS. Under the hood the HBSS was removed with a 1ml pipette and 1ml Trypsin-EDTA/HEPES was added and the 1.5ml tubes were incubated for 10minutes in the water bath. During the incubation step plugged glass pipettes were fire polished to reduce the diameter and coated with 5% BSA in PBS to reduce cell adhesion to the glass. After 10 minutes the trypsin was removed with a pipette and the tissue was washed two times with HBSS/DNase. Afterwards a washing step with HBSS/HEPES was performed to remove DNase deposits. The tissue was dissociated with the fire polished pipette until all tissue pieces were gone and the solution had a dimly appearance. A prepared 6cm dish containing 5ml N2 medium was filled with 150µl of the cell suspension and the cell concentration was examined under the microscope. If the cell concentration was dense enough, 150µl cell suspension was added to every 6cm dish with dotted coverslips. Otherwise the applied concentration was adapted. The dishes were incubated for 24h in an incubator with 5% CO_2

and 37°C and on the next day flipped with the cell side facing down (dots facing down) onto the astrocyte feeder layer. Cultures were kept in this condition for up to 4 weeks. N2 medium was changed once a week by removing only 2/3 of the old medium and adding 5ml fresh N2 media to every dish, to preserve released factors from astrocytes in the media for hippocampal neurons.

3.3.3. Analysis of cultivated primary neurons

3.3.3.1. Immunofluorescence analysis of primary neuronal cell cultures

For the analysis of the spreading process and growth cone diameter hippocampal cultures were fixed at div (days in vitro) 1, 2, 3 or 4 and stained with phalloidin and an antibody against betaIII-tubulin. Therefore the cultures were fixed with pre-warmed 4% PFA/sucrose for 20 minutes. The medium was aspirated and without any further washing step the PFA/Sucrose solution was added. After 20 minutes the PFA/Sucrose was removed and dishes were washed with PBS once for storage or three times for direct use in the immunofluorescence. Fixed cultures were stored at 4°C until all time points were collected. Cells were permeabilised for 1 minute with 0.1%Triton in PBS. Afterwards cells were washed three times with PBS. A wet chamber was prepared by placing wet Whatman filter paper into a box which was overlayed with parafilm. Cells were blocked for 1h at room temperature with 5% goat serum and 0.1% Triton in PBS. Therefore drops of 50µl blocking solution were placed on the parafilm and coverslips were put onto the drops with the cell side facing down. Before the blocking process paraffin dots were removed to obtain a flat layered coverslip. After the blocking step 200µl PBS were pipetted underneath the coverslip to lift it up. The coverslips were then transferred onto drops with primary antibody and incubated for the appropriate time depending on the used primary antibodies. The antibody solution contained 3% goat serum and 0.01% Triton in PBS. After the incubation time 200µl of PBS were pipetted underneath the coverslips and the coverslips were dipped into two 50ml beakers filled with PBS and the remaining liquid was removed carefully with a filter paper. Afterwards coverslips were placed on 50µl drops containing the secondary antibody with a dilution of 1:1000. Coverslips were incubated for 1 hour at room temperature and the washing procedure was repeated. Then coverslips were incubated for 15minutes in a DAPI solution with a final concentration of 1:1000. In the meantime glass slides were labeled and cleaned with ethanol, while Moviol was warmed up at 37°C. Coverslips were washed by dipping them again in PBS filled 50ml beakers and in the last step cells were washed in Milli-Q. With a cut 200µl tip Moviol drops were placed onto the glass slides and with a kim wipe excess of water

was removed from the coverslips. To mount the coverslips they were placed cell side facing down slowly onto the Moviol drops to avoid the generation of air bubbles. The coverslips were dried at RT overnight in the dark and stored for long-time storage at 4°C.

3.3.3.2. Analysis of spreading and growth cone diameter

Images of the stained cultures were obtained with the epifluorescence Leica microscope and a 40x objective. The obtained images were analyzed with the Keyence software and the growth cone diameter was assessed with the "specify region freehand line" tool by drawing the growth cone shape by hand. In an excel table the diameter of Cofilin $2^{+/+}$ or $^{-/-}$ neurons were recorded and also the number of neurites per cell and the polarity of each cell was noted. The average and standard error of every time point was calculated and compared between wt and mt. The significance was tested in a two-tailed independent t-test.

3.3.3.3. Immunofluorescence analysis on astrocytes

To prepare immunofluorescence on astrocytic cultures, the medium was aspirated from the coverslips and cells were immediately fixed by adding 4%PFA for 20min. Afterwards cells were washed three times with PBS, followed by the permeabilisation of cells for 60sec with 0.1% TritonX100 in PBS. Cells were washed for three times in PBS and then blocked for 1h at RT in PBT-Block with 2%BSA, 0.05% gelatine and 50mM glycine. Therefore coverslips were placed on 50µl drops placed on a parafilm in a wet chamber. After the blocking step coverslips were directly transferred onto 50µl primary antibody solution, which consisted of blocking solution with the anti-Cofilin2 antibody FHU-diluted 1:100. The coverslips were incubated for 4h at RT. Afterwards coverslips were washed by pipetting 200µl PBT underneath the coverslip to lift them up and the dipping of coverslips in two different beakers filled with PBT. During the washing steps remaining liquid was carefully removed with a paper towel, before transfer to the second beaker. Then coverslips were placed on 50µl drops containing 3%NGS and 0.01% Triton in PBS and the GFAP antibody diluted 1:700. Coverslips were incubated ON at 4°C. On the next day coverslips were washed again as mentioned above with PBS and placed on 50µl drops containing blocking solution with a 1:1000 dilution of the secondary antibodies. After the washing steps cells were incubated with DAPI diluted 1:1000 in PBS for 15minutes. Coverslips were washed again with PBS, followed by a last washing step in Milli-Q and mounted on objective slides with Moviol containing the anti-fade NPG.

3.4. Histology

3.4.1. Mouse brain dissection

Adult brains were dissected on ice and transferred immediately to a snap-cap tube filled with 10ml 4%PFA. The tissue was fixed for 48h at 4°C on a rocker. Afterwards the tissue was washed three times with PBS and stored in PBS until cut.

3.4.2. Vibratome sections

Sagittal and coronal sections with a thickness of 25µm were prepared with a Leica Vibratome VT 1200S. A razor blade was inserted into the system with an angle parallel to the object table. The vibration accuracy was measured using the Leica vibrocheck and tuned to optimal levels. Fixed brain tissue was cut near to the midline to obtain sagittal sections and the brain was glued with the cut side to an object table. For coronal sections the brain was cut near the cerebellum and the cut surface was glued to the objective table. The objective table was submerged to a chamber filled with ice cold PBS/0.01% azide and adjusted to obtain a perfect cutting plane. Areas of interest were placed at the opposite side of the razor blade so that the blade hits the tissue at last. The chamber was surrounded by ice to keep the PBS cooled. Cutting was performed at a speed of 0.16mm/s and vibration amplitude of 1.5mm. The obtained sections were stored in 24-well plates filled with PBS/0.01% azide. To obtain complete slices for the morphology analysis the fixed brains were embedded in 6% agarose and the agarose block containing the brain was glued to the objective table. The agarose was removed after the cutting process.

3.4.3. Immunofluorescence on vibratome sections

To analyze the expression of Cofilin 2 in distinct neuronal subpopulations colocalization studies were performed between FHU-I and specific markers for subpopulations on sagittal vibratome sections of adult wt brains. For the staining protocol the slices were blocked overnight at 4°C in blocking solution containing 2% NGS, 2% BSA and 1% DMSO in TBS-T. For the Cofilin 2 staining slices were incubated for 48h at room temperature with the FHU-I antibody diluted 1:100 in blocking solution. Per slice 200µl of staining solution were used. Afterwards slices were washed three times for 30min in TBS-T. The second primary antibody, as specific marker for the subpopulation, was diluted in the blocking solution according to the manufactures instruction and the slices were incubated for the appropriate time (see table 1). Slices were washed three times for 30min with TBS-T, with the last washing step overnight at 4°C to allow a complete wash-out of unbound primary antibody

and reducing unspecific background staining. The secondary antibody was diluted 1:1000 in blocking solution and the slices were incubated for 2 hours at room temperature on a shaker. Per slice 200µl of staining solution were prepared. The slices were washed three times for 30min on a shaker with TBS-T. The nuclei were stained with Draq5 diluted 1:1000 in TBS-T for 30min. Afterwards slices were also stained with DAPI diluted 1:1000 in TBS-T for 30min. Slices were washed three times for 30min in TBS-T, followed by a last washing step in Milli-Q before the mounting process. Finally slices were mounted on object slides and excess Milli-Q was removed with Whatmann paper. The slices were embedded in Moviol and a coverslip was used to cover the slice, while avoiding the generation of air bubbles. The expression of Cofilin 2 in neuronal subpopulations was analyzed with a confocal microscope.

antibody	company	dilution	host	condition	Marker
Calbindin	Sigma	IF 1:400	Ms mono	ON at 4C	Subpopulation of inhibitory neurons
Parvalbumin	SYSY	IF 1:1000	Ms	ON at 4C	Subpopulation of inhibitory neurons
Tyrosine-hydroxylase	SYSY	IF 1:500	Gp	ON at 4C	Dopaminergic neurons
Tryptophan-hydroxylase	Sigma	IF 1.250	Ms	ON at 4C	Serotonergic neurons
Choline-acetyltransferase	Abcam	IF 1:500	Ms	ON at 4C	Cholinergic neurons
vGLUT1	Millipore	IF 1:500	Gp	ON at RT	Cortical terminals of glutamatergic neurons
vGLUT2	SYSY	IF 1:500	Gp	ON at 4C	Glutamatergic neurons of the thalamus
FHU-I	polyclonal Witke lab	IF 1:100	rabbit	48h at RT	Cofilin 2
PSD95	Millipore	IF 1:500	Ms	ON at RT	Postsynaptic marker for excitatory neurons
Gephyrin	SYSY	IF 1:250	Ms	ON at 4C	Postsynaptic marker for inhibitory neurons

Table 1: Antibodies used for the colocalization studies. The expression profile of Cofilin 2 was examined in different neuronal subtypes. Therefore colocalization studies between FHU-I (Cofilin 2) and a subtype-specific antibody were prepared. The table shows the used concentrations and conditions for every antibody.

3.4.4. Golgi staining

The Golgi staining is an effective technique to study morphological alterations in neuronal dendrites and dendritic spines. The kit is based on the technique discovered by Camillo Golgi by which a tissue is impregnated in potassium dichromate and silver nitrate, which leads to a microcrystallization of silver chromate in some neurons generating a brownish color. Equal volumes of solution A and B were mixed 24 hours prior to use and covered in the dark to generate the impregnation solution. For every brain 20ml of impregnation solution was needed. The brain was dissected on ice and directly transferred to a snap-cap with 10ml of the impregnation solution and incubated for 2 weeks in the dark on a shaker at RT. After 24 hours the impregnation solution was changed. The brain was transferred into a snap-cap filled with 10ml of solution C and stored at room temperature in the dark for another 72 hours. Thereby the solution was replaced after 24 hours with fresh solution C. The brain was cut to 100µm slices with a vibratome and the slices were transferred onto gelatin-coated microscope slides, which were prepared with a drop of solution C. Excess solution was wiped away with Whatmann paper and the slices were dried at room temperature overnight. On the next day slices were placed vertically into a glass staining rack and rinsed in Milli-Q for two times 4min each. In the meantime staining solution was prepared by mixing 1 part solution D with 1 part solution E and 2 parts of Milli-Q. We used 10ml of solution D and E and 20ml Milli-Q to reach the filling level of the glass rack. The prepared staining solution can be used for up to 100 sections but should be shaken during the different staining steps. The sections were incubated for 10min in the staining solution and rinsed in Milli-Q two times for 4min each. Afterwards sections were dehydrated in 50%, 75% and 95% ethanol for 4min each, followed by four rounds in absolute ethanol for 4min each. The slices were cleared in Xylene three times for 4min each and mounted with Entellan. Sections were dried overnight under the hood. Whole cortex images were taken with the bright field dissecting microscope.

3.4.4.1. Sholl analysis

The Golgi staining was used to perform a Sholl analysis to quantify the dendritic branching and ramification richness of neurons in Cofilin $2^{fl/fl}$ and Cofilin $2^{fl/fl}$ Nestin-Cre animals. One advantage of this method is the fact that only a limited number of cells at random are stained in their entirety, which makes it possible to trace single neurons in the cortical network. Therefore images were taken with the 10x objective of the Leica microscope in the bright field mode. Separate lying neurons in layer III were traced by hand with adobe photoshop to be able to generate a binary image for the analysis with the ImageJ plugin `Sholl analysis`. The starting radius was defined to 20pixel. 50 cells for every genotype were analyzed for

their number of intersections according to the distance to the cell soma. The obtained data was transferred into an excel sheet and an average was calculated. Significance was tested in a two-tailed independent t-test and the standard error was calculated.

3.4.4.2. Dendritic spine analysis

A further advantage of the Golgi staining is the ability to analyze the number and morphology of dendritic spines. Therefore the 60x objective of the Keyence microscope was used to obtain images with the quick full focus mode. This allows the generation of images with an overlay of different layers. Pyramidal layer III neurons in the cortex were analyzed for their number of spines per 10µm. Further also the dendritic spines were classified into three distinct morphological classes: thin, stubby and mushroom. Since the number and shape of spines varies not only for the different cortical layers, but also for different dendritic areas we also divided the pyramidal neurons into three parts: proximal, basal and distal. The number and different shape of spines were counted for every area with the ImageJ software and the `cell count` plugin. For every genotype 25 cells were analyzed and an average was calculated. The significance was tested in a two-tailed independent t-test and a standard error was calculated.

3.5. Electrophysiology

The patch clamp recording technique allows the analysis of the electrical properties and functional connectivity of neurons. Several patch clamp configurations can be used depending on the research interest, but we concentrate here on the whole cell mode. Thereby the membrane patch is disrupted by briefly applying strong suction using a glass micropipette in contact with the membrane, to establish electrical and molecular access to the intracellular space. In the whole cell mode the recording of summed currents flowing through all channels in the entire cellular membrane are possible. In this configuration the diffusible contents of the pipette exchange over time with those in the cell. For this reason the composition of the solution in the pipette should be kept close to the one of the cytosol, but allows also the manipulation of the intracellular space of the cells with certain drugs. When the patch clamp whole cell mode is achieved, two different configurations can be executed, either the current clamp configuration, or the voltage clamp configuration.

3.5.1. Current clamp mode

In current clamp configuration the injected current is controlled by the amplifier, which enables the study of changes in membrane potential. The membrane potential is free to vary

and whatever voltage the cell generates on its own or as a result of stimulation via current injection is recorded. In these configuration baseline properties of the cell, like the excitability, the frequency and shape of action potentials (AP) and the input resistance of the membrane can be analyzed.

3.5.2. Voltage clamp mode

In the voltage clamp mode the membrane potential is clamped at a chosen value, which was -70 mV holding potential for the miniature postsynaptic current (mPSCs) measurements. This allows the measurement of how much ionic current crosses a cell´s membrane at a given voltage. Based on the fact that many ion channels like the NMDA-receptors are voltage-gated ion channels, which open only when the membrane voltage is within a certain range, this is an important method to study the number and kinetic of ion channels. We measured mPSCs in pyramidal neurons of the Ca1 region in the hippocampus in voltage clamp mode. Therefore the patched cell was hold at -70mV and Tetrodotoxin was added to the external solution, which blocks voltage-gated sodium channels and thereby inhibits the generation of AP. Additionally in the internal solution of the micropipettes the toxin QX-134 was added, which has the same effect on sodium channels.

3.5.2.1. Measuring mEPSCs

To analyze mEPSCs Picrotoxin was applied to block $GABA_A$-receptors and inhibited the occurrence of mIPSCs. Supplementary Trichlormethiazide was added, which blocked the desensitization of AMPA-receptors and increased the frequency of mEPSCs. Recorded events were initiated by the release of the excitatory neurotransmitter glutamate, which binds to AMPA-receptors. AMPA receptors are ion channels that conduct sodium and potassium and leads to a positive inward current into the cell. Due to the fact that the cells were hold at -70mV a second important class of glutamate receptors, the NMDA-receptors were blocked. These receptors are doubly gated, first by the neurotransmitter and second by voltage. Channels open only when the membrane potential is raised up to -40mV, due to the fact that a Mg^{2+}-ion functions as a plug at the channel as a result of ionic interactions when the membrane potential is at -70mV. When the membrane potential is increased the potential becomes positive and repels the Mg^{2+}-ion from the channel, thereby allowing the transport of calcium into the cell. The recorded mEPSCs were analyzed for their inter-event interval and their amplitude with the MiniAnalysis (Synaptosoft Inc.) software. Therefore at least 5 minutes or 300 events were recorded and analyzed.

3.5.2.2. Measuring mIPSCs

The frequency and amplitude of miniature inhibitory postsynaptic currents (mIPSCs) were also analyzed. Therefore Tetrodotoxin was used to block the generation of AP and NBQX, which blocked AMPA receptors, ensuring that exclusively inhibitory PSCs were recorded. Local inhibitory neurons in the Ca1 region of the hippocampus spontaneously release the neurotransmitter GABA, which binds on postsynaptic $GABA_A$-receptors of pyramidal neurons and generates a mIPSC. These $GABA_A$-receptors are ion channels, which conduct the passage of chloride ions into the cell and decrease the intracellular membrane potential further, which could cause a hyperpolarization or could impact on incoming depolarizing currents to prevent the generation of an AP. The inter-event interval and the amplitude of mIPSCs were calculated with the MiniAnalysis software from Synaptosoft Inc.. Therefore at least 5 minutes or 300 events were detected and analyzed.

3.5.3. General preparation of mice for electrophysiology

All electrophysiological studies were performed on P21 - P28 old animals from the Cofilin 2 Nestin-Cre mouse line. Animals were killed by decapitation. The brain of the animal was dissected and placed in ice-cold Sucrose-aCSF. The cerebellum and the frontal part of the cortex were removed and the brain was glued with the rostral part to a vibratome cutting plate. A vibratome (Leica) was used to cut the brain in 300µm coronal slices, while the brain was maintained in ice-cold Sucrose-aCSF bubbled with O_2 with 5% CO_2. Slices were transferred to 37°C bubbled Sucrose-aCSF and incubated for 30 minutes in this solution. After 30 minutes slices were transferred to room temperature aCSF and were incubated for one more hour before cells were patched. Therefore the slice was placed in a chamber filled with aCSF. The aCSF also contained reagents like TTX, Picrotoxin or NBQX. A pump was used to perfuse the aCSF through the recording chamber. With a 60x objective the Ca1 region of the hippocampus was sought and healthy cells were patched. Therefore a glass capillary puller was used to prepare recording pipettes with a resistance of 3-4MΩ. The glass pipette was tip filled and back filled with 150µl of intracellular solution. To patch a cell the glass pipette was placed on a pipette holder and put into the bath to focus on the micropipette tip. During this procedure mild pressure was applied and hold in the pipette. The brain slice was approached by the micropipette by moving the micromanipulator while focusing on the pipette. When the amplifier was set to voltage clamp, the pipette offset was corrected so that the currents measured were considered as 0pA. A test puls was given to monitor the cell resistance during the patching process. When the tip touched the cell body the pressure was released to obtain a GΩ seal. Thereby a GΩ seal is characterized by a

resistance that reaches at least 1GΩ. During the sealing process a negative voltage close to the cells resting potential was applied to hold the cell later at -70mV. To break through the membrane a short suction pulse was applied. When the membrane was opened the program Clampfit was used to acquire 1minute recordings. For every patched cell at least 10 minutes were recorded.

3.6. Behavioral analysis of Cofilin 2 Nestin and ADF Cofilin 2 Nestin animals

The deletion of Cofilin 1 in the forebrain with a CamKII-Cre leads to abnormalities in the behavior of animals (Rust el al; 2010; Zimmermann et al; 2015; Goodson et al; 2012). Western blot and colocalization studies revealed the expression of Cofilin 2 in brain areas and neuronal subpopulations responsible for anxiety, memory and locomotion. Therefore the Cofilin 2 Nestin-Cre and ADF Cofilin 2 Nestin-Cre animals were tested in some basic behavioral tests to get a first insight into cognitive functions, anxiety-related behavior or locomotion that could be altered due to the loss of Cofilin 2 or the dual deletion of ADF and Cofilin 2. For behavioral test only male mice between the age of P60 and P120 were used. As controls littermates with the genotype Cofilin $2^{fl/fl}$ or $ADF^{-/-}$ Cofilin $2^{fl/fl}$ were used, while the mutant was genotyped as Cofilin $2^{fl/fl}$ Nestin-Cre or $ADF^{-/-}$ Cofilin $2^{fl/fl}$ Nestin-Cre. Mice were held in the isolator and brought to the behavior room in their home cages. All male mice were held in a group of two animals to avoid changes due to different home caging conditions. The tail of one mouse was marked and the animals were kept untouched for 30min before the test was started to avoid an increased locomotor activity of the animals based on the transport and change in environment. Additionally the light was dimmed in the room to avoid stressful factors for the animals, which could also lead to hyperactivity. Animals were placed in the respective apparatus and filmed by a camera to analyze their movement and behavior with the software ANY-maze. During the run the center point of the animal was tracked and a maximum of 20positions/sec was recorded. Between different trials the apparatus was cleaned with ethanol to remove odor cues. Traces of urine and defecation were removed before with Milli-Q. Three different behavioral tests were performed and the exact handling of animals for every apparatus is explained in detail in the following chapters.

3.6.1. Open field

The open field test provides an opportunity to assess novel environment exploration, general locomotor activity and provides an initial screen for anxiety-related behavior in rodents. Additionally due to an elongated test session also the habituation process can be analyzed. The open field is built out of four square chambers with a size of 45x45 cm. In every chamber

one mouse can be placed so that four mice can be analyzed in parallel. The open field was divided with the AYN-maze software into two different zones: the center area and the periphery and different paradigms were recorded with the software for every zone, like zone entries, time spent there and the freezing- and immobility-times. Therefore the animal was placed in the center of the apparatus and was allowed to freely explore the apparatus for a test session of 60min, while tracking the midpoint of the animal as center point. During the test session repetitive behaviors, like rearing in the center or at the wall and the number of grooming performances were manually counted by the experimenter. To assess the number of freezing episodes and the time spent freezing the detection of freezing was based on a minimum freeze duration of 250ms and a freezing rate of 6 to 16%. The minimum immobility was based on 50% and minimum immobility duration was set to 1000ms. The locomotor activity was measured in the total distance travelled during the 60min test session. For assessing exploratory behavior the 60min test session was divided into 5min bins and the number of center entries and the time spent there were examined in these 5min bins and compared between wt and mt animals. A session lasting longer than 30min allows also the detection of habituation to an increasingly familiar chamber environment, which is due to a synaptic depression of connections involved in exploratory behavior. Therefore the total distance travelled and the immobility time was examined in 5min bins for the 60min test session and changes between wt and mt were analyzed. The open field enables also an initial screening for anxiety-like behavior which is influenced by two factors during the session: first is social isolation resulting from the physical separation from cage mates while performing the test; second is the stress created by the brightly lit and unprotected center area. Therefore the freezing rates in the center and the periphery and the number of center entries were examined. Mice will typically spend significantly more time exploring the periphery of the open field than the unprotected center area. An increased time in the center area would reflect a reduced anxious-like baseline behavior. For the Cofilin 2 Nestin mouse line nine mice per genotype were analyzed and for the ADF Cofilin 2 Nestin mouse line 10 animals per genotype.

3.6.2. Elevated Plus Maze

The elevated plus maze takes advantage of an approach-avoidance conflict between the natural tendency of mice to explore a novel environment and an anxiety evoking stimulus. Therefore this test can be used to study anxiety-like behavior in rodents. The apparatus (figure 18) consist of two sets of opposing arms with a length of 37cm and width of 5cm extending from a central area (5x5cm). During a test session of 5min mice were allowed to freely explore the maze and decide between spending time in enclosed protected arms, or in open unprotected arms. Thereby the maze was also lifted 1m above the ground. Mice tend to

avoid the open arms since they induce an anxiolytic stimulus and stay in the protected enclosed arms. At the beginning of the experiment the mouse was placed in the central region and the number of open and closed arm entries and the time spent there was determined. Additionally also the number of stretch-attend postures were counted manually by the experimenter, since they are risk-assessment behaviors which indicate that the animal is hesitant to move to a new position. A high frequency of these postures indicates a higher level of anxiety. To exclude the possibility that a higher number of open arm entries was only related to an increased locomotor activity also the total number of arm entries was compared between wt and mt animals. To compare the time wt and mt animals stayed immobile the immobility detection was set to 70% with a minimum immobility period of 2000ms. Nine mice per genotype were analyzed for the Cofilin 2 Nestin mouse line, and ten mice per genotype for the ADF Cofilin 2 Nestin mouse line.

Fig. 18: Elevated plus maze (EPM): a behavioral device to analyze anxiety-like behavior in animals. The EPM consists of four arms: two which are enclosed and protected arms, and two open and unprotected arms. The EPM is elevated 1m above the ground. Mice were placed in the middle area and could freely explore the apparatus for 5min. Thereby mice tend to avoid the open arms and mice that spent more time exploring the unprotected area reflect a reduced anxiolytic behavior.

http://www.stoeltingco.com/anymaze/mazes/anxiety-depression/elevated-plus-maze.html

3.6.3. Y-maze

Mazes are experimental devices employed for evaluation of spatial memory in rodents. The Y-maze analysis spontaneous alternations, which are a reference procedure to assess the working memory. Thereby the working memory is a type of short-term memory that allows the animal to remember which arm it had visited before. This memory function depends on the hippocampus since place cells in the hippocampus fire whenever the animal enters a specific location. The Y-maze consists of three arms with a length of 35cm and 5cm width. For this test mice were placed at the end of the X- arm and were allowed to freely explore the maze for 10min. When walking out of an arm of the maze, the animal remembers from which arm it came and explores the third arm finalizing a complete alternation or sequence (X-Y-Z). If the animal revisits the arm it had encountered before the actual one, the animal displays a failed sequence (X-Y-X). The animal could also stayed in one arm, go back to the center area and then visited exactly the same arm it had just left, which was marked as same arm

return (X-center-X). During the exploration of the maze the sequence of arm visits was written down by the experimenter and analyzed afterwards for the occurrence of sequences, fails and same arm returns. The total number of arm visits was calculated as 100% and the relative number of sequences, fails and same arm returns were calculated for every animal. An average was calculated from nine mice per genotype of the Cofilin 2 Nestin and for ten mice per genotype of the ADF Cofilin 2 Nestin mouse line. The standard error was calculated and the significance was tested in a two-tailed independent T-test.

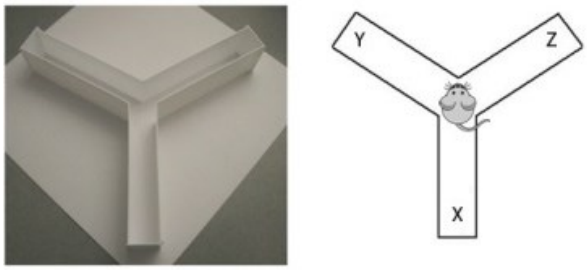

Fig. 19: Working memory was tested in a Y-maze. A behavioral test to assess working memory is the Y-maze device, which is used to count the numbers of spontaneous alternations. Therefore mice were placed in the X- arm and could freely explore the maze for 10mins. The sequence of visited arms was noted by the experimenter and afterwards analyzed for the occurrence of sequences (X-Y-Z), failed sequences (X-Y-X) and same arm returns (X-Center-X).

http://sbfnl.stanford.edu/cs/bm/lm/bml_ymaze.html

4. Results

4.1. Expression profile of Cofilin 2 in the brain

4.1.1. Cofilin 2 is ubiquitously expressed in the brain

Cofilin 1 expression in the brain is highest in the neural fold at E9.5 and the expression persists in the developing nervous system displaying a ubiquitously expression in the adult brain. In contrast ADF is expressed at low levels during embryonic development and displays a postnatal upregulation in epithelial cells and the brain (Gurniak et al., 2005; Vartiainen et al., 2002). Thereby Cofilin 1 and ADF exhibit a coexpression in the brain, while the Cofilin 2 expression was thought to be more restricted to the muscle. Gurniak et al could show that Cofilin 2 is also expressed in the brain (Gurniak et al., 2014). The complete deletion of Cofilin 2 is lethal around postnatal day 7 (P7), due to a malformation of the diaphragm which leads to respiratory problems (Gurniak et al., 2014). Morphological analysis of neuromuscular junctions did not reveal pathological changes, which leads to the conclusion that a possible neuronal function is independent of the muscular phenotype. So the question remains still open, why Cofilin 2 is also expressed in the brain although two actin depolymerization factors are already localized to the brain (Bellenchi et al., 2007; Gurniak et al., 2005). Therefore a more detailed expression profile of Cofilin 2 in wt animals and a possible overexpression of Cofilin 1 or ADF in distinct brain regions of mt animals, as compensation for the loss of Cofilin 2, were examined. Preparation of protein lysates of defined brain regions at P7 were prepared and analyzed in a SDS-PAGE. To verify that the same amount of protein was loaded for every probe the blots were also incubated with a GAPDH antibody. Thereby GAPDH displays a strong expression in every tissue and was unaffected by the Cofilin 2 knockout. For every ADF/Cofilin family member also a positive control was loaded onto the gel, to verify the functionality of the used antibodies. To analyze the expression level of Cofilin 2 the membrane was incubated with the primary antibody FHU-I and a muscle lysate served as a positive control. Protein lysates for the following brain regions were prepared from Cofilin $2^{+/+}$, Cofilin $2^{+/-}$ and Cofilin $2^{-/-}$ animals: cortex, hippocampus, striatum, olfactory bulb, cerebellum and midbrain (overview in figure 6).

With the blots shown in Fig. 20 it was possible to confirm the complete knockout of Cofilin 2 and check if Cofilin 2 was expressed in every brain region. As expected the complete absence of Cofilin 2 expression in every brain region was displayed in Cofilin 2 knockout animals. The functionality and specificity of the FHU-I antibody was confirmed through the signal in the muscle control, which served as a positive control for this antibody. Further the specificity of the antibody could be clarified by the molecular weight of the obtained band, which was located above the marker band of the 17kDa myoglobin-red band. Proteins were

separated depending on their mass, which enabled the comparison with the marker bands for their identification. Cofilin 2 has a molecular weight of 19kDa.

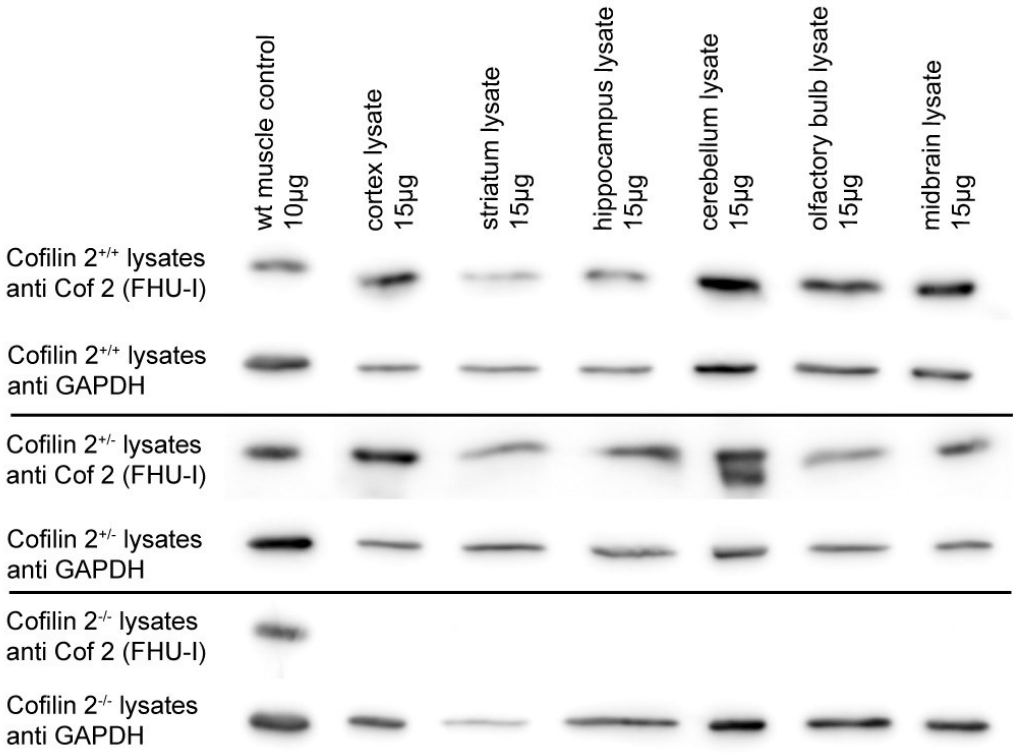

Fig. 20: Comparison of the expression levels of Cofilin 2 in different brain regions at P7 and the verification of the Cofilin 2 knockout in the brain. Protein lysates of different brain regions of P7 Cofilin 2 wt, heterozygote and knockout animals were prepared and 15µg were loaded onto a 15% SDS gel. The membrane was incubated with the specific Cofilin 2 antibody FHU-I. As a loading control the membrane was also incubated with a GAPDH antibody to verify that the same amount of total protein concentration was loaded. The muscle lysate served as a positive control for the FHU-I antibody. The Blot allowed the comparison of the Cofilin 2 expression level in different brain regions and confirmed the complete knockout of Cofilin 2 in the brain at P7.

Additionally these blots confirmed the ubiquitously expression of Cofilin 2 in all analyzed brain regions. To be able to compare the expression levels of Cofilin 2 in different brain regions, the obtained Cofilin 2 signal was normalized to the GAPDH signal. The GAPDH loading control in the wt lysates did not displayed a uniform signal and indicated a stronger signal in the cerebellum lysate. In the heterozygote lysates the GAPDH signal was more uniform and showed an equally strong signal. After normalization of the blots seen in Fig. 20, the strongest expression for Cofilin 2 in the wt lysates could be seen in the midbrain and cerebellum, followed by the cortex and the olfactory bulb lysates. The weakest expression of Cofilin 2 was displayed in the striatum and hippocampus lysates. In comparison, in the Cofilin $2^{+/-}$ lysates the highest expression level could be seen in the cerebellum, followed by the cortex, hippocampus and midbrain and the weakest expression in the olfactory bulb and the

striatum. But the bands were not reduced to about 50% due to the loss of one Cofilin 2 allele in every brain region. In the hippocampus and striatum lysates the band was also stronger than in the Cofilin 2 wt lysates. This could be explained by the fact that for every genotype a different blot was prepared so that a comparison between the signals was not possible. Only when all lysates are loaded on the same blot a direct comparison in the signal strength is possible. A direct comparison between all three genotypes was done in the Fig. 21. Another difference could be seen in the cerebellum lysate, which displayed a double band in the Cofilin 2 heterozygote lysate, which could be due to degradation in this protein lysate.

In summary Cofilin 2 displayed a ubiquitously expression in the brain at P7, the time point when the complete knockout of Cofilin 2 becames lethal.

4.1.2. The loss of Cofilin 2 leads to an upregulation of ADF and Cofilin 1 in certain brain areas

Although all three isoforms of the ADF/Cofilin family have similar biochemical properties and overlap in their expression profile in the brain, the deletion of one member in the brain leads to a distinct phenotype. Cofilin 1 is the predominant ADF/Cofilin family isoform in the adult brain (Gurniak et al., 2005) and also in the cortex of P0 animals (Bläsius 2012). The loss of Cofilin 1 is associated with an upregulation of ADF in the adult brain to compensate for the Cofilin 1 deficiency (Bläsius 2012; Rust et al., 2010). In contrast to that is the complete deletion of ADF not accompanied by an upregulation of Cofilin 1 (Bellenchi et al., 2007; Gorlich et al., 2011). In this study specific brain regions were analyzed for an upregulation of ADF or Cofilin 1, which could give a hind for a specific function of Cofilin 2 in certain brain areas. Additionally the upregulation of ADF/Cofilin family members could prevent a possible brain-restricted phenotype of Cofilin 2 knockout animals at P7. Thereby a functional compensation from ADF or Cofilin 1 has to take place, meaning that Cofilin 2 and ADF or Cofilin 1 are both involved in the same functional processes in the brain.

The expression level of all three ADF/Cofilin family members were analyzed in lysates of Cofilin 2 wt, heterozygote and knockout animals of distinct brain regions. Therefore lysates of all three genotypes were loaded onto a gel and the membrane was incubated with specific antibodies for Cofilin 2 (FHU-I), Cofilin 1 (KG60) and ADF (7D10). For every antibody also a positive control was included, which was a brain lysate for Cofilin 1, a uterus lysate for ADF and a muscle lysate for Cofilin 2. GAPDH served as a normalization control to verify equal loading. The Western Blots in Fig. 21 confirmed the complete deletion of Cofilin 2 in the different brain areas of Cofilin $2^{-/-}$ lysates. Additionally a reduction in the expression level of Cofilin 2 was observed in Cofilin $2^{+/-}$ lysates in comparison to Cofilin $2^{+/+}$ lysates.

Densitometric analysis was performed after normalization with the GAPDH signal to quantify the amount of proteins. To analyze the Cofilin 2 reduction in the different brain regions the absolute intensity of the Cofilin $2^{+/+}$ lysate was set to 100% and compared to the absolute intensity of Cofilin $2^{+/-}$ lysates. The strongest reduction in the Cofilin 2 expression level was detected in the olfactory bulb (49%), followed by the cortex (54%) and midbrain (59%). A moderate reduction was detected in the hippocampus (62%) and cerebellum (71%). Almost no reduction in the Cofilin 2 expression level was detected in Cofilin $2^{+/-}$ striatum lysates (90%).

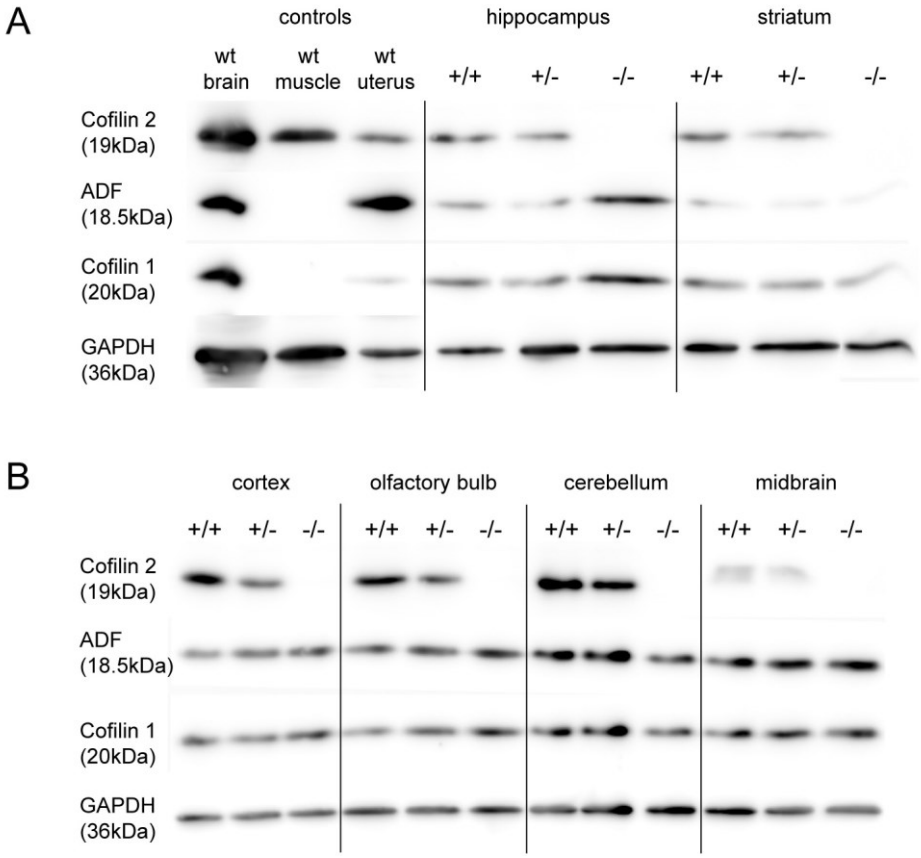

Fig. 21: Comparison of the expression levels of ADF/Cofilin family members in different brain regions at P7. Lysates of the hippocampus and striatum (A), as well as cortex, olfactory bulb, cerebellum and midbrain (B) were prepared from P7 littermates from Cofilin $2^{+/+}$, $^{+/-}$ and $^{-/-}$ animals and loaded onto a 15% SDS gel. The membrane was incubated with antibodies against Cofilin 2 (FHU-I), ADF (7D10) and Cofilin 1 (KG60) to confirm a possible upregulation of ADF or Cofilin 1 due to the loss of Cofilin 2. As a loading control the blot was also incubated with a GAPDH antibody. The antibodies for Cofilin 2 and ADF were incubated on the same blot, since both primary antibodies were made in different species (rabbit and mouse). For Cofilin 1 a second blot was prepared, due to the close molecular weight between the different isoforms and the generation of the KG60 antibody also in rabbit. Both blots were simultaneously incubated with the same antibody. The brain control served as a positive control for KG60 (Cof1), the muscle lysate for FHU-I (Cof2) and the uterus lysate for 7D10 (ADF).

The blots shown in figure 21 were also used to analyze the possible upregulation of ADF or Cofilin 1, due to the loss of Cofilin 2. Densitometric analyses were performed on the obtained

signals for Cofilin 2 after normalization to the GAPDH signal. Interesting to mention is that if an upregulation in a brain area at P7 occurred, both ADF and Cofilin 1 were upregulated, although to a various degree. In figure 21 an upregulation of ADF and Cofilin 1 in the cortex, midbrain and olfactory bulb lysates of Cofilin $2^{-/-}$ lysates could be detected. The strongest upregulation for both ADF and Cofilin 1 was observed in the hippocampus lysates of knockout animals (figure 21A). In the hippocampus the upregulation of ADF (360%) was almost double compared to the Cofilin 1 upregulation (170%). In the Cofilin $2^{-/-}$ striatum lysate a reduction for both ADF/Cofilin family members could be observed, but in this lysate also the reduction in the Cofilin 2 expression level in Cofilin $2^{+/-}$ lysates was not detected. Further could been shown that ADF also displays a broad expression in every analyzed brain region, which is important for the analysis of double knockout animals for ADF and Cofilin 1 or Cofilin 2. All three members of the ADF/Cofilin family share a 82% sequence homology. Therefore the molecular weight of all three members is in a close range, ranging from 18,5kDa for ADF to 20kDa for Cofilin 1. Therefore the control of the antibody specificity on the blots is quite important. For this reason a specific positive control was loaded for every used antibody. Cofilin 2 is known to be the muscle-specific isoform and only FHU-I generated a signal in the muscle lysate (figure 21A). For Cofilin 1 an adult brain lysate was loaded and only in this control a strong signal is detectable for Cofilin 1, but also a faint one in the uterus lysate. The positive control for ADF is a uterus lysate, which displayed a clear signal for ADF. All three isoforms could be detected in the adult brain lysate. To ensure a complete separation of all three isoforms a high-percentage gel with 15% acrylamide was used and the gel run until the lower marker bands between 17kDa and 25kDa were highly separated.

In summary the complete knockout of Cofilin 2 was compensated by an upregulation of ADF and Cofilin 1 in the hippocampus, cortex, midbrain and olfactory bulb at postnatal day 7, when the complete knockout becames lethal.

4.1.3. The highest expression of Cofilin 2 is detected at the beginning of synaptogenesis

Synapses are key structures in the neural network and the functional state of the network is reflected in the formation, rearrangement and degeneration of synapses. The formation of synapses between neurons occurs during early brain development, with a peak at P7. At the onset of synaptogenesis immature synapses are innervated by multiple axons, but during maturation a decline in the number of innervations occurs, which leaves behind only one functional axonal input. This process is known as synaptic pruning. The pruning process requires the retraction of axons from synaptic connections, which is an actin-dependent step (Tahirovic and Bradke 2009). At P10 the end of the initial growth stage is obtained and a

major transcriptional change is initiated leading to a decline in the number of synapses at P15. Oppenheimer and Schwartz showed that between P7 and P15 a large difference in the number and density of synapses develops, which is important to create a specific and mature circuitry (Oppenheimer and Schwartz 1997). After P21 a partial recovery of synapses could be detected, which is due to the process of learning. Additionally in adult animals a process called synaptic plasticity is responsible for the strengthening and weakening of mature synapses due to the process of learning and memory. Thereby a decrease in synaptic strength is associated with a decrease in the number of transmitter vesicles released from presynaptic terminals and a reduced mobilization of vesicles to the active zone, all processes which are known to be regulated by actin (Nelson et al., 2013; Rust and Maritzen 2015). Therefore the question was addressed whether the expression level of Cofilin 2 is altered during important steps of synaptogenesis. To analyze the expression levels of Cofilin 2, protein lysates of different brain regions at distinct developmental stages were analyzed. To check for changes in the expression levels of Cofilin 2 lysates of P0, P7, P15, P21 and adult (P90) wt animals were compared. To normalize the obtained Cofilin 2 expression levels to the GAPDH loading control, the Multi Gauge software was used. The average was calculated from three different litters (n = 3). To compare the Cofilin 2 expression level between the brain regions, the P0 cortex result was set as 100%. Based on the P0 cortex the relative numbers for all other brain regions were calculated and are displayed in single graphs for every brain region (figure 22). Additionally the respective Western blots are displayed in figure 22.

For all analyzed regions, except the cortex and the cerebellum, the highest expression of Cofilin 2 was around the time point P7. After P7 a decline in these regions occured. In the hippocampus the Cofilin 2 expression increased again between P15 and P21 and stayed at that level until adulthood. The striatum showed after the decline between P7 and P15 a constant Cofilin 2 expression level until an upregulation in adulthood occurred. In the olfactory bulb a further decrease in the Cofilin 2 expression from P15 to P21 took place. Between P21 and P90 the expression level stayed constant. After the decline at P7 the Cofilin 2 concentration in the hypothalamus remained constant and showed an increase in the adult animals. In the midbrain no changes in the expression level of Cofilin 2 between P15 and P21 could be detected, but a further decrease in the adult animal is reflected. The strongest Cofilin 2 expression in the cortex occurred at P0. After P0 a steady decrease in the expression level of Cofilin 2 is detected. In contrast, in the cerebellum the highest expression of Cofilin 2 is revealed in the adult animals. Between P0 and adulthood the level of Cofilin 2 did not vary greatly in the cerebellum.

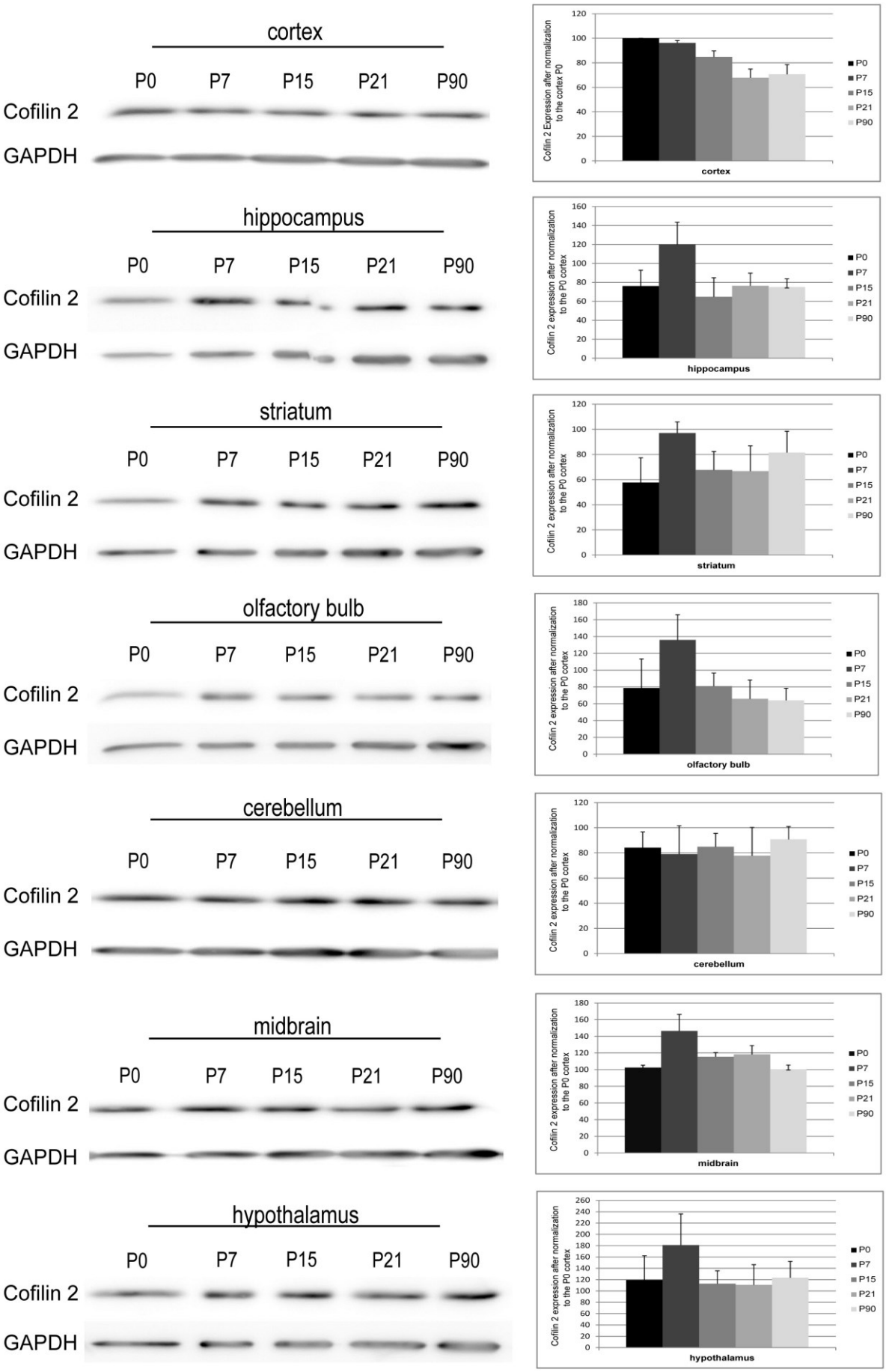
cortex
P0 P7 P15 P21 P90
Cofilin 2
GAPDH
Cofilin 2 Expression after normalization to the cortex P0
cortex
hippocampus
Cofilin 2 expression after normalization to the P0 cortex
hippocampus
striatum
striatum
olfactory bulb
olfactory bulb
cerebellum
cerebellum
midbrain
midbrain
hypothalamus
hypothalamus
P0
P7
P15
P21
P90

Fig. 22: Analysis of Cofilin 2 protein levels at developmental steps during synaptogenesis in wt animals. Protein lysates of different brain regions of wt animals were prepared at P0, P7, P15, P21 and P90 and 15µg were loaded on a 15% SDS gel. The membrane was incubated with a specific antibody for Cofilin 2 (FHU-I). GAPDH served as a loading control. The obtained Western-blot signals for the Cofilin 2 expression were normalized to the obtained GAPDH signal for every probe with the Multi Gauge software. The average was calculated (n = 3). To compare the obtained Cofilin 2 level in different brain regions, the result for the P0 cortex was set as 100% and expression level of other regions were calculated based on the P0 cortex. The standard error was calculated.

In summary the highest expression of Cofilin 2 for all analyzed brain regions was dispayed at the onset of synaptogenesis around P7, except for the cortex and cerebellum. Interestingly, around this time point also the complete knockout of Cofilin 2 becames lethal.

4.1.4. Analysis of the Cofilin 2 expression in different neuronal subtypes

During the development of the central nervous system neuronal progenitor cells generate an enormous number of distinct types of neurons and glial cells. Intrinsic genetic programs define the combinations of transcription factors that determine the cell fate, e.g. by the expression of specialized enzymes for the synthesis of neurotransmitters, which marks the cell to a specific neuronal subtype. The obtained results from the Western blot analyses displayed a broad expression pattern of Cofilin 2 in all different brain regions. Therefore the next step was to take a closure look at specific neuronal subtypes in different brain regions. Vibratome sections of adult wt animals were prepared and stained for Cofilin 2 in combination with a second antibody specific for a distinct neuronal subtype. A colocalization between both antibodies indicates an expression of Cofilin 2 in the respected neuronal subtype.

4.1.5. Cofilin 2 is expressed in distinct classes of inhibitory neurons

Only 20-25% of all neurons in the cortex are inhibitory neurons, but they convey important functions. Although the number of inhibitory neurons in contrast to excitatory neurons is relatively low, they reflect a great diversity. A classification is based on their morphology, size, intrinsic properties, connectivity patterns and gene expression. One way to classify inhibitory neurons into subgroups is the occurrence of three different calcium-binding proteins: Parvalbumin, Calbindin and Calmodulin. In this study a focus on the two proteins parvalbumin and calbindin was examined, which are localized to specific mostly non-overlapping subpopulations of inhibitory neurons, based on their association to separate

functional systems (van Brederode et al., 1991). Parvalbumin is localized to fast-spiking, non-adapting interneurons, while calbindin is present in regular-spiking interneurons (Markram et al., 2004). To analyze the expression of Cofilin 2 in inhibitory neurons immunofluorescence stainings with the Cofilin 2 specific antibody FHU-I and parvalbumin or calbindin on adult wt vibratome sections were prepared (figure 23 and 24).

An overlap in the expression of calbindin and Cofilin 2 was observed in different subtypes of inhibitory neurons. Thereby the Cofilin 2 staining in interneurons was localized to the cell soma, but was also observed in the nucleus. A first region that was analyzed for a colocalization between Cofilin 2 and inhibitory neurons was the cerebellum. Calbindin-positive cells in the cerebellum were exclusively found in the Purkinje cell layer, which only contains one type of inhibitory Purkinje cells. These Purkinje cells were also positive for Cofilin 2. Additionally a few Cofilin 2-positive cells were found in the molecular layer, which contains stellate and basket cells. A second region that was analyzed for the colocalization between calbindin and Cofilin 2 was the cortex. In the cortex calbindin positive cells in the layer II/III of the motor cortex were analyzed, which marks them as inhibitory smooth non-pyramidal neurons. Calbindin mainly marks double bouquet cells and Martinotti cells in the cortex. Thereby Martinotti cells are found in layer II – VI and are specialized in projecting their axons towards layer I, where they inhibit the tuft dendrites of pyramidal neurons. Additionally their axons can also project horizontally in layer I to inhibit dendrites in neighboring columns and are thereby the only source for cross-columnar inhibition (DeFelipe 2002). These cells can also target multiple domains including proximal and perisomatic dendrites, as well as cell somata. Thereby Cofilin 2 could fulfill an important function in the remodeling of the actin cytoskeleton in presynaptic terminals to regulate synaptic vesicle release that controls firing patterns of pyramidal neurons in layer I. In contrast, double bouquet cells are only dendritic-targeting cells with a bitufted dendritic morphology that seems to be involved in the inhibition of basal dendrites (DeFelipe et al., 1990). Their axons branch frequently to form higher-order branches with densely studded boutons. These calbindin-positive cells were also positive for Cofilin 2, showing that Cofilin 2 was expressed in smooth non-pyramidal neurons. In these cells Cofilin 2 could fulfill a function in the actin remodeling during the dendritic arborization and axon branching process. But most of the cells in the cortex were exclusively positive for Cofilin 2, which leads to the suggestion that Cofilin 2 could be also localized to excitatory pyramidal cells, which represent the main class of neurons in the cortex. Another possibility would be excitatory spiny stellate cells, which are not positive for calbindin. In the third analyzed region, the striatum, Cofilin 2 colocalized with calbindin-positive cells that mark medium spiny neurons (Bennett and Bolam 1993). These medium spiny neurons are GABAergic and make up 90% of all cells in the striatum. Besides the localization of Cofilin 2 to the cell soma, a punctate staining of FHU-I could be also

examined in the striatum, which could result from afferent terminal endings, which innervate the striatum.

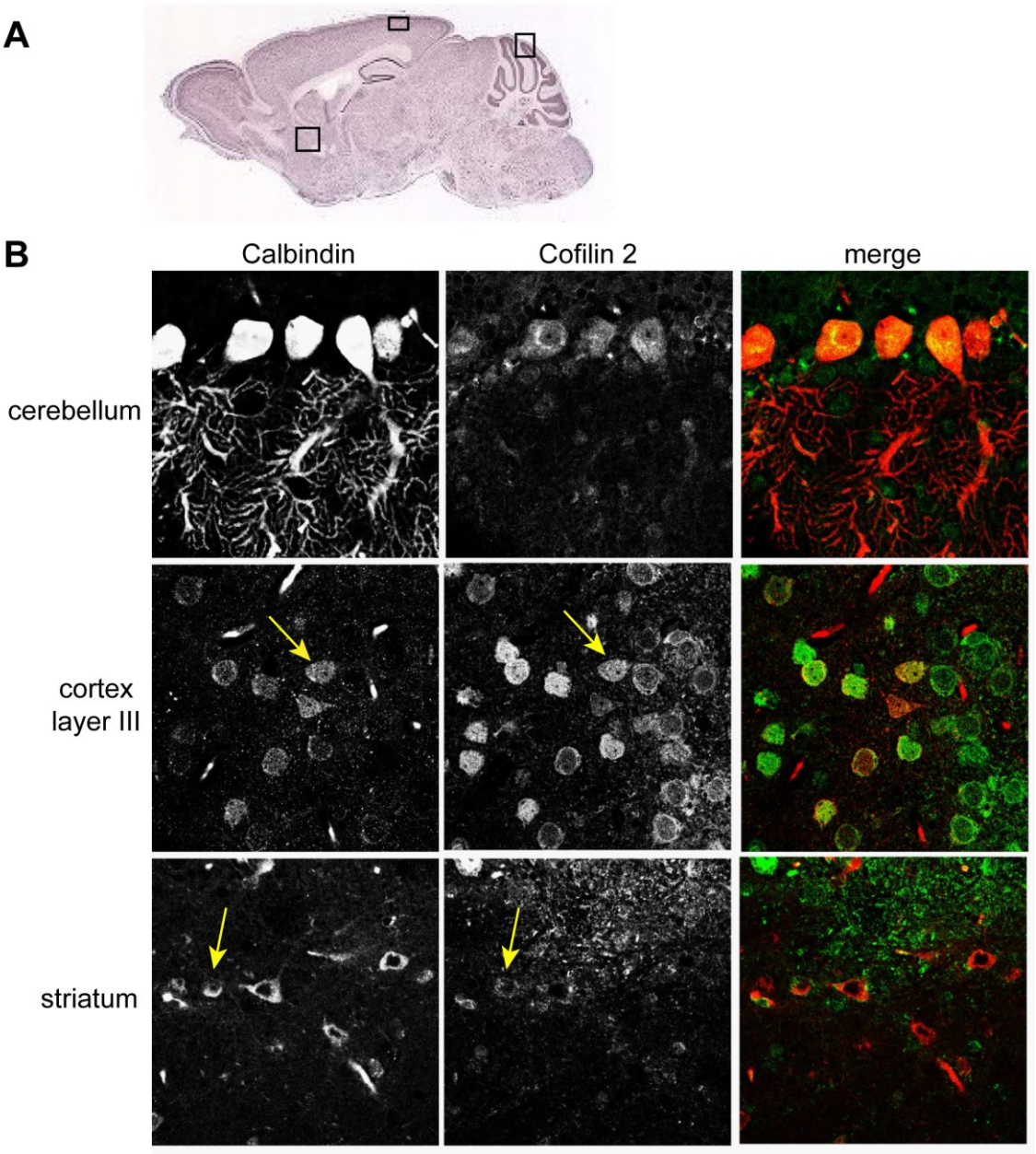

Fig.23: Cofilin 2 is expressed in Purkinje cells of the cerebellum, smooth non-pyramidal neurons in the cortex and in medium spiny neurons of the striatum. A Nissl staining of a sagittal mouse brain section. Analyzed regions were marked. **B** Vibratome sections of adult wt animals were stained with the antibodies FHU-I for Cofilin 2 and Calbindin, which marks inhibitory neurons. The cerebellum, cortex and striatum were analyzed for a possible colocalization between Cofilin 2- and Calbindin-positive cells. The FHU-I staining was detected via the secondary antibody Alexa488, and the Calbindin staining via Alexa594. Nuclei were stained with Draq5 and are shown in blue. Yellow arrows indicate cells which showed a colocalization between both antibodies, but not all FHU-I positive cells displayed also a staining for Calbindin. Images were obtained at 63x magnification. Scale bar: 20µm

A second marker for a subset of inhibitory neurons is parvalbumin, which is also a calcium-binding protein that is localized to fast-spiking interneurons. The parvalbumin antibody displayed a punctate neuropil labeling and a strong staining of the cell soma.
A colocalization between parvalbumin and Cofilin 2 was analyzed in the cerebellum. In figure 23 Cofilin 2-positive cells were found in the molecular layer, which were not stained by calbindin. These cells can be marked by parvalbumin and are inhibitory stellate and basket cells (figure 24). These cells in the molecular layer form GABAergic synapses onto dendritic branches of Purkinje cells. Therefore a colocalization between parvalbumin and FHU-I could be examined in these stellate and basket cells (figure 24). Additionally parvalbumin was also localized to Purkinje cells, which displayed again a colocalization with the Cofilin 2 antibody.
Parvalbumin is also expressed in principal sensory and motor relay nuclei in the thalamus, which project back to the cortex and form the sensory input that is used as a basis for perception (Jones and Pons 1998). In these cells a Cofilin 2 expression was also examined. Additionally a few more cells were positive for Cofilin 2, which were not stained by parvalbumin. These could be relay cells which were only positive for calbindin (data not shown) and project to layer I of the somatosensory cortex (Rausell et al., 1992). These calbindin positive cells form a basis for the engagement of multiple aspects of sensory experience into a single framework of consciousness. In the thalamus nuclei could be distinguished by different patterns of parvalbumin- and calbindin-positive cells, and reflect that thalamic cells belong to different functional systems that also project differentially into the cortex (Magnusson et al., 1996). Cofilin 2 was expressed in both analyzed thalamic systems, since principal sensory and motor relay cells (marked by parvalbumin) and relay cells stained by calbindin were positive for Cofilin 2.
In the striatum we already confirmed the expression of Cofilin 2 in medium spiny neurons. A second cell type in the striatum are fast-spiking GABAergic interneurons, which participate in feed-forward inhibition of principal neurons and are positive for parvalbumin. In these cells no colocalization between FHU-I and parvalbumin was observed, excluding the expression of Cofilin 2 in fast-spiking interneurons (figure 24).

In summary Cofilin 2 was localized to a subset of inhibitory neurons in different brain regions, but no expression of Cofilin 2 was detected in fast-spiking inhibitory neurons.

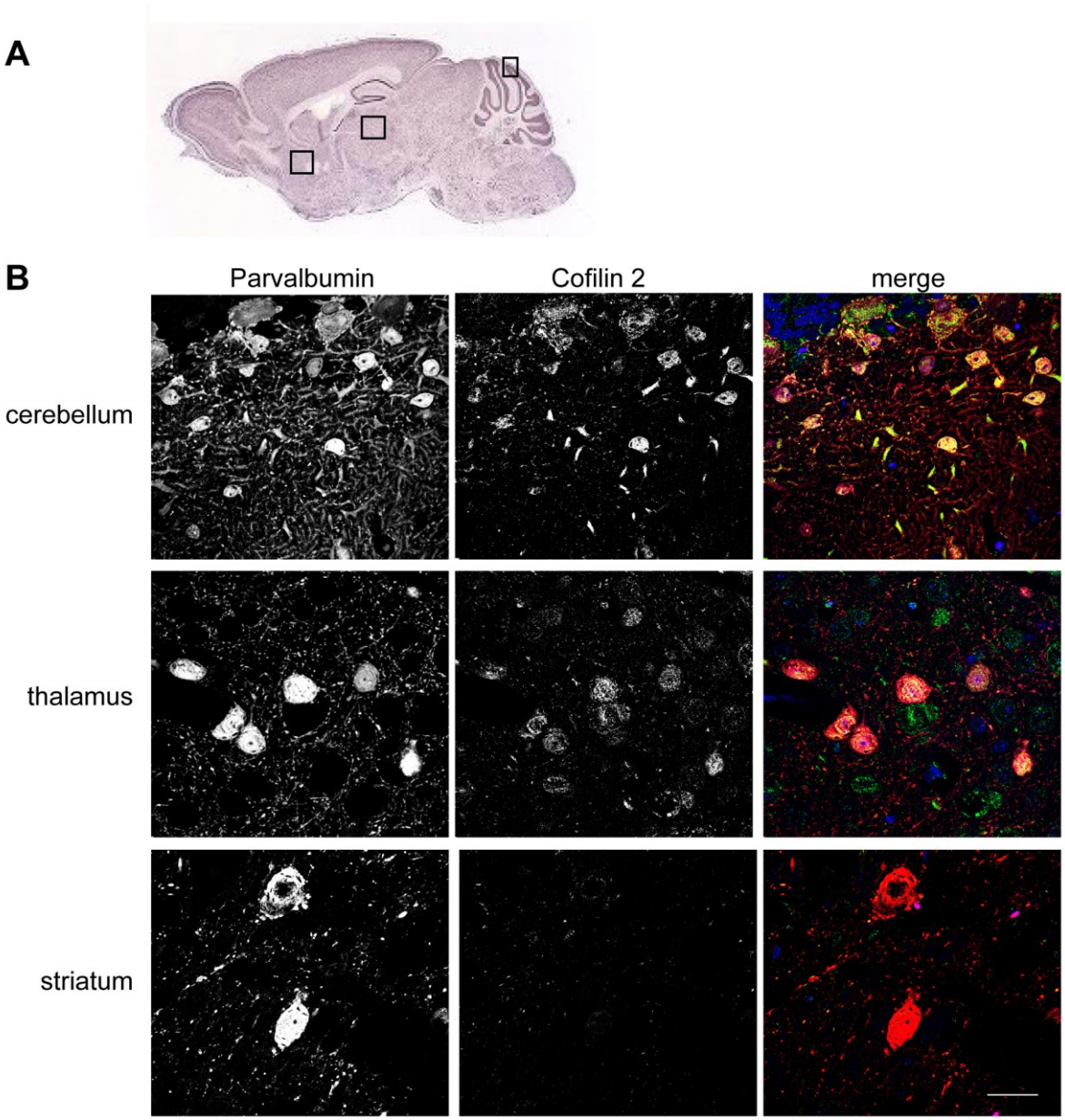

Fig.24: Cofilin 2 is expressed in stellate and basket cells of the cerebellum, principal sensory relay nuclei in the thalamus, but not in fast spiking interneurons of the striatum. A Nissl staining of a sagittal mouse brain section. Analyzed regions were marked. **B** Vibratome sections of adult wt animals were stained with the antibodies FHU-I for Cofilin 2 and parvalbumin, which marks inhibitory neurons. The FHU-I staining is displayed via the secondary antibody Alexa488, and the parvalbumin staining via Alexa594. Nuclei were stained with Draq5 (blue). The cerebellum, thalamus and striatum were analyzed for a possible colocalization between Cofilin 2- and parvalbumin-positive cells. Images were obtained at 63x magnification. Scale bar: 20µm

4.1.6. Cofilin 2 is expressed in dopaminergic neurons

Dopamine is one of the most intensively studied neurotransmitter in the brain due to its involvement in several mental and neurological disorders. Although dopaminergic neurons only correspond to approximately 3-5% of total neurons in the substantia nigra, they play a significant role in the control of voluntary movement and behavioral processes like mood,

addiction and stress (Chinta and Andersen 2005). Dopaminergic neurons are mainly localized to two areas, which build two different pathways: the nigrostriatal pathway, which originates in the substantia nigra and extends fibers into the dorsal striatum. The second one is the mesolimbic pathway and arises from the ventral tegmental area into the nucleus accumbens, the septum, amygdala and the hippocampus. The biogenic neurotransmitter dopamine is synthesized from the amino acid tyrosine via the enzyme Tyrosine-hydroxylase (Daubner et al., 2011). An antibody against this enzyme was used to check for a possible expression of Cofilin 2 in dopaminergic neurons. Therefore adult wt vibratome sections were incubated with the Tyr-hydroxylase antibody and FHU-I, which is specific for Cofilin 2.

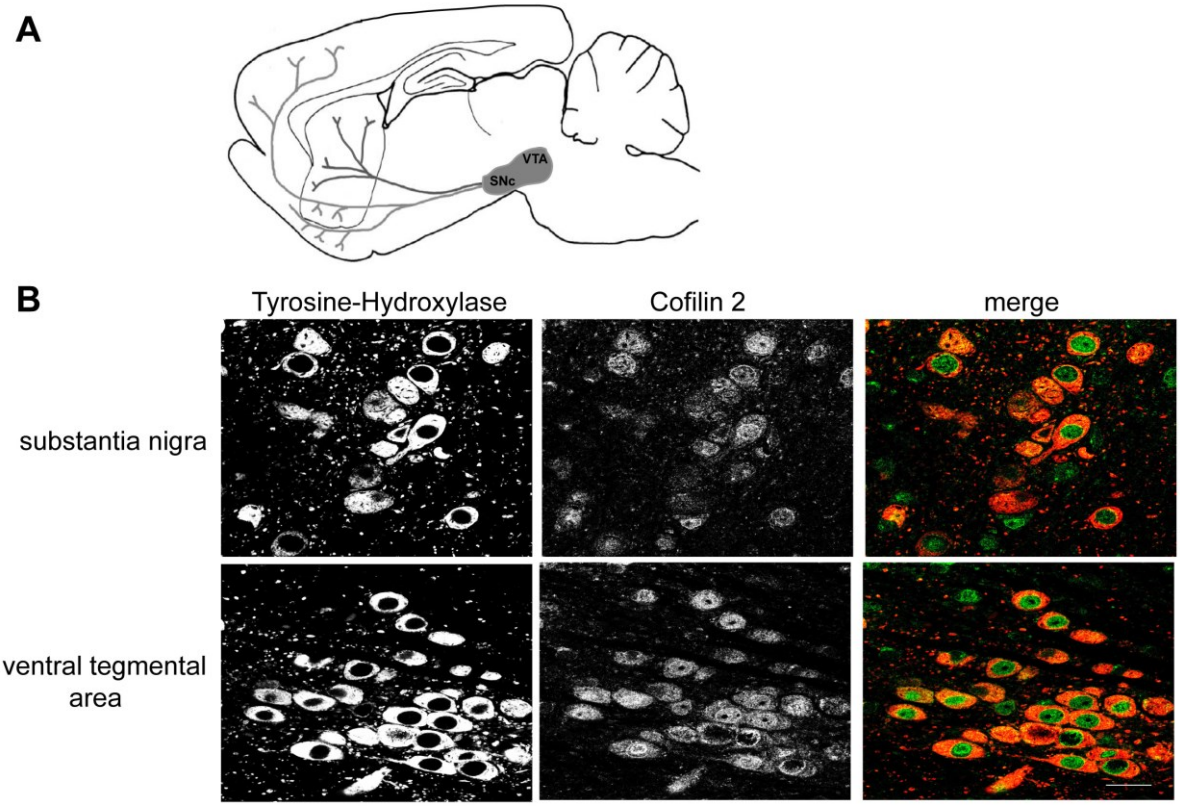

Fig. 25: Cofilin 2 localizes to dopaminergic neurons. A Position of the ventral tegmental area (VTA) and substantia nigra (SNc) in a sagittal section of a mouse brain. Dopaminergic neurons are localized to these areas. **B** Vibratome sections of adult wt animals were stained for Cofilin 2 (FHU-I) and Tyr-Hydroxylase, an enzyme for the synthesis of the neurotransmitter dopamine. A colocalization between Cofilin 2 and dopaminergic neurons was analyzed in the substantia nigra and the ventral tegmental area. The FHU-I staining is displayed via the secondary antibody Alexa488, and the Tyr-Hydroxylase staining via Alexa594. Nuclei were stained with Draq5 and are marked in blue. Cofilin 2 was found in the cell soma and nucleus of dopaminergic neurons. Images were taken at a magnification of 63x. Scale bar: 20µm

A colocalization between Cofilin 2 and Tyr-hydroxylase could be detected in two pathways (figure 25). An expression of Cofilin 2 was seen in dopaminergic neurons in the substantia nigra, as well as in the ventral tegmental area (VTA). Thereby Cofilin 2 was not only localized

to the cytoplasm, but also detectable perinuclear. The antibody Tyr-Hydroxylase showed an cytoplasmic staining, together with a punctuate staining surrounding the cells.

4.1.7. Serotonergic neurons express Cofilin 2

Serotonin is involved in the inhibition of sensory input and behavioral output. The neurotransmitter is associated with cognitive disorders like depression, bipolar disorder or schizophrenia (Carr and Lucki 2011). Serotonergic neurons are localized in two midbrain areas, called dorsal raphe nucleus and median raphe nucleus. Both structures innervate most cortical and subcortical structures and build an extensive system of innervation which allows serotonergic neurons to affect many different brain functions. Serotonin is derived from the amino acid tryptophan via the enzyme Tryptophan-hydroxylase (Walther et al., 2003). To analyze the expression of Cofilin 2 in serotonergic neurons vibratome sections were incubated with antibodies against Cofilin 2 and Tryptophan hydroxylase.

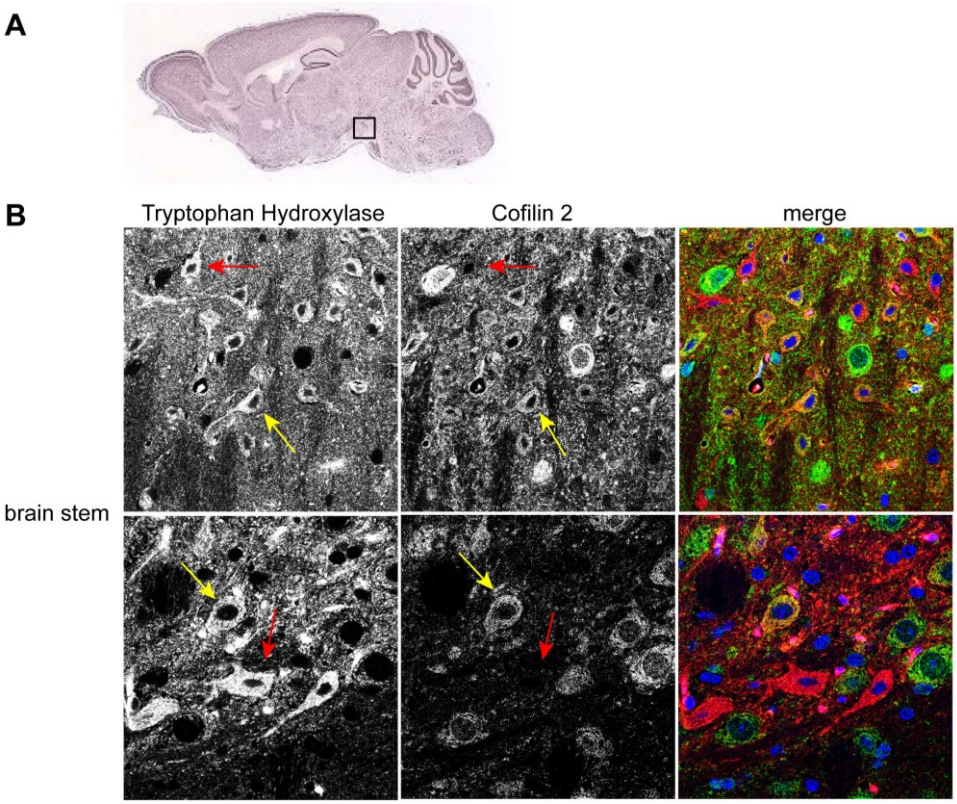

Fig.26: Cofilin 2 is expressed in serotonergic neurons. A Nissl staining of a sagittal mouse brain section. Analyzed regions were marked. **B** Vibratome sections of wt adult animals were stained for Cofilin 2 (FHU-I) and Tryptophan Hydroxylase (TPH), which is a marker for serotonergic neurons. The FHU-I staining is displayed via the secondary antibody Alexa488, and the TPH staining via Alexa594. Nuclei were stained with Draq5 (blue). The colocalization of both antibodies was analyzed in the raphe nuclei of the brain stem. Red arrows indicate cells which are positive for TPH, but not for FHU-I. Yellow arrows mark cells that are positive for both antibodies. Images were taken at a magnification of 63x. Scale bar: 20µm

The colocalization study between FHU-I and Tryptophan Hydroxylase revealed a few positive cells for both antibodies, indicated by the yellow arrows in figure 26. Additionally cells which were only positive for the antibody Tryptophan Hydroxylase could be observed (red arrows). Thereby Cofilin 2 seemed to be expressed only in a small subpopulation of serotonergic neurons in the brain stem. A few FHU-I positive cells were also localized to the brain stem, which were not positive for TPH and were therefore non-serotonergic. These cells could be cholinergic neurons, which synthesize the neurotransmitter acetylcholine. Thereby the Cofilin 2 staining in the brain stem was localized to the cytoplasm and synaptic terminals, indicated in a punctual staining pattern throughout the brain stem. The antibody Tryptophan Hydroxylase was mainly localized to the cytoplasm, but also showed a staining in some neurites.

In summary Cofilin 2 was expressed in a subset of serotonergic neurons in the brain stem that are involved in the processing of information from various sensory pathways and the control of motor output.

4.1.8. Cofilin 2 is localized to cholinergic neurons

Scopolamine, an anti-cholinergic drug, blocks cholinergic activity and induces memory impairments in the long-term and working memory (Polster 1993). The cholinergic system is composed of organized cells in the basal forebrain that project to the neocortex and hippocampus to fulfill memory functions. A second system in the brain stem (tegmental cholinergic system) is involved in the sleep-wake cycle. Choline acetyltransferase is an enzyme found only in acetylcholinergic neurons that produce the neurotransmitter acetylcholine (Oda 1999). Therefore an antibody specific for the enzyme choline acetyltransferase was used to analyze a possible colocalization with the specific Cofilin 2 antibody FHU-I in vibratome sections of adult wt animals. The antibody choline acetyltransferase displayed a cytoplasmic staining, while the Cofilin 2 specific antibody FHU-I also displayed a cytosplasmic staining in cholinergic neurons.

In the hypothalamus all choline acetyltransferase-positive cells were also positive for FHU-I, which indicates an expression of Cofilin 2 in cholinergic neurons that are involved in memory functions. On the contrary not all cholinergic neurons in the brain stem were positive for FHU-I, which indicates that in the tegmental cholinergic system only a subpopulation of cholinergic neurons express Cofilin 2 (red and yellow arrows figure 27). Additionally also a few FHU-I positive cells in the brain stem could be found, which were not positive for the enzyme choline acetyltransferase and are therefore non-cholinergic. These cells could be serotonergic cells since Cofilin 2-positive cells in the brain stem also colocalized with a serotonergic marker (figure 26).

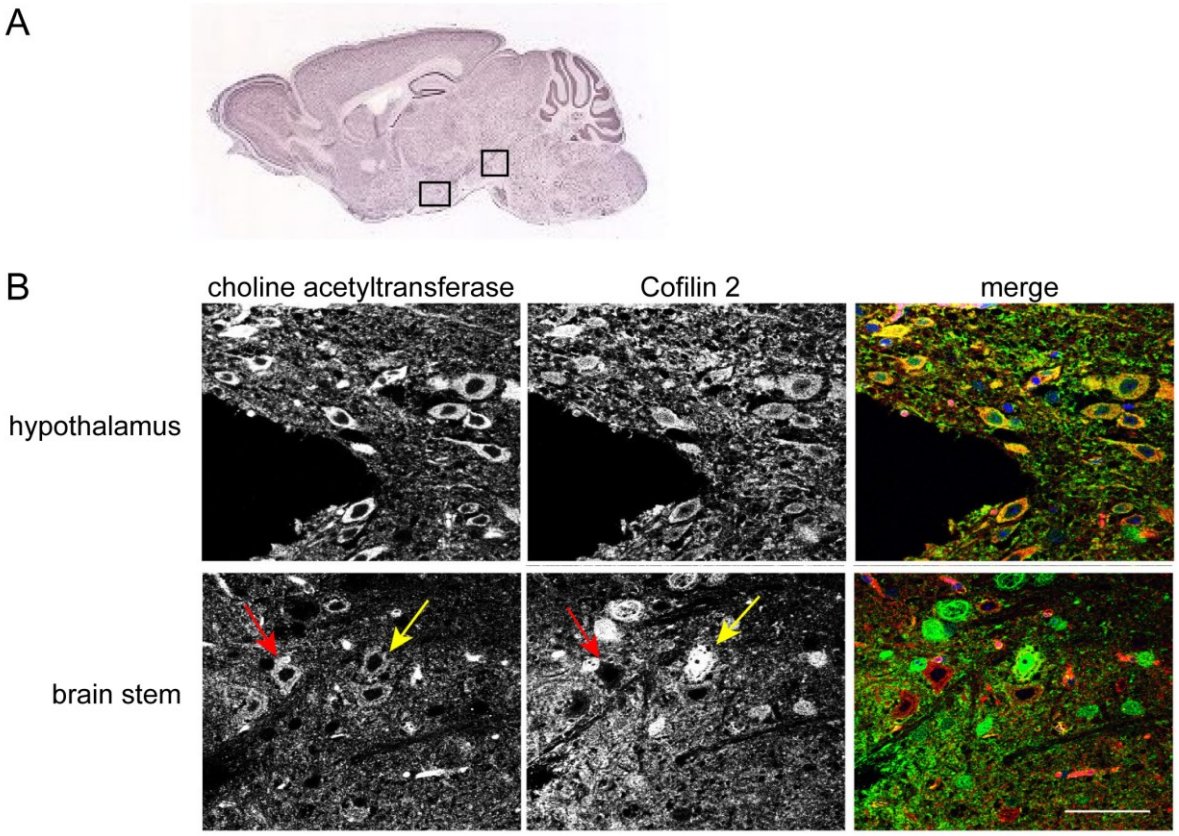

Fig.27: Cholinergic neurons express Cofilin 2. A Nissl staining of a sagittal mouse brain section. Analyzed regions were marked. **B** To analyze the expression of Cofilin 2 in cholinergic neurons adult wt vibratome sections were stained with the antibodies FHU-I, which is specific for Cofilin 2 and choline acetyltransferase (ChT) that marks cholinergic neurons. The FHU-I staining is displayed via the secondary antibody Alexa488 (green), and the ChT staining via Alexa594 (red). Cell nuclei were stained with Draq5 (blue). Areas in the hypothalamus and the brain stem were analyzed for a possible colocalization. Yellow arrows mark cells that are positive for both antibodies. A red arrow indicates the expression of only one antibody. In the hypothalamus all ChT-positive cells were also positive for Cofilin 2, while in the brain stem a few cells did not show a colocalization of both antibodies. Images were taken at a magnification of 63x with a confocal microscope. Scale bar: 20µm

In summary Cofilin 2 expression was found in both cholinergic systems, although in the tegmental cholinergic pathway only a subset of cholinergic neurons were positive for Cofilin 2, while all cholinergic neurons involved in memory functions seemed to express Cofilin 2.

4.1.9. Cofilin 2 is expressed in glutamatergic terminals with low-release probability

Glutamate is the predominant excitatory neurotransmitter in the central nervous system and glutamatergic transmission is critical for controlling neuronal activity. The homeostasis of the glutamatergic system is maintained by a set of transporters present in the plasma membrane and presynaptic vesicles. Three highly homologous proteins are known as vesicular glutamate transporters (vGLUT 1-3), which transport glutamate from the cytoplasm into

vesicles. VGLUT transporters are developmentally regulated and mark functionally distinct populations of glutamatergic neurons (Liguz-Lecznar and Skangiel-Kramska 2007). While vGLUT 1 and 2 are known to appear in all known glutamatergic neurons, vGLUT3 is localized to dopaminergic and serotonergic neurons, as well as to astrocytes that are also capable to release glutamate. The expression of vGLUT 1 and 2 seems to be largely complementary with only limited overlap (Liguz-Lecznar and Skangiel-Kramska 2007). Fremeau et al found out that synapses with low release probability, which are known to exhibit long-term-potentiation (LTP) express vGLUT1 (Fremeau et al., 2001). In contrast vGLUT2 is expressed in synapses that exhibit high release probabilities for long-term depression (LTD). To analyze the localization of Cofilin 2 in both circuits colocalization studies on adult wt vibratome sections were prepared with FHU-I in combination with antibodies either against vGLUT1 or vGLUT2.

The vGLUT1 and 2 antibodies displayed a punctate staining in both areas, which relies on the localization of these antibodies to the membrane of synaptic vesicles (figure 28). FHU-I showed an overall expression in the cell body, the nucleus and neurites of cortical neurons. The zoom into the overlay of the vGLUT1 and FHU-I staining displayed a colocalization between both antibodies in presynaptic terminals of cortical glutamatergic neurons, indicated in the obtained yellow spots (figure 28B). On the other hand no complete colocalization between vGLUT 2 and FHU-I could be detected in the overlay of thalamic glutamatergic terminals (figure 28C). In this staining the Cofilin 2 expression was localized in close proximity to the vGLUT2 staining, indicated by the fact that the green staining for FHU-I is found next to the red signal for the vGLUT2 staining, with a few spots that display a small overlap area between both signals (yellow spots). These spots could represent functional synapses indicated by the red vGLUT2 staining as presynaptic marker and the green FHU-I staining highlighting the postsynaptic part. Therefore Cofilin 2 seemed to be expressed in synapses with low release probability, while no Cofilin 2 could be found in synapses with high release probability.

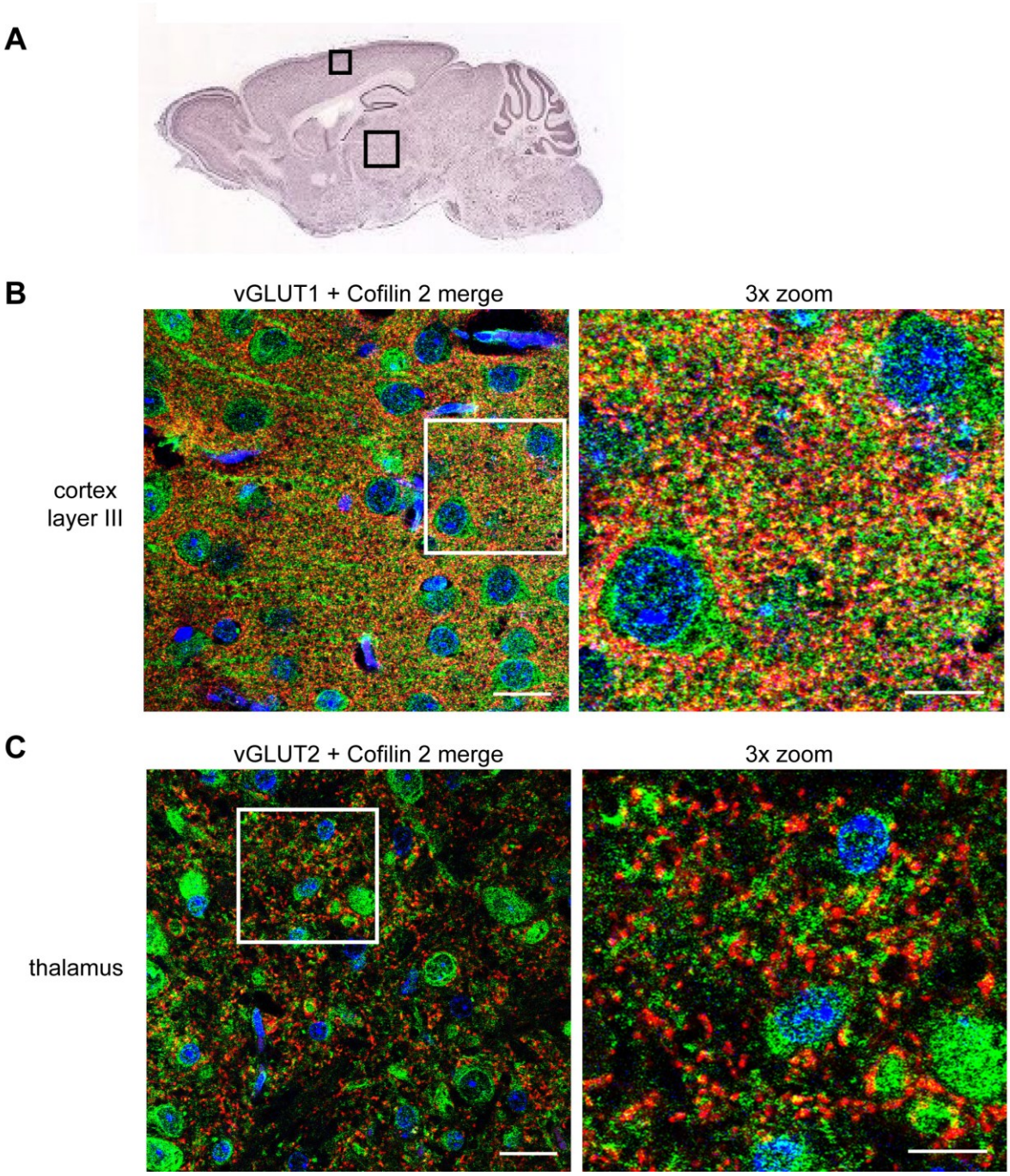

Fig.28: Cofilin 2 is localized to cortical terminals of glutamatergic neurons. A Nissl staining of a sagittal mouse brain section. Analyzed regions were marked. **B** Adult wt vibratome sections were incubated with an Cofilin 2 specific antibody (FHU-I) and an antibody against the vesicular glutamate transporter (vGLUT1), which is mainly localized to presynaptic cortical terminals in glutamatergic neurons. Yellow spots indicate a colocalization of vGLUT1 and Cofilin 2 in glutamatergic terminals of the somatosensory cortex. **C** To analyze a possible expression of Cofilin 2 in glutamatergic terminals of the thalamus, adult wt vibratome sections were stained with FHU-I, a specific antibody against Cofilin 2 and vGLUT2, a vesicular glutamate transporter protein found in presynaptic thalamic terminals of glutamatergic neurons. Signals for both antibodies display a signal in close proximity, without a direct overlap. Glutamatergic terminals of thalamic origin do not express Cofilin 2.
The FHU-I staining is indicated by Alexa488 (green) and the vGLUT stainings by the secondary antibody Alexa594 (red). Nuclei were stained in blue with Draq5. Images were taken at a magnification of 63x. Scale bar:20µm The right panel shows a 3x zoom of the merged overlay. Zoom area is marked by a white box in the merged overlay. Scale bar: 10µm

A summary over all performed colocalization studies and the localization of Cofilin 2 in defined neuronal subtypes is listed in the following table 2:

Brain area	Marker protein	Cell type	Cofilin 2 expression
cortex	Calbindin Parvalbumin	smooth nonpyramidal interneurons in layer II/III of the motor cortex	+
cerebellum	Calbindin Parvalbumin	Purkinje cells	+
	Parvalbumin	Stellate and basket cells	+
striatum	Calbindin	Medium spiny neurons	+
	Parvalbumin	Fast-spiking interneurons	-
thalamus	Parvalbumin	Principal sensory and motor relay nuclei	+
Substantia nigra	Tyrosine hydroxylase	Dopaminergic neurons of the nigrostriatal pathway	+
Ventral tegmental area	Tyrosine hydroxylase	Dopaminergic neurons of the mesolimbic pathway	+
Midbrain (dorsal and median raphe nuclei)	Tryptophan hydroxylase	Serotonergic neurons	+- (subset)
hypothalamus	Choline acetyltransferase	Cholinergic neurons involved in memory function	+
Brain stem	Choline acetyltransferase	Cholinergic neurons in the tegmental cholinergic system	+- (subset)
cortex	vGLUT1	Glutamatergic neurons with low-release probability	+
thalamus	vGLUT2	Glutamatergic neurons with high-release probability	-

Table 2: Overview over the colocalization studies with a Cofilin 2-specific antibody FHU-I and different markers for neuronal subtypes in defined brain regions.

4.2. Subcellular localization of Cofilin 2 in neurons

The β- and γ-isoforms of actin are highly expressed in neurons and contribute to important processes like cell division, polarity and cell migration. Additionally, actin is localized to sub compartments of neuronal cells fulfilling specialized functions there. Actin is the most abundant cytoskeletal protein in dendritic spines, regulating dynamic morphological changes during synaptogenesis and synaptic plasticity (Nimchinsky et al., 2002). Furthermore actin is implicated in the transport and anchoring of receptors for neurotransmitters in the postsynaptic membrane. Rust et al. showed that the loss of Cofilin 1 leads to postsynaptic changes in LTP and LTD, as well as changes in the number and morphology of dendritic spines (Rust et al., 2010). Two-photon-time-lapse imaging of dendritic spines in acute hippocampal slices showed that the induction of LTD by low-frequency stimulation is

accompanied by a marked shrinkage of spines. Thereby spine shrinkage is mediated by the activity of Cofilin, which implicates actin depolymerization to activity-induced reduction in the number of synaptic connections (Zhou et al., 2004). Additionally, actin is localized to the presynaptic site and there seems to be important for the formation of the active zone and the clustering of synaptic vesicles into defined pools (Nelson et al., 2013). Although the loss of Cofilin 1 in the forebrain only affected postsynaptic mechanisms (Rust et al., 2010), a double knockout of ADF and Cofilin 1 also displayed a presynaptic phenotype (Gorlich et al., 2011). Thereby an enrichment of ADF in presynaptic terminals was observed, but the analysis of $ADF^{-/-}$ mutant mice revealed no changes in presynaptic recruitment or exocytosis of synaptic vesicles. Additionally, postsynaptic mechanisms were unchanged in mice lacking ADF. Görlich et al found an elevated level of Cofilin 1 in mice deficient for ADF, suggesting a compensatory effect of Cofilin 1 and a cooperated function of ADF and Cofilin 1 in regulation actin rearrangement at synapses. Additionally in mice deficient for ADF and Cofilin 1 a disturbed morphology of striatal excitatory neurons, accompanied by an increased glutamate release was observed, resulting in hyper-locomotion of $ADF^{-/-}$ Cofilin $1^{fl/fl}$ CaMKII-Cre knockout animals. This phenotype was not detected in single mutants for Cofilin $1^{fl/fl}$ CaMKII-Cre or $ADF^{-/-}$, showing a functional redundancy for both proteins in synapses (Zimmermann et al., 2015). In this study the pre- and postsynaptic localization of Cofilin 2 was examined, which could play a role in specific synaptic functions.

4.2.1. Cofilin 2 is localized in pre and postsynaptic compartments

To analyze the expression of Cofilin 2 in synapses synaptosomes were prepared from the cortex of adult wt animals. Thereby synaptosomes are isolated synaptic terminals that have detached from the axon. After homogenization of cortical tissue and subsequent fractionation by centrifugation steps, a reseal of the plasma membrane encloses parts of the pre- and postsynaptic membrane, leaving behind functional synapses, which could be examined to study synaptic transmission. The synaptosomes were further fractionated to separate the pre- and postsynaptic site, as well as extrasynaptic proteins. The obtained lysates were incubated with PSD-95, as a marker for the postsynaptic site, Syntaxin-I as a marker for the presynaptic site and Synapthophysin as a general marker for synaptosomes. The expression of ADF/Cofilin family members was analyzed with specific antibodies for all three isoforms.

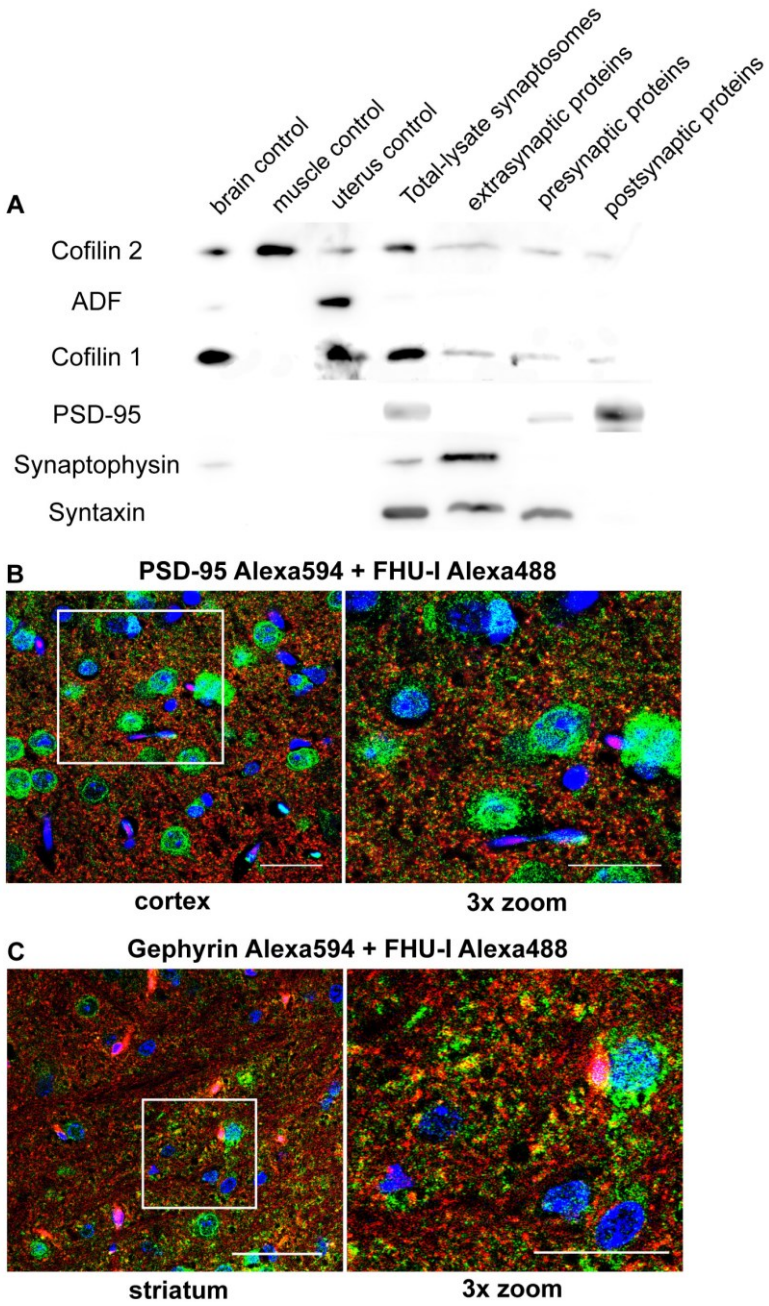

Fig. 29: Cofilin 2 is expressed in pre- and post-synaptic terminals. A To examine the synaptic localization of Cofilin 2 synaptosomes from adult wt cortices were prepared. 10µg of every probe were loaded on a 10% and 15% gel and analyzed with antibodies against the ADF/Cofilin family and marker for the presynaptic site (Syntaxin), postsynaptic site (PSD-95) and a general marker for synaptosomes (synaptophysin). Controls for every protein of the ADF/Cofilin family were also loaded on the gel: brain control for Cofilin 1, muscle control for Cofilin 2 and a uterus control for ADF. **B** Immunofluorescence analysis on adult wt vibratome sections with an excitatory postsynaptic marker PSD-95 (Alexa594 red) and a Cofilin 2 specific antibody FHU-I (Alexa488 green) in the cortex. Nuclei were stained with Draq5 (blue). Yellow spots indicate and overlap between both signals. Images were taken at a magnification of 63x. Scale bar: 20µm The right panel shows a 3x zoom. Scale bar: 10µm **C** Colocalization studies between Cofilin 2 (Alexa488 green) and Gephyrin (Alexa594 red), which is an inhibitory postsynaptic marker. Yellow spots indicate an overlap between both signals. Adult wt vibratome sections were stained and the striatum was analyzed. Nuclei were stained with Draq5 (blue). Images were taken at a magnification of 63x. Scale bar: 20µm The right panel shows a 3x zoom. Scale bar: 10µm

The Western blots of synaptosomes indicated an expression of Cofilin 2 in pre- and postsynaptic terminals (figure 29A). Also a pre- and postsynaptic expression of Cofilin 1 could be verified as already shown by Rust et al (2010). Only for ADF no signal could be observed in pre- and postsynaptic lysates. This is unexpected since the expression of ADF was already examined by Görlich et al via immunofluorescence analysis between ADF and synaptophysin or PSD-95, indicating a pre- and postsynaptic localization of ADF (Gorlich et al., 2011). Additionally, Rust et al also obtained a band for ADF in the presynaptic fraction of synaptosomal lysates (Rust et al., 2010). The functionality of the used antibody against ADF could be proven by the loaded uterus control, which exhibited a band at the height of ADF. The successful preparation of synaptosomes was controlled with the antibody synapthophysin, which is a general marker for nerve terminals. This membrane glycoprotein of synaptic vesicles is ubiquitously expressed in all neurons and should give a signal in the total lysate of synaptosomes and the soluble extrasynaptic fraction. A band for synapthophysin could be examined in the total lysate of synaptosomes and the soluble extrasynaptic fraction, as expected. As a presynaptic marker served the membrane-protein syntaxin, which is associated with the docking of synaptic vesicles to the active zone. A signal for syntaxin could be observed in the total lysate, the extrasynaptic lysate and the presynaptic fractionation, which is expected since syntaxin is a soluble protein. PSD-95 was used as postsynaptic marker, due to its function in the anchoring of NMDA receptors in the postsynaptic membrane. Enrichment in the PSD-95 signal could be observed from the total synaptosomal lysate to the postsynaptic fractionation. Also a weak band for PSD-95 could be seen in the presynaptic lysate, showing that the first fractionation between the pre- and postsynaptic proteins was not sufficient enough and a small amount of postsynaptic proteins could be found in the presynaptic lysate. A fractionation of presynaptic proteins still occurred since the staining of syntaxin-1 displayed a signal in the presynaptic fraction. Additionally, Rust et al already confirmed the presynaptic localization of Cofilin 1 in synaptosomal preparations, which could be also seen in this blot (Rust et al., 2010). To confirm the obtained results from the Western blot, immunofluorescence analyses on adult wt vibratome sections were performed. In a colocalization staining between vGLUT1 and FHU-I a presynaptic localization of Cofilin 2 could be further affirmed (figure 28). The localization of Cofilin 2 to postsynaptic sites was further examined with a staining of PSD-95 for excitatory synapses and FHU-I. Also in this staining a colocalization between Cofilin 2 and PSD-95 was observed (figure 29B). To also analyze inhibitory synapses stainings with FHU-I and Gephyrin were performed, which anchors GABA and Glycine receptors in the postsynaptic membrane. A few yellow spots were examined in this staining, but more frequently the signals were in close proximity to one another and only displayed a small overlap (figure 29C).

In summary all three ADF/Cofilin family members are found in synapses and display a pre- and postsynaptic localization. Thereby Cofilin 2 seemed to be localized only in a subset of excitatory and inhibitory postsynaptic compartments.

4.2.2. Cofilin 2 displays a broad expression in primary cortical cultures

To gain insight into the distribution of Cofilin 2 to specific neuronal structures, which exhibit different functions, the subcellular localization of Cofilin 2 in neurons was further analyzed *in vitro* in primary cultures. Therefore primary cortical neurons were prepared and the cells were fixed after 4 days in culture. Immunostainings with the neuronal marker betaIII-tubulin and a Cofilin 2-specific marker FHU-I were prepared. Thereby tubulin is the major component of microtubules and is a dimer composed of one alpha and one beta tubulin molecule. There are several isoforms of beta tubulin, which are expressed in a tissue-specific manner. BetaIII-tubulin is regarded to be a neuron-specific marker and has been suggested to be one of the earliest markers to signal neuronal commitment in the primitive neuroepithelium (Fanarrage et al., 1999). Thereby BetaIII-tubulin stained the cell soma, neurites and fine neurite branches. As seen in figure 30 Cofilin 2 displayed a broad expression in cortical neurons and was not restricted to a specific sub-compartment. Cofilin 2 expression was observed in every neurite, including fine branches and growth cones at the tips of neurites. Additionally a strong signal for Cofilin 2 was detected in the cell soma.

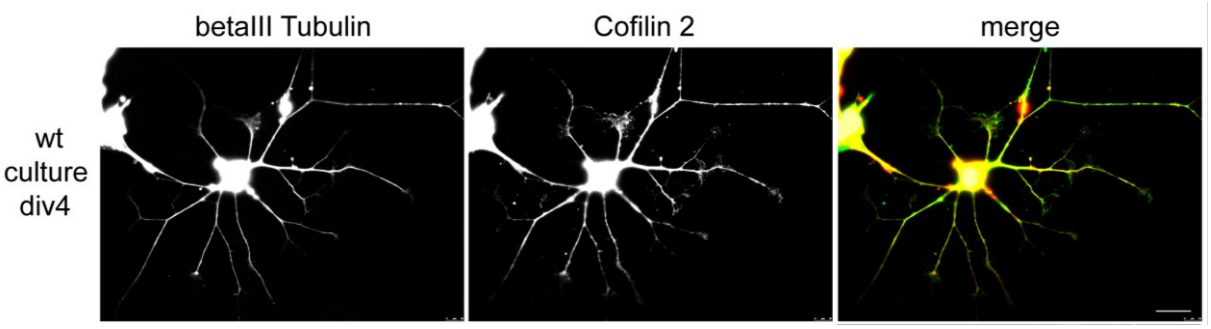

Fig.30: Subcellular localization of Cofilin 2 in primary cortical neurons. To analyze the localization of Cofilin 2 in neurons primary cortical cultures were prepared and the cells were fixed at div4 (4 days *in vitro*). The cells were stained with the neuronal marker betaIII-tubulin (A594 red) and the Cofilin 2-specific marker FHU-I (A488 green). Cofilin 2 was localized all over the cell, with a staining in the cell soma and neurites, as well as fine branches at the end of neurites. Images were taken at a magnification of 40x. The image was overexposed to analyze the localization of Cofilin 2 also in fine neurite branches. Scale bar: 20µm

4.3. Expression of the ADF/Cofilin family in glial cells

In the mature central nervous system three different types of non-neuronal glia cells exist, which exceeds the number of neuronal cells by a ratio of 3 to 1. They fulfill important functions like the supply of nutrients, the insulation of neurons, the destruction of pathogens and the removal of cell debris. In this thesis we will focus on two types, the astrocytes and the microglia. The third type are oligodendrocytes, which were not further analyzed here. Dumont et al used a proteomic approach to identify proteins in mature rat oligodendrocytes via two-dimensional liquid chromatography and two-dimensional gel electrophoresis followed by mass spectrometry (Dumont et al., 2007). In this study all three ADF/Cofilin family members were identified in oligodendrocytes. A further study in oligodendrocyte progenitor cells (OPC) identified an association of Cofilin with the pro-apoptotic protein Bax (Simonishvili et al., 2013). Thereby in healthy OPCs Cofilin and Bax are associated, while this interaction is disrupted in cells undergoing excitotoxic death. A defined role for Cofilin in oligodendrocytes was not further analyzed in the literature and could be a future research point.

4.3.1. Cofilin 1 is the main isoform expressed in microglia

Microglia cells derive from hematopoetic stem cells and migrate into the brain via the bloodstream. Therefore Cofilin 2 is not deleted in microglia in the Cofilin 2 Nestin and ADF Cofilin 2 Nestin knockout animals, due to the fact that Nestin is only expressed in the forebrain of the CNS (Tronche et al., 1999). They are primarily scavenger cells that remove cell debris. During a brain injury the number of microglia cells increases and they migrate to the site of injury. The possible expression of ADF/Cofilin family members in microglia was analyzed via Western Blot with protein lysates from cultured microglia and isolated microglia from brain tissue using the MACS (magnetic cell separation) technology. Thereby, Micro-beads coated with the microglia-marker CD11b, which is a key subunit of the membrane attack complex, were used to positively isolate microglia. Both lysates were a kind gift from the Fuhrmann lab. To estimate the expression levels of all ADF/Cofilin isoforms in microglia different concentrations of recombinant Strep-tag protein for either Cofilin 2, ADF or Cofilin 1 were also loaded on the same blot.

The Western blots with microglia lysates indicated no expression of Cofilin 2 *in vitro* or *in vivo* in microglia (figure 31). For ADF only a very faint band in the MACS microglia probe was observed. The expression level for ADF was even lower than 20ng as shown by comparison between the obtained band and the loaded recombinant Strep-tag concentration of 20ng, as the lowest concentration analyzed. The band for the recombinant Strep-tag protein run

different in the gel, due to the 1kDa of the Strep-tag protein that was linked to the N-terminus of the ADF protein. Cofilin 1 displayed the strongest expression in microglia with an estimated concentration of 500ng in cultured microglia, and between 80 – 160ng in MACS microglia. Therefore the amount of Cofilin 1 in MACS microglia was fourfold to eightfold higher than the amount of ADF in 10µg of loaded MACS lysate.

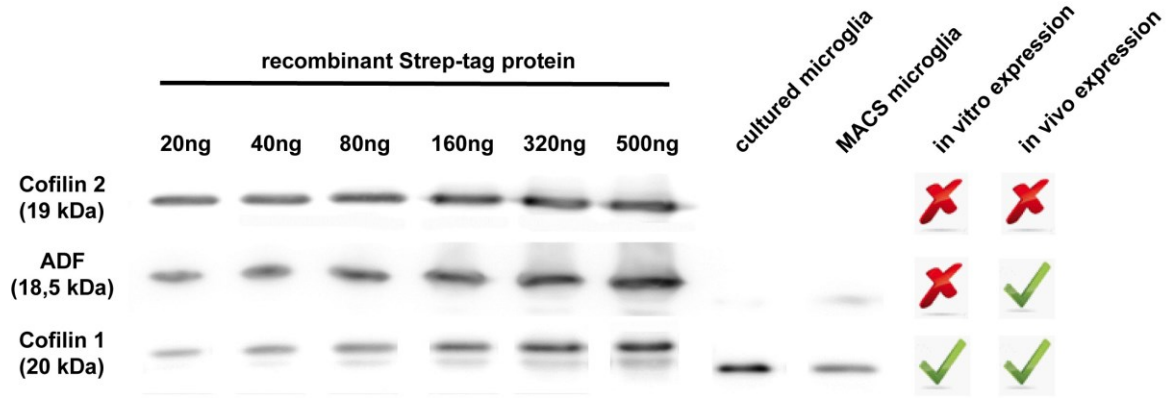

Figure 31: Cofilin 1 is the predominantly expressed ADF/Cofilin isoform in microglia. The expression of ADF/Cofilin family members was analyzed in protein lysates of cultured microglia and isolated microglia from brain tissue using the MACS technology in combination with the Microglia-marker CD11b on a Western blot. The single blots were incubated with antibodies specific for Cofilin 2 (FHU-I), ADF (7D10) and Cofilin 1 (KG60). To estimate the expression levels of all three isoforms different concentrations from a recombinant Strep-tag protein of the respected isoform were also loaded on the same gel. The recombinant proteins ran slower in the gel and are located above the signals for the proteins in the cultured microglia lysate and the MACS microglia. Thereby the recombinant proteins have an increased size according to the Strep-tag, which has a molecular weight of 1kDa. All three isoforms share a close molecular weight ranking from 18.5kDa for ADF, 19kDa for Cofilin 2 and 20kDa for Cofilin 1.

4.3.2. Cofilin 2 is only expressed in culture in astrocytes

Astrocytes have elaborate local processes that give these cells a star-like appearance. They have supportive functions in maintaining the brain homeostasis and signaling abilities of neurons, and additionally help to define synaptic contacts. These cells derive from the same progenitor cells in the subventricular zone as neurons. A deletion of Cofilin 2 via the Nestin promotor would also affect astrocytes, due to the deletion around E10.5 in neuron and glial cell precursors (Tronche et al., 1999). The onset of astrocytic development starts around E17.5 and has a peak in the early postnatal days. A specific marker for astrocytes is the glial fibrillary acidic protein, which is an intermediate filament protein found in the CNS only in astrocytes (Sofroniew and Vinters 2010). To analyze the Cofilin 2 localization in astrocytes a staining with GFAP and FHU-I was prepared *in vitro* in cultured astrocytes, as well as *in vivo* in adult wt vibratome sections.

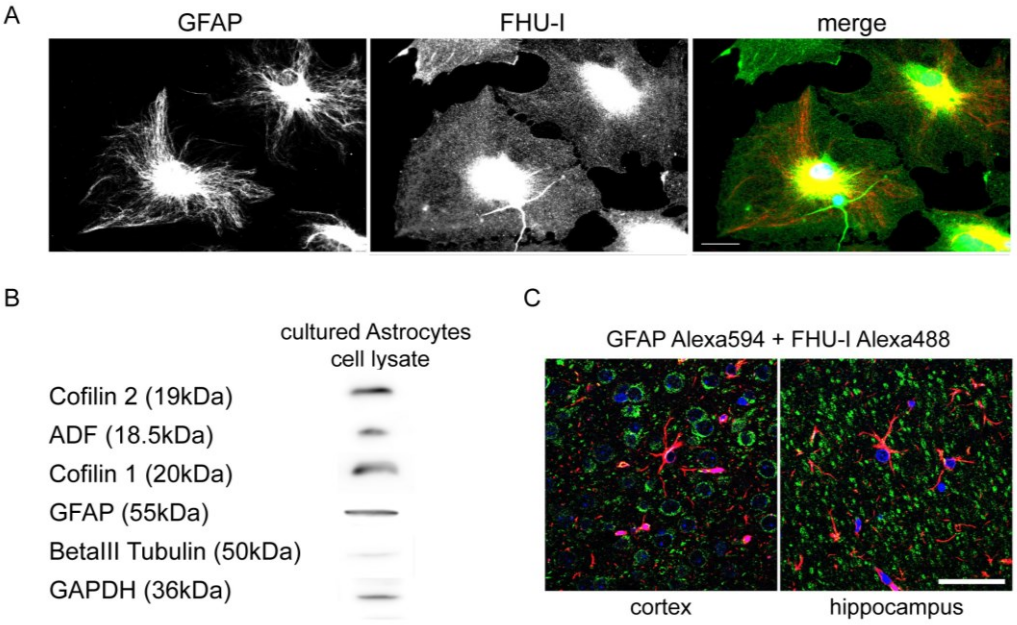

Figure 32: Cofilin 2 is expressed *in vitro* in cultured astrocytes but not *in vivo*. A To analyze a possible expression of Cofilin 2 in astrocytes wt astrocytic cultures were prepared from the cortex and fixed after 3 weeks in culture. The cultures were stained with GFAP (Alexa594 red), a marker for astrocytes and FHU-I (Alexa488 green) a specific marker for Cofilin 2. The nuclei were stained with DAPI (blue). Images were taken at a magnification of 63x at an epifluorescence microscope. Scale bar: 25µm **B** Additionally, protein lysates from astrocytic cultures were prepared and loaded onto a 15% gel. The membrane was incubated with antibodies against the ADF/Cofilin family. GAPDH served as a loading control. To verify the cultivation of astrocytes the antibody GFAP was used. To analyze a possible neuronal contamination of the cultures, the membrane was incubated with betaIII-tubulin, as a marker for immature neurons. **C** Immunofluorescence analysis of adult wt vibratome sections revealed no colocalization between the antibodies GFAP (Alexa594 red) and FHU-I (Alexa488 green), excluding an expression of Cofilin 2 *in vivo* in astrocytes. Nuclei were stained with Draq5 (blue). Images were taken at a magnification of 63x at a confocal microscope. Scale bar: 20µm

The GFAP staining indicated a filamentous network, which was consistent with the antibody that is directed against an intermediate filament protein. The specificity of the GFAP antibody was further proven by the fact that no GFAP signal could be detected in the neuron attached to one astrocyte (figure 32A). Immunostaining on astrocytic cultures revealed a ubiquitous expression of Cofilin 2 in astrocytes and displayed a cytosolic, as well as a nuclear localization of Cofilin 2. Additionally Cofilin 2 was also localized to a neuron, which grew on top of the astrocytic layer, proving again an expression of Cofilin 2 in neurons (figure 32A). Additionally the obtained lysates from cultured astrocytes displayed a signal for Cofilin 2. All three ADF/Cofilin family members were tested on the Western blot and revealed an expression in astrocytes *in vitro*. To confirm that a pure astrocytic culture was prepared the Western blot was also incubated with a specific marker for astrocytes (GFAP) and a neuronal marker (betaIII-tubulin). Only a faint band at the height of 50kDa for betaIII-tubulin could be observed, which proved that an almost pure astrocytic culture was generated. Additionally a

band at 36kDa for the GFAP protein was obtained. As second step immunostainings with GFAP and FHU-I on wt vibratome slices were prepared to analyze if Cofilin 2 was also expressed *in vivo* in astrocytes. As seen in figure 32C no colocalization between GFAP and FHU-I was found in the cortex and hippocampus of vibratome slices, excluding the expression of Cofilin 2 *in vivo* in astrocytes. Thereby the cortex and hippocampus were analyzed, due to the fact that a GFAP staining was only localized to these two regions.

In summary Cofilin 2 only seemed to be expressed in astrocytes after cultivation. In culture astrocytes displayed a different morphology with a more flattened and spread out morphology *in vitro*, compared to a star-like appearance of astrocytes *in vivo*. The changed conditions in culture were astrocytes grow on a plastic layer without coating could lead to the expression of Cofilin 2 to enable the cells to migrate and attach to the new surface. Further the preparation of astrocytic cultures from cortical tissue with a trypsination step leads to a shift in the differentiation state of cells. This could also alter the expression of proteins. In microglia also an elevated level of Cofilin 1 was detected in culture lysates, compared to MACS microglia. Cofilin 2 is not expressed in microglia at all.

5. Analysis of a conditional knockout of Cofilin 2 in the brain

5.1. The deletion of Cofilin 2 is still compensated by an upregulation of ADF and Cofilin 1 in adult animals

The complete deletion of Cofilin 2 is lethal around postnatal day 7, due to a muscle specific phenotype. The analysis of neuromuscular junctions did not reveal any changes in Cofilin $2^{-/-}$ mutants. However, Gurniak et al found a strong Cofilin 2 expression in the adult brain (Gurniak et al., 2014), leading to the question why all three members of the same protein family with similar functions were expressed in the same tissue. To be able to study the role of Cofilin 2 in the brain a conditional deletion of Cofilin 2 under the brain-specific promotor Nestin was generated. The Cre-recombinase expression under the Nestin promoter starts at embryonic day 10.5 in neuronal and glial cell precursors of the forebrain (Tronche et al., 1999). Nestin-Cre animals were crossed with floxed Cofilin 2 animals to obtain animals with a restricted deletion of Cofilin 2 in the brain. Obtained Cofilin $2^{fl/fl}$ Nestin-Cre animals were viable, which allowed us to study the Cofilin 2 expression also in adult brain regions. Dahlstrand et al revealed that the Nestin protein is also expressed in a wide variety of other progenitor cell types during development (Dahlstrand et al., 1995). Another group found the presence of enhancer elements in the rat Nestin gene that were sufficient to target

expression to the CNS (Zimmerman et al., 1994). We wanted to know whether the deletion of Cofilin 2 is restricted to the forebrain or could be also found in the adult animals in brain regions which are generated by the mid- and hindbrain. Therefore protein lysates from the following brain regions were generated from Cofilin $2^{fl/fl}$ and Cofilin $2^{fl/fl}$ Nestin-Cre animals: cortex, hippocampus, striatum, olfactory bulb, cerebellum, midbrain and hypothalamus. The lysates were loaded onto a 15% SDS gel and incubated with a Cofilin 2 specific antibody to check the expression of Cofilin 2 in adult brain regions, as well as the deletion of Cofilin 2 in defined brain areas. Further it was analyzed whether the loss of Cofilin 2 leads to a brain region restricted upregulation of Cofilin 1 or ADF.

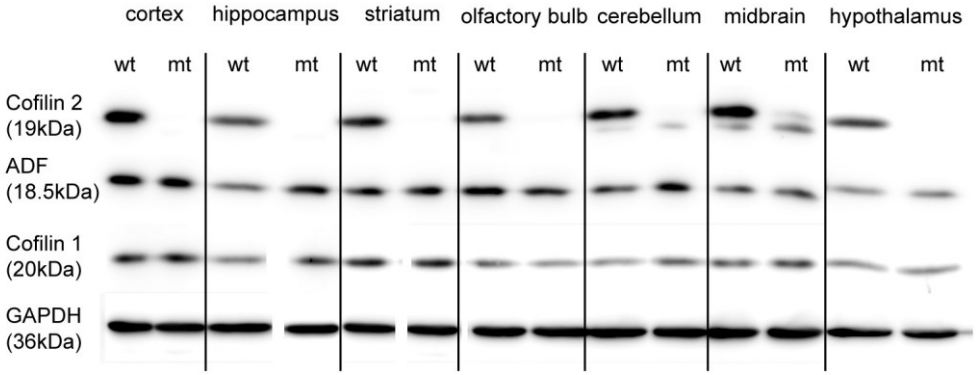

Fig. 33: The deletion of Cofilin 2 with the Nestin-Cre recombinase is detectable in all brain regions. To analyze the Nestin-Cre deletion in the brain Cofilin $2^{fl/fl}$ (wt) and Cofilin $2^{fl/fl}$ Nestin-cre (mt) lysates of different adult brain areas were loaded onto a 15% SDS gel. The membrane was incubated with specific antibodies for Cofilin 2 (FHU-I), ADF (7D10) and Cofilin 1 (KG60) to analyze a possible upregulation of other ADF/Cofilin family members upon loss of Cofilin 2. The antibodies for Cofilin 2 and ADF were incubated on the same blot, since both primary antibodies were made in different species (rabbit and mouse). For Cofilin 1 a second blot was prepared, due to the close molecular weight between the different isoforms and the generation of the KG60 antibody also in rabbit. Both blots were simultaneously incubated with the same antibody. The shown GAPDH signal is from the Cofilin 2/ADF blot, since the GAPDH-signal for the Cofilin 1 blot was comparable.

The deletion of Cofilin 2 could be verified for all analyzed brain regions, due to the fact that no band for Cofilin 2 was detectable in the Cofilin $2^{fl/fl}$ Nestin-Cre lysates (figure 33). Only for the midbrain and cerebellum a faint band at the height of 19kDa could be detected. Additionally both regions also showed two bands in close proximity. This phenomenon could be also detected in cerebellum lysates of P7 animals (Fig. 20). The strongest expression level for Cofilin 2 was detected in the midbrain and cortex lysates of adult Cofilin $2^{fl/fl}$ lysates, followed by the cerebellum, hypothalamus and hippocampus. The weakest expression in adult brain could be seen in the striatum and olfactory bulb. Additionally the hippocampus displayed the strongest upregulation of ADF (159%) and Cofilin 1 (133%) in adult brain tissue, which was also reflected in knockout animals at P7. A second brain region with an upregulation of ADF and Cofilin 1 at P7 and in adult animals was the midbrain (ADF: 132%;

Cofilin 1: 122%). In the cerebellum lysate of adult Cofilin $2^{fl/fl}$ Nestin-Cre animals only a weak upregulation of Cofilin 1 could be detected, which was not shown in younger animals. The upregulation of ADF and Cofilin 1 in the olfactory bulb lysates was lost in adult animals. The GAPDH antibody served as a loading control and confirmed that the same protein concentration was loaded for every probe.

In summary Cofilin 2 was also ubiquitously expressed in the adult brain and the Nestin-Cre recombinase leads to the deletion of Cofilin 2 in the whole brain. Also in adult animals the brain-specific loss of Cofilin 2 was compensated by an upregulation of ADF and Cofilin 1 in certain brain areas (hippocampus and midbrain).

5.2. The brain-specific loss of Cofilin 2 does not lead to obvious brain malformations

In this study the conditional deletion of Cofilin 2 was used to analyze whether the loss of Cofilin 2 also leads to obvious malformations in the brain. Therefore vibratome sections were analyzed under the brightfield microscope to get a first overview over the brain structure of Cofilin $2^{fl/fl}$ Nestin-Cre animals. In coronal and sagittal vibratome sections no malformations of the brain from Cofilin $2^{fl/fl}$ Nestin-Cre animals were observed (figure 34). The cortex had the same thickness as in Cofilin $2^{fl/fl}$ controls, which indicated that no cortical layers were missing. The hippocampus showed the regular assembly and also the ventricles were not enlarged. Also the striatum, thalamus and the hypothalamus displayed no alterations. The sagittal sections did not revealed any changes in the cerebellum, due to the fact that all layers were present, the white matter thickness was not decreased and the number of gyri was comparable to the control animals.

In summary these results could show that the brain-specific deletion of Cofilin 2 did not show obvious brain malformations and displayed therefore a milder phenotype than the brain restricted deletion of Cofilin 1, which shows a reduced cortical thickness and enlarged ventricles.

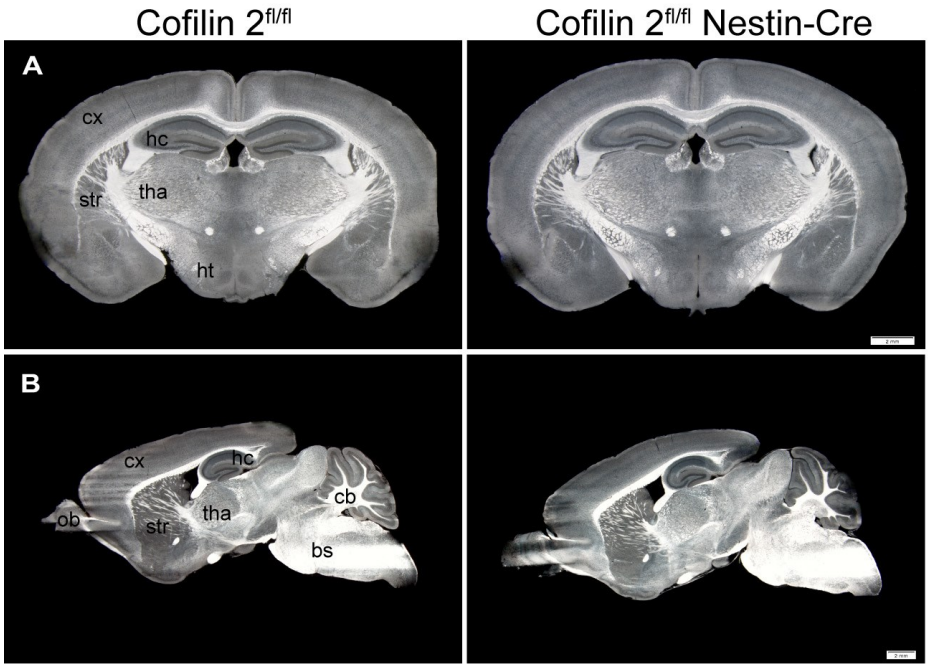

Fig. 34: The deletion of Cofilin 2 does not lead to obvious malformations in the brain. A Coronal vibratome sections of adult Cofilin $2^{fl/fl}$ and Cofilin $2^{fl/fl}$ Nes-Cre animals (300µm). At intervals of 600µm pictures were taken at a brightfield microscope and analyzed for the occurrence of brain malformations. No abnormalities could be observed in analyzed mt brains. Scale bar: 2mm **B** Sagittal vibratome sections of adult Cofilin $2^{fl/fl}$ and Cofilin $2^{fl/fl}$ Nes-Cre animals (300µm). Pictures were taken at a brightfield microscope every 600µm to analyze morphological changes in the brain tissue. Sagittal sections also revealed no abnormalities in the brain architecture of mt animals. Scale bar: 2mm Three different control and mt animals were analyzed. cx = cortex; hc = hippocampus; str = striatum; tha = thalamus; cb = cerebellum; ht = hypothalamus; ob = olfactory bulb; bs = brain stem

5.3. Cofilin 2 is also expressed in the pituitary gland

The complete deletion of Cofilin 2 leads to a growth retardation in Cofilin $2^{-/-}$ animals, starting directly after birth. Knockouts were much smaller than their littermates (Gurniak et al., 2014). This phenotype was also observed in the conditional knockouts of Cofilin $2^{fl/fl}$ Nestin-Cre and ADF$^{-/-}$ Cofilin $2^{fl/fl}$ Nestin-Cre animals. The weight of litters was analyzed and compared over the first month during development. Starting at P21 the knockout animals were much smaller and displayed a 36% reduction in weight compared to control littermates (control 10.7g ± 1.08g; mutant 6.8g ± 1.2g; $p<0.05$; $n = 6$). This growth retardation maintained into adulthood, although the difference in weight reduces to 11% at P56 (control 18.5g ± 0.62g; mutant 16.4g ± 0.4g; $p<0.05$; $n = 6$). An expression of Cofilin 2 was observed in the hypothalamus, which is known to release hormones that control the metabolism and growth of animals (figure 35). These hormones stimulate the pituitary gland to secrete hormones that govern physiological functions, like growth, development and metabolism. Therefore it was examined whether Cofilin 2 was also expressed in the pituitary gland and if Nestin-Cre deletion also includes the pituitary gland. Lysates from pituitary glands of Cofilin $2^{fl/fl}$ and Cofilin $2^{fl/fl}$ Nestin-Cre were prepared and analyzed on a Western blot.

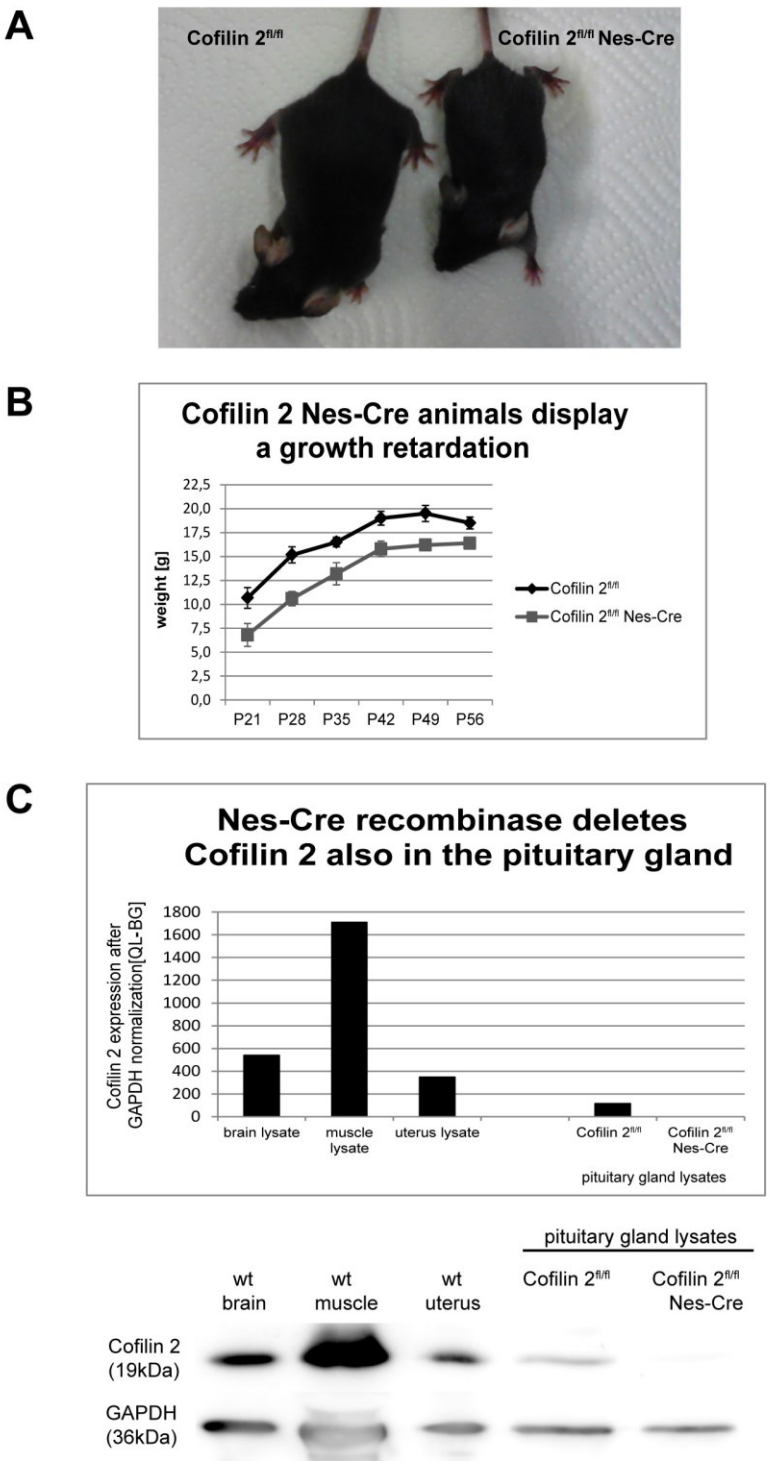

Fig. 35: Nestin-Cre deletion also affects the expression of Cofilin 2 in the pituitary gland. A Cofilin $2^{fl/fl}$ Nes-Cre animals were much smaller than their littermates and displayed a growth retardation. Images were taken from P35 old Cofilin $2^{fl/fl}$ control and Cofilin $2^{fl/fl}$ Nes-Cre knockout animals. **B** The weight of litters was measured every week starting at P21 and the average and standard error were calculated. Note that the knockout animals displayed a reduced weight over the entire analyzed time in comparison to their littermates. Six different control and knockout animals were studied. Student-t-test: $p<0.05$ **C** Pituitary gland lysates of Cofilin $2^{fl/fl}$ and Cofilin $2^{fl/fl}$ Nes-Cre animals were prepared and loaded onto a Western blot to analyze the expression of Cofilin 2 in the pituitary gland. A band at the height of 19kDa can be observed for the control, while in the knockout lysate no band for Cofilin 2 was detectable, leading to the conclusion that Nes-Cre was also expressed in the pituitary gland.

As seen in figure 35C Cofilin 2 was also expressed in the pituitary gland, although to a low level in comparison with the brain and muscle lysates. Additionally the Nestin-Cre expression was also localized to the pituitary gland since no band for Cofilin 2 could be obtained in the pituitary lysates of Cofilin $2^{fl/fl}$ Nestin-Cre animals. Thereby the loss of Cofilin 2 in the hypothalamus and pituitary gland could contribute to the observed growth retardation in conditional knockout animals.

5.4. The deletion of Cofilin 2 in neuronal cells does not lead to significant alterations in the F-actin levels

The deletion of a depolymerization factor could alter the ratio between G (globular)- and F (filamentous)-actin. A reduced depolymerization rate of actin filaments can lead to a shift towards F-actin and thereby inhibit the re-arrangement of actin during important neurodevelopmental processes. An impact on the G- and F-actin pool was also detected in Cofilin $1^{fl/fl}$ CamKII-Cre animals (Rust et al., 2010). In these mutants a reduction in the level of G-actin was observed in synaptosomes of the cortex and hippocampus. Although Cofilin 1 seems to be the predominant depolymerization factor in the brain, the question was if the deletion of Cofilin 2 would also impact on F-actin levels. To answer this question cortical lysates of Cofilin $2^{fl/fl}$ and Cofilin $2^{fl/fl}$ Nestin-Cre animals were prepared and the G- and F-actin pool was separated through differential centrifugation steps. The G-actin monomers were localized in the supernatant, while the F-actin filaments were pelleted. Equivalent volumes of the obtained lysates were loaded onto a 10% gel and analyzed with the antibody C4 against actin. The antibody C4 reacts with all six isoforms of vertebrate actin (Lessard 1988) and detects both globular and filamentous forms of actin, without affecting actin polymerization. GAPDH served as a control to prove the separation between the cytoplasmic/soluble and pelleted fractions. GAPDH is a cytoplasmic protein and should not be found in the pellet fraction. In figure 36A a faint signal for GAPDH was also detectable in the pelleted fraction, which contained the F-actin. This indicates that the separation between the globular and filamentous actin was not completely and a small amount of G-actin could be also detected in the pelleted fraction. This contamination was recalculated during the densitometric determination of the F/G-actin ratio. The comparison between the obtained signals for the C4 antibody in the Cofilin $2^{fl/fl}$ and Cofilin $2^{fl/fl}$ Nestin-Cre animals revealed a reduction in the G-actin signal and an increase in the F-actin signal in the mutant. Three different litters were analyzed for their G- and F-actin levels and the statistical analysis is shown in figure 36B. An increase in the F/G-actin ratio could be observed in Cofilin $2^{fl/fl}$ Nestin-Cre animals (control 1.0 ± 0.08; mutant 1.46 ± 0.166; n = 3; ns), although the change in the F- to G-actin ratio was not significant. This increase in the F-actin level could influence the dynamic of migrational

structures that rely on actin filaments, like growth cones or dendritic spines. Therefore an examination of these highly motile structures was done to see if they were affected by the loss of Cofilin 2.

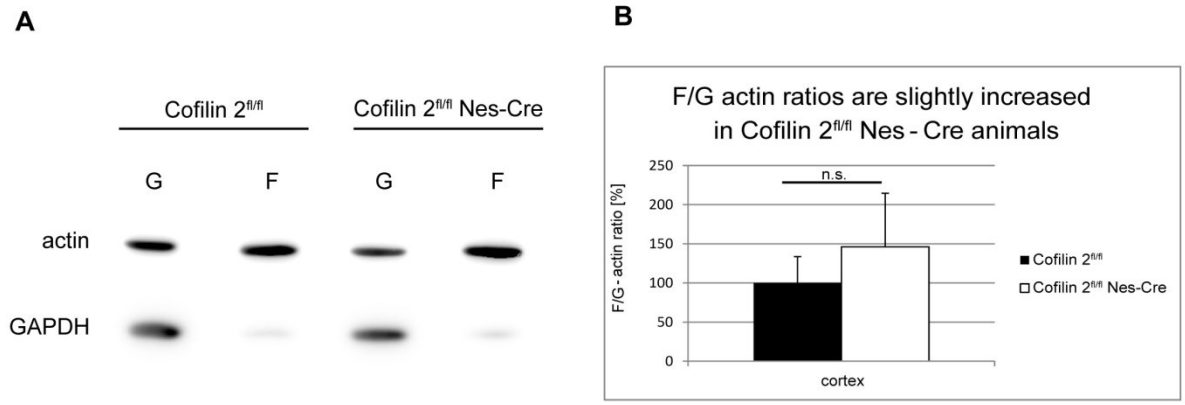

Fig. 36: Cofilin 2$^{fl/fl}$ Nestin-Cre animals showed a slightly increased F-actin level. A The G- and F-actin levels of Cofilin 2$^{fl/fl}$ and Cofilin 2$^{fl/fl}$ Nes-Cre cortical lysates were examined by Western blot. The G-actin level in the supernatant, as well as the F-actin level in the pellet was examined to calculate the F/G-actin ratio. Thereby C4 served as an antibody against actin and GAPDH as confirmation for the separation between the G- and F-actin pool. **B** An increased F/G-actin ratio was detected in Cofilin 2$^{fl/fl}$ Nes-Cre animals (control 1.0 ± 0.08; mutant 1.46 ± 0.166; n = 3; ns), although the obtained results were statistically not significant. The standard error was calculated and the significance was analyzed in a two-sampled independent t-test. Three different controls and mutants were analyzed (n = 3).

In summary the brain-specific loss of Cofilin 2 did not lead to a significant shift in the F/G-actin ratio, but a slightly increased level of F-actin was observed.

5.5. The deletion of Cofilin 2 leads to an increase in the growth cone diameter

Neurons are generated in the SVZ and VZ and have to migrate over long distances to their final position in the cortex. Actin plays an important role during these migrational processes (Ayala et al., 2007). A highly dynamic structure, termed growth cone, at the tip of neurites senses guidance cues and determines the migrational direction. This structure has a defined assembly with microtubules in the core, surrounded by a branched network of actin filaments, which inhibits the protrusion of microtubules. The depolymerization of actin filaments is necessary to disassemble the branched network, which leads to the protrusion of microtubuli and the movement of the neurite. The loss of Cofilin 1 leads to an accumulation of F-actin in growth cones (Bläsius Diploma thesis; 2012). In this study it was analyzed whether the loss of Cofilin 2 also had an impact on these highly dynamic structures, which were necessary to establish the polarity of neurons and influence migrational processes. The

analysis of growth cone structures was performed on primary hippocampal cultures, which were fixed at div1, 2, 3 and 4. This enabled the study of the outgrowth of the first neurites from round neuronal spheres in the first few days of culture and the assembly of the growth cones at the tips of these neurites. The fixed cultures were stained for betaIII-tubulin as a marker for immature neurons and phalloidin, which binds specifically to F-actin.

Starting with the growth cone analysis at div1, the Cofilin $2^{+/+}$ neurons displayed a phalloidin staining in the cell soma, at the periphery of the growth cone and also in fine structures like filopodia at the tip of the growth cone (figure 37). In contrast to that revealed the Cofilin $2^{-/-}$ neurons a staining of phalloidin mainly at the core center where the microtubuli were typically localized and only a weak staining at the periphery. The BetaIII tubulin staining was found all over the neuron in the cell soma, neurites and growth cones. At div2 an increase in the diameter of growth cones in Cofilin $2^{-/-}$ neurons could be observed and they displayed a malformed morphology. Although several outgrowing neurites were found, they showed a high diversity in their length and morphology. Cofilin $2^{+/+}$ neurons fixed at div3 displayed already a polarization of neurons with one longer neurite that inhibited the outgrowth of all other neurites. Therefore the phalloidin staining in the shorter neurites showed a more intense staining than in the fast elongating neurite, with a finer growth cone at the tip. Additionally fine branches could be detected along the neurites, which displayed a phalloidin staining. In comparison, the Cofilin $2^{-/-}$ neurons showed also a polarization of neurites, but all neurites displayed a reduced outgrowth and a stronger signal for phalloidin in all tips. In addition the phalloidin signal was strongly enhanced and localized to the core center of the growth cone, instead of the periphery where actin filaments were normally localized. At div4 Cofilin $2^{+/+}$ neurons seemed to be polarized and also the neurites already started to branch. In this stage only very small growth cones could be detected. In strong contrast, the Cofilin $2^{-/-}$ neurons displayed one neurite with a highly increased growth cone diameter and an accumulation of F-actin.

Im summary these results could show that the brain-specific loss of Cofilin 2 impacts on actin-based structures like the growth cone. An increased growth cone diameter was observed in Cofilin 2-deficient neurons and the outgrowth of neurites was reduced. Further an altered localization of the F-actin staining was detected upon the loss of Cofilin 2.

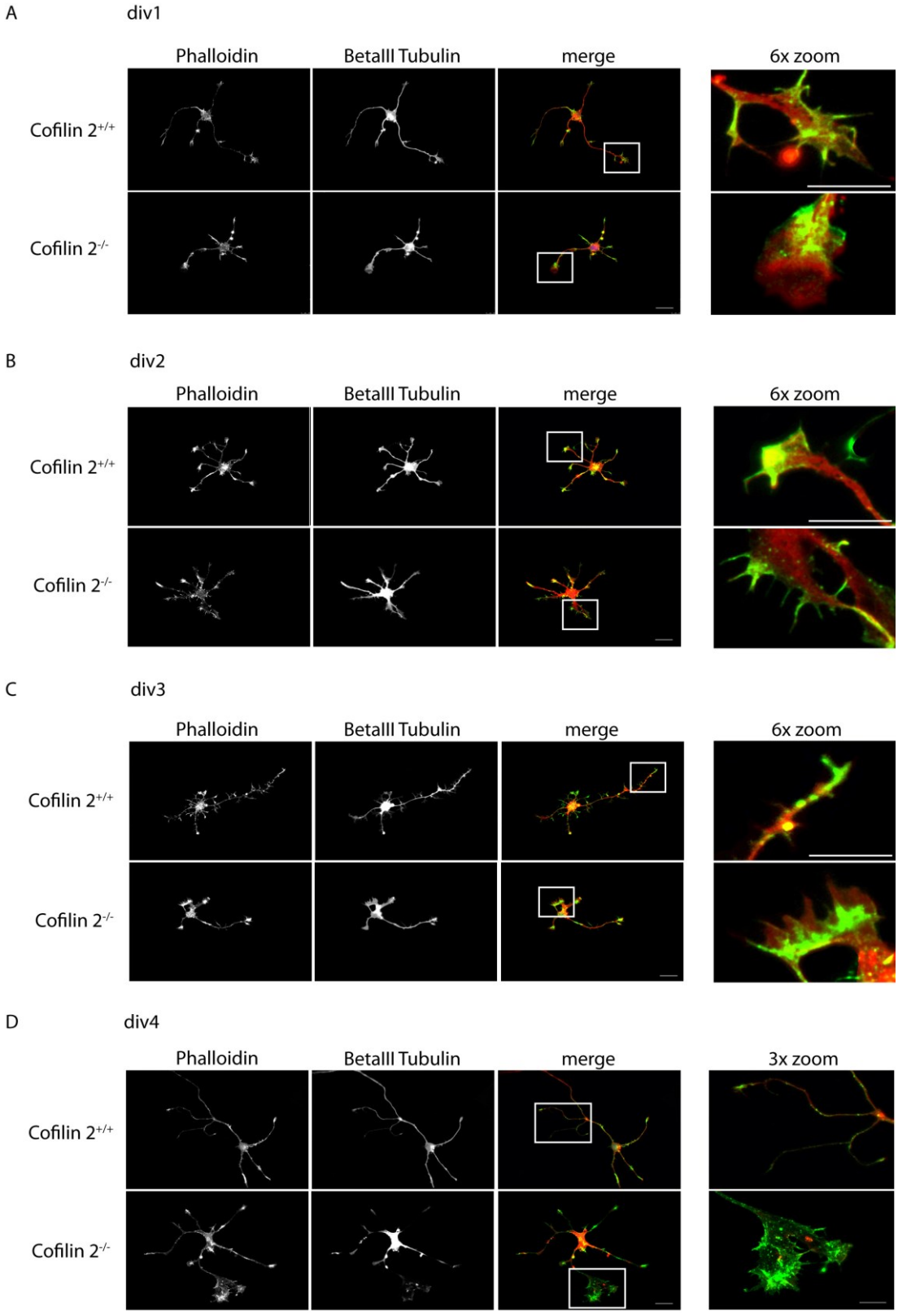

Fig. 37: The growth cone dynamic is reduced upon the loss of Cofilin 2. Primary hippocampal cultures were prepared from E17.5 embryos. Cultures from Cofilin $2^{+/+}$ and Cofilin $2^{-/-}$ animals were fixed after div1 (**A**), div2 (**B**), div3 (**C**) and div4 (**D**) and stained with the immature neuronal marker BetaIII-tubulin (Alexa594 red) and phalloidin-Alexa488 (green), which binds specifically to F-actin. Images were taken at a magnification of 40x at an epifluorescence microscope. Scale bar: 20µm The right panel shows a 6x zoom (for div 1 – 3) and a 3x zoom (for div 4) of growth cones at the tips of neurites. Scale bar: 10µm

A statistical evaluation of the increased growth cone diameter is shown in figure 38. Neurons were obtained from two different litters and 21 – 28 cells from every genotype were analyzed for the first four days *in vitro*. For every examined time point an increase in the growth cone diameter could be observed in Cofilin 2 deficient neurons. Additionally the diameter of the growth cone in Cofilin 2 mutant neurons further increased over time.

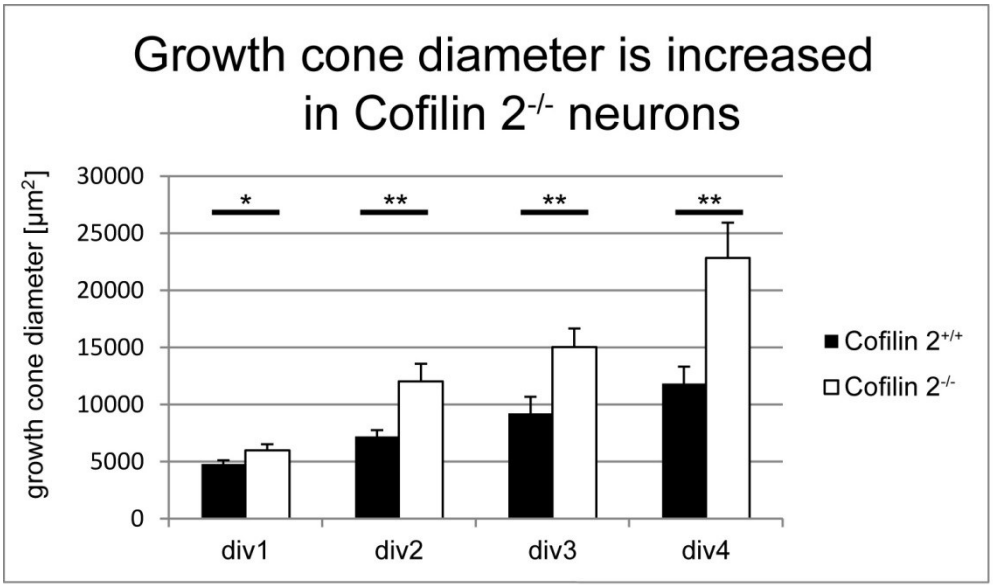

Figure 38: Increase in the growth cone diameter upon deletion of Cofilin 2. Statistical analysis of the growth cone diameter in Cofilin $2^{+/+}$ and Cofilin $2^{-/-}$ neurons at the time points div1, 2, 3 and 4. The diameter of the growth cone at every tip of neurons from two different litters were analyzed with the Keyence software The standard error was calculated and the significance was analyzed in a two-sampled independent t-test ($p < 0.05$ *; $p< 0.01$ **).

5.6. Cortical migration is not affected by the loss of Cofilin 2

A reduced motility of migrational structures like the growth cone could influence the migration of neurons from the SVZ to the cortical layers. Bellenchi et al already postulated a contribution of Cofilin 1 during cortical migration processes. The conditional deletion of Cofilin 1 leads to migration dependent malformations of the cortex. In the Cofilin $1^{fl/fl}$ Nestin-Cre animals layers II – IV were completely missing (Bellenchi et al., 2007). This result implicates an important role for actin depolymerization factors during neuronal migration. To analyze a contribution of Cofilin 2 during cortical migration between E13 and E19 a Golgi staining was performed on Cofilin $2^{fl/fl}$ Nestin-Cre animals. In this staining method the nervous tissue is impregnated with potassium dichromate and silver nitrate, which leads to a microcrystallization of silver chromate in neurons and generates a black color. This procedure stained a limited number of cells at random in their entirety. The Golgi staining did not revealed changes in the cortical layering of Cofilin $2^{fl/fl}$ Nestin-Cre animals. All six layers

could be identified and no clustering of cells in any layer could be observed. Also the cell number of cortical neurons did not seemed to be affected, which could result from changes in cell division or increased apoptosis rates.

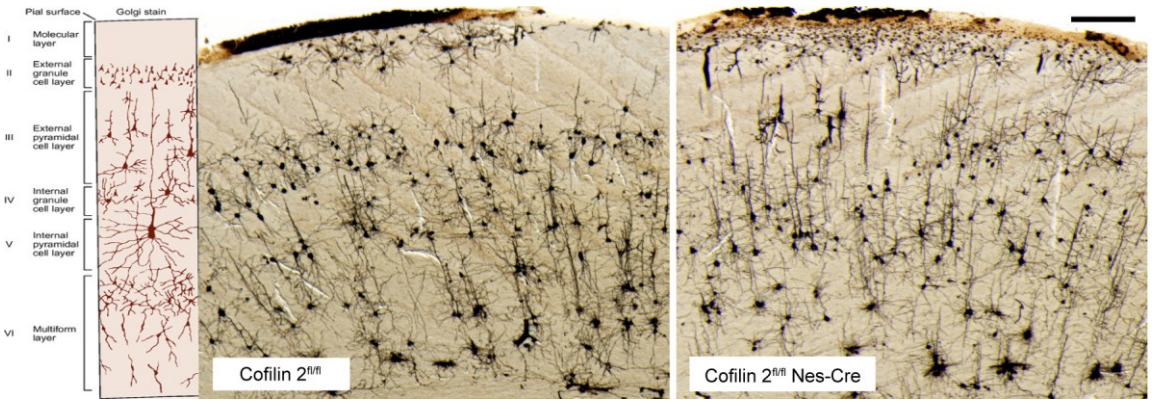

Figure 39: Directed migration of neurons into the cortical layers is independent of Cofilin 2. Adult brains of Cofilin $2^{fl/fl}$ and Cofilin $2^{fl/fl}$ Nes-Cre animals were stained with a Golgi Staining Kit. Images were taken at a brightfield microscope from the cortex, to analyze the cortical migration of neurons into the six layered structure. The Golgi staining of Cofilin $2^{fl/fl}$ Nes-Cre animals did not revealed any migrational defects in the cortex. All six layers were present and no clustering of cells occurred. Scale bar: 50µm (right upper corner)

In summary the loss of Cofilin 2 did not impact on cortical migration or proliferation in the SVZ, since all six cortical layers are present and the cell number was not affected. Therefore Cofilin 1 is the only actin depolymerization factor regulating cortical migration and cell division.

5.7. The loss of Cofilin 2 leads to a reduced complexity of pyramidal neurons in the cortex

An advantage of the Golgi staining is the fact that only a limited number of cells were stained at random in their entirety. This enables the analysis of morphological details of neurons as well as the examination of dendritic spines. Dendrites and axons were clearly stained and could be followed in their entire length. Therefore a Sholl analysis on small pyramidal neurons in the cortical layers II and III was performed, due to the fact that in these layers no overlap between neighboring neurons occurred and therefore single neuronal branches could be tract in their entirety. This method allowed the analysis of morphological characteristics of neurons, as well as their dendritic branching and ramification richness. Therefore the number of intersections in accordance to the distance from the cell soma was examined (figure 40).

The Cofilin $2^{fl/fl}$ Nestin-Cre animals revealed a decrease in the number of intersections starting from the earliest analyzed area-point of 25µm from the cell soma. This reduction was found throughout the entire analysis until a distance of 125µm was reached. Afterwards the Cofilin $2^{fl/fl}$ and Cofilin $2^{fl/fl}$ Nestin-Cre animals displayed a comparable number of intersections. The difference in the number of intersections was highly significant, as tested in a two-tailed independent t-test. This result leads to the conclusion that Cofilin $2^{fl/fl}$ Nestin-Cre animals displayed a reduced branching of dendrites over the distance to the cell soma and thereby also a reduced complexity of neurons. This reduction in complexity could alter the connectivity of neurons in defined circuits and the establishment of synapses between pre- and postsynaptic partners, based on the decreased dendritic area for the formation of dendritic spines. Therefore the next step was to analyze whether these neurons also showed a decreased number of dendritic spines or alterations in dendritic spine morphology based on the slightly increased F-actin level (see figure 36), which could inhibit the dynamic rearrangement of these highly motile compartments that rely on actin as the prominent cytoskeletal protein (Cingolani and Goda 2008).

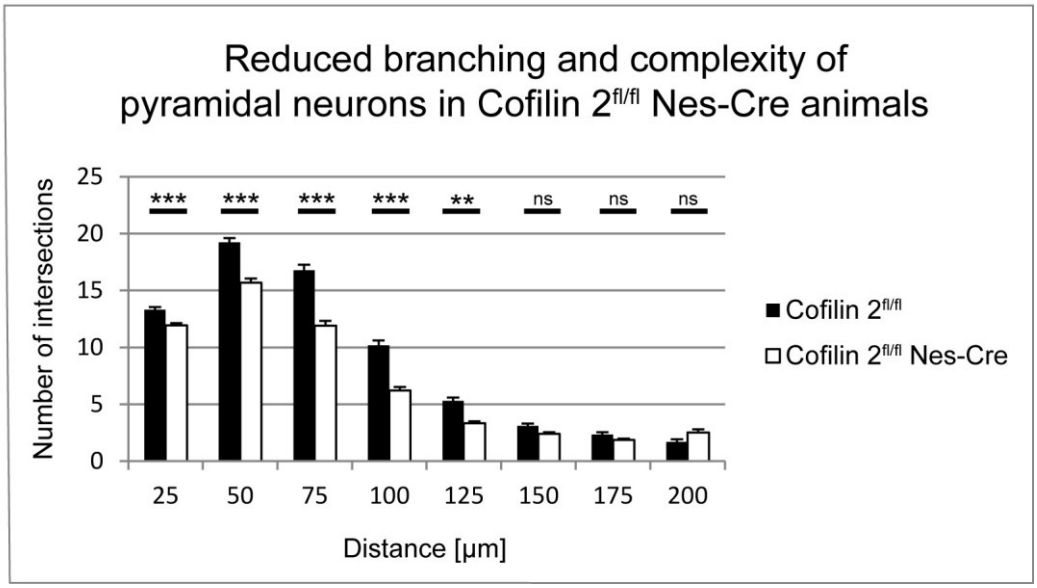

Fig. 40: Pyramidal neurons in the cortical layers II and III displayed a reduced branching and complexity due to the loss of Cofilin 2. The Golgi staining was used to perform a Sholl analysis with the ImageJ software. The number of intersections was calculated based on the distance to the cell soma. Experiments were performed on two different litters and 50 cells per genotype were analyzed. The standard deviation was calculated. The significance was tested in a two-tailed independent t-test. ($p < 0.01$ **; $p < 0{,}001$ ***)

In summary the brain-specific loss of Cofilin 2 affects the dendritic branching and results in a reduced complexity of pyramidal neurons in the cortical layers II and III.

5.8. The brain-specific loss of Cofilin 2 leads to alterations in the morphology of dendritic spines

Spines are neuronal protrusions, which receive presynaptic input and contain therefore neurotransmitter receptors and signaling systems essential for synaptic function and plasticity. More than 90% of excitatory synapses terminate on dendritic spines. The spine density varies across cortical areas, but a link between spine density and the level of cortical processing was proposed (Jacobs et al., 2001). Thereby spines undergo morphological changes based on the synaptic activity. These changes are accompanied by dynamic rearrangements of actin filaments, which are the prominent cytoskeletal protein in spine heads. Based on their morphology spines can be classified into three main groups: mushroom spines with a large head and a narrow neck; thin spines with a smaller head and a narrow neck; and stubby spines with no obvious constriction between the head and the dendrite. Actin is highly dynamic in spines with about 85% of it being exchanged within two minutes as analyzed in studies using fluorescently labeled actin (Honkura et al., 2008). Thereby a deletion of an important actin depolymerization factor could impact the dynamic rearrangement of actin filaments in dendritic spines, which would be reflected in a decrease in the number of spines or changes in their morphology. Therefore the Golgi staining was used to examine the number of dendritic spines in cortical pyramidal neurons in layers II and III. Due to the fact that the number of spines varies upon dendritic areas, pyramidal dendritic branches were classified into basal, proximal and distal parts in reference to the nature review by Spruston (Spruston 2008). For all three areas the overall number of spines was analyzed, as well as their morphology based on the classification into the three main groups: thin, mushroom and stubby spines. As shown in figure 41C, no alterations in the overall number of spines between Cofilin $2^{fl/fl}$ and Cofilin $2^{fl/fl}$ Nestin-Cre neurons were detected. A closer look at the different spine types revealed an increase in the number of thin spines on basal and proximal dendrites, accompanied by a decrease in the number of mushroom-like spines in all three analyzed regions, which kept the total number constant between wt and mt. This result was surprising since the deletion of Cofilin 1 leads to the opposite effect with an increase in the number of mushroom-shaped spines, together with a small increase in the overall number of spines (Rust et al., 2010). The number of stubby-shaped spines was only increased in the distal region of pyramidal neurons in Cofilin $2^{fl/fl}$ Nestin-Cre animals. Changes in the morphology of spines could result from alterations in the presynaptic vesicle release, which would also induce LTP or LTD in the first place. To analyze if changes in the synaptic activity could contribute to the observed morphological changes in spines electrophysiological studies were performed.

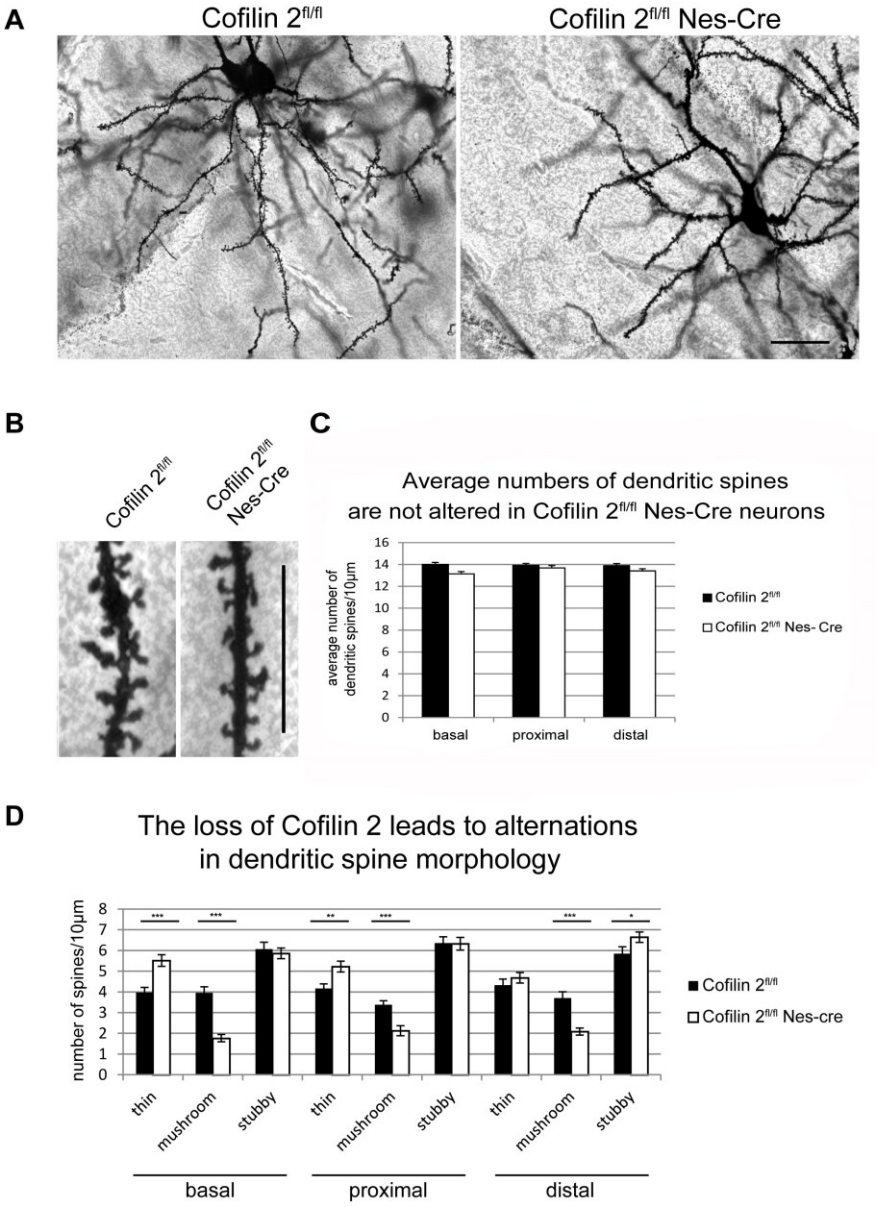

Fig. 41: The deletion of Cofilin 2 does not change the number of dendritic spines, but their morphology. A The Golgi staining was used to obtain pictures from cortical pyramidal neurons in the layers II and III and divide these neurons into basal, proximal and distal dendritic areas. Images were taken at the inverse Keyence microscope (63x) with the quick full focus function. Scale bar: 20µm **B** The number and morphology of spines based on their dendritic location was analyzed per 10µm (black lines) and compared between the Cofilin $2^{fl/fl}$ and Cofilin $2^{fl/fl}$ Nes-Cre animals. **C** To investigate the role of Cofilin 2 during dendritic spine formation the Golgi staining was used to count the number of dendritic spines per 10µm. The average numbers of dendritic spines were not altered between Cofilin $2^{fl/fl}$ and Cofilin $2^{fl/fl}$ Nes-Cre animals in basal, proximal and distal areas. **D** The morphology of dendritic spines was analyzed for all three dendritic areas (basal, proximal, distal) in pyramidal neurons. Spines were divided into three different groups (thin, mushroom and stubby) and the number of spines per 10µm was counted for every group. A reduction in the number of mushroom-shaped spines could be observed for all three dendritic regions with a concomitant increase in the number of thin spines in Cofilin $2^{fl/fl}$ Nes-Cre neurons, which kept the total number of spines constant between wt and mt. Experiments, were performed on two different litters and 50 cells per genotype were analyzed. The standard error was calculated and the significance was tested in a two-tailed independent t-test. ($p< 0,05$ *; $p< 0.01$ **; $p< 0,001$ ***)

In summary these results could show that the loss of Cofilin 2 did not impact on the overall number of spines, but rather leads to morphological changes with an increased number of thin (immature) spines, accompanied by a reduced number of mushroom-shaped (strong) spines in cortical layers.

5.9. Examination of the Cofilin $2^{fl/fl}$ Nestin-Cre animals in electrophysiological studies

Neurons are specialized for the integration and propagation of electrical signals, through which neurons communicate. The understanding of basic electrophysiological properties is fundamental to appreciate the function and dysfunction of neurons and neuronal systems. To study electrical properties of hippocampal pyramidal neurons the whole cell patch clamp technique was performed. This technique enables the recording of the intracellular electrical activity of a single cell and allows conclusions about the synaptic input that this single neuron receives. In this study pyramidal neurons in the Ca1 region of the hippocampus were examined, due to the fact that there are defined routes for information flow making the hippocampus a useful target to study synaptic functions (Deng et al., 2010). Thereby the hippocampus is implicated in important learning and memory processes (Lewis et al., 2012; McClelland et al., 1995). Additionally in this study an upregulation of ADF and Cofilin 1 was found in the hippocampus of Cofilin 2 deficient animals at P7 and in adult animals (figure 21 and 33).This upregulation suggest a possible compensatory effect of ADF or Cofilin 1 upon the loss of Cofilin 2, which could indicate an important role of Cofilin 2 in hippocampal processes.

5.9.1. The loss of Cofilin 2 does not alter miniature excitatory postsynaptic currents in the hippocampus

Actin has important presynaptic functions in the formation of the active zone and the transport of synaptic vesicles from the reserve pool to the active zone. Thereby actin plays a role in the organization of synaptic vesicles into these distinct pools (Nelson et al., 2013; Rust and Maritzen 2015). These functions are fulfilled through synaptic signaling cascades that alter the activity of actin-binding proteins and thereby induce rearrangements of the actin cytoskeleton. An altered organization of synaptic vesicles was observed in mice lacking the actin-depolymerizing factors ADF and Cofilin 1 (Zimmermann et al., 2015). This result leads to the hypothesis that actin stabilization impairs vesicle recruitment. Additionally, electrophysiological recordings revealed elevated levels of excitatory synaptic vesicle release (Zimmermann et al., 2015). To analyze whether a deletion of Cofilin 2 also influences the

synaptic vesicle release, whole cell patch clamp experiments on pyramidal neurons in the Ca1 region of the hippocampus were performed. Through the application of Tetrodotoxin (TTX) voltage-gated sodium-channels were blocked, which inhibited the generation of action potentials. This enabled the detection of miniature postsynaptic currents (mPSCs). These currents could be further classified into excitatory and inhibitory mPSCs, based on the neurotransmitter which gets released and opens specific ion channels on the postsynaptic site. Thereby mPSCs are classified as spontaneous releases of single synaptic vesicles on the presynaptic site, which occur without a stimulation of synaptic connections. First excitatory mPSCs were analyzed (figure 42 and 43). Therefore picrotoxin was applied, which blocked $GABA_A$-receptors and inhibited the generation of mIPSCs. Further Trichlormethazide (TCM) was used to inhibit the desensitization of AMPA receptors. The time between the recorded mEPCSs was used to calculate an average inter-event interval, which indicates the number of spontaneous synaptic vesicle releases from excitatory neurons. 20 cells from control and mutant animals were analyzed and no alterations in the frequency of spontaneous synaptic vesicle releases were detected. The control displayed an inter-event interval of 1.4sec ± 0.116sec (n = 20) and was thereby comparable to the mutant with 1.1sec ± 0.108sec (n = 20, Mann-Whitney test p = 0.75656; figure 42B). Since the obtained data was not normally distributed, as tested in an Shapiro-Wilk test, also a Kolmogorov-Smirnov test was prepared to compare the distribution of the single data points between wt and mt. Also in the cumulative distribution no alterations in the release of mEPSCs could be observed, which is also reflected in the p-value of 0.786.

On the postsynaptic site actin plays an important role in structural plasticity of spines during LTP and LTD (Cingolani and Goda 2008). Therefore actin is implicated in the regulation of surface-receptor diffusion, the exo-endocytic trafficking of receptors to the postsynaptic membrane and their anchoring in the postsynaptic density. The inactivation of Cofilin 1 increased the density and head volume of dendritic spines and impaired LTP (Rust et al., 2010). Also an increased level of AMPA receptors in the postsynaptic density was found upon the deletion of Cofilin 1. To address the question whether the loss of Cofilin 2 leads to postsynaptic impairments in AMPA receptor mobility the amplitude of recorded mEPSCs was analyzed (figure 43). Thereby the amplitude of the obtained mEPSCs reflected only AMPA receptors, due to the fact that NMDA receptors are also gated through voltage and the channel is blocked by an Mg^{2+} ion when the cell is at its resting potential. The obtained mean for the amplitude of Cofilin $2^{fl/fl}$ animals with 12.6pA ± 0.69pA (n = 20) was comparable to the Cofilin $2^{fl/fl}$ Nestin-Cre animals with a mean amplitude of 12pA ± 1.26pA (n = 20, Mann-Whitney test p-value 0.58232). To test for a possible shift in the amplitude a cumulative distribution was performed since the data was not normally distributed (Shapiro-Wilk test). A

Kolmogorov-Smirnov test revealed no changes in the amplitude of mEPSCs of wt and mt pyramidal neurons.

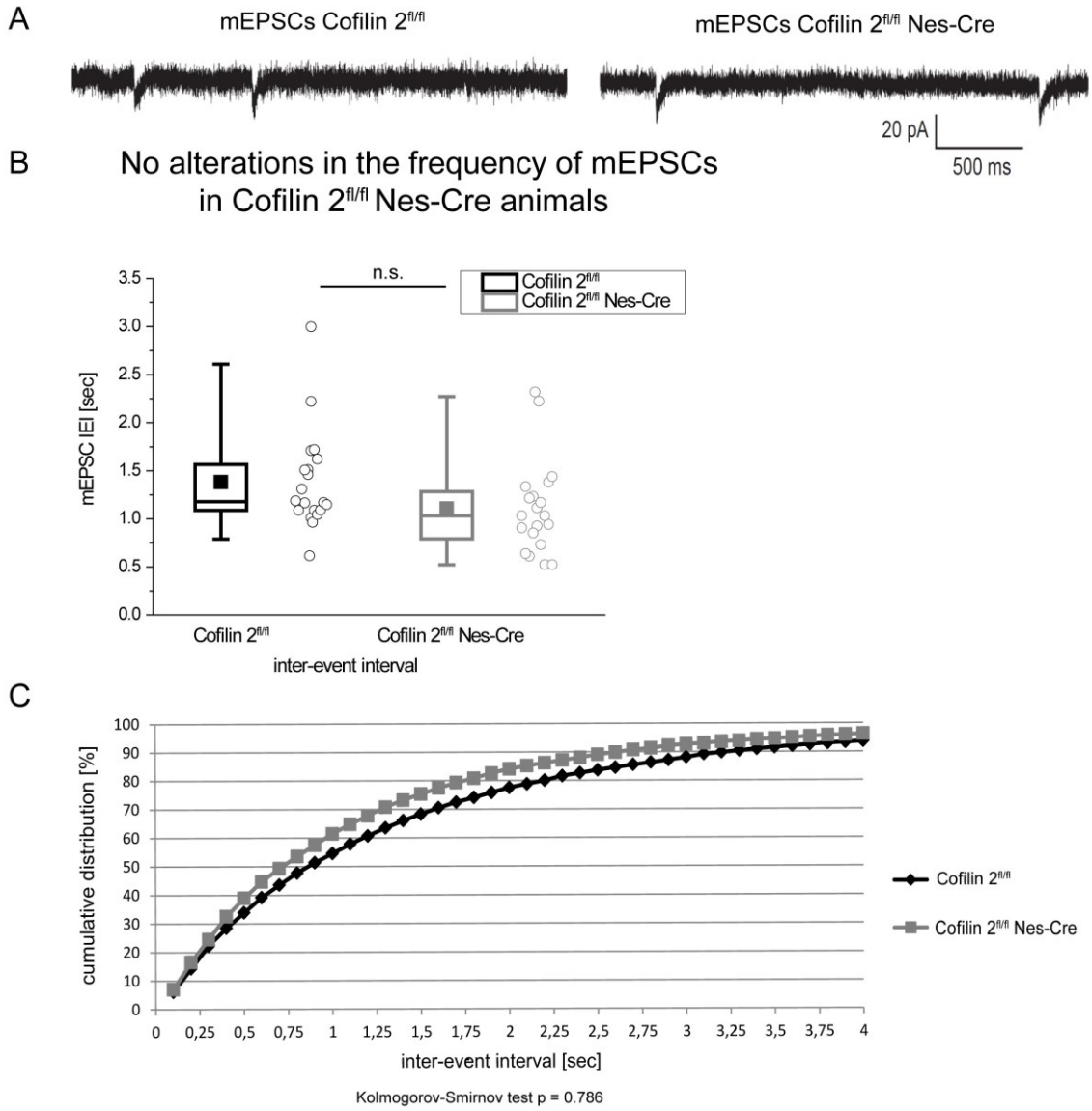

Fig. 42: The inter-event interval (IEI) of spontaneous mEPSCs is not altered in Cofilin 2$^{fl/fl}$ Nestin-Cre animals. Hippocampal Ca1 pyramidal neurons were patched in brain slices of P20 – 22 old mice with TTX (blocks the generation of AP), picrotoxin (inhibits the occurrence of mIPSCs) and TCM (blocks the desensitization of AMPA receptors) in the external solution. For each genotype 20 cells from 4 distinct animals were analyzed for the occurrence of spontaneous mEPSCs in voltage clamp mode, holding the membrane potential at -70mV. **A** Exemplary showcase for the recorded mEPSCs of Cofilin 2$^{fl/fl}$ and Cofilin 2$^{fl/fl}$ Nes-Cre animals. Note that the number of events was similar between control and mutant animals. **B** Analyzed cells were plotted as individual points in a box graph, which enabled the comparison between the distribution of the wt and mt cells. The mean and standard error for the IEI was calculated and a comparable mean was detected for the control (1.4sec ± 0.116sec; n = 20) and the mutant (1.1sec ± 0.108sec;n = 20). Mann-Whitney test p-value 0.75656. **C** The obtained data was not normally distributed (Shapiro-Wilk test) and therefore a cumulative distribution was prepared to analyze shifts in the IEI between the control and mutant cells. The significance was tested with a Kolmogorov-Smirnov test for nonparametric data. With a p-value of 0.786 no significance was detected.

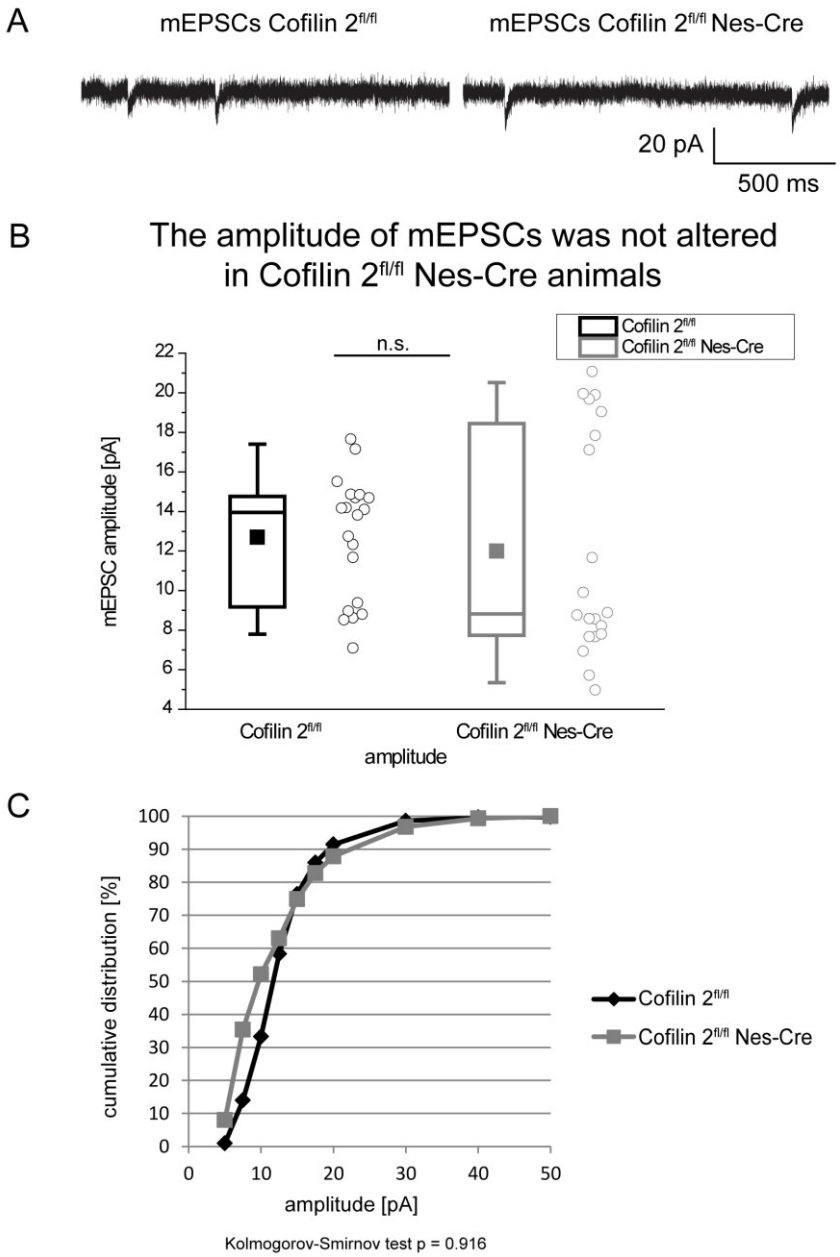

Fig. 43: The amplitude of mEPSCs is unaffected upon the deletion of Cofilin 2 in neuronal cells. Hippocampal Ca1 pyramidal neurons were patched in P20 – 22 old mice with TTX (blocks the generation of AP), picrotoxin (inhibits the occurrence of mIPSCs) and TCM (blocks the desensitization of AMPA receptors) in the external solution. For each genotype 20 cells from 4 distinct animals were analyzed for the occurrence of spontaneous mEPSCs in voltage clamp mode, holding the membrane potential at -70mV. Note that NMDA-receptors are blocked when holding the cell at -70mV and the observed amplitude was based only an AMPA-receptors. **A** Exemplary showcases for the recorded mEPSCs of Cofilin $2^{fl/fl}$ and Cofilin $2^{fl/fl}$ Nes-Cre animals. Note that the amplitude of recorded events for the control and mutant were comparable. **B** Every analyzed cell was plotted as individual point in a box graph, which enabled the comparison between the distribution of the collected wt and mt cells. The average and standard error were calculated for Cofilin $2^{fl/fl}$ and Cofilin $2^{fl/fl}$ Nes-Cre animals. The mean for the control is with a value of 12.6pA ± 0.69pA, comparable to the mutant with a value of 12pA ± 1.26pA (Mann-Whitney test p-value 0.58232. **C** A cumulative distribution was prepared since the data is not normally distributed (Shapiro-Wilk test) and a shift in the amplitude is not reflected in the average. Therefore the significance was tested in a nonparametric Kolmogorov-Smirnov test. With a p-Value of 0.916 no significant alteration between the control and mutant animals could be observed.

In summary the loss of Cofilin 2 did not significantly alter the frequency or amplitude of mEPSCs, although the cumulative distribution indicated a slight shift towards a smaller amplitude of Cofilin 2-deficient cells. This would fit to the obtained results from dendritic spine analysis were an increased number of thin (immature) spines was observed, which contain a lower number of AMPA receptors.

5.9.2. Elevated frequency of spontaneous inhibitory vesicle release upon the brain-specific loss of Cofilin 2

The balance between excitation and inhibition plays an important role for neuronal connectivity, due to the fact that an increased level of glutamate displays also neurotoxic effects (Lau and Tymianski 2010). The release of inhibitory neurotransmitters is important for the regulation of synaptic integration, as well as the probability and timing of action potential generation. A single inhibitory neuron can innervate 100 principle neurons to synchronize the network activity (Isaacson and Scanziani 2011). Additionally inhibitory neurons are involved in feed-forward inhibition to regulate the excitatory output in neuronal circuits. The frequency of mIPSCs generated from inhibitory neurons in the hippocampus was measured. Therefore TTX was applied to block the generation of action potentials and NBQX, which blocks AMPA-receptors. The main inhibitory neurotransmitter in the CNS is GABA, which is synthesized from glutamate by the glutamic acid decarboxylase. This enzyme is expressed by inhibitory neurons in the spinal cord, in basket cells of the hippocampus, in Purkinje cells and basket cells of the cerebellum and in granule cells of the olfactory bulb (Lujan et al., 2005). The release of vesicles that contain GABA as a neurotransmitter was analyzed in the Ca1 region of the hippocampus by analyzing the inter-event interval IEI in recordings of mIPSCs (figure 44).

The average of the Cofilin $2^{fl/fl}$ control animals was with about 0.659sec ± 0.069sec (n = 20) between the occurrences of two events more than double as in the knockout with about 0.284sec ± 0.027sec (n = 20, Mann-Whitney test p-value 0.56868). Although no significant was detected in a Mann-Whitney test we also performed a cumulative distribution analysis. In this test a shift in the inter-event interval (IEI) was visible, since in the control 50% of the analyzed cells had an IEI below or equal to 0.4sec, while in knockout cells 50% was already reached at 0.250sec. A Kolmogorov-Smirnov test displayed significance with a value of p = 0.0001. The knockout animals showed a decreased IEI, which could be related to an increased spontaneous release of GABA vesicles in the hippocampus.

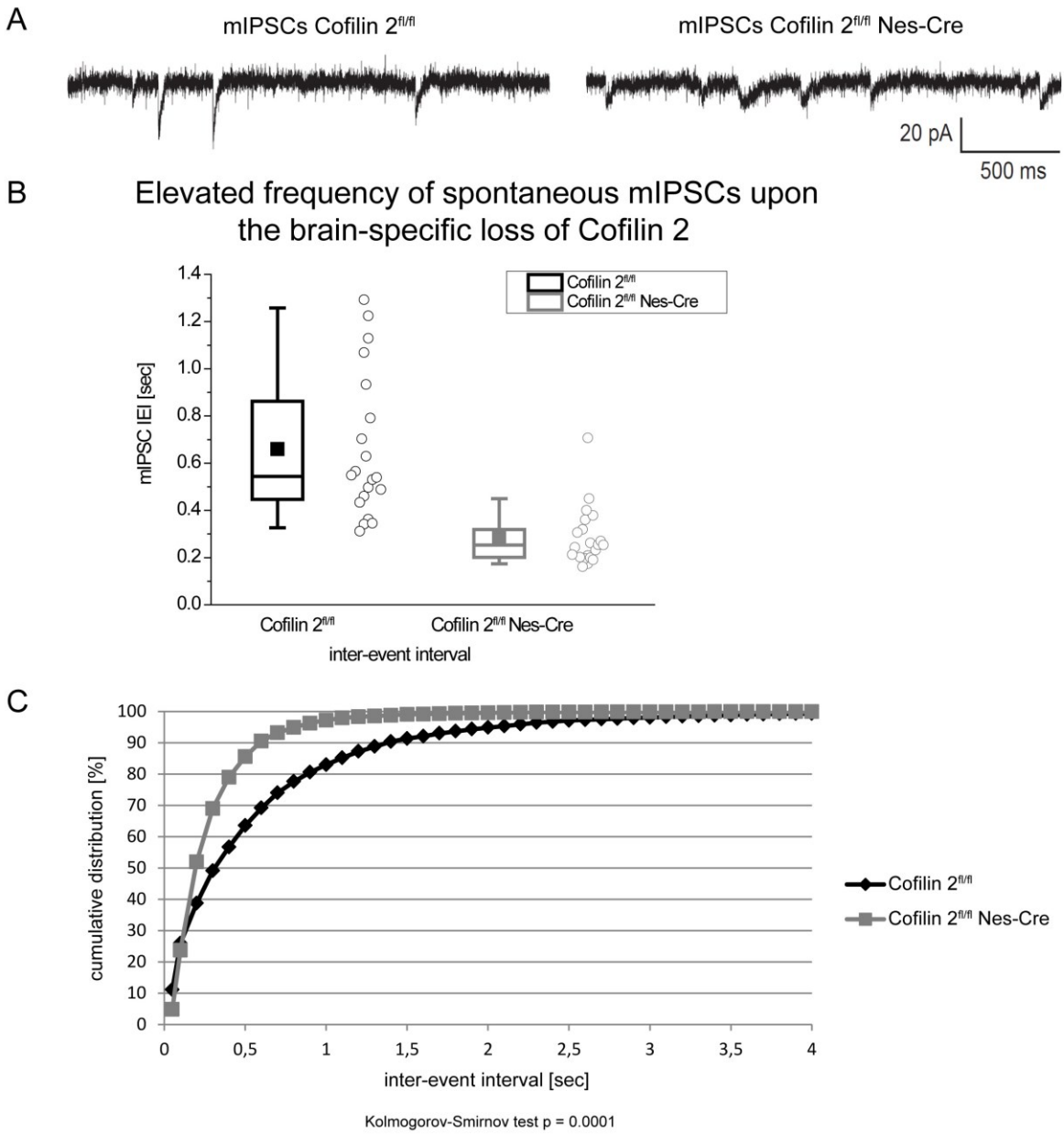

Fig. 44: Upon the brain-specific loss of Cofilin 2 an elevated frequency of mIPSCs is detected. Hippocampal Ca1 pyramidal neurons were patched in P20 – 22 old mice with TTX and NBQX in the external solution to block the generation of AP and mEPSCs. For the Cofilin $2^{fl/fl}$ control 20 cells and the Cofilin $2^{fl/fl}$ Nes-Cre mutant 21 cells from 3 distinct animals were analyzed for the occurrence of spontaneous mIPSCs in voltage clamp mode, holding the membrane potential at -70mV. **A** Exemplary showcases for the recorded mIPSCs of Cofilin $2^{fl/fl}$ and Cofilin $2^{fl/fl}$ Nes-Cre animals. Note that the number of events is increased in the mutant animals. **B** Every analyzed cell was plotted as individual point in a box graph, which enabled the comparison between the distribution of the collected wt and mt cells. The average and standard error of 20 cells from the Cofilin $2^{fl/fl}$ control and 21 cells from the Cofilin $2^{fl/fl}$ Nes-cre animals was calculated. Note that the inter-event-interval was decreased for the mutant to 0.284sec ± 0.027sec compared to the control with 0.65sec ± 0.069sec (Mann-Whitney test p-value 0.56868). **C** To see where the shift in the data between control and mutant animals occured a cumulative distribution plot was prepared, since the data was not normally distributed (Shapiro-Wilk test). 50% of the wt had an inter-event-interval below or equal to 0.4sec, while 50% of the mutant was already included at 0.250sec. The significance was tested in a nonparametric Kolmogorov-Smirnov test, with a significant p-Value of 0.0001.

The recorded events relied mainly on ionotropic $GABA_A$-receptors, which conduct chloride ions. To obtain a sufficient signal an internal solution with an increased concentration of chloride ions was used. $GABA_B$-receptors are metabotropic and have to activate internal signaling cascades to open potassium channels, which lead to a decelerated postsynaptic response and do not contribute to the measured events here. A second important inhibitory neurotransmitter is Glycine, which is the main inhibitory neurotransmitter in the brain stem and spinal cord and is only rarely expressed in the hippocampus. An important difference between excitatory and inhibitory actions exists in the fact that excitatory synapses often innervate dendritic spines, while synapses on cell bodies are often inhibitory (Markram et al., 2004). Inhibitory actions are more significant when they are initiated at the cell body near the axon segment, because a depolarization produced by an excitatory current from a dendrite must pass through the cell body as it moves toward the axon segment. Inhibitory actions at the cell body open chloride channels, which hyperpolarizes the cell and reduces the outcome of an excitatory current. Therefore most $GABA_A$-receptors are localized at the cell soma, where the actin cytoskeleton is differently organized and regulated than in dendritic spines.

The recorded mIPSCs were also analyzed for changes in the amplitude of events (figure 45). The average amplitude was slightly distinct between control 18.94pA ± 1.02pA and knockout animals 14.94pA ± 1.05pA and displayed a reduced amplitude for the Cofilin $2^{fl/fl}$ Nestin-Cre animals. In a Mann-Whitney test the data was not significant ($p = 0.54186$, figure 45B). Therefore the distribution of the single data points was also analyzed in a cumulative distribution to detect a possible shift between control and knockout animals (figure 45C). With a Kolmogorov-Smirnov test a tendency for a reduced amplitude in mutant animals was observed, however the difference was not statistically different (p-value 0.531). In control animals 50% of the analyzed cells had amplitudes below or equal to 15 pA, while in the knockout 50% were reached at 10pA.

To be able to compare miniature postsynaptic currents between wt and mt cells it must be considered that the cell capacitance or serial resistance should be comparable between both genotypes. According to Ohm´s law ($R = U*I$): the higher the resistance, the less current is needed to introduce voltage changes. Thereby if the resistance of the wt cells was increased in comparison to the mt, these wt cells would need less current to introduce a change in the membrane potential, which leads to the generation of an event. Therefore changes in mPSCs can only be analyzed between wt and mt cells when the capacitance and resistance is examined and comparable for both genotypes. A direct examination of the resistance and capacitance was not done in this thesis, but if changes in the resistance would be responsible for the detected changes in mIPSCs of mutant cells, then both postsynaptic currents (mEPSCs and mIPSCs) should display a phenotype that is proportional to one

another. Since we could not detect changes in mEPSCs it is unlikely that a difference in the resistance or capacitance exist between wt and mt cells and that these changes account for the observed phenotype in mIPSCs.

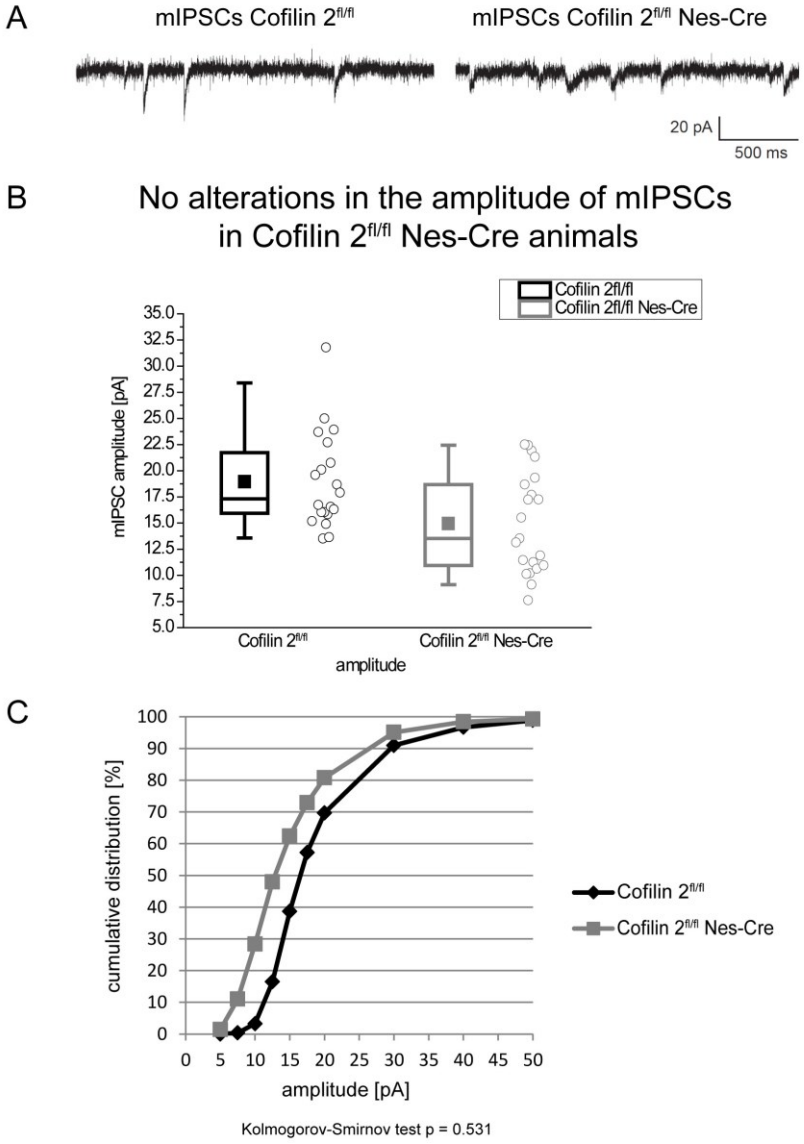

Fig. 45: The amplitude of mIPSCs is not altered in the hippocampus upon the brain-specific loss of Cofilin 2. Hippocampal Ca1 pyramidal neurons were patched in P20 – 22 old mice with TTX and NBQX in the external solution to block the generation of AP and mEPSCs. For the Cofilin $2^{fl/fl}$ control 20 cells and the Cofilin $2^{fl/fl}$ Nes-Cre mutant 21 cells from 3 distinct animals were analyzed. The occurrence of spontaneous mIPSCs in voltage clamp mode was analyzed, holding the membrane potential at -70mV. **A** Exemplary showcases for the recorded mIPSCs of Cofilin $2^{fl/fl}$l and Cofilin $2^{fl/fl}$ Nes-Cre animals. Note that the amplitude is decreased in Cofilin $2^{fl/fl}$ Nes-Cre animals. Additionally an increase in the delay time of the recorded events could be observed. **B** Every analyzed cell was plotted as individual point in a box graph, which enabled the comparison between the distribution of the collected wt and mt cells. The average and standard error was calculated for both genotypes. Note that the average amplitude of the mutant animals with 14.94pA ± 1.05pA was slightly decreased compared to the control with an average amplitude of 18.94pA ± 1.02pA (Mann-Whitney test p-value 0.54186). **C** Since the data was not normally distributed the distribution was analyzed in a nonparametric Kolmogorov-Smirnov test. With a p-Value of 0.531 the data was not significantly different.

In summary the loss of Cofilin 2 leads to a significant increase in inhibitory synaptic vesicle release in the Ca1 region of the hippocampus. No significant alteration in the amplitude of mIPSCs was observed, but an increased number of Cofilin 2-deficient cells with a smaller amplitude were detected. The same observation was also made during the analysis of mEPSCs.

5.9.3. The resting potential is reduced in Cofilin $2^{fl/fl}$ Nestin-Cre cells

The cell membrane is 2 – 3 nm thick and is impermeable to most charged molecules, separating the cytoplasm of a cell from extracellular environment. This leads to different ion concentrations between the inside of a cell and the surrounding fluid. Thereby the cell membrane acts as both an insulator and an diffusion barrier for the movement of ions, leading to the generation of an electrical potential between the interior and the exterior of a cell (membrane potential). Different types of ion channels span the cell membrane and are selectively for the conductance of specific ions. Thereby each ionic current is associated with a conductance (inverse of resistance) and a driving force, which is due to the different concentrations of ions between the intracellular and extracellular space. The capacity of channels to conduct ions can be modified by voltage (changes in the membrane potential), concentration of intracellular messengers (Ca^{2+}-dependent) or external concentration of neurotransmitters. In an excitable neuron ion channels are represented by conductance. Thereby the conductance is important to understand mechanisms that contribute to AP-generation, repetitive firing and bursting.

During the analysis of mPSCs also the holding current at the beginning of the measurement was noted. As seen in figure 46A, the holding current of Cofilin $2^{fl/fl}$ Nestin-Cre animals was with -111.86pA ± 10.75pA (n = 21) significantly more positive than the holding current of control animals with -146.92pA ± 10.49pA (n = 20, Mann-Whitney test p-value 0.0096) at the beginning of the measurement. The holding current is thereby determined as the current injected by the system to keep the neuron at -70mV. If the system needs to apply more negative current to be able to hold the cell at -70mV, as observed for control cells, these cells displayed a more positive membrane potential. That means the membrane potential of mt cells was more negative, compared to wt cells, and the system applied less current to hold the cell at -70mV. Therefore a reduced holding current could be due to changes in the membrane conductance or potential. One reason for the altered holding current in Cofilin $2^{fl/fl}$ Nestin-Cre animals could be changes in the intracellular ion concentrations, since after 5 min of recording an exchange between ions in the cell plasma and the filled micropipette took place, which lead to a reduction in the differences between the holding current (figure 46B),

albeit still less current was needed in Cofilin 2 deficient neurons to maintain at -70mV. The ion exchange leads to an holding current of -130.35pA ± 11.15pA in the control (n = 20) compared to -109.39pA ± 11.74pA in the mutant (n = 21, Mann-Whitney test p-value 0.07346).

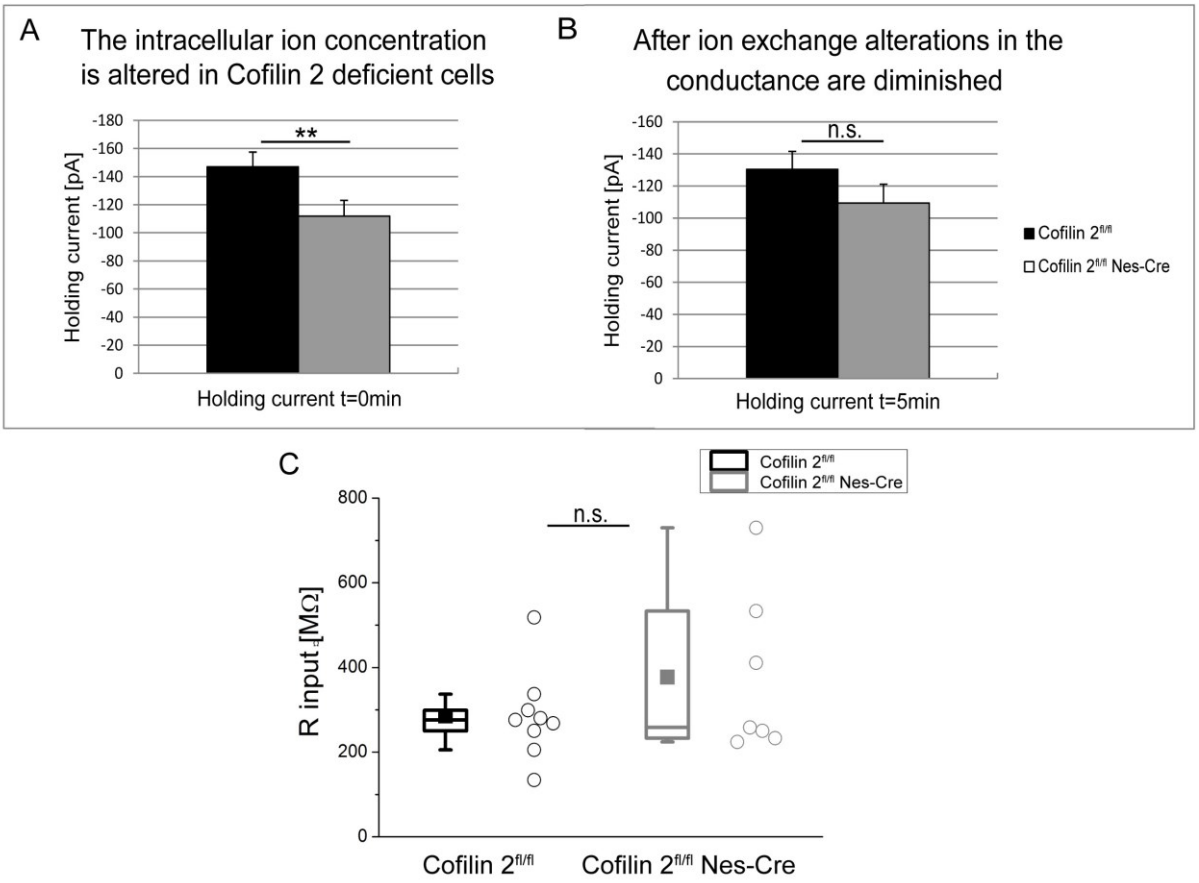

Fig. 46: The holding current that is needed to hold the membrane potential at -70 mV is significantly less negative in Cofilin 2$^{fl/fl}$ Nestin-Cre animals. The examined cells for the evaluation of mPSCs were also analyzed for their holding current at -70 mV after the cell was successfully patched. Therefore the holding current was taken at the beginning of the measurement and after 5 min of recording. In these 5 min an ion exchange between the cell plasma and the intracellular solution of the micropipette occurred. Changes in the holding current could also arise from an altered excitability of cells. **A** The holding current between Cofilin 2$^{fl/fl}$ and Cofilin 2$^{fl/fl}$ Nes-Cre animals was compared at the beginning of the recordings. At that time point the ion concentration in the cell plasma differs from the intracellular recording solution in the pipette. Note that for the Cofilin 2$^{fl/fl}$ Nes-Cre animals (-111.86pA ± 10.75pA, n = 21) a significantly lower holding current is needed, indicating a more negative membrane potential than in control animals (-146.92pA ± 10.49pA; Mann-Whitney test 0.0096). **B** After 5min the holding current was again analyzed for both genotypes, but this time the current became comparable potentially due to diffusion of ions between both compartments. Note that the difference in the holding current had decreased between control (-130.35pA ± 11.15pA, n = 20) and mutant animals (-109.39pA ± 11.74pA, n = 21; Mann-Whitney test 0.07346). **C** Cofilin 2$^{fl/fl}$ Nes-Cre cells displayed an increased input resistance 377MΩ ± 73.12MΩ, in comparison with control cells 285.2MΩ ± 34.96MΩ, although changes were not significant (t-test 0.243). This means that mutant cells had a reduced conductance and were less leaky for ions.

In the current clamp mode also intrinsic proberties were measured and revealed a slightly increased input resistance in Cofilin 2-deficient cells (377MΩ ± 73.12MΩ; n = 7) compared to controls (285.2MΩ ± 34.96MΩ; n = 9; t-test 0.243). Changes in the input resistance result in a reduced conductance, which means that the cell membrane is less permeable for ions. This could result in an increased excitability of cells, since the diffusion rate of ions out of the cell is decreased upon the increased membrane conductance.

In summary Cofilin 2-deficient neurons need a reduced holding current to keep the membrane potential at -70mV during the recordings. The analysis of intrinsic cell properties revealed a slightly increased input resistance of Cofilin $2^{fl/fl}$ Nestin-Cre neurons, which leads to a reduced conductance. That means that Cofilin $2^{fl/fl}$ Nestin-Cre neurons displayed an increased excitability, since the cells were less leaky for ions that could diffuse through the cell membrane and alter therefore the membrane potential. These observations could be a hint for a role of actin in ion channel regulation.

5.10. Behavioral analysis of Cofilin 2 deficient animals

5.10.1. The brain-specific deletion of Cofilin 2 does not alter locomotor or exploratory behavior in an open field

The open field is a quadratic apparatus, which is divided into a periphery- and a center-area. This center area is an open brightly illuminated and unprotected environment, which is avoided by the animals. Therefore mice spent most of the time exploring the periphery of the apparatus, typically in contact with the walls. Mice were allowed to freely explore the open field for a test session of 60 minutes. This test provides the opportunity to assess novel environment exploration, general locomotor activity, habituation and provides an initial screen for anxiety-related behavior in rodents. Goodson et al showed an increased total activity of Cofilin $1^{fl/fl}$ CaMKII-Cre animals in the open field, reflecting a locomotor hyperactivity (Goodson et al., 2012). Cofilin $2^{fl/fl}$ and Cofilin $2^{fl/fl}$ Nestin-Cre animals were analyzed in the open field to observe if an increased activity could be also detected in these animals. The most commonly used measure for locomotor activity is the total distance travelled. Therefore the total distance traveled was calculated for the Cofilin $2^{fl/fl}$ control animals and normalized to 100% and compared to the total distance travelled in the mt. As seen in figure 47A the total distance travelled for the Cofilin $2^{fl/fl}$ Nestin-Cre animals was not increased (control 100% ± 15.11; mutant 109.65% ± 12.08; ns; n = 9) .

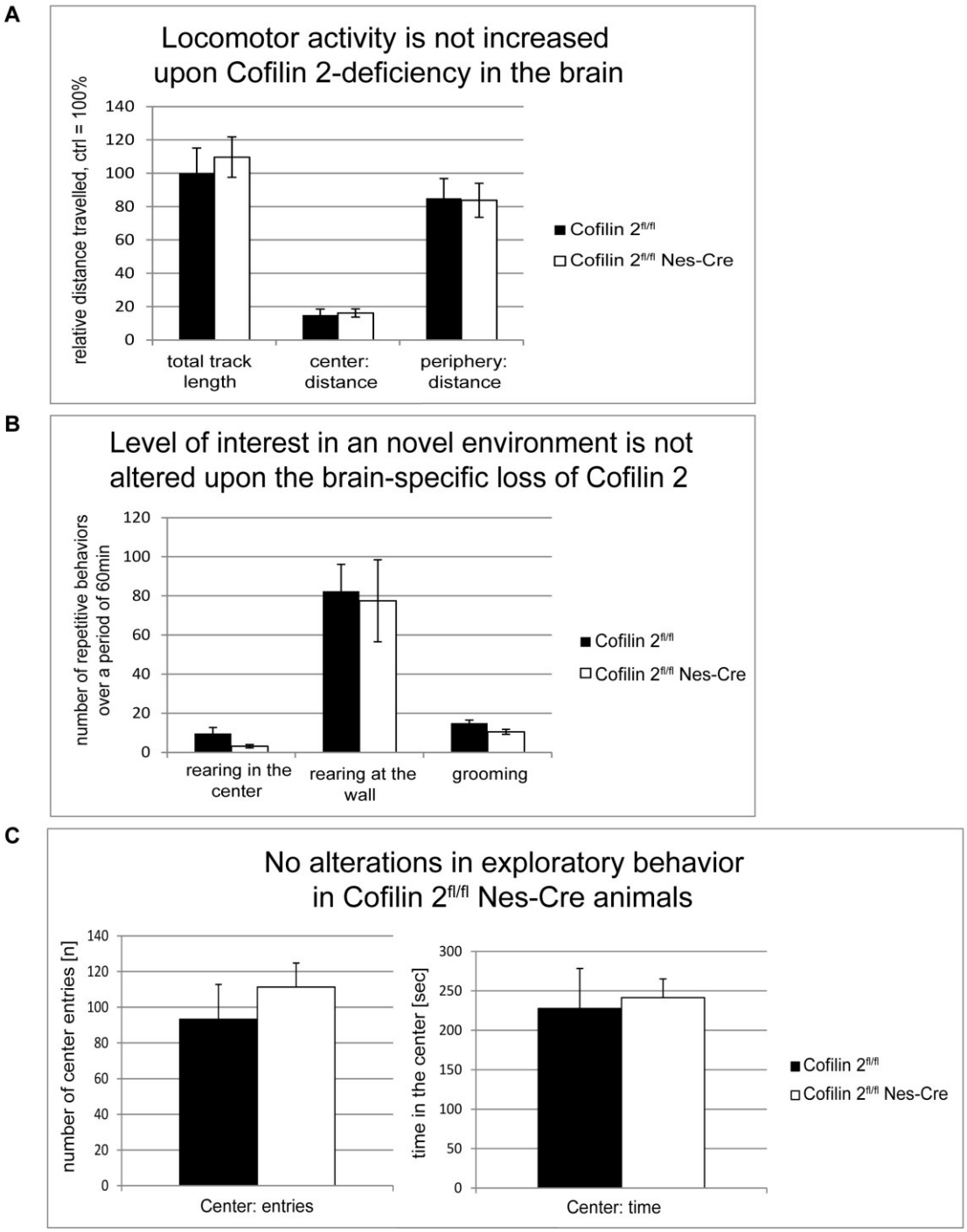

Fig. 47: Locomotor activity and exploratory behavior is not altered upon the brain-specific loss of Cofilin 2. A The total distance travelled during a period of 60 minutes was calculated in the open field and the relative distance of Cofilin $2^{fl/fl}$ animals were normalized to 100%. No increase in locomotor activity for the Cofilin $2^{fl/fl}$ Nes-Cre animals could be observed. Also the distances travelled in the center and in the periphery of the open field were comparable. **B** Repetitive behaviors were analyzed during the 60min test phase. An elevated frequency of repetitive behaviors indicates increased locomotor activity and an increased level of interest in novel environments. The loss of Cofilin 2 did not alter the number of repetitive behaviors. **C** The number (n) of center entries and the time spent in the center of the open field were examined for the Cofilin $2^{fl/fl}$ and Cofilin $2^{fl/fl}$ Nes-Cre animals. No changes in the exploratory behavior of Cofilin $2^{fl/fl}$ Nes-Cre animals could be detected. Experiments were performed on 2 – 3 month old male wt (n=9) and mt (n=9) animals. The standard error was calculated and the significance was tested in a two-tailed independent t-test. Changes were not significant.

The total distance travelled was sub-divided into distance travelled in the center and periphery to analyze if the mt animals spent more time in one of these areas compared to the controls. Also the distance travelled in the center and periphery of the open field was comparable and both groups spent only one fifth of the total distance in the center area. An increased level in the novelty of a new environment and locomotor activity is also reflected in an elevated frequency of repetitive behaviors, like grooming or rearing. A change in the number of repetitive behaviors was not detected in Cofilin $2^{fl/fl}$ Nestin-Cre animals. When mice are placed in a new environment the hippocampus signals a lack of information about the current environment and mice start exploratory behavior. Therefore the level of exploratory behavior can be measured in the number of center entries and time spent in the center. In figure 47C a change in exploratory behavior was not observed in Cofilin $2^{fl/fl}$ Nestin-Cre animals, due to the fact that no alterations in the number of center entries (control 93.25 ± 19.54; mutant 111.33 ± 13.41; ns; n = 9) or time spent in the center could be detected (control 227.675sec ± 50.67sec; mutant 241.4sec ± 23.73sec; ns; n = 9).

If the duration of the open field analysis exceeds 30minutes also the process of habituation can be analyzed. In habituation an animal first responds to a new stimulus, in this experiment the open field as a new environment, by attending to it with a series of orienting responses, like repetitive behaviors or increased locomotion and then learns to ignore the stimulus if the stimulus is neither beneficial nor harmful. This is reflected in the fact that mice calm down over the 60min period of the test session, with an increased level of activity at the beginning of the test and a decline over time. Additionally the number of immobile episodes increases over time. A decrease in the intensity of a stimulus results from a diminished synaptic effectiveness within a pathway. As seen in figure 48 the habituation was not affected in Cofilin $2^{fl/fl}$ Nestin-Cre animals. A reduction in the response to the given stimulus could be detected in Cofilin $2^{fl/fl}$ and Cofilin $2^{fl/fl}$ Nestin-Cre animals, reflected in a decrease in the total distance travelled over time as analyzed for 5min bins of the 60min test session. Additionally the time immobile increased the longer the test ran for both genotypes.

In summary, in the open field test no alterations in locomotor activity and exploratory behavior could be observed in Cofilin $2^{fl/fl}$ Nestin-Cre animals. The brain-specific deletion of Cofilin 2 also did not impact on the habituation process to a new environment.

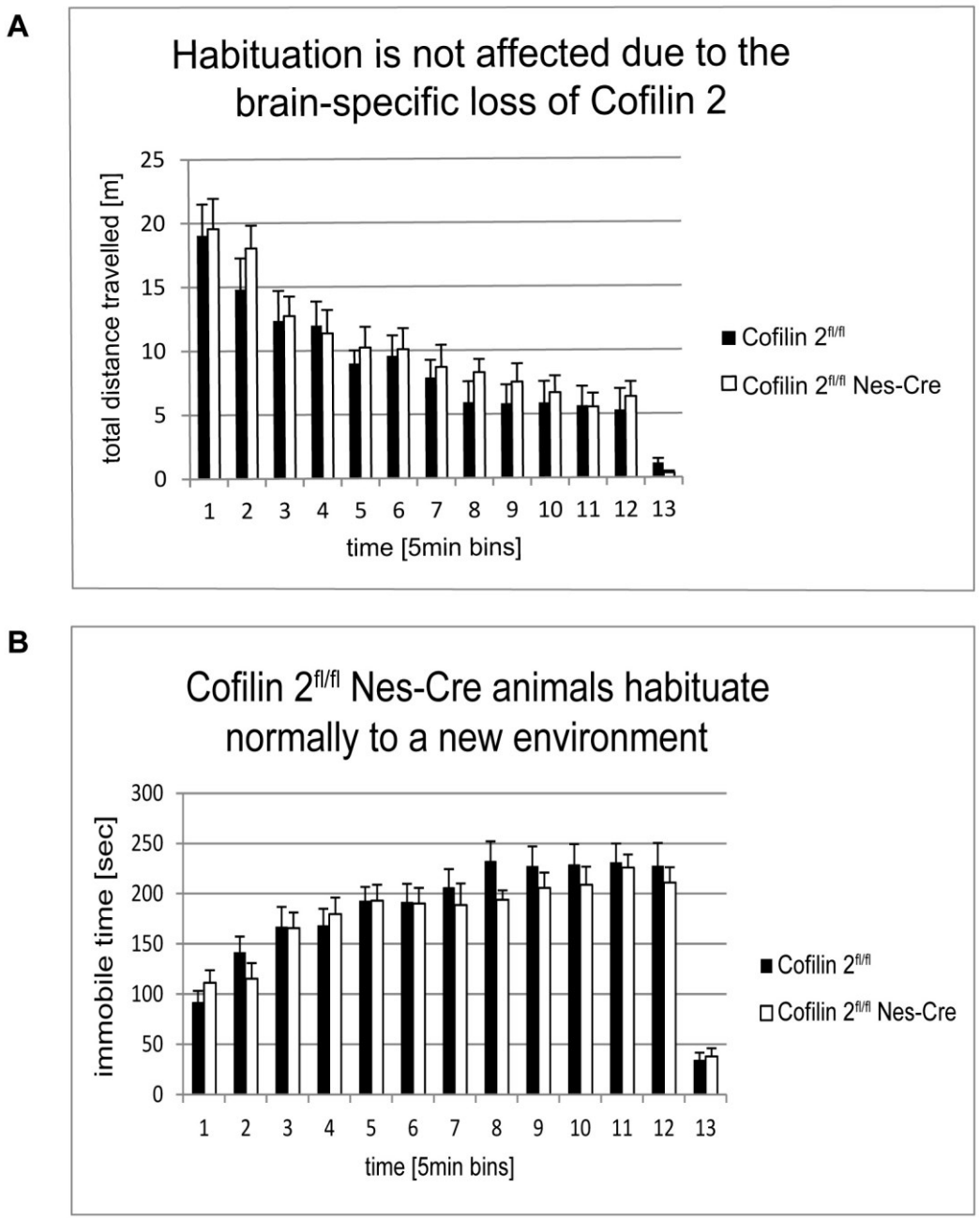

Fig. 48: Cofilin $2^{fl/fl}$ Nestin-Cre animals habituate normally to a new environment. A Prolonged test duration of the open field also enables the analysis of the habituation process. The total distance travelled was analyzed for 5min intervals (bins) of the 60min test session. A reduction in the total distance travelled over time could be observed for the Cofilin $2^{fl/fl}$ and Cofilin $2^{fl/fl}$ Nes-Cre animals. **B** A reduction in the total distance travelled should be also reflected in an increased time of immobility. Therefore the time immobile was analyzed in 5min intervals (bins) of the 60min test duration. An increase in the time immobile for Cofilin $2^{fl/fl}$ and Cofilin $2^{fl/fl}$ Nes-Cre animals could be observed during the 60min test phase. Results were obtained from nine different 2 to 3 month old male animals for every genotype. The standard error was calculated and significance was tested in a two-tailed independent student t-test. Changes were not significant.

5.10.2. The brain-specifc loss of Cofilin 2 does not alter anxiety

An experimental approach to assess anxiety-like behavior in rodents is the elevated plus maze (EPM). This test is based on an approach-avoidance conflict that takes advantage of the natural tendency of mice to explore a novel environment against a fearful stimulus. In the EPM mice are allowed to freely explore the apparatus for 5 minutes and can decide between the exploration of two open, unprotected arms or two enclosed, protected arms. The fearful stimuli in the EPM are the open unprotected maze arms, which are avoided by animals, because they are the potentially more dangerous areas. An increased number of open arm entries and/or the amount of time spent there reflect a decreased anxiety-like behavior in rodents. A conditional deletion of Cofilin 1 in the brain resulted in less anxious animals in the open field and EPM and an increased total activity (Goodson et al., 2012). In this study it was analyzed whether the loss of Cofilin 2 also impacts on neuronal circuits responsible for anxiety in mice. Although an increased anxiety in Cofilin $2^{fl/fl}$ Nestin-Cre animals could not be detected in the open field (see figure 47), the EPM is a more preferable method to analyze anxious behavior in rodents.

The overall activity of mice in the EPM was analyzed to exclude the possibility that an increased number of open arm entries could only result from a generalized hyperactivity. Hyperactive animals would show an increased number of total arm entries (open + closed arms). Thereby the number of total arm entries in the EPM should not differ between both groups to exclude hyperactivity as cause for behavioral abnormalities. In figure 49A a comparable number of total arm entries for Cofilin $2^{fl/fl}$ and Cofilin $2^{fl/fl}$ Nestin-Cre animals was observed, which exclude hyperactivity in the knockout animals (control 21.4 ± 1.705; mutant 19.5 ± 1.33; ns; n = 9). An anxious animal will make fewer open arm entries and spent less time in this unprotected area. As a next step the number of open arm entries and the time spent there were compared. The number of open arm entries were nearly the same for Cofilin $2^{fl/fl}$ and Cofilin $2^{fl/fl}$ Nestin-Cre animals (control 4.2 ± 1.29; mutant 4.3 ± 0.99; ns; n = 9), although the mutant mice spent slightly more time in the open arms than the controls (control 14.3sec ± 5.53sec; mutant 18.5sec ± 7.06sec; ns; n = 9)(figure 49B). This result indicated that the single knockout of Cofilin 2 was not sufficient to significantly alter anxiety-like behavior. According to this observation also the tracking plots of Cofilin $2^{fl/fl}$ and Cofilin $2^{fl/fl}$ Nestin-Cre animals did not differ in the paths of the single animals over the entire 5 minutes test phase (figure 49C). Cofilin $2^{fl/fl}$ Nestin-Cre animals avoided the open, unprotected arms like the controls and mostly stayed in the closed, protected arms.

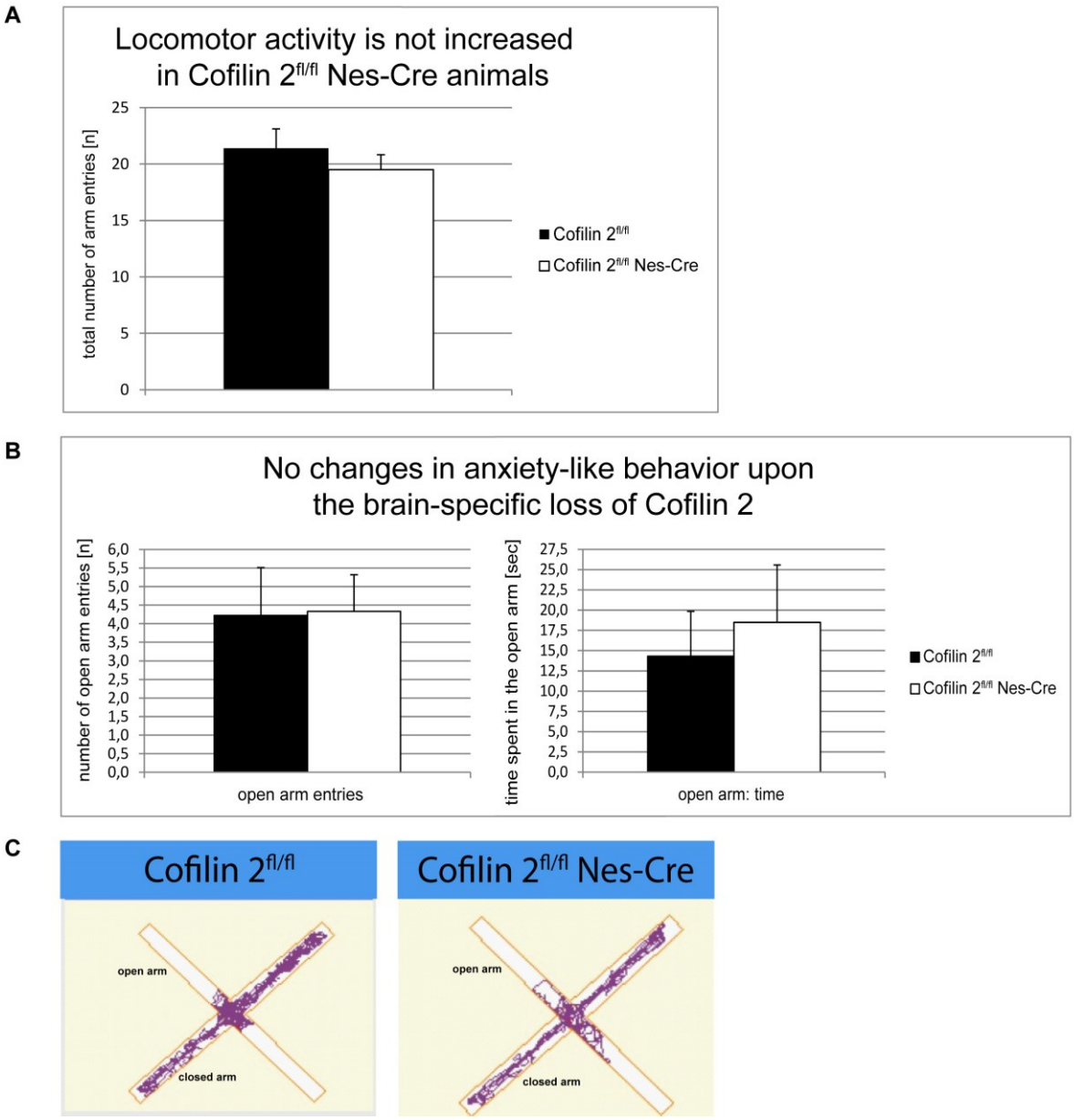

Fig.49: No alterations in anxiety-like behavior could be observed in Cofilin 2$^{fl/fl}$ Nestin-Cre animals. To assess anxiety-like behavior EPM experiments were performed. Mice were allowed to freely explore the apparatus for 5 minutes and had to decide between the visit of open, unprotected arms or enclosed, protected arms. **A** The overall activity was measured through the total number (n) of arm entries. No alterations between Cofilin 2$^{fl/fl}$ and Cofilin 2$^{fl/fl}$ Nes-Cre animals could be observed, which excludes changes in the locomotor activity, which could mimic anxiety-like abnormalities in this test. **B** The number of open arm entries and time spent there were compared between control and mutant animals. No alterations could be observed upon the loss of Cofilin 2 in neuronal cells. **C** As an example two tracking plots were shown for one Cofilin 2$^{fl/fl}$ control and one Cofilin 2$^{fl/fl}$ Nes-Cre animal each. In these plots the head position of animals were reflected over the entire 5minutes in the open and closed arms. The Cofilin 2$^{fl/fl}$ Nes-Cre animals avoided the open arms like the Cofilin 2$^{fl/fl}$ animals. Most of the time both genotypes explored the closed and protected arms. Results were obtained from nine different 2 to 3 months old male animals for every genotype. The standard error was calculated and significance was tested in a two-tailed independent student t-test. Changes were not significant.

In summary the single brain-specific loss of Cofilin 2 did not lead to changes in anxiety-related behavior in the open field or elevated plus maze. These results suggest that Cofilin 1 is the main isoform involved in anxiety-related circuits or that the loss of Cofilin 2 is compensated by the expression of Cofilin 1 and/or ADF.

5.10.3. No significant changes in the working memory upon the brain-specific deletion of Cofilin 2

During the exploration of an apparatus latent learning processes in the hippocampus occur to acquire information about the new environment. The input to the brain is thereby first processed into a working memory. The working memory is required for the encoding and recall of explicit knowledge over a short duration of seconds. This type of memory can be analyzed in spontaneous alternations of arm visits in the Y-maze. When walking out of an arm of the maze the animal remembers from which arm it had come and explores a second new arm, followed by the visit of the third arm, finalizing a complete sequence (X-Y-Z) without a re-visiting of an already attended arm. Impairments in the working memory could result in same arm returns (X-X) or a failed alternations (X-Y-X). Mice were analyzed in the Y-maze over a period of 10minutes and the obtained sequence of arm visits was examined for same arm returns, fails or absolved sequences. The single deletion of Cofilin 1 with the CaMKII-Cre results in impairments of associative learning, whereas exploratory learning like the working memory is not affected (Rust et al., 2010). The combined deletion of ADF and Cofilin 1 in the brain lead to an impaired working memory, implicating a role for actin depolymerization factors during exploratory learning (Zimmermann et al., 2015). In this study the question was examined whether Cofilin 2 could influence short-term memory functions. Therefore 2 to 3 months old male animals with a genotype of Cofilin $2^{fl/fl}$ (n=9) and Cofilin $2^{fl/fl}$ Nestin-Cre (n=9) were analyzed in a Y-maze.

The working memory belongs to the type of exploratory learning, which is performed by neural circuits in the hippocampus and prefrontal cortex. Impairments in working memory would be reflected in an increased level of same arm returns and failed alternations and an accompanied decrease in the number of correctly performed sequences, in which every arm is visited only once. This observation was made in the Cofilin $2^{fl/fl}$ Nestin-Cre animals although the changes were statistically not significant as tested in a two-tailed independent t-test (figure 50). Only a tendency for the reduction in the number of sequences and an increase in the number of failed alternations could be made. Due to the high variance of test results for every animal most studies use a minimum of 12 – 15 animals per experimental group to insure sufficient power for a statistical analysis. We only analyzed 9 animals per

genotype, which could explain that the obtained data was not significant. The value for the failed alternation in the t-test is 0.08 and therefore nearly significant.

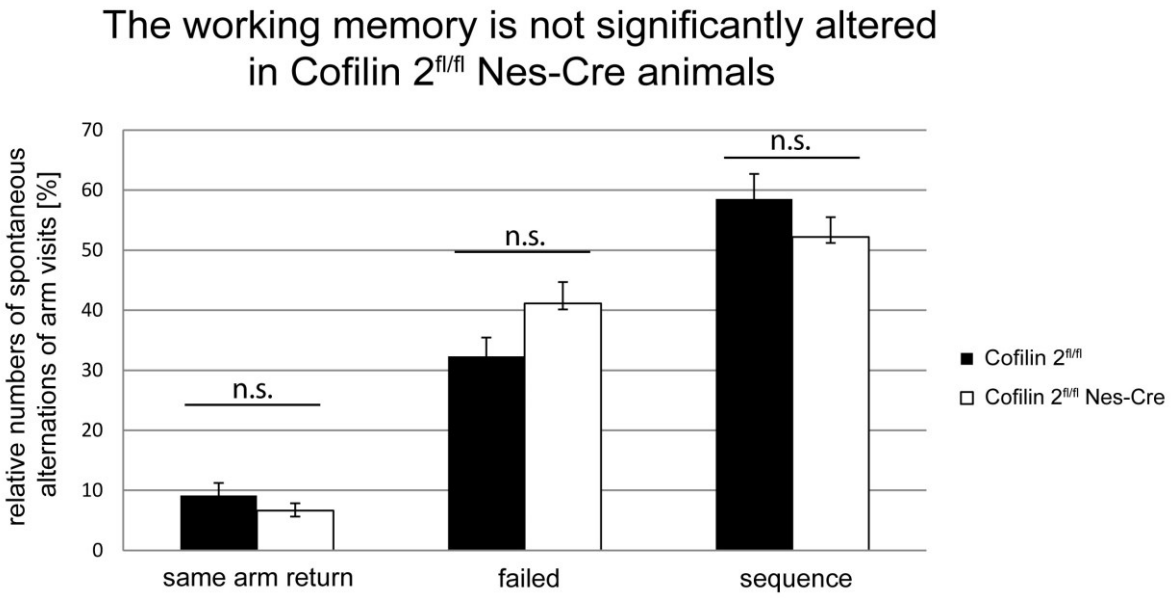

Fig.50: The loss of Cofilin 2 has a slight impact on exploratory learning. Animals were tested for 10 minutes in a Y-maze to assess spontaneous alternations. The obtained visited arm sequence was analyzed for same arm returns (X-X), failed alternations (X-Y-X) and sequences (X-Y-Z) for Cofilin $2^{fl/fl}$ (n=9) and Cofilin $2^{fl/fl}$ Nes-Cre (n=9) animals. For the Cofilin $2^{fl/fl}$ Nes-Cre animals a slight decrease in the number of sequences could be observed, which is accompanied by an increase in the number of failed alternations. These observed changes were not significant as tested in a two-tailed independent t-test. The standard error was calculated.

In summary the loss of Cofilin 2 did not result in significant alterations of the working memory as tested in a Y-maze. Although a tendency for working memory impairments could be detected in Cofilin $2^{fl/fl}$ Nestin-Cre animals, as implicated in a reduction in the number of sequences, accompanied by an increased number of same arm returns.

6. Brain-specific ADF/Cofilin 2 double knockout animals

6.1. No upregulation of Cofilin 1 upon the dual loss of ADF and Cofilin 2 in the brain

Although all three isoforms are widely expressed in the brain and show functional redundancy (Nakashima et al., 2005; Vartiainen et al., 2002), the upregulation of one isoform cannot always compensate the complete loss of another family member. Especially in cases when the expression is localized to defined neuronal sub-compartments like pre- and postsynaptic sites. Therefore it was first analyzed whether an upregulation of Cofilin 1 in the brain of double knockout animals for ADF and Cofilin 2 could be detected. The complete knockout of Cofilin 2 displayed a strong upregulation of ADF and Cofilin 1 in the

hippocampus and a mild upregulation of both proteins in the cortex, olfactory bulb and midbrain in younger animals (P7). In adult conditional knockout animals with a brain-specific deletion of Cofilin 2 a weak upregulation of Cofilin 1 could be detected in the hippocampus and midbrain, while a stronger upregulation of ADF was found in these regions. Additionally an upregulation of Cofilin 1 was detected in the adult cerebellum. To analyze a potential upregulation of Cofilin 1, adult brain lysates of ADF$^{-/-}$ Cofilin 2$^{fl/fl}$, ADF$^{-/-}$ Cofilin 2$^{fl/del}$ and ADF$^{-/-}$ Cofilin 2$^{fl/fl}$ Nestin-Cre animals were prepared and loaded onto a 15% SDS gel. In these animals a complete deletion of ADF and a conditional deletion of Cofilin 2 was generated. For the conditional deletion the enzyme Cre-recombinase was expressed under the Nestin promotor. This enabled an expression of the Cre-recombinase in neuronal and glial cell precursors starting around embryonic day 10.5.

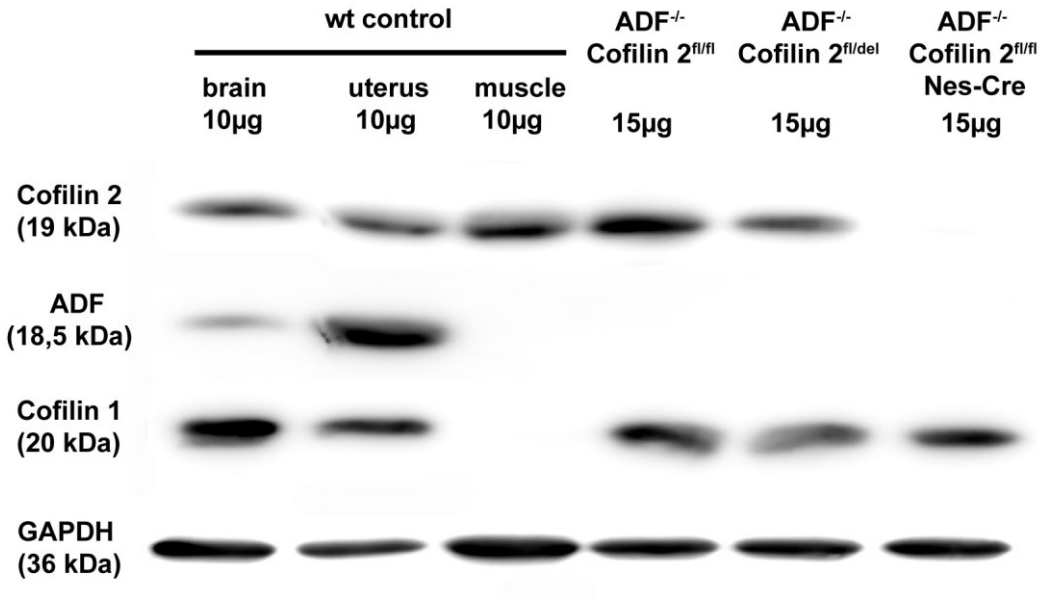

Fig. 51: The loss of Cofilin 2 and ADF in the adult brain is not compensated by an upregulation of Cofilin 1. Adult brain lysates of ADF$^{-/-}$ Cofilin 2$^{fl/fl}$, ADF$^{-/-}$ Cofilin 2$^{fl/del}$ and ADF$^{-/-}$ Cofilin 2$^{fl/fl}$ Nes-Cre double knockout animals were prepared and 15µg were loaded onto a 15% SDS gel. As controls 10µg of a wt brain lysate (Cofilin 1), wt uterus lysate (ADF) and wt muscle lysate (Cofilin 2) were loaded. GAPDH served as a loading control. The membrane was incubated with antibodies against Cofilin 2 (FHU-I), ADF (GV13) and Cofilin 1 (KG60), to analyze the expression level of Cofilin 1 upon the complete deletion of ADF and Cofilin 2 in brain. Additionally the complete knockout of ADF was confirmed. A 56% reduction in the level of Cofilin 2 was observed in ADF$^{-/-}$ Cofilin 2$^{fl/del}$ and a complete deletion of Cofilin 2 in ADF$^{-/-}$ Cofilin 2$^{fl/fl}$ Nes-Cre.

After densitometric analysis the ADF$^{-/-}$ Cofilin 2$^{fl/del}$ lysate displayed a 56% reduction in the Cofilin 2 expression level compared to the ADF$^{-/-}$ Cofilin 2$^{fl/fl}$ lysate. In the double knockout lysate no signal for Cofilin 2 could be detected. As expected a complete absence of ADF in all three prepared brain lysates verified the complete deletion of ADF in this mouse line. The functionality of the antibody was tested with the uterus lysate, which displayed a signal for the GV13 antibody. Additionally a signal could be obtained for ADF in the wt brain lysate.

The GAPDH signal displayed an equal loading of all probes. No upregulation of Cofilin 1 in either the ADF$^{-/-}$ Cofilin 2$^{fl/del}$ (77%) or the ADF$^{-/-}$ Cofilin 2$^{fl/fl}$ Nestin-Cre double knockout animals (78%) could be observed, since the intensity of the Cofilin 1 band was comparable in all three brain lysates. Note that all three members of the ADF/Cofilin family were expressed in the brain lysate. Additionally no upregulation of Cofilin 1 could be detected in brain area lysates of ADF$^{-/-}$ animals (Bellenchi et al., 2007; Gorlich et al., 2011), but an upregulation of Cofilin 1 was detected in synaptosomal lysates (Gorlich et al., 2011). This means that although no upregulation of Cofilin 1 was detected in total brain lysates, specific subcompartments could still display an upregulation of Cofilin 1 upon the dual loss of ADF and Cofilin 2.

In summary the results of this Western blot revealed the complete deletion of ADF in all three genotypes (control, heterozygote and homozygote animals) and the conditional deletion of Cofilin 2 in knockout animals. Surprisingly no compensatory upregulation of Cofilin 1 was detected in total brain lysates of adult knockout animals.

6.2. The expression of Cofilin 1 alone is sufficient to maintain brain architecture

All three ADF/Cofilin family members share similar biochemical function and are co-expressed in the brain, but the deletion of one member leads to a distinct phenotype in the brain. This leads to the hypothesis that these proteins fulfill different functions during brain development. Since the deletion of Cofilin 2 alone did not lead to any gross brain malformations and additionally an upregulation of ADF and Cofilin 1 could be observed in the hippocampus, cortex, midbrain and olfactory bulb, the brain architecture was analyzed in animals with a dual loss of ADF and Cofilin 2, in which Cofilin 1 was the only ADF/Cofilin family member expressed in the brain.

To get a first overview about brain areas that could be affected upon the dual loss of ADF and Cofilin 2, coronal and sagittal brain sections of an ADF$^{-/-}$ Cofilin 2$^{fl/fl}$ and an ADF$^{-/-}$ Cofilin 2$^{fl/fl}$ Nestin-Cre brain were prepared with a vibratome. Pictures were taken every 300µm with a brightfield microscope. As seen in figure 52 no gross brain malformations were detected upon the dual deletion of ADF and Cofilin 2. All brain areas were distinguishable and displayed no reduction in size or morphological alterations in the double knockout. This result indicates that Cofilin 1 alone was sufficient to maintain the basal brain architecture and was the only isoform needed to fulfill important migrational processes for the generation of the cortex, cerebellum and hippocampus.

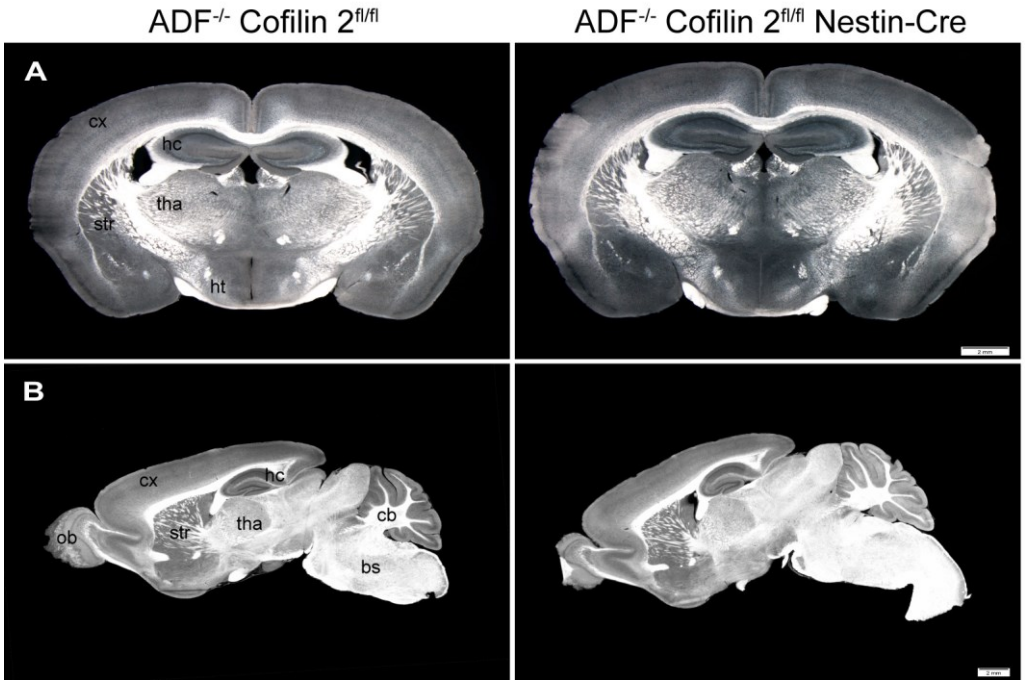

Fig. 52: The expression of Cofilin 1 as only actin depolymerization protein is sufficient to maintain brain architecture. A Coronal vibratome sections of adult ADF$^{-/-}$ Cofilin 2$^{fl/fl}$ and ADF$^{-/-}$ Cofilin 2$^{fl/fl}$ Nes-Cre animals were produced (30µm). At intervals of 300µm pictures were taken at a brightfield microscope and analyzed for the occurrence of brain malformations. Scale bar: 2mm **B** Sagittal vibratome sections of adult ADF$^{-/-}$ Cofilin 2$^{fl/fl}$ and ADF$^{-/-}$ Cofilin 2$^{fl/fl}$ Nes-Cre animals were yielded (300µm). Pictures were taken at a brightfield microcope every 300µm to analyze changes in the brain tissue. Scale bar: 2mm cx = cortex; hc = hippocampus; str = striatum; tha = thalamus; cb = cerebellum; ht = hypothalamus; ob = olfactory bulb; bs = brain stem

In summary these results could show that Cofilin 1 is the predominant actin depolymerization factor in the brain in terms of cortical migration and cell proliferation and that the expression of Cofilin 1 alone was sufficient to maintain brain architecture. The dual loss of ADF and Cofilin 2 in the brain did not lead to obvious malformations, like the loss of Cofilin 1 with a reduced cortical thickness and enlarged ventricles.

6.3. The dual loss of ADF and Cofilin 2 does not lead to a significant impact on the F/G actin ratio

The ADF/Cofilin family members depolymerize actin filaments at the minus-end and thereby replenish the G-actin pool. This is important to maintain a constant flux of G-actin monomers to the barbed end of actin filaments, which leads to the assembly of new dendritic spines or is able to regulate the transport of vesicles to the active zone of synapses. Thereby signaling cascades regulate the activation of ADF/Cofilin family members. The deletion of a depolymerization factor should shift the G- to F-actin level towards filamentous actin. Upon deletion of Cofilin 1 Rust et al detected significantly increased F/G actin ratios in hippocampal and striatal lysates (Rust et al., 2010). The loss of ADF alone did not alter the

F/G actin ratio, but the double knockout of ADF and Cofilin 1 showed significantly higher F-actin levels in synaptosomes, which were further increased compared to Cofilin $1^{fl/fl}$ CaMKII-Cre animals alone (Gorlich et al., 2011). A deletion of Cofilin 2 alone indicated a slightly increased F/G actin ratio (1.46) in the cortex of Cofilin $2^{fl/fl}$ Nestin-Cre knockout animals, but no significance could be detected. We also separated G-actin monomers from the filamentous actin for ADF/Cofilin 2 double knockout animals (figure 53). Also in these mutant animals a slight increase in the F-actin levels could be observed, but again no significance could be detected (control 1.0 ± 0.04; mutant 1.37 ± 0.06; ns; n = 3).

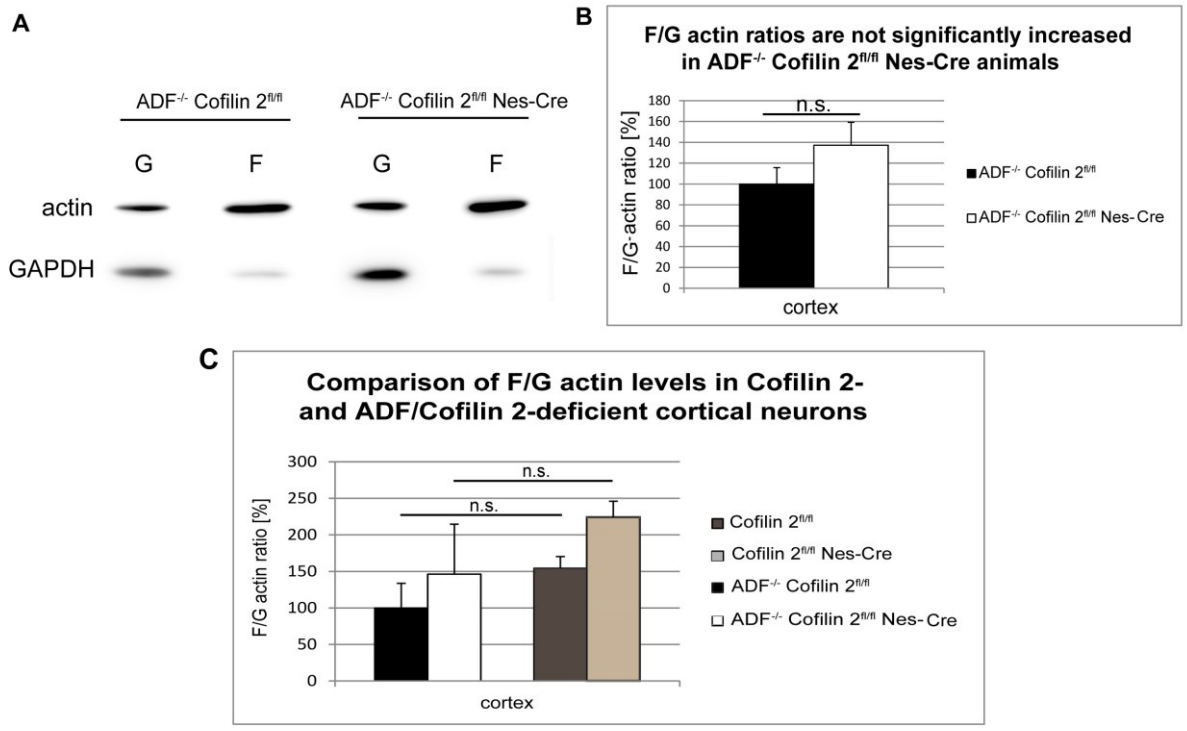

Fig. 53: The dual loss of ADF and Cofilin 2 does not lead to a significant impact on the F/G-actin levels in the cortex. A Protein lysates from the cortex of $ADF^{-/-}$ Cofilin $2^{fl/fl}$ and $ADF^{-/-}$ Cofilin $2^{fl/fl}$ Nes-Cre animals were prepared and the monomeric G-actin was separated from the filamentous F-actin through the incubation in PHEM buffer, followed by a centrifugation step. 1µg of every probe was loaded onto a 10% gel and incubated with the actin-antibody C4. The separation was controlled with the GAPDH antibody, which should only give a signal in the G-actin supernatant probe. For both genotypes a slight signal for GAPDH could be also observed in the pellet fractions, which suggest a supernatant contamination in the pellet fraction. This contamination was comparable between wt and mt animals. **B** The F/G actin ratio was calculated and the control was set to 100%. Three mice were analyzed for every genotype (n=3) and the average and standard error were calculated. Significance was analyzed in a two-sampled independent t-test. The obtained results were statistically not significant. **C** Comparison of the cortical F/G actin ratio between mice deficient of Cofilin 2 and mice with a double knockout for ADF and Cofilin 2. The Cofilin $2^{fl/fl}$ control was set as 100%. Both isoforms alter the F/G actin ratio in the cortex, but differences between Cofilin $2^{fl/fl}$ Nes-Cre and $ADF^{-/-}$ Cofilin $2^{fl/fl}$ Nes-Cre animals were not significant.

In summary the dual loss of the two actin depolymerization factors ADF and Cofilin 2 still did not impact significantly on the F/G-actin ratio in the cortex. Only a slight increase in the F-actin level was observed

6.4. Locomotor activity and novelty seeking behavior is not affected in ADF/Cofilin 2 double knockout animals

In ADF single mutants synapse morphology and physiology are unchanged and no behavioral abnormalities or learning defects are detected in $ADF^{-/-}$ animals (Gorlich et al., 2011). In contrast to that leads the deletion of Cofilin 1 with a CaMKII-Cre to postsynaptic defects, reflected in morphological alterations of dendritic spines, increased number of AMPA receptors and the impact on postsynaptic mechanisms like LTP or LTD (Rust et al., 2010). No alteration in presynaptic function could be observed upon the deletion of Cofilin 1. Surprisingly the loss of ADF and Cofilin 1 leads to a presynaptic phenotype with an altered recruitment and exocytosis of synaptic vesicles in the hippocampus and striatum. The increased glutamate release is also likely to account for the observed behavioral phenotype with a hyper-locomotion of $ADF^{-/-}$ Cofilin $1^{fl/fl}$ CamKII-Cre animals (Zimmermann et al., 2015). Therefore a relevance of presynaptic actin dynamics for mouse behavior was detected by the analysis of ADF/Cofilin 1 mutant mice (Zimmermann et al., 2015). Since Cofilin 1 does not affect the presynaptic site, but presynaptic defects could be observed upon the dual deletion of ADF and Cofilin 1, the combined loss of ADF and Cofilin 2 in double knockout animals was analyzed for changes in the locomotor activity. Cofilin 2 was localized to the pre- and postsynaptic site, albeit no changes in the locomotor activity and exploratory behavior could be detected in Cofilin $2^{fl/fl}$ Nestin-Cre single mutants. Therefore $ADF^{-/-}$ Cofilin $2^{fl/fl}$ animals as controls and the $ADF^{-/-}$ Cofilin $2^{fl/fl}$ Nestin-Cre mutants were analyzed in an open field over a period of 60min. As seen in figure 54A no significant changes in the locomotor activity between control and knockout animals were detectable as measured in the total distance travelled (control 100% ± 14.36; n = 7; mutant 122.9% ± 9.52; n = 9; ns). Additionally the center distance and periphery distance was comparable between control and knockout mice. Also the numbers of repetitive behaviors, which reflected the interest in the novelty of the environment, did not indicate changes in the exploratory behavior of control and knockout animals.

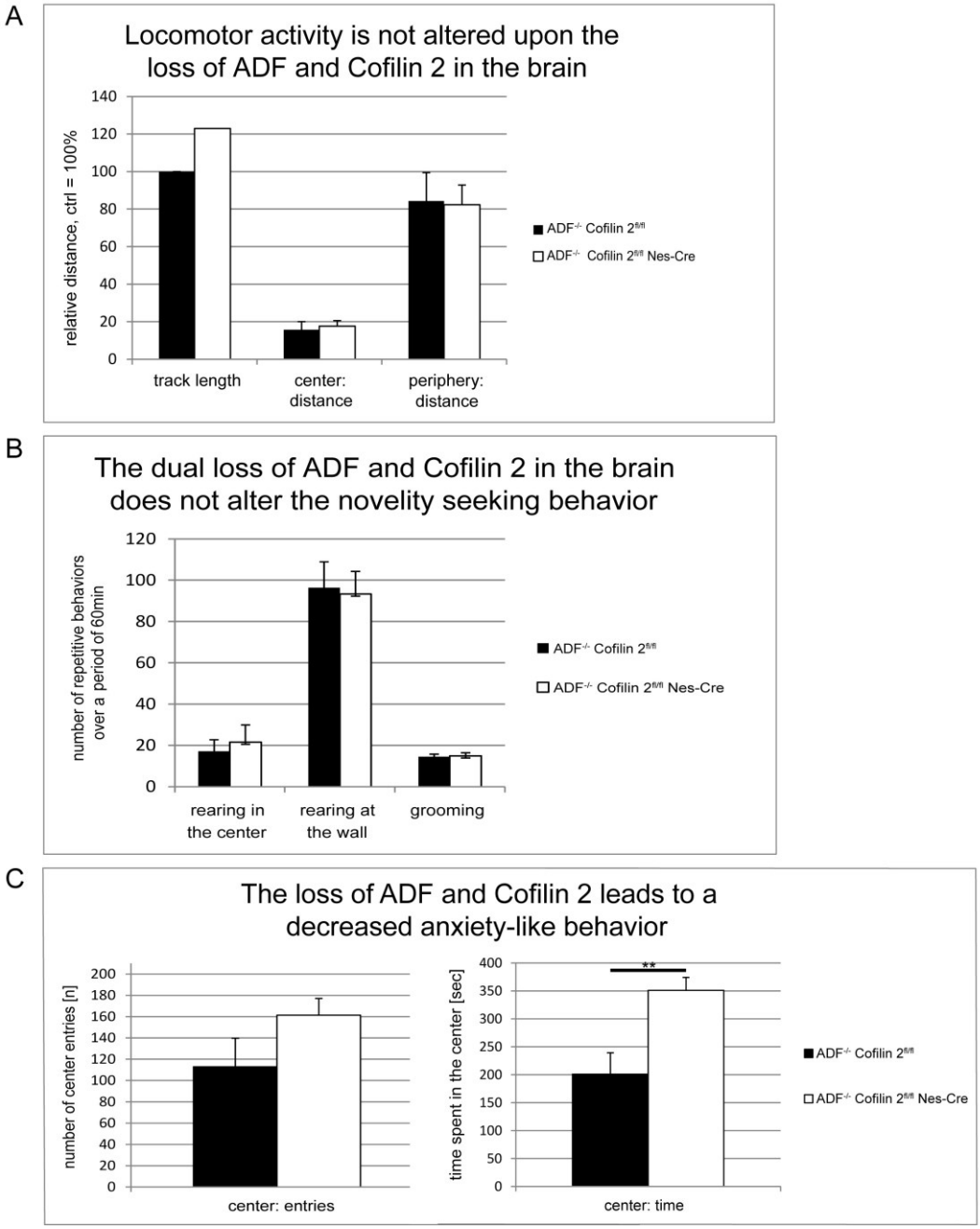

Fig.54: The complete loss of ADF together with a brain-specific deletion of Cofilin 2 alters the anxiety-like behavior in mice, but did not reveal changes in exploratory behavior. A Mice were analyzed over a period of 60 min in an open field, which was divided into a central zone and a periphery; the track length by the ADF$^{-/-}$ Cofilin 2$^{fl/fl}$ control was set to 100%. The ADF$^{-/-}$ Cofilin 2$^{fl/fl}$ Nes-Cre animals did not reveal an increased locomotor activity, and the distances travelled in the center, as well as in the periphery were comparable between control and knockout. **B** Repetitive behaviors were counted as novelity-seeking behaviors and an increased number would indicate an elevated exploratory behavior. No changes in the ADF$^{-/-}$ Cofilin 2$^{fl/fl}$ and ADF$^{-/-}$ Cofilin 2$^{fl/fl}$ Nes-Cre animals could be observed in rearing and grooming behavior over the 60min test period. **C** The ADF$^{-/-}$ Cofilin 2$^{fl/fl}$ Nes-Cre animals showed an increased number of center entries and also spent significantly more time there. This indicates a diminution in the anxiety-related behavior of these animals. The time spent in the center and periphery was calculated based on the controls and set as 100%. In the open field n=7 ADF$^{-/-}$ Cofilin 2$^{fl/fl}$ and n=9 ADF$^{-/-}$ Cofilin 2$^{fl/fl}$ Nes-Cre animals were analyzed and the average and standard error were calculated. The significance was tested in a two-tailed independent t-test ($p<0.05$ *; $p<0.01$ **).

The open field also provides an initial screen for anxiety-related behavior in rodents. It has been suggested that two factors influence anxiety-like behavior in the open field: the first is the social isolation caused by the physical separation from cage mates while performing the test, and second is the stress created by the brightly lit and unprotected center area. Mice will typically spent significantly more time exploring the periphery of the open field, than the unprotected center area. As seen in figure 54C the ADF$^{-/-}$ Cofilin 2$^{fl/fl}$ Nestin-Cre mutant mice spent significantly more time in the center of the open field (control 201sec ± 38.36sec; n = 7; mutant 350.74sec ± 23.36sec; n = 9; $p<0.01$) and also performed more center entries than the controls (control 113 ± 26.67; n = 7; mutant 161.33 ± 15.84; n = 9; ns). Mice that spent more time exploring the unprotected center area demonstrate a reduced anxiety-related behavior. For that reason an elevated plus maze test was also performed, which further divides exploratory behavior from anxiety-related characteristics.

In summary the dual loss of ADF and Cofilin 2 did not alter locomotor activity and exploratory behavior in an open field, as also observed for the single brain-specific loss of Cofilin 2. A difference was detected in anxiety-related behavior, since the dual loss of ADF and Cofilin 2 resulted in an elevated number of center area entries and a significantly increased center time.

6.5. ADF$^{-/-}$ Cofilin 2$^{fl/fl}$ Nestin-Cre animals habituate normally to a new environment

A prolonged duration in the open field also enables the examination of the process of habituation, in which an animal responds to a new environment with an increased locomotor activity and elevated exploratory behavior. This activity declines over time if no harmful stimulus is presented and the animal calms down. A reason for that is the activity dependent synaptic depression of specific synaptic connections. In Cofilin 1$^{fl/fl}$ CamKII-Cre mutants Ca1 synapses in the hippocampus were resistant to a LTD induced by a paired pulse LSF (low frequency stimulation), while in control animals a depression of about 15% could be observed. Therefore Cofilin 1 seems to be important for postsynaptic mechanism like LTP and LTD (Rust et al., 2010). Since the single deletion of Cofilin 2 did not lead to alterations in LTD, as seen in the habituation process during the open field test, also double knockout animals for ADF and Cofilin 2 were analyzed for changes at the postsynaptic site. The habituation process during the open field trial can be measured by examining the total distance travelled and the time immobile in 5min bins of the 60min test duration. As seen in figure 55 the ADF$^{-/-}$ Cofilin 2$^{fl/fl}$ controls and the ADF$^{-/-}$ Cofilin 2$^{fl/fl}$ Nestin-Cre knockouts displayed a reduction in the total distance travelled over the 60min time period, with an increase in the time immobile. This indicated for both groups a reduced response of animals

to the new environment due to the habituation process, which is reflected in the diminished behavior.

In summary the results of the open field test indicated that also the dual loss of ADF and Cofilin 2 in the brain did not impact on the habituation process and therefore did not lead to changes in postsynaptic parameters like LTD.

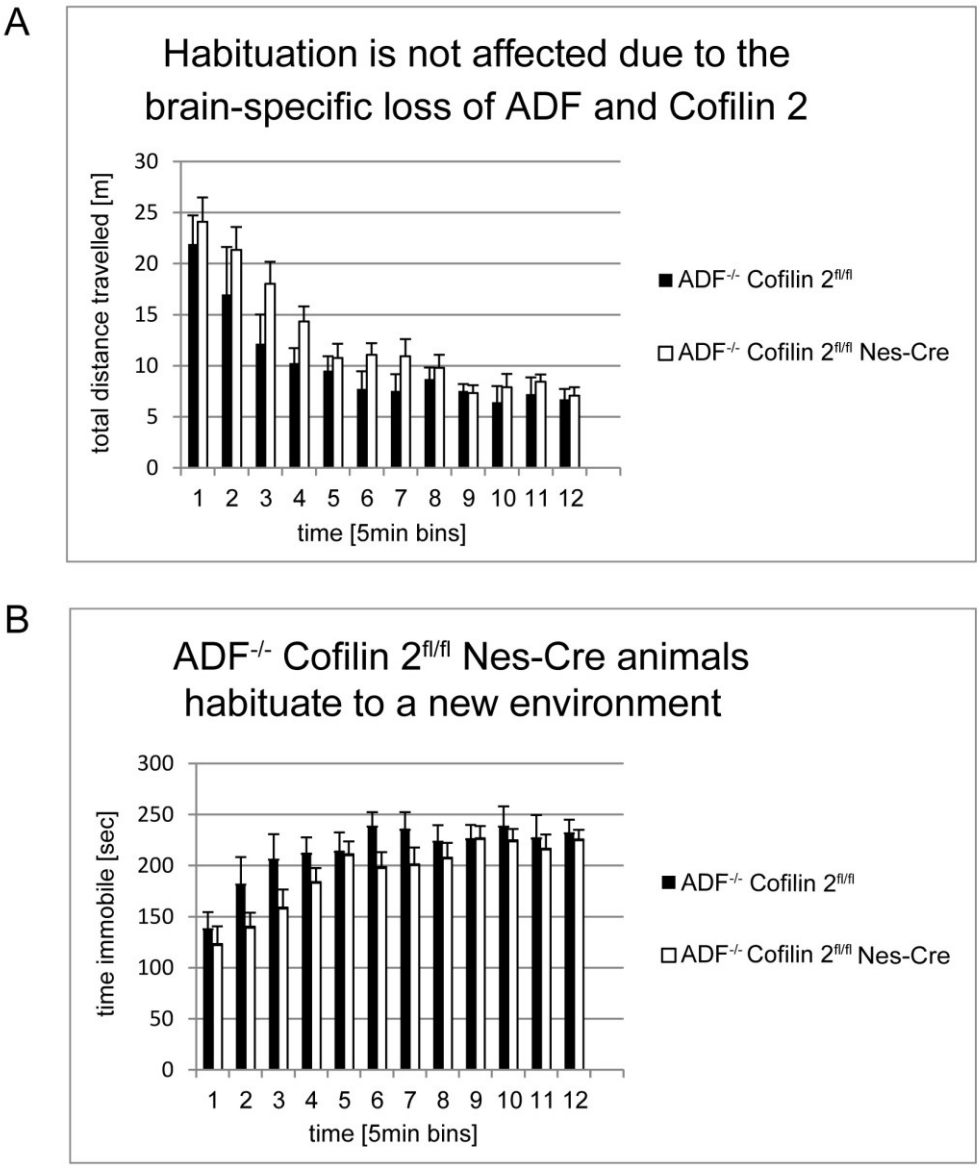

Fig.55: The habituation process is not affected upon the dual loss of ADF and Cofilin 2 in the brain. A The 60min period of the open field was divided into 5min bins and the total distance travelled was analyzed for every bin. Both the ADF$^{-/-}$ Cofilin 2$^{fl/fl}$ control and the ADF$^{-/-}$ Cofilin 2$^{fl/fl}$ Nes-Cre knockout mice revealed a decrease in the distance travelled over time, which reflects a reduction in exploratory behavior. **B** In accordance to the reduced total distance travelled during the 60min period the time immobile of control and knockout animals increased over time in the open field, which indicated a habituation process to the new environment and thereby a synaptic depression of specific connections. In the open field n=7 ADF$^{-/-}$ Cofilin 2$^{fl/fl}$ and n=9 ADF$^{-/-}$ Cofilin 2$^{fl/fl}$ Nes-Cre animals were analyzed and the average and standard error were calculated. The significance was tested in a two-tailed independent t-test, no significance could be observed.

6.6. A combined deletion of ADF and Cofilin 2 in the brain leads to a reduced anxiety-related behavior

The analysis of ADF$^{-/-}$ Cofilin 2$^{fl/fl}$ Nestin-Cre animals in the open field already gave a first hint for a diminished anxiety-related behavior in these animals, as seen in an increased number of center entries and also time spent there. Therefore we analyzed their behavior further in an elevated plus maze (EPM), which is a specialized test to assess anxiety-like behavior in mice. This test takes advantage of the natural tendency of mice to explore a new environment. Mice are allowed to freely explore the apparatus for 5min and can choose between the visit of enclosed, protected arms or open, unprotected arms, the latter give a fearful stimulus to the animals. The number of open arm entries and the amount of time spent in the open and closed arms were recorded during the trial. To exclude the possibility that changes in the number of open arm entries were related to an increased locomotor activity rather than an anxiety-like phenotype of ADF$^{-/-}$ Cofilin 2$^{fl/fl}$ Nestin-Cre animals, it was first examined whether animals displayed an elevated locomotor activity. As seen in figure 56A the total locomotor activity was not altered in ADF$^{-/-}$ Cofilin 2$^{fl/fl}$ Nestin-Cre mutants and therefore changes in the number of open arm visits were related to a decrease in anxiety in these animals (control 25.2 ± 8.56; n = 7; mutant 31.4 ± 4.79; n = 9; ns). According to that also a significant increase in the number of open arm visits of knockout animals was detected (control 7.6 ± 3.5; n = 7; mutant 14.4 ± 2.94; n = 9; ns) (figure 56B and D). The comparison between the track plots of control and knockout animals showed that the mutant animals frequently visited both open arms over the whole length, while the control animals only displayed stretch attend postures on the corner between the open arms and the central area and therefore did not move completely out to the open arms, but stayed closed to the protected area. Additionally the knockout animals reflected a reduced number of freezing episodes and time spent freezing in comparison with the controls. All these findings reflected a decreased anxiety-related behavior in animals with a complete loss of ADF and a conditional loss of Cofilin 2 using the Cre recombinase under the Nestin promotor. The single deletion of Cofilin 2 with Nestin-Cre did not lead to the same phenotype. Even the Cofilin 2$^{fl/fl}$ Nestin-Cre animals did not visit the whole length of the open arms (figure 49C) and the number of open arm visits was nearly the same between control and mutant animals. Since the single knockout of ADF also did not displayed any behavioral abnormalities the observed phenotype is due to the combined loss of ADF and Cofilin 2 in the brain.

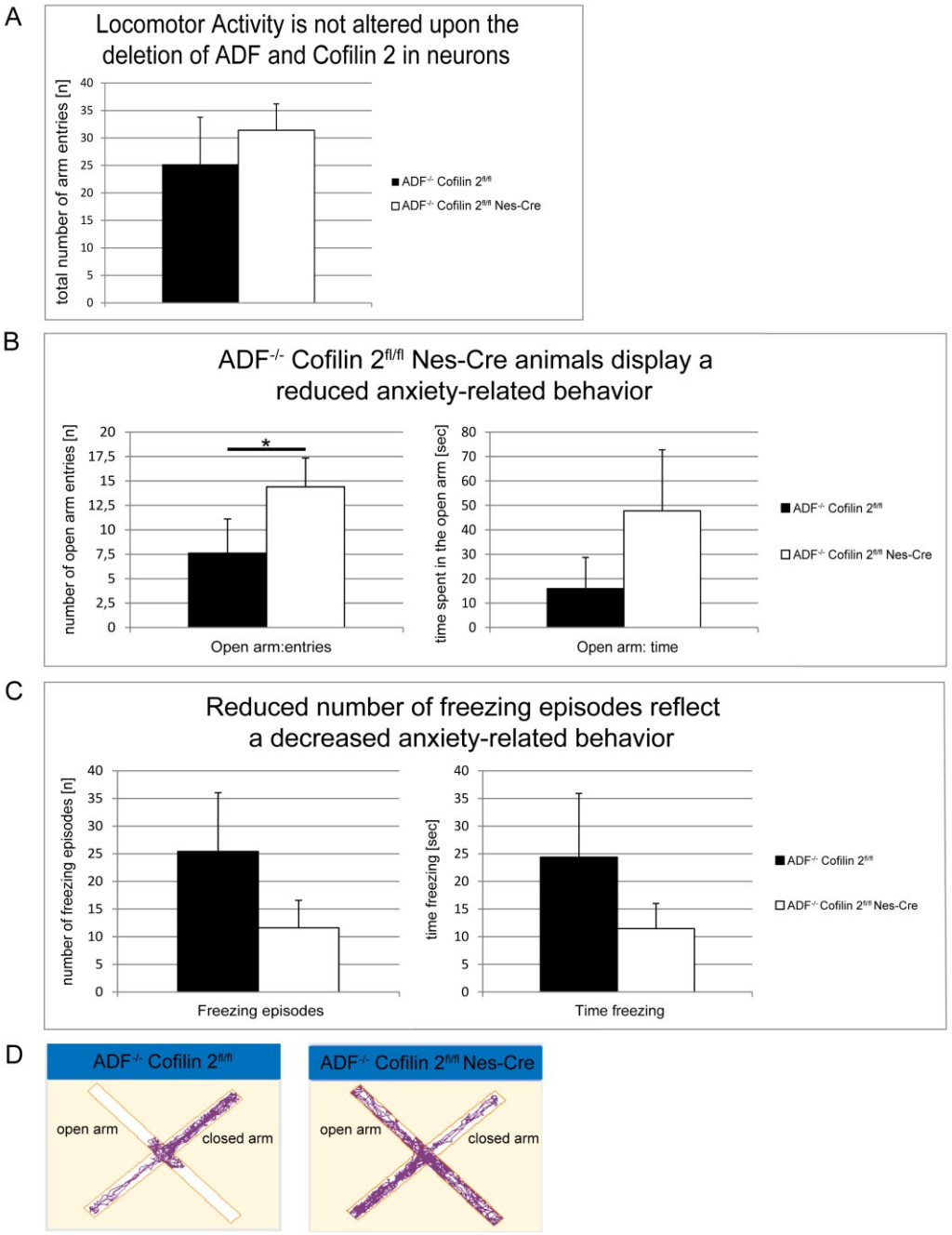

Fig.56: A dual loss of ADF and Cofilin 2 reduces anxiety-like behavior in mice. A To exclude that an increased number of open arm entries just reflected an increased locomotor activity, the total distance travelled over the 5min period in the elevated plus maze (EPM) was analyzed and compared between ADF$^{-/-}$ Cofilin 2$^{fl/fl}$ and ADF$^{-/-}$ Cofilin 2$^{fl/fl}$ Nes-Cre animals. No significant changes in the locomotor activity could be observed between control and knockout animals. **B** The open arm entries and the time spent on the open arms were compared between control and knockout animals and an increased number of open arm entries for the knockout animals could be observed. **C** A slight decrease in the number of freezing episodes and freezing time was displayed for ADF$^{-/-}$ Cofilin 2$^{fl/fl}$ Nes-Cre animals (not significant; p-Value 0.09). This indicates a reduced anxiety-like behavior. **D** Track plot examples of one ADF$^{-/-}$ Cofilin 2$^{fl/fl}$ and one ADF$^{-/-}$ Cofilin 2$^{fl/fl}$ Nes-Cre animal each are shown. A track plot indicates the head position of the animal over the 5min trial in the EPM and reflects thereby the visit of the open arms. The control track plot revealed that the animal only visited the open arm close to the central area and did not move out to the end of the open arm. In contrast the track plot of the knockout animal reflected a frequent visit of the entire open arm up to the end point.

In summary only the combined loss of ADF and Cofilin 2 lead to a reduced anxiety-related behavior in the open field and elevated plus maze. No alterations in anxiety were detected in the single brain-specific knockout of Cofilin 2, suggesting overlapping functions of ADF and Cofilin 2 in neuronal circuits regulating anxiety-related behavior.

6.7. A dual deletion of ADF and Cofilin 2 in neurons affects the working memory in the Y-maze

When an animal is placed for the first time into a Y-shaped maze, the hippocampus signals a lack of information about the current environment. The exploration of the new maze is a latent learning process, which leads to the strengthening of synaptic connections or even the establishment of new synapses. When the animal walks out of an arm it remembers which arm it had visited before and explores the other two arms, finalizing a complete alternation. The working memory is required for the encoding and recall of explicit knowledge over a short duration of seconds during the exploration of the Y-maze. This type of memory can be analyzed in spontaneous alternations of arm visits during the Y-maze test. These spontaneous alternations are analyzed and the number of failed sequences (revisit of the just encountered arm) or same arm returns indicates an impairment of the working memory. An impaired working memory is found in double knockout animals for ADF$^{-/-}$ and Cofilin 1$^{fl/fl}$ CaMKII-Cre (Zimmermann et al., 2015), while a deletion of Cofilin 1 alone using the CaMKII-Cre does not affect working memory (Rust et al., 2010). The deletion of Cofilin 2 displayed a tendency for an impaired working memory, reflected in a decreased number of sequences, combined with an increase in the number of fails, although no significance could be detected (figure 50). To address the question whether the combined deletion of ADF and Cofilin 2 would augment the observed phenotype in exploratory learning, ADF$^{-/-}$ Cofilin 2$^{fl/fl}$ controls and ADF$^{-/-}$ Cofilin 2$^{fl/fl}$ Nestin-Cre animals were examined over 10min in a Y-maze. As seen in figure 57 a significant increase in the number of same arm returns and a decline in the number of sequences could be observed in knockout animals lacking ADF and Cofilin 2. The number of fails was only slightly decreased in ADF$^{-/-}$ Cofilin 2$^{fl/fl}$ Nestin-Cre animals. Therefore ADF in combination with Cofilin 2 seemed to play a role in the establishment of the working memory in rodents.

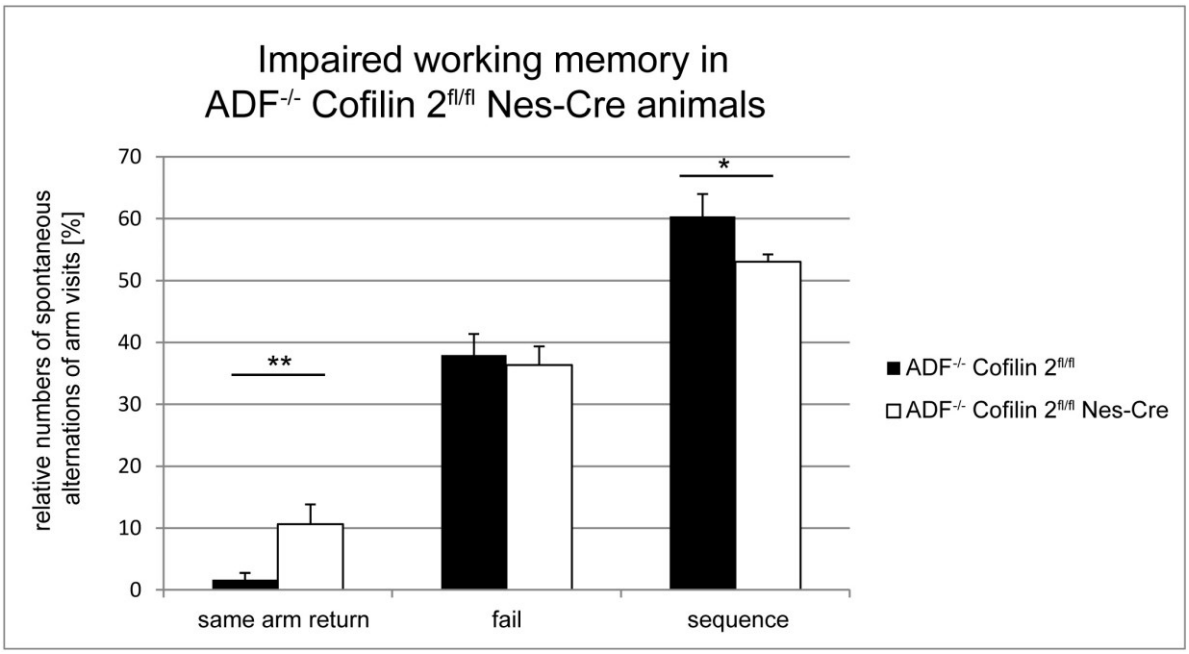

Fig. 57: The simultaneous deletion of ADF and Cofilin 2 in the brain affects the working memory in the hippocampus. In a Y-maze n=7 ADF$^{-/-}$ Cofilin 2$^{fl/fl}$ and n=9 ADF$^{-/-}$ Cofilin 2$^{fl/fl}$ Nes-Cre animals were analyzed for their spontaneous alternation sequences during a 10min trial. A consecutive visit of all three arms was marked as sequence (X;Y;Z), while the re-visit of the arm the animal had encountered before was taken as fail (X;Y;X). Also the direct re-visit of an arm was measured as same arm return (X;X). The average and standard error were calculated and significance was tested in a two-tailed independent t-test ($p<0.05$ *; $p<0.01$ **). The animal's deficit for ADF and Cofilin 2 revealed an increased number of same arm returns accompanied by a decrease in the number of correct sequences. This result indicated that the brain-specific dual deletion of ADF and Cofilin 2 affected working memory functions in the hippocampus.

In summary the dual deletion of ADF and Cofilin 2 results in impairments of exploratory learning as tested in a Y-maze. In Cofilin 2-deficient animals only a tendency for an impact on the working memory was detected, while changes were not significantly different. These results suggest overlapping functions for ADF and Cofilin 2 in hippocampal circuits that are involved in working memory functions.

7. Discussion

7.1. Cofilin 2 expression and upregulation

The actin cytoskeleton plays crucial roles during brain development and the establishment of functional neuronal circuits. Alterations in the organization and dynamics of the actin cytoskeleton are linked to various neurodegenerative diseases (Hoogenraad et al., 2004; Maloney and Bamburg 2007). Actin depolymerization factors are important to refill the G-actin pool to enable a constant incorporation of actin monomers at the barbed end of existing fibers, a process that drives the outgrowth of neurites, the arborization of dendrites or the activity dependent changes in dendritic spines. Actin filaments are depolymerized and severed by the ADF/Cofilin family, which consist out of three members: ADF, Cofilin 1 and Cofilin 2. All three proteins are expressed in the brain, but the deletion of either protein leads to a distinct brain phenotype, suggesting different functions and subcellular localization of all three proteins. Most studies on the role of depolymerization factors were performed on ADF and Cofilin 1, since Cofilin 2 was long suggested to be the muscle-specific isoform.

Cofilin 1 is ubiquitously expressed in the CNS (Bellenchi et al., 2007). The complete deletion of Cofilin 1 is embryonic lethal around E9.5, due to a neural tube closure defect (Gurniak et al., 2005). To examine the exact role of Cofilin 1 in the brain a mouse-line with a brain-specific deletion, using Nestin-Cre expression, was examined. The loss of Cofilin 1 impairs radial migration, which results in the loss of cortical layers II – IV (Bellenchi et al., 2007). In Cofilin $1^{fl/fl}$ Nestin-Cre animals an upregulation of ADF could be detected, indicating that Cofilin 1 and ADF could have overlapping functions (Hotulainen et al., 2005). Western blot analysis displayed a comparable pattern for Cofilin 1 and ADF in the adult brain, although the signal for ADF was weaker (Bellenchi et al., 2007; Gorlich et al., 2011). During embryonic brain development ADF and Cofilin 1 were also coexpressed. The complete deletion of ADF is viable and $ADF^{-/-}$ mice only showed a mild hyperplasia of the cornea, while no alterations in brain morphology or behavior could be observed (Bellenchi et al., 2007; Ikeda et al., 2003). In $ADF^{-/-}$ mice no compensatory upregulation of Cofilin 1 could be detected in total brain lysates. Cofilin 2 was perceived to be the muscle-specific isoform of the ADF/Cofilin family members and mutations in the human Cofilin 2 gene result in an autosomal dominant form of nemaline myopathy (Agrawal et al., 2007). The complete knockout of Cofilin 2 in mouse is lethal around postnatal day 7 (P7), based on respiratory and circulation problems. In Cofilin 2 knockout animals a progressive muscle degeneration was observed between P3 – P7, due to an impaired exchange of α-actin isoforms during early postnatal remodeling of the sarcomere (Gurniak et al., 2014). Surprisingly the muscle-specific isoform Cofilin 2 was also expressed in total brain lysates, but no characteristic alterations were found in neuromuscular junctions of knockout animals. A brain phenotype in Cofilin $2^{-/-}$ animals was not obvious and needed further investigation. To gain insight into the role of Cofilin 2 in

neuronal development, biochemical analysis on different brain area lysates were performed to establish an expression profile of Cofilin 2 in the brain. The expression of Cofilin 2 was also analyzed during different developmental time points to detect a possible contribution of Cofilin 2 to neurodevelopmental processes in different brain regions.

7.1.1. The loss of Cofilin 2 leads to the upregulation of Cofilin 1 and ADF in distinct brain regions

The expression of Cofilin 2 was analyzed in different brain regions of P7 animals via Western blot. Lysates from Cofilin $2^{+/+}$ animals at P7 were prepared, due to the fact that it is the latest time point before the complete deletion of Cofilin 2 is lethal. In every analyzed brain region a signal for the Cofilin 2 antibody could be observed, showing a broad expression of Cofilin 2 in the brain of 7 day old newborn (figure 21). The highest expression of Cofilin 2 at P7 was found in the cortex and cerebellum, which are the brain regions with the highest migrational rates during development, followed by the midbrain and the hippocampus. The brain-specific knockout of Cofilin 1 affects migrational processes of postmitotic neurons from the subventricular zone to the cortical layers (Bellenchi et al., 2007). The areas with lowest Cofilin 2 expression at P7 were the striatum and olfactory bulb. Interestingly, the areas with an increased Cofilin 2 expression also showed an upregulation of ADF and Cofilin 1 upon the loss of Cofilin 2. An upregulation of another ADF/Cofilin family member upon the deletion of one isoform is a common mechanism in knockout animals of this family. All three members display 82% sequence homology and share therefore the same basic function, which could compensate a loss and attenuate a specific phenotype. Nevertheless all three members also show distinct biochemical properties. For example Cofilin 2 has a higher binding affinity to F-actin than Cofilin 1 or ADF and therefore an increased severing activity, while the depolymerization rate is lower, compared to ADF and Cofilin 1. Therefore the loss of Cofilin 2 could still lead to a specific phenotype, since some actin-dependent processes could rely more on a high severing activity, which cannot be achieved by ADF or Cofilin 1.

Since a broad expression of Cofilin 2 was examined in the brain, the next step was the analysis of different developmental time points for their Cofilin 2 expression. The expression profile of Cofilin 2 during different developmental time points ranking from P0, P7, P15, P21 to adult animals were examined in distinct brain regions of wt animals (figure 22). Interestingly in almost all brain regions the expression of Cofilin 2 was highest at P7, the time point when the deletion of Cofilin 2 was starting to become lethal. The only exception was the cortex where the expression peaks at P0 and the cerebellum where the highest expression was found in adult animals. A conditional deletion of Cofilin 1 in the brain using Nestin-Cre expression leads to a cortical migrational defect, resulting in the absence of the layers II – IV

(Bellenchi et al., 2007). These result link actin depolymerization factors with cortical layer formation defects and resemble the pathology of type 1 lissencephaly patients (Bellenchi et al., 2007). The cortical proliferation and migration wave starts at E13.5 and the layering is completed until E19.5. Cofilin 2 could have a role during these processes and the expression could then decline after birth when the development of the cortex is terminated. Therefore it would be interesting to analyze also the expression of Cofilin 2 during embryonic stages that are important for cortical development. Since the Cofilin $2^{fl/fl}$ Nestin-Cre brains did not showed a translucent appearance of the cerebral cortex (figure 34), the loss of Cofilin 2 seemed to be compensated by the expression of ADF and Cofilin 1. An elevated level of ADF and Cofilin 1 was detected in cortical lysates of Cofilin $2^{-/-}$ animals around P7 (figure 21), which could lead to a milder phenotype.

Also the process of synaptogenesis starts at P7 with an elevated number of synaptic contacts that are built, followed by a fine-tuning around P15 leading to the pruning of synapses that are not frequently used. The establishment of synapses requires a breakup of the actin cytoskeleton for the protrusion of filopodia-like structures, which are then reassembled to dendritic spines or presynaptic terminals. Actin is also the main cytoskeletal protein in dendritic spines and the assembly of the postsynaptic compartment needs a highly dynamic actin cytoskeleton. Thereby Cofilin 2 is important to depolymerize existing actin filaments for the protrusion of new filaments and also the recycling of older filaments to maintain the G/F-actin pool. Further the severing activity of Cofilin 2 is important to obtain a high number of shorter actin filaments, which can be used to assemble the branched actin cytoskeleton in dendritic spines and presynaptic terminals. Only this branched actin network can fulfill the important function of actin filaments in this specialized compartments. Rust et al analyzed the phosphorylation level of Cofilin 1 during synaptogenesis and also found higher phosphorylation levels at early postnatal stages, which dramatically decreased during synaptogenesis (P21 – P50) and therefore confirm the observed results here (Rust et al., 2010).

The next step was the confirmation of the complete Cofilin 2 knockout and the respected altered levels of ADF or Cofilin 1. Therefore lysates for every region of Cofilin $2^{+/+}$, Cofilin $2^{+/-}$ and Cofilin $2^{-/-}$ animals were loaded on one gel and the blot was incubated with antibodies against all three ADF/Cofilin family members. The Cofilin $2^{+/-}$ lysates should contain a 50% reduction in the Cofilin 2 expression, due to the loss of Cofilin 2 on only one allele. Densitometric analysis revealed an almost 50% reduction in the cortex, hippocampus, olfactory bulb and midbrain lysates. Only in the striatum (90%) and cerebellum (71%) a higher Cofilin 2 expression rate was left. This could result from an unsteady Cofilin 2 expression level around P7 in these brain regions compared with the other brain regions. Additionally the Cofilin 2 protein has a long half-life and could result in an elevated protein

level, although the reduction in the Cofilin 2 expression is there, due to the loss of one Cofilin 2 allele. Another explanation would be that every animal is unique and has its own metabolism and hormone balance and reacts to environmental stimuli differently. Therefore the number of analyzed animals should be increased to obtain a representative mean.

In figure 20 the complete knockout of Cofilin 2 was verified, since in Cofilin $2^{-/-}$ lysates no band at the height of Cofilin 2 was detectable. Additionally a slight upregulation of ADF and Cofilin 1 in the cortex, midbrain and olfactory bulb could be observed, but the strongest upregulation of ADF and Cofilin 1 at P7 was reflected in the hippocampus (figure 21). In the hippocampus actin plays an important role for learning processes like LTP and the establishment of synapses (Fukazawa et al., 2003). An increased F-actin content was found in cortical and hippocampal synaptosomes of Cofilin $1^{fl/fl}$ CaMKII-Cre animals, which leads to an enlargement of dendritic spines and altered postsynaptic parameters like L-LTP and LTD (Rust et al., 2010). Görlich et al detected an upregulation of Cofilin 1 in synaptic structures of $ADF^{-/-}$ mice and suggested that the lack of synaptic defects in $ADF^{-/-}$ mice could be explained by the elevated Cofilin 1 levels that compensate for the loss of ADF (Gorlich et al., 2011). This hypothesis was confirmed in $ADF^{-/-}$ Cofilin $1^{fl/fl}$ CaMKII-Cre animals, which showed an additive effect of ADF, since the F-actin level in synaptosomes was further increased in double knockout animals in comparison to Cofilin $1^{fl/fl}$ CaMKII-Cre animals (Zimmermann et al., 2015). Additionally a presynaptic phenotype was observed in double knockout animals for ADF and Cofilin 1, while the single brain-specific knockout of Cofilin 1 only leads to postsynaptic defects. The observed upregulation of ADF and Cofilin 1 in certain brain regions could attenuate a possible Cofilin 2 based brain phenotype and indicates that Cofilin 2 expression is important in these brain regions, since the loss needs to be compensated by an upregulation of other ADF/Cofilin family members.

Since the complete deletion of Cofilin 2 is lethal around P7, a brain specific deletion of Cofilin 2 using Cre-expression under the Nestin promotor was analyzed. In this mouse line Cofilin 2 was deleted in neuronal and glial cell precursors of the forebrain, starting around E10.5 (Tronche et al., 1999). Cofilin $2^{fl/fl}$ Nestin-Cre animals were viable, but smaller than their littermates, and allowed the study of adult animals. With the help of this conditional mouse line it was examined whether the conditional deletion of Cofilin 2 was restricted to specific brain regions and if the deletion rate of the Nestin-Cre recombinase was sufficient enough in every brain region. Additionally a possible upregulation of ADF or Cofilin 1 was analyzed in adult animals. Therefore lysates from different brain regions from adult Cofilin $2^{fl/fl}$ and Cofilin $2^{fl/fl}$ Nestin-Cre animals were prepared. In adult animals the highest expression level of Cofilin 2 was found again in the cortex, midbrain and cerebellum, followed by the striatum, hippocampus and olfactory bulb (figure 33). The deletion of Cofilin 2 was efficient in almost every brain region, since no band for Cofilin 2 was detected in the Cofilin $2^{fl/fl}$ Nestin-Cre

lysates. Only for the midbrain a faint band at the height of Cofilin 2 was detected, indicating that in the midbrain the deletion of Cofilin 2 was not complete. Only the midbrain and hippocampus showed an upregulation of ADF and Cofilin 1 in both P7 and adult animals, whereas the hippocampus showed the highest upregulation of ADF and Cofilin 1 at both time points, highlighting an important function of ADF/Cofilin family members in this brain region. This leads to the suggestion that especially in the hippocampus the deletion of Cofilin 2 seems to be compensated by other ADF/Cofilin family members. A compensatory effect of other ADF/Cofilin family members upon the loss of one member was also detected in ADF$^{-/-}$ mice and Cofilin 1$^{fl/fl}$ CaMKII-Cre mouse models, suggesting a functional redundancy (Gorlich et al., 2011; Rust et al., 2010). In the cerebellum only an upregulation of Cofilin 1 was detected in adult animals, indicating that both Cofilins could be necessary for synaptic processes in the adult cerebellar cortex. The upregulation of ADF and Cofilin 1 was lost between P7 and adulthood in the cortex and olfactory bulb, leading to the suggestion that ADF/Cofilin family members could contribute to migrational processes that assemble brain structures.

Since an upregulation of other ADF/Cofilin family members occurred upon the loss of Cofilin 2, the analysis of double knockout animals was important and necessary to check whether these upregulations prevent or attenuate a possible Cofilin 2-based phenotype. To analyze if the combined loss of ADF and Cofilin 2 in the brain displayed a stronger phenotype than the single conditional knockout of Cofilin 2, lysates of adult ADF$^{-/-}$ Cofilin 2$^{fl/fl}$ Nestin-Cre knockout animals were analyzed for a possible upregulation of Cofilin 1. The complete knockout of ADF was viable and showed no obvious brain phenotype, but an additive effect of ADF was detected in ADF$^{-/-}$ Cofilin 1$^{fl/fl}$ CaMKII-Cre animals (Gorlich et al., 2011; Wolf et al., 2015; Zimmermann et al., 2015). Total brain lysates of adult ADF$^{-/-}$ Cofilin 2$^{fl/fl}$ control animals and ADF$^{-/-}$ Cofilin 2$^{fl/fl}$ Nestin-Cre knockout animals were prepared. In adult animals the dual loss of both ADF and Cofilin 2 does not lead to an upregulation of Cofilin 1 in total brain lysates (figure 51). This could suggest overlapping functions or a subcellular localization for ADF and Cofilin 2 that is distinct to the brain specific function and localization of Cofilin 1. The upregulation of ADF was not sufficient to compensate for the loss of Cofilin 1 in Cofilin 1$^{fl/fl}$ CaMKII-Cre animals, which displayed a postsynaptic phenotype (Rust et al., 2010). An explanation for this observation could be the fact that ADF is predominantly enriched in presynaptic terminals and therefore fails to countervail the loss of Cofilin 1 in postsynaptic structures (Gorlich et al., 2011). On the other hand displayed ADF$^{-/-}$ Cofilin 1$^{fl/fl}$ CaMKII-Cre animals an additive effect of ADF, since in knockout animals also a presynaptic phenotype could be observed (Wolf et al., 2015; Zimmermann et al., 2015). This could suggest that the loss of Cofilin 2 might be more compensated by ADF than Cofilin 1. The fact that ADF and Cofilin 2 could have overlapping functions in the brain makes the analysis of double knockout

animals quite interesting, since it could have a more severe phenotype than the single knockout of Cofilin 2. A second explanation could be that the normal expression of Cofilin 1 is sufficient to maintain the brain morphology and function. In this study only total brain lysates of ADF$^{-/-}$ Cofilin 2$^{fl/fl}$ and ADF$^{-/-}$ Cofilin 2$^{fl/fl}$ Nestin-Cre animals were analyzed for alterations in the Cofilin 1 level. A better insight into the possible upregulation of Cofilin 1, due to the loss of ADF and Cofilin 2, should be analyzed in brain lysates of different brain regions, since the complete lysate could hide a weak upregulation of Cofilin 1 in distinct brain regions. Görlich et al also detected no upregulation of Cofilin 1 in ADF$^{-/-}$ mice in brain area lysates of the cortex and hippocampus, while an upregulation of Cofilin 1 was detected in synaptosomal lysates (Gorlich et al., 2011). As seen in figure 51 a complete knockout of ADF and Cofilin 2 was verified, since no band for ADF or Cofilin 2 was detected in the brain lysate of ADF$^{-/-}$ Cofilin 2$^{fl/fl}$ Nes-Cre animals.

Since Cofilin 2 displayed a broad expression profile in different brain regions, a further examination of distinct neuronal subtypes in these brain regions was performed. A possible role of Cofilin 2 in certain brain regions will be further discussed in the next chapters.

7.2. Cofilin 2 expression in different brain regions and a possible role of Cofilin 2 in distinct neuronal populations

7.2.1. Expression of Cofilin 2 in cholinergic neurons indicates a role for Cofilin 2 in memory processes

Acetylcholine is one of the major neurotransmitters involved in cognitive function (Levin and Simon 1998). A block of cholinergic activity induces memory impairments, including working memory deficits and a loss of cholinergic neurons is associated with Alzheimer´s Disease (AD). Actin rearrangements are known to play an essential role in learning and memory processes (Nelson et al., 2012; Rust et al., 2010). Colocalization studies revealed an expression of Cofilin 2 in cholinergic neurons of the basal forebrain (figure 27). These cholinergic neurons provide the major cholinergic innervation to the cortex and hippocampus and play a key role in memory processes. In Cofilin 2$^{fl/fl}$ Nestin-Cre animals a tendency for impairments in working memory could be detected, although changes were not significant. The dual loss of ADF and Cofilin 2 in ADF$^{-/-}$ Cofilin 2$^{fl/fl}$ Nestin-Cre animals displayed a significant impairment in working memory (figure 57). A reduction in cholinergic neurons is closely linked with a dysfunction of the neurotrophin NGF and its TrkA receptor. Thereby NGF-mediated cell signaling is required for long-term-survival of cholinergic neurons and

requires the binding of NGF to TrkA receptors at the presynaptic ending of cholinergic neurons and the internalization of these complexes for their retrograde axonal transport to the soma, where it alters gene transcription (Niewiadomska et al., 2011). Harrington et al showed that actin depolymerization is essential for initiation of NGF/TrkA endosome trafficking, since the stabilization of actin via Jasplakinolide induces a complete loss of TrkA endosome retrograde transport (Harrington et al., 2011). Additionally an association of Cofilin-Rac1 with TrkA in early endosomes was found that implicates Rac1-Cofilin signaling in the maturation of early endosomes to retrograde transport-competent endosomes. According to these findings it would be interesting to analyze the number of cholinergic neurons in knockout animals for either Cofilin 2 or ADF and Cofilin 2. If changes in the number of cholinergic neurons appear it would be further necessary to proof the association of different ADF/Cofilin family members to NGF/TrkA endosomal pathways.

7.2.2. Cofilin 2 in serotonergic neurons could contribute to dendritic elaboration and synaptogenesis

Serotonergic neurons are localized to raphe nuclei and innervate the cortex and thalamus (Takeuchi et al., 1983). Thereby the axons arborize over a large area and many do not form classical synapses, but rather exhibit paracrine or volume transmission. The outgrowth of axons depends on a highly motile structure at the tip, called growth cone. It was shown that the elongation of axons is accompanied by a depolymerization of actin filaments, which build a physical barrier for the outgrowth of microtubules. ADF/Cofilin family members were localized to growth cones to enable the depolymerization of actin filaments for the protrusion of the growth cone (Flynn et al., 2012; Garvalov et al., 2007). A deletion of Cofilin 2 could impact on the dynamic actin rearrangement upon guidance cues for the direction of axon guidance to specific targets. *In vitro* studies on cultured hippocampal neurons revealed an increased diameter of growth cones in Cofilin 2 deficient neurons and an altered localization of F-actin at these structures. These results implicate that due to the loss of Cofilin 2 the outgrowth of axons to their specific targets could be also altered *in vivo*, resulting in a reduced or delayed innervation of serotonergic neurons to their cortical target cells. Thereby serotonergic axons arborize over a large distance to reach the cortical area, which could amplify an effect upon the loss of Cofilin 2 on these cells and could be an explanation why changes could be more severe in the serotonergic system compared to cortical innervations within the same cortical column. During brain development serotonin has been shown to influence the maturation of tissues, including dendritic elaboration, synaptogenesis and organization of the cortex (Buznikov et al., 2001; Kondoh et al., 2004). Further it was shown that abnormalities in synaptic connections induced by a reduced or excess serotonin

concentration greatly reduced the number of dendrites in the cortex and hippocampus (Kondoh et al., 2004). A reduced dendritic branching of cortical neurons was observed in Cofilin $2^{fl/fl}$ Nestin-Cre animals via analysis of Golgi stained neurons in layers II and III (figure 40). Altered serotonin levels could be also linked to a disturbance of the actin cytoskeleton. The signaling by the neurotransmitter serotonin relies on the efficient transporter-mediated re-uptake of serotonin to terminate the synaptic signal. Treatment of Cos7 cells with cytochalasin D, an inhibitor of actin polymerization, inhibited the uptake activity of the serotonin transporter SERT (Sakai et al., 1997). This implicates that SERT uptake activity is regulated by the state of the actin cytoskeleton and that a disruption of F-actin reduces uptake activity. A block in the actin dynamic by the deletion of Cofilin 2 could alter actin rearrangements and thereby the recycling activity of serotonin transporters. This could lead to altered levels of serotonin in the extracellular space and thereby alter dendritic elaboration. Further is an altered regulation of SERT also implicated in anxiety, depression and autism. Anxiety is related to a reduced serotonin level (Briley et al., 1990). In $ADF^{-/-}$ Cofilin $2^{fl/fl}$ Nestin-Cre animals an altered response to fearful stimuli could be detected, raising the question of altered serotonin levels in the brain (figure 56). Additionally actin-based mechanisms were found to dictate p38MAPK-dependent transporter activity. Activation of this pathway leads to mobilization of transporters by un-tethering of the C-terminus of SERT from actin (Chang et al., 2012). Actin cytoskeletal disruption by cytochalasin D mobilizes SERT molecules, which is reflected in increased diffusion rates. Therefore the actin cytoskeleton is also implicated in the restriction of SERT mobility within membrane microdomains and the incorporation of transporters in the membrane. A more static F-actin could lead to altered transport of SERT to the membrane and therefore could modify serotonin levels. A slight increase in the F-actin content was also shown in cortical lysates of Cofilin 2 deficient, as well as ADF and Cofilin 2 deficient animals (figure 36 and 53). Therefore it would be of interest to study the mobilization of SERT in Cofilin $2^{fl/fl}$ Nestin-Cre animals by using Antagonist-conjugated quantum dots to study single molecules of SERT and there localization and mobilization within the cell.

7.2.3. Cofilin 2 is only expressed in glutamatergic presynaptic terminals with low-release probability

Vesicular glutamate transporters (vGLUTs) define distinct subsets of glutamatergic neurons and both transporters could be classified upon their localization to synapses with different release probabilities. VGLUT1 is expressed in synapses with low release probabilities, which are involved in LTP, while vGLUT2 is localized to synapses with high release probability implicated in LTD. Cofilin 2 is only localized to vGLUT1 positive presynaptic terminals (figure

28B). Since no colocalization between Cofilin 2 and vGLUT2 could be detected only a subset of glutamatergic presynaptic terminals contains Cofilin 2 (figure 28C). Studies showed that actin fulfills positive and negative functions on the vesicle pool in presynaptic terminals (Rust 2015; Rust and Maritzen 2015). On the one hand actin guides arriving vesicles to facilitate their docking and thereby regulates the size of the readily releasable pool. On the other side actin forms a physical barrier for the priming reaction and prevents the fusion of vesicles with the active zone. Thereby the role of actin depends on the particular synapse type (Dillon and Goda 2005). A bouton with high release probability depends on actin for the recruiting of vesicles into the readily releasable pool to support exocytosis. In contrast boutons with low release probability would use actin as a physical barrier to limit vesicle fusion. This model suggests that synapses differently modify the activity of actin-binding proteins and could therefore also rely to a different extent on Cofilin 2. The absence of Cofilin 2 in high release synapses go together with the observed behavioral studies, which displayed no changes in the habituation process upon Cofilin 2 deletion, suggesting no alterations in LTD (figure 48). In contrast the activation or deactivation of Cofilin 2 upon signaling pathways that induce LTP could be important to fulfill the role of actin as barrier to restrict an increased vesicle priming, but simultaneously enabling the rearrangement of actin filaments during LTP which is accompanied by spine enlargement. Therefore the loss of Cofilin 2 could impact on the process of LTP. A contribution of Cofilin 2 to the process of LTP should be analyzed in electrophysiological studies by applying one single 1sec 100Hz train or by a theta-burst stimulation (Larson and Munkacsy 2015). A further role for Cofilin 2 in pre- and postsynaptic compartments will be discussed in the chapter 5.3.2.

7.2.4. Cofilin 2 is localized to dopaminergic neurons and could influence cognitive functions

Dopamine plays an important role as modulator of the interplay between excitatory and inhibitory projections in the striatum that control voluntary movement and cognitive processes. Thereby dopaminergic neurons in the substantia nigra build synaptic connections on striatal medium spiny neurons, which release GABA (Pollack 2001). Thereby dopamine executes an excitatory effect on GABAergic neurons via D1-receptors, while an inhibitory effect is accompanied by D2–receptors. These GABAergic interneurons in the striatum influence the signal transmission to the thalamus that filters information and projects fibers back to the cortex to induce a behavioral response. Thereby hyperlocomotion is often associated with impaired dopamine function, due to the fact that a reciprocal modulation of dopamine and glutamate was described in the striatum, where glutamate facilitates dopamine release (Krebs et al., 1991). In the study from Zimmermann et al only double

knockout mutants for ADF and Cofilin 1 exhibited hyperlocomotion and impaired working memory, whereas the single mutants did not reveal changes (Zimmermann et al., 2015). The block of dopamine or glutamate transmission resulted in normal locomotion in double knockout animals. These observations indicate that the deregulation of actin dynamics enhanced glutamate release from medium spiny neurons, which deregulate dopamine release that resulted in hyperlocomotion. Since the single knockouts for ADF and Cofilin 1 did not exhibit this phenotype, both ADF and Cofilin 1 have a crucial role in the neurotransmitter release of excitatory synapses. In this study no alterations in locomotion could be detected in the single Cofilin 2 knockout (figure 47), as well as the double knockout for ADF and Cofilin 2 (figure 54). This leads to the suggestion that Cofilin 2 is dispensable for excitatory vesicle release, since even the dual loss of two ADF/Cofilin members did not lead to hyperlocomotion. Additionally also no alterations in the frequency of mEPSCs were detected in the Ca1 region of the hippocampus (figure 42).

The ADF$^{-/-}$ Cofilin 1$^{fl/fl}$ CaMKII-Cre animals analyzed by Zimmermann et al also revealed an impact on the working memory and the dopamine system is known to play a role in cognitive processes of working memory (Brozoski et al., 1979; Castner et al., 2000). An impaired working memory was detected in double knockout animals for Cofilin 2 and ADF (figure 57), although the single knockout of Cofilin 2 only showed a tendency for an affected working memory (figure 50). Thereby cognitive performance depends on the basal level of dopamine function in cortico-striatal circuitry. An expression of Cofilin 2 in dopaminergic neurons was verified in colocalization studies between Cofilin 2 and Tyr-hydroxylase, an enzyme necessary for the synthesis of dopamine (figure 25). Cofilin 2 was localized to dopaminergic neurons in the VTA and substantia nigra. Electrophysiological studies on hippocampal Ca1 neurons revealed that a loss of Cofilin 2 increases the frequency of mIPSCs (figure 44). These results implicate Cofilin 2 in the release probability of GABAergic inhibitory neurons. A lack of dopamine leads to an increased GABAergic inhibition of the thalamus, which alters the information processing in the thalamus and leads to a reduced signal propagation to the cortex, which then influence cognitive functions. Thereby the loss of Cofilin 2 in dopaminergic neurons could alter the synaptic input to the striatum, which could result in a shift towards inhibition and thereby reduce excitatory stimulation of cortical neurons that could impact on the working memory.

Actin is also implicated in maintaining the structure and function of dopaminergic neurons (Hao et al., 1997). The neurofilament light subunit is able to form a stable interaction with G-actin and the application of cytochalasin induces the depolymerization of filaments, which shifts the F/G-actin ratio towards G-actin. This shift causes an aggregation of neurofilaments in cultured dopaminergic neurons (Hao et al., 1997). In contrast neurofilaments do not display binding towards F-actin. The loss of Cofilin 2 induces a slight shift from G- to F-actin

and could thereby reduce the interaction between neurofilaments and actin, which could result in morphological or functional changes in dopaminergic neurons or even induce the loss of dopaminergic neurons.

Next steps should be to examine the possible loss of dopaminergic neurons in Cofilin 2, as well as ADF and Cofilin 2 deficient animals, by immunofluorescence staining with Tyr-hydroxylase, followed by counting of the number of marked dopaminergic neurons in the substantia nigra and ventral tegmental area. Additionally a possible colocalization between Cofilin 2 or ADF and antibodies against D1- or D2-receptors should be performed to analyze the localization of Cofilin 2 to specific presynaptic dopaminergic terminals. Also the number of receptors could be analyzed in control and knockout animals. If an alteration in the number of receptors exists, a dopamine receptor antagonist can be used to block the dopamine transmission and thereby inhibit the modulation of neuronal circuits to the thalamus and prefrontal cortex (PFC).

7.2.5. Cofilin 2 could fulfill an important function in inhibitory vesicle release and $GABA_A$-receptor clustering

Interneurons play an important role in establishing a functional balance, as well as the complexity and architecture of neuronal circuits. Thereby a single inhibitory neuron can innervate up to 100 principle neurons to synchronize cortical network activity. In the spinal cord the principal inhibitory neurotransmitter is glycine, whereas in the brain the principal neurotransmitter that mediates fast inhibitory synaptic transmission is γ-aminobutyric acid GABA (Rang 1995). GABA and glycine receptors are anchored postsynaptically by gephyrin, which assembles into a scaffold and interacts with actin (Bausen et al., 2006; Charrier et al., 2006). The application of cytochalasin D, which blocks the polymerization of actin, leads to a reduction in the number of gephyrin clusters (Bausen et al., 2006). Colocalization studies between Cofilin 2 and gephyrin generated only a few yellow spots with a small overlap in both signals, but in most cases only signals in close proximity to one another (figure 29). Therefore Cofilin 2 is not directly associated with gephyrin but mainly localized in close proximity, which could makes sense since gephyrin is linked to the barbed end of actin filaments, while Cofilin 2 as a depolymerization factor is localized to the pointed end of filaments. The other possibility would be that Cofilin 2 is mainly localized in presynaptic terminals of GABAergic neurons. In this study an elevated frequency of mIPSCs were detected in hippocampal pyramidal neurons upon the loss of Cofilin 2, which indicates a role for Cofilin 2 in inhibitory vesicle release (figure 44). Thereby the loss of Cofilin 2 could lead to a more static F-actin organization that provides tracks for the transport of vesicles to the

readily releasable pool and the priming of vesicles for the release. This would lead to an increased size of the readily releasable pool and thereby to an increased frequency of mIPSCs. This increased release of GABA could hyperpolarize pyramidal neurons in the hippocampus and inhibit a depolarization by an incoming postsynaptic current. An altered excitability of hippocampal neurons could impact on learning and memory processes and inhibit the signal propagation to the cortex and thereby alter the behavioral outcome of an animal.

Further a shift towards decreased amplitude of mIPSCs in the CA1 region of the hippocampus was found in Cofilin 2 deficient animals, leading to the suggestion that a reduced number of $GABA_A$-receptors were found in the postsynaptic membrane of hippocampal neurons (figure 45). Surprisinlgy the Kolmogorov-Smirnov test did not reveal significant changes, although in the box blots a pool of neurons with reduced amplitude was detected in Cofilin $2^{fl/fl}$ Nestin-Cre animals, which were not present in the control. Charrier et al showed that F-actin depolymerization by Latrunculin A reduces the clusters of gephyrin and thereby the backbone of inhibitory postsynaptic scaffolding (Charrier et al., 2006). The actin cytoskeleton determines trafficking, anchoring and synaptic clustering of receptors and is also implicated in the differential organization of distinct pools of receptors to fulfill postsynaptic specialization (Charrier et al., 2006; Hanus et al., 2006). The depletion of gephyrin also alters the clustering of many $GABA_A$-receptor subtypes (Kneussel et al., 1999) and shows that GABA-receptors are also anchored via F-actin. Thereby $GABA_A$-receptors mediate the tonic inhibition and are of particular interest in cognitive processing. The α5-subunit of $GABA_A$ receptors is predominantly expressed in the hippocampus (Wisden et al., 1992) and a depletion of this subunit facilitates fear conditioning or improves spatial learning in mice (Collinson et al., 2002; Crestani et al., 2002). Double knockout animals for ADF and Cofilin 2 displayed impairments in working memory and reduced anxiety-related behavior (figure 56 and 57). These observed phenotypes could be caused by an altered number of GABA-receptors in the postsynaptic membrane. A more static actin cytoskeleton could inhibit the lateral diffusion of receptors to the postsynaptic membrane or the number of receptors anchored via gephyrin in the membrane could be affected The subunit composition of $GABA_A$-receptors is also developmentally regulated and changes from the embryonic stage to the formation of synapses (Wang and Kriegstein 2009). Thereby 19 different subunits exist, which exhibit different functional properties and kinetics (Verdoorn et al., 1990). For example the incorporation of specific α-subunits determines the kinetics of receptor deactivation and desensitization, while the β-subunits affect channel properties. A more static actin cytoskeleton in knockout animals could alter the transport of receptors to the postsynaptic membrane and thereby consequently the developmentally regulated exchange of GABA-receptor subunits, which are necessary for example for the establishment of

synapses and their maturation. Note that the kinetics of recorded mIPSCs differed between control and Cofilin $2^{fl/fl}$ Nestin-Cre neurons (figure 44A). Events from mt animals had a broader appearance, suggesting an elongated opening time. This could be a hint for an altered receptor-subunit composition in the mt. Additionally the kinetics of receptors could be altered in ADF/Cofilin 2 knockout animals and change the outcome of neuronal circuits for learning or behavioral processes. Further an antagonist of $GABA_A$-receptors could be used to study the distribution and number of receptors in the postsynaptic membrane. If changes in the number of receptors occur, it would be also possible to check for alterations in subunit composition due to the Cofilin 2 loss. Therefore it would be possible to check the expression of subunits via qPCR in cortical preparations of control and knockout animals.

Inhibitory synapses often connect to the cell soma, due to the fact that they are more efficient when they are generated at the cell body near the axon hillock. Thereby inhibitory actions at the cell body open chloride channels that increase the Cl^- conductance and reduce the incoming depolarization by excitatory currents. In the cell soma actin filaments build a cortical cytoskeletal ring at the inner site of the membrane to support cell shape and enable the anchoring of adhesion receptors for cell-surface contacts. This cortical actin displays a different arrangement than the fine branched and specialized network localized in dendritic spines. Additionally in dendritic spines actin is the most abundant cytoskeletal protein, since microtubule protrusions into the spine are only encountered randomly for a few milliseconds (Kapitein and Hoogenraad 2011). In contrary in the cell soma microtubule are also arranged into cytoskeletal tracks that define the transport of vesicles. This increased cytoskeletal content could impede a fast trafficking of neurotransmitter receptors, in comparison with a specialized compartment for neurotransmitter anchoring and diffusion, like the postsynaptic membrane. Additionally different actin-binding proteins could be localized to the postsynaptic terminals in comparison to the cell soma, leading to the suggestion that distinct signaling pathways could be involved in the regulation of the actin cytoskeleton in the cell soma. Actin also fulfills multiple functions in the cell soma and an actin rearrangement is therefore regulated via multiple signaling pathways and not a view specialized pathways for the regulation of neuronal activity. Therefore the trafficking, anchoring and clustering of neurotransmitter receptors in the cell soma could be regulated quite differently than in dendritic spines in terms of receptor numbers and channel activity. Shoop et al showed that application of Latrunculin A on chick ciliary ganglion neurons stabilizes F-actin and retains large clusters of acetylcholine receptors on the cell soma and prevents receptor loss from the cell surface (Shoop et al., 2000). The analysis of mIPSCs did not reveal significant changes in the amplitude, which would indicate alterations in the number of $GABA_A$-receptors (figure 45), but an increased release of inhibitory vesicles was examined in the Ca1 region of the hippocampus (figure 44), which can induce a shift in the balance towards inhibition, altering

the outcome of neuronal circuits. Cofilin 2 is expressed in the cell soma of different inhibitory subgroups (figure 23 and 24) and could therefore be more essential for the rearrangement of actin in the cell soma to modulate the number of GABAergic receptors.

Interneurons were analyzed for Parvalbumin and calbindin expression, which are localized in different non-overlapping subgroups of interneurons. In the striatum parvalbumin is localized to fast-spiking non-adapting interneurons (FSI), which did not show an expression of Cofilin 2. These neurons are connected via gap junctions and exhibit therefore electrical synapses (Hjorth et al., 2009). These electrical synapses most likely do not rely on a rearrangement of the actin cytoskeleton, so that the expression of ADF/Cofilin family members is not required in these neurons. In contrast to that Cofilin 2 was expressed in medium spiny neurons (MSN) of the striatum, which build neuronal circuits with the thalamus and cortex by chemical synapses. In contrast these neurons express Cofilin 2 to enable a rearrangement of the actin cytoskeleton at synapses. Cofilin 2 could have a role in maintaining actin dynamics for receptor trafficking and anchoring in MSN. MSN are also inhibitory cells that release GABA. An increased frequency of mIPSCs was detected in the hippocampus, which suggests that Cofilin 2 could play a role in inhibitory vesicle release. An altered inhibitory release in the striatum can alter the balance between excitation and inhibition and induce a shift towards inhibition. This shift could reduce input from the striatum to the cortex and reduce the excitation of cortical neurons. Working memory deficits, as observed in double knockout animals for ADF and Cofilin2, could also result from a reduced excitation of cortical neurons (figure 57).

7.2.6. Cofilin 2 is expressed in the hypothalamus and pituitary gland and could contribute to hormonal release

The hypothalamus is the link between the endocrine and nervous system and produces hormones, which activate or deactivate the production of other hormones in the pituitary gland. Therefore it is responsible for the production of essential hormones that govern physiological functions, like growth, development and metabolism. The complete knockout of Cofilin 2 leads to a growth retardation in Cofilin $2^{-/-}$ animals, which starts early after birth and is displayed in smaller knockout animals in comparison to their littermates (Gurniak et al., 2014). This growth defect is only a secondary effect in the complete Cofilin 2 knockout, since the growth is restricted by the reduced exchange of α-actin isoforms during the early postnatal remodeling of sarcomeres. But also adult animals with a conditional deletion of Cofilin 2 showed this growth retardation (figure 35) and also the analysis of the body weight

over the first weeks after birth displayed a reduced weight due to the loss of Cofilin 2. Western blot analysis of control and Cofilin $2^{fl/fl}$ Nestin-Cre animals revealed an expression of Cofilin 2 in the hypothalamus and the pituitary gland and also displayed that the Nestin-Cre deletion also affects both of these regions (figure 33 and 35). To regulate metabolism and growth of animals the hypothalamus secretes growth hormone releasing hormones (GHRH) that prompt the pituitary gland to release growth hormones (GH) or growth hormone inhibiting hormones (GHIH). It would be interesting to analyze the hormone level of control and Cofilin $2^{fl/fl}$ Nestin-Cre animals in the blood to check for a possible increase or decrease of certain hormones involved in the regulation of growth and metabolism. Leptin is a hormone that helps to regulate energy balance by stimulation of GH secretion. Thereby Leptin inhibits or excites specific hypothalamic neurons via activation of PI3K that lead to the induction of actin rearrangements (Harvey et al., 2000). These actin rearrangements open K/ATP-channels and elevate their activity, which results in a hyperpolarization of hypothalamic neurons. A treatment of hippocampal neurons with Leptin led to a decreased level of F-actin (Ning et al., 2006), implicating a depolymerization of actin filaments for the regulation of energy homeostasis. A shift towards F-actin due to the loss of Cofilin 2, could impact on the activity of certain hypothalamic neurons that lead to an altered secretion of hormones by the hypothalamus and/or the pituitary gland. This in turn could result in a reduced body weight of Cofilin 2 deficient animals.

7.2.7. Cofilin 2 is not expressed in astrocytes and microglia

Dynamic reorganizations of the actin cytoskeleton are also pivotal for cell shape changes and migrational processes in microglia and astrocytes and are also coupled to the activation of members of the Rho family of small GTPases (Hall 1998). Microglia derive from hematopoietic stem cells and during development migrate into the CNS. Cofilin 1 is the only expressed ADF/Cofilin family member *in vivo* in microglia. For ADF only a signal in the cell culture lysate of microglia could be detected. The expression of Cofilin 2 was excluded from microglia cells *in vitro* and *in vivo* (figure 31). Additionally Cofilin 2 was also not expressed *in vivo* in astrocytes and only displayed a signal *in vitro* in astrocytic cell culture lysates (figure 32). Adhesion and homeostasis conditions are quite distinct between the brain and cell culture conditions. These altered environmental conditions in the cell culture could lead to an activation of Cofilin 2 expression, to enable cells to adhere and migrate in the new cell culture environment. Due to the fact that neurons and glia cells are generated by the same progenitor cells the use of the Nestin-Cre mouse line would also lead to the deletion of the protein-of-interest in glial cells. This could result in secondary side effects as it is shown for

the Nestin-Cre deletion of Cofilin 1 (Bellenchi et al., 2007). The deletion of Cofilin 1 via Nestin-Cre recombinase displayed a more severe phenotype than the deletion of Cofilin 1 by the Nex-Cre recombinase (Schütz; unpublished data), suggesting that Cofilin 1 also plays a role in glial cells and the deletion of Cofilin 1 impacts on glial and neuronal development. Since astrocytes are involved in important mechanisms to maintain the brain homeostasis, interference in astrocytic functions, could change the brain homeostasis, which then influence the functionality of neurons. For example one function of astrocytes is the uptake and clearance of neurotransmitters. The loss of Cofilin 1 in astrocytes could decrease this uptake, which would increase the concentration of neurotransmitter in the extracellular fluid that can activate receptors on neurons for a longer period. That would lead to an increased excitability of neurons, although the receptor number or function in neuronal synapses is not directly affected. Since Cofilin 2 was not present in glia cells the observed phenotype in Cofilin $2^{fl/fl}$ Nestin-Cre animals was only related to neuronal processes, which makes the results easier to interpret.

7.3. The role of Cofilin 2 in distinct morphological and functional processes in the CNS

7.3.1. The loss of Cofilin 2 affects dendritic branching

Dendrites are the site of most synaptic contacts and dendritic development determines the number and pattern of synapses received by each neuron (Hume and Purves 1981). A proper dendritic arborization is a critical process for accurate development of neuronal circuits and for activity-dependent plasticity in mature neurons (Libersat and Duch 2004; Scott and Luo 2001). Thereby dendritic abnormalities are the most consistent pathologic cause correlated with mental retardation. The outgrowth of neurites for the polarization into axon and dendrites, depends on a highly dynamic structure at the tips of these neurites, the growth cone. Small GTPases of the Rho family control the activation of ADF/Cofilin family members, which are necessary to depolymerize the actin cytoskeleton in the growth cone that builds a barrier for the protrusion of microtubuli. The loss of Cofilin 2 leads to an increased growth cone diameter in primary hippocampal cell cultures, reflecting a more static structure than the highly motile structures in control neurons (figure 37 and 38). In this study no live-cell imaging was performed, which should be a next step to examine the exact role of Cofilin 2 in growth cone dynamics, which also influences dendritic branching.

Additionally actin is involved in modulating dendritic morphology during development. Real-time imaging has demonstrated that dendritic elaboration occurs through a net growth of highly dynamic filopodia that each extend and retract many times per minute (Dailey and

Smith 1996). The extension, retraction and branching of dendritic processes are regulated by an intrinsic genetic program (Jan and Jan 2003) and extrinsic factors (McAllister 2002). For the retraction of dendritic structures during developmental processes extrinsic factors also stimulate the Rac pathway that regulates the activation state of ADF/Cofilin family members (Rosso et al., 2005). A block of Rac or Cdc42 reduces the number of primary dendrites, whereas an increased RhoA activity causes a retraction of dendrites (Li et al., 2002). Therefore Cofilin 2 could be necessary for the retraction of filopodia during the establishment of dendritic branches and additionally for the breakup of cortical actin in the cell soma, as well as the dense actin network in growth cones, for the outgrowth of neurites, which will later differentiate into dendrites. This would result in a reduced dendritic branching as observed in cortical pyramidal neurons of Cofilin $2^{fl/fl}$ Nestin-Cre animals (figure 40). Together with the observed growth cone defect, which further impairs the elongation of dendrites, Cofilin 2 seems to play a role in neurite elongation and dendritic branching.

Neuronal activity also regulates the number of dendritic filopodia, which display the substrate for new branch formations (Dailey and Smith 1996). Cultured hippocampal neurons formed dendritic branches only in the presence of afferent innervation. This lead to the suggestion that the formation of synaptic contacts guide dendritic growth (Vaughn 1989) and those new dendritic branches are also stabilized by synapses (Wu et al., 1999). An increased number of immature (thin) spines was detected in Cofilin 2-deficient cortical neurons (figure 41). Since these thin spines represent weaker synaptic contacts, due to the fact that a reduced number of receptors are anchored in the postsynaptic density, also a reduction in the stabilization of dendritic branches could occur. In Cofilin $2^{fl/fl}$ Nestin-Cre animals a reduction in dendritic branching could be observed in cortical pyramidal neurons, which is reflected in a reduced number of intersections in a Sholl analysis (figure 40). This result showed that the loss of Cofilin 2 impacts on the outgrowth or stabilization of newly formed dendrites. Studies on the number of dendritic spines in knockout animals did not reveal changes between control and knockout animals, showing that the number of spines is not altered upon the loss of Cofilin 2. Additionally an upregulation of ADF and Cofilin 1 was observed in the cortex of Cofilin $2^{-/-}$ brains, at the beginning of synaptogenesis (P7). Nevertheless the loss of Cofilin 2 could inhibit the maturation of dendritic spines. In addition the block of NMDA-receptors early in development, when synapses only contain NMDA-receptors, leads to a loss of dendrites (Rajan and Cline 1998), since dendritic branches are stabilized by synaptic activity. Impairment in actin reorganization, due to the loss of Cofilin 2, could alter the transport and anchoring of NMDA receptors and thereby reduce the number and clustering of receptors at the PSD, which could alter the neuronal activity and thereby contribute to a loss of dendrites. Changes in the number of mature synapses can be detected upon a staining with vGLUT1 (presynaptic marker) and PSD-95 (postsynaptic marker), which marks mature functional

synapses. Thereby the number of mature synapses in Cofilin $2^{fl/fl}$ and Cofilin $2^{fl/fl}$ Nestin-Cre animals could be compared.

7.3.2. Dendritic spine maturation could be affected by the loss of Cofilin 2

Within the first week of murine development dendritic protrusions begin to increase in density. These protrusions are also capable of extreme movements, especially early during development with an accelerated synaptogenesis starting around postnatal day 7. Interestingly Cofilin 2 expression analysis during different developmental time points indicated the highest expression of Cofilin 2 at P7, when the complete knockout of Cofilin 2 is starting to became lethal. At that time point the Cofilin 2 expression reaches a peak in most brain areas, except for the cortex and cerebellum, which showed the highest expression at P0 and adulthood (figure 22). The protrusion of dendritic spines for the establishment of synapses needs a constant rearrangement of the actin cytoskeleton, since actin is the most prominent cytoskeletal protein in spines. Spines are highly dynamic structures and their formation and maturation depends on actin remodeling (Cingolani and Goda 2008). ADF/Cofilin family members are localized at spines and enable the rapid rearrangement of actin, due to the depolymerization of filaments (Hotulainen et al., 2005; Racz and Weinberg 2006). During the second and third week of life, the density of dendritic spines further increases, in coincidence with the rate of synaptogenesis. During this time period (P15 – P21) a prominent expression of Cofilin 2 could be observed in all brain regions, although weaker in comparison to P7. The motility of spines is developmentally regulated and decreases during the first postnatal weeks as synaptic circuits mature. During the next month a pruning process with a loss of spines is observed in animals, which generates the mature spine density after several months. An expression of Cofilin 2 is also found at P90 showing a broad expression in all brain regions (figure 22). Additionally also the spine morphology changes during the development. Early in development most spines are stubby or thin with quite long filopodia. Over the next weeks the number of thin spines decreases and the spine maturation can be seen in the occurrence of mushroom shaped spines, which display the site of strong synapses. Thereby the spine volume is proportional to the area of the PSD and PSD area correlates with the number of incorporated receptors. In Cofilin 2 deficient animals a reduction in the number of mushroom-shaped spines could be observed (figure 41), which could implicate Cofilin 2 in the maturation process of dendritic spines. The overall number of spines was not altered and an concurrent increase in the number of thin spines was also detected. This suggests that Cofilin 2 was not necessary for the formation of spines, but rather was important for the transition from immature to mature spines. The incorporation of

new receptors as well as the enlargement of the PSD needs a dynamic actin cytoskeleton, which allows the expansion of the spine volume. A loss of Cofilin 2 could lead to an impaired rearrangement of actin filaments blocking the transport of proteins for the increment in spine volume and also the transport of receptors to the postsynaptic membrane.

Glutamate is the main excitatory neurotransmitter in the brain and can fulfill its function via the activation of three receptors: AMPA, NMDA and kainate receptors. In this study the frequency and amplitude of mEPSCs in the Ca1 region of the hippocampus were examined. These mEPSCs are generated by spontaneous glutamate vesicle release and the binding of glutamate to the AMPA receptor, which is an ionotropic transmembrane receptor for the fast excitatory synaptic transmission that enables the opening of further glutamate-gated receptors. The AMPA receptor number seemed to be not affected in Cofilin $2^{fl/fl}$ Nestin-Cre animals, since no changes in the amplitude of mEPSCs in the Ca1 region of the hippocampus was detected (figure 43). To directly analyze the lateral diffusion and clustering of AMPA receptors, hippocampal cultures should be incubated with quantum dots conjugated with a primary antibody directed against the AMPA receptor subunit GluR2. Live cell imaging of stained hippocampal neurons should be performed to track the transport and clustering of AMPA receptors to the postsynaptic membrane in Cofilin $2^{fl/fl}$ Nestin-Cre animals. An altered lateral diffusion of AMPA receptors was observed in Cofilin $1^{fl/fl}$ CaMKII-Cre mice, while no alterations in the surface expression of NMDA receptors could be observed (Rust et al., 2010). NMDA-receptors are a second class of ionotropic glutamate receptors that mediates the fast and slow components of excitatory synaptic transmission. Since an increased number of immature (thin) spines, accompanied with a reduced level of mushroom shaped spines, were observed in Cofilin $2^{fl/fl}$ Nestin-Cre animals and thin spines mainly contain NMDA-receptors, this class of glutamate receptors should also be analyzed. The NMDA receptor surface expression should be analyzed by radio-ligand binding of [^{3}H]-labelled MK-801, an uncompetitive antagonist of the NMDA receptor. Changes in the number of NMDA receptors cannot be detected in mEPSCs, since these receptors are voltage-gated and open when the cell is depolymerized to -40mV. During the electrophysiological recordings cells were patched at -70mV, restricting the opening of NMDA receptors and their contribution to the recorded mEPSCs. Another possibility would be to examine the ratio between the NMDA- and AMPA response in electrophysiological studies. These studies could show that different types of glutamate receptors depend differently on Cofilin 2 for their transport and clustering and are therefore distinctly affected by the loss of Cofilin 2. Further it was also shown that NMDA and AMPA receptors are differently sensitive to drugs altering actin dynamics (Allison et al., 1998; Kirsch and Betz 1995). This indicates that actin contributes to the differential organization of distinct pools of postsynaptic receptors to obtain a postsynaptic specialization. Thin spines represent immature spines and mainly contain

NMDA receptors, while the maturation of spines is accompanied with an occurrence of AMPA receptors in the postsynaptic density. Thereby the maturation of spines results from the lateral transport of AMPA-receptors from the extrasynaptic space into the postsynaptic density (Fortin et al., 2012; Takahashi et al., 2009). The finding of an increased number of immature spines suggests a role for Cofilin 2 in AMPA receptor transport during the maturation process, although our preliminary electrophysiology findings did not reveal changes in the number of AMPA receptors in Cofilin2$^{fl/fl}$ Nestin-Cre animals. One possibility would be the fact that the recordings were performed on P21 old mice and therefore at a developmental time point were synaptogenesis was still not completed. At that early time point the pruning of synaptic connections takes place removing synaptic contacts that are not used rather than the maturation of spines to strengthen synaptic contacts. Therefore the transport of AMPA receptors could be more important and frequently at a later time point, masking a defect in AMPA receptor number in electrophysiological studies performed on young Cofilin 2 deficient animals. Zhou et al showed that F-actin stabilization by jasplakinolide results in a reduced endocytosis of AMPA receptors from the PSD, while actin depolymerization via latrunculin accelerates AMPA receptor internalization into the PSD (Zhou et al., 2001). In Cofilin 1$^{fl/fl}$ CamKII-Cre mutants an altered number of AMPA receptors were found, implicating Cofilin 1 in the lateral diffusion of AMPA-receptors (Rust et al., 2010). Additionally an increase in mushroom-shaped spines was observed, highlighting the possibility that the loss of Cofilin 1 blocks AMPA receptor endocytosis, which leads to an increase in the number of AMPA receptors and therefore to an increased PSD area. This increase in the PSD area then elevates the number of mushroom-shaped spines.

In the Cofilin 2$^{fl/fl}$ Nestin-Cre knockout mice no changes in the number of AMPA-receptors (figure 43) and further the opposite effect on mushroom shaped spines was detected, with a decreased number on cortical pyramidal neurons (figure 41). Studies with GFP-tagged actin revealed two distinct actin pools in dendritic spines (Honkura et al., 2008). On the one hand stable longitudinal filaments present along the core of spines that are involved in the exo - endocytic trafficking of receptors, as well as the overall stability of the spine. On the other hand the dynamic sub-plasmalemmal actin network at the postsynaptic scaffold responsible for the anchoring and organization of receptor pools and thereby for the morphological remodeling of the spine head. Differences in the turnover rates and structures of these filaments are important for different postsynaptic mechanisms. One possibility is that the transport of AMPA-receptors was not affected due to the loss of Cofilin 2, but the increase in spine size upon maturation was blocked due to the increased level of F-actin by the loss of an actin depolymerizing factor. The more static actin filaments in dendritic spines could interfere with the anchoring and organization of AMPA receptors, necessary for the maturation of spines, while the basic synaptic transmission could be fulfilled. Thereby it was

also shown that the trafficking of AMPA receptors and the internalization can occur independently of spine shape changes (Cingolani and Goda 2008). The loss of Cofilin 2 could have a stronger impact on the more dynamic sub-plasmalemmal actin network, responsible for the anchoring and clustering of receptors, than the more static longitudinal filaments along the core of spines for the trafficking of receptors. Thereby Cofilin 2 could fulfill a role in receptor anchoring and clustering rather than in the transport, while Cofilin 1 seems to be involved in both processes.

A positive correlation between the dimension of the spine head and the PSD area, and between the PSD area and the number of synaptic glutamate receptors exists. Therefore spine head size and synaptic efficiency are highly correlated and a reduced number of mushroom-shaped spines, which represent ´strong synapses´, could lead to a reduced synaptic efficiency. Additionally alternations in actin dynamics in dendritic spines are associated with mental retardation (Meng et al., 2002; Pontrello and Ethell 2009). Therefore reduced actin rearrangements at spines can impact on learning and memory processes. Impairment in working memory processes were detected in ADF$^{-/-}$ Cofilin 2$^{fl/fl}$ Nestin-Cre animals (figure 57). The single knockout of Cofilin 2 did not lead to significant changes in working memory, although a tendency for an impaired working memory was detected (figure 50). In the hippocampus of newborn and adult animals an upregulation of ADF and Cofilin 1 was detected in Cofilin 2$^{fl/fl}$ Nestin-Cre animals, which could compensate the loss of Cofilin 2 and milder the effect on the working memory (figure 21 and 33). Additionally a link exists between morphological changes and increased synaptic efficiency due to the process of LTP. After induction of LTP an increase in the PSD area could be observed (Hering and Sheng 2001), which also reflects an increase in the number of mushroom-shaped spines. Therefore the reduced number of mushroom-shaped spines in Cofilin 2 deficient animals could also indicate an impaired induction of LTP. Actin is the major cytoskeletal protein found in pre- and postsynaptic terminals and a modulation of actin is likely to drive cytoarchitectural changes that are associated within synaptic plasticity. Rust et al showed with electrophysiological studies that the deletion of Cofilin 1 impairs the late phase of LTP, although the induction of LTP is not affected (Rust et al., 2010). The analysis of LTP in Cofilin 2$^{fl/fl}$ Nestin-Cre animals should be conducted in further electrophysiological experiments to clarify the role of Cofilin 2 for LTP.

Further the presence of F-actin at synapses is most critical during early development, while the disruption of actin in mature synapses does not disrupt clustering of synaptic proteins (Yao et al., 2006). This observation implicates actin in the establishment and maturation of synapses during development. In young synapses the depolymerization of F-actin results in dispersion of synaptic vesicles and N-cadherin clusters. This shows that during early developmental stages adhesion molecules are both recruited and stabilized by F-actin and F-

actin clustering is required downstream of neuronal adhesion for the clustering of vesicles. The specification of synapses is mediated via cell-cell contact between transmembrane molecules and therefore specifies the sites for presynaptic assembly. Cadherins are adhesion molecules that form trans-synaptic homophilic dimers and engage F-actin rearrangements through catenins both on pre- and postsynaptic sides. Thereby cadherin-mediated adhesion directly triggers presynaptic actin polymerization and vesicle trapping through Rac GEFßPix. Reduced actin dynamics through the loss of Cofilin 2 could inhibit the active actin reorganization upon signaling of cell-cell contact and thereby prevent the assembly of presynaptic compartments. This could result in a decreased number of functional synapses and could explain the increased number of thin immature spines. The maturation of spines also depends on synaptic activity. An increased neuronal excitability by application of a $GABA_A$ receptor antagonist, results in an increased spine density and area, while an inhibition of vesicle release by botulinum toxin causes a significant decrease in spine density (McKinney et al., 1999). This means that thin spines represent immature spines without a presynaptic partner. Therefore the increased number of thin spines could indicate a decreased number of functional synapses. This hypothesis could be tested with a staining of vGLUT1 and PSD-95, whose colocalization indicates a functional synapse or by EM micrographs.

7.3.3. Cofilin 2 fulfills distinct functions in the presynaptic compartment

Actin is also abundantly present at the presynaptic terminals of mature synapses and fulfills two opposite functions: First it maintains and regulates vesicle pools by serving as a scaffold to restrict vesicle mobility. Second it provides a conduit to direct the transfer of vesicles between the pools. Thereby boutons that are large or release neurotransmitter at a fast rate dependent on actin for recruiting vesicles into the readily releasable pool to support exocytosis. Boutons that are small and release only small amounts of neurotransmitter use actin as a physical barrier to limit vesicle fusion. Therefore the synaptic activities of small or large synapses activate different signaling machineries for the modification of the activity of defined actin binding proteins. In colocalization studies an expression of Cofilin 2 was restricted to presynaptic terminals that express vGLUT1, which marks synapses with low release probability (figure 28). No colocalization between vGLUT2 as a marker for synapses with high release probability and Cofilin 2 could be observed, but a signal in close proximity suggesting that Cofilin 2 is rather localized to the postsynaptic compartment of large synapses (figure 28). The use of actin filaments as a physical barrier needs a regulated activity of actin depolymerization factors to restrict vesicle mobility on the one hand, while on

the other hand also enable enough mobility to induce synaptic plasticity. A loss of Cofilin 2 could further increase the block of vesicle mobility and inhibit the induction of LTP and the refill of the readily releasable vesicle pool. To analyze a possible role of Cofilin 2 in vesicle mobility and exocytosis Paired-pulse ratios in Cofilin $2^{fl/fl}$ Nestin-Cre animals could be analyzed. Thereby vesicle trafficking along F-actin filaments is facilitated by myosin V and vesicles are captured at the active zone by binding of myosin to syntaxin (Watanabe et al., 2005). An increase in F-actin is known to block the activity of myosin V. A slight shift towards F-actin was observed in cortical lysates of Cofilin 2 deficient animals and this increase in F-actin could decrease the activity of myosin V and thereby reduce the transport of vesicles to the active zone. Wolf et al performed EM micrographs on the Ca1 stratum radiatum of $ADF^{-/-}$ Cofilin $1^{fl/fl}$ CaMKII-Cre animals (ACC mice) to analyze the distribution of vesicles within presynaptic terminals (Wolf et al., 2015). They found a reduced number of vesicles within a region close to the active zone, while an increased number was found in a region >250nm away from the active zone, showing a shift in vesicle distribution. Additionally an increased number of docked vesicles were detected at the plasma membrane. These observations support a role of actin depolymerization factors in presynaptic vesicle mobilization. Interestingly the loss of Cofilin 1, as the major ADF/Cofilin isoform in excitatory synapses did not result in a presynaptic phenotype. Görlich et al also did not reveal presynaptic changes in $ADF^{-/-}$ mice (Gorlich et al., 2011). Only the dual loss of ADF and Cofilin 1 affects presynaptic physiology, leading to the suggestion that ADF is able to compensate for the loss of Cofilin in presynaptic terminals, which is also reflected in elevated ADF levels upon the loss of Cofilin 1. This indicates that ADF and Cofilin 1 display overlapping functions in presynaptic physiology and highlights how important it is to compare single Cofilin 2 knockout animals with double knockout animals for ADF and Cofilin 2.

In this study electrophysiological recordings were performed on Cofilin $2^{fl/fl}$ Nestin-Cre animals to detect possible changes in spontaneous synaptic vesicle release. No alterations in the frequency of mEPSCs were observed due to the loss of Cofilin 2, whereas an increased release of GABAergic vesicles was observed in Cofilin 2 deficient animals (figure 42 and 44). Interestingly Wolf et al also found no alterations in the amplitude and inter-event interval of mEPSCs, although further electrophysiological studies revealed an impaired glutamate release. They concluded that changes were not detected in mEPSCs, because the number of dendritic spines and synapses was reduced in ACC mice. A reduction in the number of spines was not detected in Cofilin $2^{fl/fl}$ Nestin-Cre animals although studies were only performed on pyramidal neurons in the cortex and not on the hippocampus (figure 41). The number of functional synapses was not studied so far in knockout animals, but a reduced dendritic arborization was found in cortical pyramidal neurons of Cofilin $2^{fl/fl}$ Nestin-Cre animals, which decreases the area for the establishment of excitatory synapses (figure

40). Thereby a reduced number of functional synapses could distort an increased release probability of small synapses in electrophysiological recordings. This means that the release probabilities of small synapses could be altered, although in this study no changes in the frequency of mEPSCs were detected. An increased stability of actin filaments in low release probability synapses could lead to an altered function of actin in these synapses, switching from a barrier function to the acceleration of vesicle transport and release. This could alter the outcome of neuronal circuits and affect learning and memory processes. Therefore it would be necessary to count the number of functional excitatory synapses in Cofilin 2 deficient animals. To test whether the neurotransmitter release is affected, isolated synaptosomes from both mutants should be depolarized by the application of KCl. The glutamate or GABA release could then be analyzed by performing an enzyme-linked fluorometric assay (Nicholls et al., 1987). To exclude the possibility that changes in neurotransmitter release are caused by alterations in the overall glutamate or GABA levels, also the total neurotransmitter content should be quantified by lysis of synaptosomes with Triton X-100.

The presynaptic actin cytoskeleton has also a role in the organization of vesicle pools. Thereby the vesicle pools can be classified into three different pools: First the readily-releasable pool (RRP) for immediate release that is docked to the active zone; second the reserve pool that is organized into clusters and third the recycling pool with vesicles that undergo exo/- endocytosis during sustained stimulation. Actin surrounds these clusters and is linked to vesicles via synapsin and also forms long actin filaments that interconnect the reserve pool with the readily releasable pool at the active zone and provides a track for the vesicle transport between pools. The treatment of synapses with latrunculin A revealed that large synapses that have to transport vesicles over longer distances are more dependent on F-actin tracks then small synapses were no alterations in the refilling of the RRP could be observed. Thereby actin also guides the fine positioning of synaptic vesicles since the stabilization of actin by application of jasplakinolide abolished the distribution of recycled vesicles towards the actin zone. An altered organization of vesicles was also observed in ADF$^{-/-}$ Cofilin 1$^{fl/fl}$ CaMKII-Cre mutant mice (Gorlich et al., 2011). In these mutants the number of docked and primed vesicles was increased in the Ca1 region of the hippocampus, resulting in an elevated level of vesicle exocytosis. Therefore it would be interesting to see whether the loss of Cofilin 2, or the dual loss of ADF and Cofilin 2, also affects the organization and positioning of vesicles. This could be done by electron microscopy of Cofilin 2$^{fl/fl}$ Nestin-Cre, as well as ADF$^{-/-}$ Cofilin 2$^{fl/fl}$ Nestin-Cre brains. In that way the presynaptic bouton size, active zone length, synapse density and the clustering of vesicles could be observed. The vesicle distribution of Cofilin 2$^{fl/fl}$ and ADF$^{-/-}$ Cofilin 2$^{fl/fl}$ Nestin-Cre animals should be analyzed to examine if the relative vesicle number is altered or a shift in vesicle

distribution between the reserve pool and RRP occurred. A role for Cofilin 2 in vesicle recruitment to the release site should be further examined in a short-term depression protocol on hippocampal slices by stimulation of Schaffer collaterals to deplete the readily releasable pool and then record excitatory postsynaptic field potentials (fEPSP) to analyze changes in the baseline that reveals defects in vesicle recruitment. Additionally a change in the fEPSP slope indicates alterations in vesicle release. The refill of the readily releasable pool by transport of vesicles from the reserve pool to the active zone along actin filaments can be further analyzed in electrophysiological Paired-pulse ratio protocols, which would also reflect changes in the kinetics of receptors due to changes in subunit composition of receptors. This electrophysiological study could give insight into the possibility that an elevated vesicle release is covered by a reduced number of functional synapses.
Actin plays also an important role in the endocytosis of synaptic vesicles. Cdc42 removes synaptic vesicles from the active zone after endocytosis in an actin-dependent mechanism. Thereby actin is involved in the generation of forces needed for the bending or fission of the membrane and provides tracks for the transport of endocytosed vesicles with the help of motor proteins (Haucke et al., 2011). Endocytosis in presynaptic terminals can be monitored by using pH-sensitive GFP variant pHluorin linked to vesicles. Thereby vesicles light up upon exposure to the extracellular pH during exocytosis and the signal is quenched again during vesicle acidification that follows endocytosis.

7.4. The role of actin depolymerization factors in the outcome of behavioral responses

Alterations in neuronal circuits can contribute to changes in behavioral outcome. Behavioral abnormalities were reported for Cofilin $1^{fl/fl}$ CaMKII-Cre animals with impairments in associative learning and a reduced anxiety-related behavior (Goodson et al., 2012; Rust et al., 2010). The double knockout for ADF and Cofilin 1 also revealed a role for actin depolymerization factors at the presynaptic site, since double knockout animals displayed a hyperlocomotion and impaired working memory functions (Zimmermann et al., 2015). Furthermore a localization of Cofilin 2 at the pre- and postsynaptic site was detected in this study, suggesting that Cofilin 2 could alter vesicle release, which could be reflected in elevated locomotion, or postsynaptic parameters like learning and memory. Therefore Cofilin 2 deficient, as well as ADF and Cofilin 2 deficient animals were analyzed in different behavioral paradigms testing exploratory behavior, locomotion, spatial memory and anxiety.

Spatial memory was analyzed in the Y-maze and working memory deficits were only significant in double knockout animals for ADF and Cofilin 2 (figure 57), while the single

knockout of Cofilin 2 displayed the same tendency, but results were not significant (figure 50). This suggests that ADF and Cofilin 1 are able to compensate the single loss of Cofilin 2. Additionally an upregulation of ADF and Cofilin 1 was observed in the hippocampus of newborn and adult animals, which could cover the loss of Cofilin 2 in learning and memory paradigms (figure 21 and 33). Thereby the Y-maze is a paradigm to test working memory in rodents. The working memory functions as a moment-to-moment utilization of information, which is processed in the hippocampus and prefrontal cortex (PFC) by feedforward excitation and local circuits. In the PFC memory fields exist, that are defined as maximal firing of a neuron to the representation of a visual target in a certain location. Thereby the same memory field encodes the same location in every trial. Additionally the pyramidal-nonpyramdial interactions are critical for the formation of memory fields in the PFC and pyramidal cells of different memory fields communicate via interneurons. A shift in the balance between excitation and inhibition could thereby impair the formation of memory fields for a new environment and could contribute to working memory deficits in the Y-maze. An elevated frequency of mIPSCs in the hippocampus of Cofilin 2 deficient animals was detected (figure 44) and could mark a shift towards inhibition, which could block the formation of memory fields. The role of actin in LTP was mentioned in several chapters of this discussion and will not be further explained here for the role of the hc in learning and memory processes.

ADF$^{-/-}$ Cofilin 2$^{fl/fl}$ Nes-Cre animals showed a significantly increased center time in the open field and additionally an increased number of open arm entries in the elevated plus maze (EPM). These observations lead to the conclusion that ADF/Cofilin 2 mutants were significantly less anxious than controls. Additionally the total number of arm entries in the EPM did not differ between control and knockout animals, implicating that changes in behavior do not simply reflect locomotor hyperactivity in knockout animals. An increased locomotor activity was also not detected during a test session in the open field. A similar phenotype was also observed in animals with a forebrain-specific deletion of Cofilin 1 using CamKII-Cre (Goodson et al., 2012). Also here, Cofilin 1 deficient animals reflect a decreased anxiety-related behavior in the open field and EPM. These observations in knockout animals reveal an important mechanism of actin filament depolymerization in anxiety. Since changes in spatial working memory were also observed in ADF$^{-/-}$ Cofilin 2$^{fl/fl}$ Nestin-Cre animals one could argue that deficits in spatial working memory could contribute to an anxiety-like phenotype, since knockout animals could have an altered discrimination between spatial locations. The hippocampus (hc) fulfills multiple functions that are associated with different sub-regions. For example lesions in the ventral hc have no effect on spatial learning and memory performance, but affect anxiety. In contrast to that are lesions of the dorsal hc associated with impaired spatial learning and memory, while no changes in anxiety were

reported (Bannerman et al., 2004). Therefore changes in anxiety are unlikely to be related to differences in spatial memory abilities.

Dysfunctional cytoskeletal remodeling in the ventral hc, which lead to alterations in synaptic plasticity are most likely the cause of changes in anxiety levels. Thereby synaptic plasticity is associated with the growth and shrinkage of dendritic spines, which are the sites of most excitatory synapses. Actin is highly abundant in dendritic spines and the main cytoskeletal protein. Additionally stress-induced changes in anxiety are associated with alterations in spine morphology and density, where reduced actin mobility in spines caused a retraction of mushroom-shaped spines and an inhibition in spine maturation (Mucha et al., 2011). A similar phenotype could be observed in this study in Cofilin 2-deficient animals were we detected a reduced number of mushroom shaped spines, accompanied with an increased number of thin spines in pyramidal neurons of the cortex (figure 41). Thin spines are known to represent more immature spines and correlates therefore with the observed phenotype observed by Mucha et al. It would be interesting to see whether these alterations in spine morphology could be also detected in the hippocampus upon the loss of Cofilin 2. The analysis of mIPSCs in the Ca1 region of the hippocampus revealed an increased spontaneous inhibitory vesicle release. This could lead to an elevated inhibition of cells, which results in a reduced excitatory stimulation. Thereby the incorporation of further glutamate receptors for the strengthening of synapses upon synaptic activity, accompanied with an increment in PSD area, could be prevented, which would result in a reduced number of mushroom-shaped spines.

Additionally in this study spine analysis were only performed on the single Cofilin 2 deletion. Therefore a next step should also the analysis of $ADF^{-/-}$ Cofilin $2^{fl/fl}$ Nestin-Cre animals to assess whether the observed phenotype is even stronger upon the dual loss of ADF and Cofilin 2. Additionally an upregulation of ADF and Cofilin 1 was detected in the hippocampus of newborn and adult animals, which could attenuate a Cofilin 2-based phenotype (figure 21 and 33). Further the NMDA receptor-mediated synaptic plasticity is a key determinant of anxiety levels (Barkus et al., 2010). It was shown that NMDA-receptor antagonists affect fear and anxiety by exhibiting anxiolytic effects. Niewoehner et al showed that the deletion of NR1, an NMDA receptor subunit, in the dentate gyrus of the ventral hc reduces anxiety (Niewoehner et al., 2007). Since a correlation between the size of the PSD and the number of NMDA receptors exists, mushroom shaped spines are the site of strong synapses. A reduced number in mushroom shaped spines was observed in the single brain-specific Cofilin 2 deletion, which could show that a more static actin cytoskeleton could block the growth of spines, which would be accompanied with an increase in the number of NMDA receptors in the PSD. A loss in the number of NMDA receptors could thereby lead to a reduced anxiety as the blocking of NMDA receptors also alters anxiety levels.

8. References

Agrawal, P. B., R. S. Greenleaf, et al. (2007). "Nemaline myopathy with minicores caused by mutation of the CFL2 gene encoding the skeletal muscle actin-binding protein, cofilin-2." Am J Hum Genet **80**(1): 162-167.

Allison, D. W., V. I. Gelfand, et al. (1998). "Role of actin in anchoring postsynaptic receptors in cultured hippocampal neurons: differential attachment of NMDA versus AMPA receptors." J Neurosci **18**(7): 2423-2436.

Anagnostaras, S. G., G. D. Gale, et al. (2002). "The hippocampus and Pavlovian fear conditioning: reply to Bast et al." Hippocampus **12**(4): 561-565.

Arikkath, J. and L. F. Reichardt (2008). "Cadherins and catenins at synapses: roles in synaptogenesis and synaptic plasticity." Trends Neurosci **31**(9): 487-494.

Ayala, R., T. Shu, et al. (2007). "Trekking across the brain: the journey of neuronal migration." Cell **128**(1): 29-43.

Bamburg, J. R. (1999). "Proteins of the ADF/cofilin family: essential regulators of actin dynamics." Annu Rev Cell Dev Biol **15**: 185-230.

Bamburg, J. R. and D. Bray (1987). "Distribution and cellular localization of actin depolymerizing factor." J Cell Biol **105**(6 Pt 1): 2817-2825.

Bamburg, J. R. and O. P. Wiggan (2002). "ADF/cofilin and actin dynamics in disease." Trends Cell Biol **12**(12): 598-605.

Bannerman, D. M., J. N. Rawlins, et al. (2004). "Regional dissociations within the hippocampus--memory and anxiety." Neurosci Biobehav Rev **28**(3): 273-283.

Bardoni, B. and J. L. Mandel (2002). "Advances in understanding of fragile X pathogenesis and FMRP function, and in identification of X linked mental retardation genes." Curr Opin Genet Dev **12**(3): 284-293.

Barkus, C., S. B. McHugh, et al. (2010). "Hippocampal NMDA receptors and anxiety: at the interface between cognition and emotion." Eur J Pharmacol **626**(1): 49-56.

Bausen, M., J. C. Fuhrmann, et al. (2006). "The state of the actin cytoskeleton determines its association with gephyrin: role of ena/VASP family members." Mol Cell Neurosci **31**(2): 376-386.

Bellenchi, G. C., C. B. Gurniak, et al. (2007). "N-cofilin is associated with neuronal migration disorders and cell cycle control in the cerebral cortex." Genes Dev **21**(18): 2347-2357.

Bennett, B. D. and J. P. Bolam (1993). "Two populations of calbindin D28k-immunoreactive neurones in the striatum of the rat." Brain Res **610**(2): 305-310.

Benson, D. L., D. R. Colman, et al. (2001). "Molecules, maps and synapse specificity." Nat Rev Neurosci **2**(12): 899-909.

Bentley, D. and A. Toroian-Raymond (1986). "Disoriented pathfinding by pioneer neurone growth cones deprived of filopodia by cytochalasin treatment." Nature **323**(6090): 712-715.

Bernstein, B. W., W. B. Painter, et al. (2000). "Intracellular pH modulation of ADF/cofilin proteins." Cell Motil Cytoskeleton **47**(4): 319-336.

Bläsius, K. (2012). Migration in the Cofilin 1 mutant mice. Institut of genetics. Bonn, Rheinische-Friedrich Wilhelms Universität. **diploma**.

Bolam, J. P., J. J. Hanley, et al. (2000). "Synaptic organisation of the basal ganglia." J Anat **196 (Pt 4)**: 527-542.

Bowman, G. D., I. M. Nodelman, et al. (2000). "A comparative structural analysis of the ADF/cofilin family." Proteins **41**(3): 374-384.

Bradford, M. M. (1976). "A rapid and sensitive mehtod for the quantiation of microgram quantities of protein utilizing the principle of protein-dye binding." Analytical Biochemistry **72**: 248 - 254.

Bradke, F. and C. G. Dotti (1999). "The role of local actin instability in axon formation." Science **283**(5409): 1931-1934.

Briley, M., P. Chopin, et al. (1990). "Effect of serotonergic lesion on "anxious" behaviour measured in the elevated plus-maze test in the rat." Psychopharmacology (Berl) **101**(2): 187-189.

Brozoski, T. J., R. M. Brown, et al. (1979). "Cognitive deficit caused by regional depletion of dopamine in prefrontal cortex of rhesus monkey." Science **205**(4409): 929-932.

Butz, S., M. Okamoto, et al. (1998). "A tripartite protein complex with the potential to couple synaptic vesicle exocytosis to cell adhesion in brain." Cell **94**(6): 773-782.

Buznikov, G. A., H. W. Lambert, et al. (2001). "Serotonin and serotonin-like substances as regulators of early embryogenesis and morphogenesis." Springer Link.

Carr, G. V. and I. Lucki (2011). "The role of serotonin receptor subtypes in treating depression: a review of animal studies." Psychopharmacology (Berl) **213**(2-3): 265-287.

Castner, S. A., G. V. Williams, et al. (2000). "Reversal of antipsychotic-induced working memory deficits by short-term dopamine D1 receptor stimulation." Science **287**(5460): 2020-2022.

Cenquizca, L. A. and L. W. Swanson (2007). "Spatial organization of direct hippocampal field CA1 axonal projections to the rest of the cerebral cortex." Brain Res Rev **56**(1): 1-26.

Chang, J. C., I. D. Tomlinson, et al. (2012). "Single molecule analysis of serotonin transporter regulation using antagonist-conjugated quantum dots reveals restricted, p38 MAPK-dependent mobilization underlying uptake activation." J Neurosci **32**(26): 8919-8929.

Charrier, C., M. V. Ehrensperger, et al. (2006). "Cytoskeleton regulation of glycine receptor number at synapses and diffusion in the plasma membrane." J Neurosci **26**(33): 8502-8511.

Chechik, G., I. Meilijson, et al. (1999). "Neuronal regulation: A mechanism for synaptic pruning during brain maturation." Neural Comput **11**(8): 2061-2080.

Chinta, S. J. and J. K. Andersen (2005). "Dopaminergic neurons." Int J Biochem Cell Biol **37**(5): 942-946.

Cingolani, L. A. and Y. Goda (2008). "Actin in action: the interplay between the actin cytoskeleton and synaptic efficacy." Nat Rev Neurosci **9**(5): 344-356.

Collinson, N., F. M. Kuenzi, et al. (2002). "Enhanced learning and memory and altered GABAergic synaptic transmission in mice lacking the alpha 5 subunit of the GABAA receptor." J Neurosci **22**(13): 5572-5580.

Craig, A. M. and Y. Kang (2007). "Neurexin-neuroligin signaling in synapse development." Curr Opin Neurobiol **17**(1): 43-52.

Crestani, F., R. Keist, et al. (2002). "Trace fear conditioning involves hippocampal alpha5 GABA(A) receptors." Proc Natl Acad Sci U S A **99**(13): 8980-8985.

Dahlstrand, J., M. Lardelli, et al. (1995). "Nestin mRNA expression correlates with the central nervous system progenitor cell state in many, but not all, regions of developing central nervous system." Brain Res Dev Brain Res **84**(1): 109-129.

Dailey, M. E. and S. J. Smith (1996). "The dynamics of dendritic structure in developing hippocampal slices." J Neurosci **16**(9): 2983-2994.

Daubner, S. C., T. Le, et al. (2011). "Tyrosine hydroxylase and regulation of dopamine synthesis." Arch Biochem Biophys **508**(1): 1-12.

Davis, H. P. and L. R. Squire (1984). "Protein synthesis and memory: a review." Psychol Bull **96**(3): 518-559.

de Wit, H., L. N. Cornelisse, et al. (2006). "Docking of secretory vesicles is syntaxin dependent." PLoS One **1**: e126.

DeFelipe, J. (2002). "Cortical interneurons: from Cajal to 2001." Prog Brain Res **136**: 215-238.

DeFelipe, J., S. H. Hendry, et al. (1990). "A microcolumnar structure of monkey cerebral cortex revealed by immunocytochemical studies of double bouquet cell axons." Neuroscience **37**(3): 655-673.

Delorme-Walker, V., J. Y. Seo, et al. (2015). "Chronophin coordinates cell leading edge dynamics by controlling active cofilin levels." Proc Natl Acad Sci U S A **112**(37): E5150-5159.

Deng, W., J. B. Aimone, et al. (2010). "New neurons and new memories: how does adult hippocampal neurogenesis affect learning and memory?" Nat Rev Neurosci **11**(5): 339-350.

Dent, E. W., S. L. Gupton, et al. (2011). "The growth cone cytoskeleton in axon outgrowth and guidance." Cold Spring Harb Perspect Biol **3**(3).

Dickson, B. J. (2002). "Molecular mechanisms of axon guidance." Science **298**(5600): 1959-1964.

Dillon, C. and Y. Goda (2005). "The actin cytoskeleton: integrating form and function at the synapse." Annu Rev Neurosci **28**: 25-55.

dos Remedios, C. G. (2003). "Actin binding proteins: regulation of cytoskeletal microfilaments." Physiological Reviews **83**.

Dumont, D., J. P. Noben, et al. (2007). "Characterization of mature rat oligodendrocytes: a proteomic approach." J Neurochem **102**(2): 562-576.

El-Husseini, A. E., E. Schnell, et al. (2000). "PSD-95 involvement in maturation of excitatory synapses." Science **290**(5495): 1364-1368.

Endo, M., K. Ohashi, et al. (2003). "Control of growth cone motility and morphology by LIM kinase and Slingshot via phosphorylation and dephosphorylation of cofilin." J Neurosci **23**(7): 2527-2537.

Engert, F. and T. Bonhoeffer (1999). "Dendritic spine changes associated with hippocampal long-term synaptic plasticity." Nature **399**(6731): 66-70.

Fanarrage, M. L., J. Avila, et al. (1999). "Expression of unphosphorylated class III β-tubulin isotype in neuroepithelial cells demonstrates neuroblast commitment and differentiation." European Journal of Neuroscience.

Fifkova, E. and R. J. Delay (1982). "Cytoplasmic actin in neuronal processes as a possible mediator of synaptic plasticity." J Cell Biol **95**(1): 345-350.

Fischer, M., S. Kaech, et al. (2000). "Glutamate receptors regulate actin-based plasticity in dendritic spines." Nat Neurosci **3**(9): 887-894.

Flynn, K. C., F. Hellal, et al. (2012). "ADF/cofilin-mediated actin retrograde flow directs neurite formation in the developing brain." Neuron **76**(6): 1091-1107.

Fortin, D. A., T. Srivastava, et al. (2012). "Structural modulation of dendritic spines during synaptic plasticity." Neuroscientist **18**(4): 326-341.

Frangiskakis, J. M., A. K. Ewart, et al. (1996). "LIM-kinase1 hemizygosity implicated in impaired visuospatial constructive cognition." Cell **86**(1): 59-69.

Fremeau, R. T., Jr., M. D. Troyer, et al. (2001). "The expression of vesicular glutamate transporters defines two classes of excitatory synapse." Neuron **31**(2): 247-260.

Fu, H. A., R. R. Subramanian, et al. (2000). "14-3-3 proteins: Structure, function, and regulation." Annual Review of Pharmacology and Toxicology **40**: 617-647.

Fukazawa, Y., Y. Saitoh, et al. (2003). "Hippocampal LTP is accompanied by enhanced F-actin content within the dendritic spine that is essential for late LTP maintenance in vivo." Neuron **38**(3): 447-460.

Garvalov, B. K., K. C. Flynn, et al. (2007). "Cdc42 regulates cofilin during the establishment of neuronal polarity." J Neurosci **27**(48): 13117-13129.

Gohla, A., J. Birkenfeld, et al. (2005). "Chronophin, a novel HAD-type serine protein phosphatase, regulates cofilin-dependent actin dynamics." Nat Cell Biol **7**(1): 21-29.

Goodson, M., M. B. Rust, et al. (2012). "Cofilin-1: a modulator of anxiety in mice." PLoS Genet **8**(10): e1002970.

Gorlich, A., M. Wolf, et al. (2011). "N-cofilin can compensate for the loss of ADF in excitatory synapses." PLoS One **6**(10): e26789.

Graus-Porta, D., S. Blaess, et al. (2001). "Beta1-class integrins regulate the development of laminae and folia in the cerebral and cerebellar cortex." Neuron **31**(3): 367-379.

Greengard, P., F. Valtorta, et al. (1993). "Synaptic vesicle phosphoproteins and regulation of synaptic function." Science **259**(5096): 780-785.

Gunsalus, K. C., S. Bonaccorsi, et al. (1995). "Mutations in twinstar, a Drosophila gene encoding a cofilin/ADF homologue, result in defects in centrosome migration and cytokinesis." J Cell Biol **131**(5): 1243-1259.

Gupta, A., L. H. Tsai, et al. (2002). "Life is a journey: a genetic look at neocortical development." Nat Rev Genet **3**(5): 342-355.

Gurniak, C. B., F. Chevessier, et al. (2014). "Severe protein aggregate myopathy in a knockout mouse model points to an essential role of cofilin2 in sarcomeric actin exchange and muscle maintenance." Eur J Cell Biol **93**(5-6): 252-266.

Gurniak, C. B., E. Perlas, et al. (2005). "The actin depolymerizing factor n-cofilin is essential for neural tube morphogenesis and neural crest cell migration." Dev Biol **278**(1): 231-241.

Hall, A. (1998). "Rho GTPases and the actin cytoskeleton." Science **279**(5350): 509-514.

Halpain, S., A. Hipolito, et al. (1998). "Regulation of F-actin stability in dendritic spines by glutamate receptors and calcineurin." J Neurosci **18**(23): 9835-9844.

Hanus, C., M. V. Ehrensperger, et al. (2006). "Activity-dependent movements of postsynaptic scaffolds at inhibitory synapses." J Neurosci **26**(17): 4586-4595.

Hao, R., R. G. MacDonald, et al. (1997). "Stable interaction between G-actin and neurofilament light subunit in dopaminergic neurons." Neurochem Int **31**(6): 825-834.

Harrington, A. W., C. St Hillaire, et al. (2011). "Recruitment of actin modifiers to TrkA endosomes governs retrograde NGF signaling and survival." Cell **146**(3): 421-434.

Harvey, J., N. G. McKay, et al. (2000). "Essential role of phosphoinositide 3-kinase in leptin-induced K(ATP) channel activation in the rat CRI-G1 insulinoma cell line." J Biol Chem **275**(7): 4660-4669.

Haucke, V., E. Neher, et al. (2011). "Protein scaffolds in the coupling of synaptic exocytosis and endocytosis." Nat Rev Neurosci **12**(3): 127-138.

Hayden, S. M., P. S. Miller, et al. (1993). "Analysis of the interactions of actin depolymerizing factor with G- and F-actin." Biochemistry **32**(38): 9994-10004.

Hering, H. and M. Sheng (2001). "Dendritic spines: structure, dynamics and regulation." Nat Rev Neurosci **2**(12): 880-888.

Hirokawa, N., K. Sobue, et al. (1989). "The cytoskeletal architecture of the presynaptic terminal and molecular structure of synapsin 1." J Cell Biol **108**(1): 111-126.

Hjorth, J., K. T. Blackwell, et al. (2009). "Gap junctions between striatal fast-spiking interneurons regulate spiking activity and synchronization as a function of cortical activity." J Neurosci **29**(16): 5276-5286.

Holtmaat, A. and K. Svoboda (2009). "Experience-dependent structural synaptic plasticity in the mammalian brain." Nat Rev Neurosci **10**(9): 647-658.

Honkura, N., M. Matsuzaki, et al. (2008). "The subspine organization of actin fibers regulates the structure and plasticity of dendritic spines." Neuron **57**(5): 719-729.

Hoogenraad, C. C., A. Akhmanova, et al. (2004). "LIMK1 and CLIP-115: linking cytoskeletal defects to Williams syndrome." Bioessays **26**(2): 141-150.

Hotulainen, P., E. Paunola, et al. (2005). "Actin-depolymerizing factor and cofilin-1 play overlapping roles in promoting rapid F-actin depolymerization in mammalian nonmuscle cells." Mol Biol Cell **16**(2): 649-664.

Huang, T. Y., C. DerMardirossian, et al. (2006). "Cofilin phosphatases and regulation of actin dynamics." Curr Opin Cell Biol **18**(1): 26-31.

Hume, R. I. and D. Purves (1981). "Geometry of neonatal neurones and the regulation of synapse elimination." Nature **293**(5832): 469-471.

Iida, K., S. Matsumoto, et al. (1992). "The KKRKK sequence is involved in heat shock-induced nuclear translocation of the 18-kDa actin-binding protein, cofilin." Cell Struct Funct **17**(1): 39-46.

Ikeda, S., L. A. Cunningham, et al. (2003). "Aberrant actin cytoskeleton leads to accelerated proliferation of corneal epithelial cells in mice deficient for destrin (actin depolymerizing factor)." Hum Mol Genet **12**(9): 1029-1037.

Isaacson, J. S. and M. Scanziani (2011). "How inhibition shapes cortical activity." Neuron **72**(2): 231-243.

Ishikawa, R. and K. Kohama (2007). "Actin-binding proteins in nerve cell growth cones." J Pharmacol Sci **105**(1): 6-11.

Jacobs, B., M. Schall, et al. (2001). "Regional dendritic and spine variation in human cerebral cortex: a quantitative golgi study." Cereb Cortex **11**(6): 558-571.

Jan, Y. N. and L. Y. Jan (2003). "The control of dendrite development." Neuron **40**(2): 229-242.

Jones, E. G. and T. P. Pons (1998). "Thalamic and brainstem contributions to large-scale plasticity of primate somatosensory cortex." Science **282**(5391): 1121-1125.

Kapitein, L. C. and C. C. Hoogenraad (2011). "Which way to go? Cytoskeletal organization and polarized transport in neurons." Mol Cell Neurosci **46**(1): 9-20.

Khaitlina, S. Y. (2001). "Functional specificity of actin isoforms." Int Rev Cytol **202**: 35-98.

Kim, C. H. and J. E. Lisman (1999). "A role of actin filament in synaptic transmission and long-term potentiation." J Neurosci **19**(11): 4314-4324.

Kirsch, J. and H. Betz (1995). "The postsynaptic localization of the glycine receptor-associated protein gephyrin is regulated by the cytoskeleton." J Neurosci **15**(6): 4148-4156.

Kneussel, M., J. H. Brandstatter, et al. (1999). "Loss of postsynaptic GABA(A) receptor clustering in gephyrin-deficient mice." J Neurosci **19**(21): 9289-9297.

Kondoh, M., T. Shiga, et al. (2004). "Regulation of dendrite formation of Purkinje cells by serotonin through serotonin1A and serotonin2A receptors in culture." Neurosci Res **48**(1): 101-109.

Kononenko, N. L., D. Puchkov, et al. (2014). "Clathrin/AP-2 mediate synaptic vesicle reformation from endosome-like vacuoles but are not essential for membrane retrieval at central synapses." Neuron **82**(5): 981-988.

Kossel, A. H., C. V. Williams, et al. (1997). "Afferent innervation influences the development of dendritic branches and spines via both activity-dependent and non-activity-dependent mechanisms." J Neurosci **17**(16): 6314-6324.

Krause, M., J. D. Leslie, et al. (2004). "Lamellipodin, an Ena/VASP ligand, is implicated in the regulation of lamellipodial dynamics." Dev Cell **7**(4): 571-583.

Krebs, M. O., J. M. Desce, et al. (1991). "Glutamatergic control of dopamine release in the rat striatum: evidence for presynaptic N-methyl-D-aspartate receptors on dopaminergic nerve terminals." J Neurochem **56**(1): 81-85.

Kriegstein, A. R. and S. C. Noctor (2004). "Patterns of neuronal migration in the embryonic cortex." Trends Neurosci **27**(7): 392-399.

Krucker, T., G. R. Siggins, et al. (2000). "Dynamic actin filaments are required for stable long-term potentiation (LTP) in area CA1 of the hippocampus." Proc Natl Acad Sci U S A **97**(12): 6856-6861.

Kuhn, J. R. and T. D. Pollard (2005). "Real-time measurements of actin filament polymerization by total internal reflection fluorescence microscopy." Biophys J **88**(2): 1387-1402.

Kusano, K., H. Abe, et al. (1999). "Detection of a sequence involved in actin-binding and phosphoinositide-binding in the N-terminal side of cofilin." Mol Cell Biochem **190**(1-2): 133-141.

Laemmli, U. K. (1970). "Cleavage of structural proteins during the assembly of the head of bacteriophage T4." Nature.

Landis, D. M., A. K. Hall, et al. (1988). "The organization of cytoplasm at the presynaptic active zone of a central nervous system synapse." Neuron **1**(3): 201-209.

Larson, J. and E. Munkacsy (2015). "Theta-burst LTP." Brain Res **1621**: 38-50.

Lau, A. and M. Tymianski (2010). "Glutamate receptors, neurotoxicity and neurodegeneration." Pflugers Arch **460**(2): 525-542.

Lessard, J. L. (1988). "Two monoclonal antibodies to actin: one muscle selective and one generally reactive." Cell Motil Cytoskeleton **10**(3): 349-362.

Levin, E. D. and B. B. Simon (1998). "Nicotinic acetylcholine involvement in cognitive function in animals." Psychopharmacology (Berl) **138**(3-4): 217-230.

Lewis, D. A., A. A. Curley, et al. (2012). "Cortical parvalbumin interneurons and cognitive dysfunction in schizophrenia." Trends Neurosci **35**(1): 57-67.

Li, M., Z. Cui, et al. (2010). "Synaptogenesis in the developing mouse visual cortex." Brain Res Bull **81**(1): 107-113.

Li, Z., C. D. Aizenman, et al. (2002). "Regulation of rho GTPases by crosstalk and neuronal activity in vivo." Neuron **33**(5): 741-750.

Li, Z., L. Van Aelst, et al. (2000). "Rho GTPases regulate distinct aspects of dendritic arbor growth in Xenopus central neurons in vivo." Nat Neurosci **3**(3): 217-225.

Libersat, F. and C. Duch (2004). "Mechanisms of dendritic maturation." Mol Neurobiol **29**(3): 303-320.

Liguz-Lecznar, M. and J. Skangiel-Kramska (2007). "Vesicular glutamate transporters (VGLUTs): the three musketeers of glutamatergic system." Acta Neurobiol Exp (Wars) **67**(3): 207-218.

Lim, S. A. O., U. J. Khang, et al. (2014). "Striatal cholinergic interneuron regulation and circuit effects." Frontiers in synaptic neuroscience.

Loisel, T. P., R. Boujemaa, et al. (1999). "Reconstitution of actin-based motility of Listeria and Shigella using pure proteins." Nature **401**(6753): 613-616.

Lucido, A. L., F. Suarez Sanchez, et al. (2009). "Rapid assembly of functional presynaptic boutons triggered by adhesive contacts." J Neurosci **29**(40): 12449-12466.

Lujan, R., R. Shigemoto, et al. (2005). "Glutamate and GABA receptor signalling in the developing brain." Neuroscience **130**(3): 567-580.

Luo, L. (2000). "Rho GTPases in neuronal morphogenesis." Nat Rev Neurosci **1**(3): 173-180.

Magnusson, A., G. Dahlfors, et al. (1996). "Differential distribution of calcium-binding proteins in the dorsal column nuclei of rats: a combined immunohistochemical and retrograde tract tracing study." Neuroscience **73**(2): 497-508.

Mallet, N., B. Ballion, et al. (2006). "Cortical inputs and GABA interneurons imbalance projection neurons in the striatum of parkinsonian rats." J Neurosci **26**(14): 3875-3884.

Maloney, M. T. and J. R. Bamburg (2007). "Cofilin-mediated neurodegeneration in Alzheimer's disease and other amyloidopathies." Mol Neurobiol **35**(1): 21-44.

Markram, H., M. Toledo-Rodriguez, et al. (2004). "Interneurons of the neocortical inhibitory system." Nat Rev Neurosci **5**(10): 793-807.

Marra, V., J. J. Burden, et al. (2012). "A preferentially segregated recycling vesicle pool of limited size supports neurotransmission in native central synapses." Neuron **76**(3): 579-589.

Matus, A. (2000). "Actin-based plasticity in dendritic spines." Science **290**(5492): 754-758.

Mazur, A. J., D. Gremm, et al. (2010). "Modulation of actin filament dynamics by actin-binding proteins residing in lamellipodia." Eur J Cell Biol **89**(5): 402-413.

McAllister, A. K. (2000). "Cellular and molecular mechanisms of dendrite growth." Cereb Cortex **10**(10): 963-973.

McAllister, A. K. (2002). "Conserved cues for axon and dendrite growth in the developing cortex." Neuron **33**(1): 2-4.

McClelland, J. L., B. L. McNaughton, et al. (1995). "Why there are complementary learning systems in the hippocampus and neocortex: insights from the successes and failures of connectionist models of learning and memory." Psychol Rev **102**(3): 419-457.

McGough, A. and W. Chiu (1999). "ADF/cofilin weakens lateral contacts in the actin filament." J Mol Biol **291**(3): 513-519.

McKim, K. S., C. Matheson, et al. (1994). "The Caenorhabditis elegans unc-60 gene encodes proteins homologous to a family of actin-binding proteins." Mol Gen Genet **242**(3): 346-357.

McKinney, R. A., M. Capogna, et al. (1999). "Miniature synaptic events maintain dendritic spines via AMPA receptor activation." Nat Neurosci **2**(1): 44-49.

Meberg, P. J., S. Ono, et al. (1998). "Actin depolymerizing factor and cofilin phosphorylation dynamics: response to signals that regulate neurite extension." Cell Motil Cytoskeleton **39**(2): 172-190.

Meng, Y., Y. Zhang, et al. (2002). "Abnormal spine morphology and enhanced LTP in LIMK-1 knockout mice." Neuron **35**(1): 121-133.

Miller, E. M., T. C. Thomas, et al. (2013). Dopamine and Glutamate interactions in ADHD: Implications for the future neurophamacology of ADHD. Mental and Behavioural Disorders and Diseases of the Nervous System, INTECH.

Moon, A. L., P. A. Janmey, et al. (1993). "Cofilin Is an Essential Component of the Yeast Cortical Cytoskeleton." Journal of Cell Biology **120**(2): 421-435.

Morales, M., M. A. Colicos, et al. (2000). "Actin-dependent regulation of neurotransmitter release at central synapses." Neuron **27**(3): 539-550.

Moriyama, K., K. Iida, et al. (1996). "Phosphorylation of Ser-3 of cofilin regulates its essential function on actin." Genes Cells **1**(1): 73-86.

Moser, E. I. (2011). "The multi-laned hippocampus." Nat Neurosci **14**(4): 407-408.

Mucha, M., A. E. Skrzypiec, et al. (2011). "Lipocalin-2 controls neuronal excitability and anxiety by regulating dendritic spine formation and maturation." Proc Natl Acad Sci U S A **108**(45): 18436-18441.

Mueller, B. K. (1999). "Growth cone guidance: first steps towards a deeper understanding." Annu Rev Neurosci **22**: 351-388.

Mulkey, R. M., S. Endo, et al. (1994). "Involvement of a calcineurin/inhibitor-1 phosphatase cascade in hippocampal long-term depression." Nature **369**(6480): 486-488.

Mulkey, R. M. and R. C. Malenka (1992). "Mechanisms underlying induction of homosynaptic long-term depression in area CA1 of the hippocampus." Neuron **9**(5): 967-975.

Munno, D. W. and N. Syed (2003). "Synaptogenesis in the CNS: An odyssey from wiring together to firing together." The Journal of Physiology.

Nadarajah, B. and J. G. Parnavelas (2002). "Modes of neuronal migration in the developing cerebral cortex." Nat Rev Neurosci **3**(6): 423-432.

Nakashima, K., N. Sato, et al. (2005). "Two mouse cofilin isoforms, muscle-type (MCF) and non-muscle type (NMCF), interact with F-actin with different efficiencies." J Biochem **138**(4): 519-526.

Nelson, B. S., C. F. Witty, et al. (2012). "A role for hippocampal actin rearrangement in object placement memory in female rats." Neurobiol Learn Mem **98**(3): 284-290.

Nelson, J. C., A. K. Stavoe, et al. (2013). "The actin cytoskeleton in presynaptic assembly." Cell Adh Migr **7**(4): 379-387.

Nguyen, P. V., T. Abel, et al. (1994). "Requirement of a critical period of transcription for induction of a late phase of LTP." Science **265**(5175): 1104-1107.

Nicholls, D. G., T. S. Sihra, et al. (1987). "Calcium-dependent and -independent release of glutamate from synaptosomes monitored by continuous fluorometry." J Neurochem **49**(1): 50-57.

Niewiadomska, G., A. Mietelska-Porowska, et al. (2011). "The cholinergic system, nerve growth factor and the cytoskeleton." Behav Brain Res **221**(2): 515-526.

Niewoehner, B., F. N. Single, et al. (2007). "Impaired spatial working memory but spared spatial reference memory following functional loss of NMDA receptors in the dentate gyrus." Eur J Neurosci **25**(3): 837-846.

Nimchinsky, E. A., A. M. Oberlander, et al. (2001). "Abnormal development of dendritic spines in FMR1 knock-out mice." J Neurosci **21**(14): 5139-5146.

Nimchinsky, E. A., B. L. Sabatini, et al. (2002). "Structure and function of dendritic spines." Annu Rev Physiol **64**: 313-353.

Ning, K., L. C. Miller, et al. (2006). "A novel leptin signalling pathway via PTEN inhibition in hypothalamic cell lines and pancreatic beta-cells." EMBO J **25**(11): 2377-2387.

Nishi, A., M. Kuroiwa, et al. (2011). "Mechanisms for the modulation of dopamine d(1) receptor signaling in striatal neurons." Front Neuroanat **5**: 43.

O'Brien, R. J., L. F. Lau, et al. (1998). "Molecular mechanisms of glutamate receptor clustering at excitatory synapses." Curr Opin Neurobiol **8**(3): 364-369.

O´Keefe, J. and L. Nadel (1978). "The hippocampus as cognitive map." Oxford University Press.

Obinata, T., R. Nagaoka-Yasuda, et al. (1997). "Low molecular-weight G-actin binding proteins involved in the regulation of actin assembly during myofibrillogenesis." Cell Struct Funct **22**(1): 181-189.

Oda, Y. (1999). "Choline acetyltransferase: the structure, distribution and pathologic changes in the central nervous system." Pathol Int **49**(11): 921-937.

Ono, S. (2003). "Regulation of actin filament dynamics by actin depolymerizing factor/cofilin and actin-interacting protein 1: new blades for twisted filaments." Biochemistry **42**(46): 13363-13370.

Ono, S., N. Minami, et al. (1994). "Characterization of a novel cofilin isoform that is predominantly expressed in mammalian skeletal muscle." J Biol Chem **269**(21): 15280-15286.

Oppenheimer, J. H. and H. L. Schwartz (1997). "Molecular basis of thyroid hormone-dependent brain development." Endocr Rev **18**(4): 462-475.

Otterbein, L. R., P. Graceffa, et al. (2001). "The crystal structure of uncomplexed actin in the ADP state." Science **293**(5530): 708-711.

Pak, C. W., K. C. Flynn, et al. (2008). "Actin-binding proteins take the reins in growth cones." Nat Rev Neurosci **9**(2): 136-147.

Pollack, A. E. (2001). "Anatomy, physiology, and pharmacology of the basal ganglia." Neurol Clin **19**(3): 523-534, v.

Pollard, T. D. and G. G. Borisy (2003). "Cellular motility driven by assembly and disassembly of actin filaments." Cell **112**(4): 453-465.

Pollard, T. D. and J. A. Cooper (1986). "Actin and actin-binding proteins. A critical evaluation of mechanisms and functions." Annu Rev Biochem **55**: 987-1035.

Pollard, T. D. E. and W. C. Earnshaw (2008). Cell Biology. Heidelberg, Springer.

Polster, M. R. (1993). "Drug-induced amnesia: implications for cognitive neuropsychological investigations of memory." Psychol Bull **114**(3): 477-493.

Pontrello, C. G. and I. M. Ethell (2009). "Accelerators, Brakes, and Gears of Actin Dynamics in Dendritic Spines." Open Neurosci J **3**: 67-86.

Pothuizen, H. H., W. N. Zhang, et al. (2004). "Dissociation of function between the dorsal and the ventral hippocampus in spatial learning abilities of the rat: a within-subject, within-task comparison of reference and working spatial memory." Eur J Neurosci **19**(3): 705-712.

Racz, B. and R. J. Weinberg (2006). "Spatial organization of cofilin in dendritic spines." Neuroscience **138**(2): 447-456.

Rajan, I. and H. T. Cline (1998). "Glutamate receptor activity is required for normal development of tectal cell dendrites in vivo." J Neurosci **18**(19): 7836-7846.

Rando, O. J., K. Zhao, et al. (2000). "Searching for a function for nuclear actin." Trends Cell Biol **10**(3): 92-97.

Rang, H. P. (1995). Pharmacology, Churchill Livingstone.

Rausell, E., C. S. Bae, et al. (1992). "Calbindin and parvalbumin cells in monkey VPL thalamic nucleus: distribution, laminar cortical projections, and relations to spinothalamic terminations." J Neurosci **12**(10): 4088-4111.

Regehr, W. G., M. R. Carey, et al. (2009). "Activity-dependent regulation of synapses by retrograde messengers." Neuron **63**(2): 154-170.

Rizzoli, S. O. and W. J. Betz (2005). "Synaptic vesicle pools." Nat Rev Neurosci **6**(1): 57-69.

Rosso, S. B. and N. C. Inestrosa (2013). "WNT signaling in neuronal maturation and synaptogenesis." Front Cell Neurosci **7**: 103.

Rosso, S. B., D. Sussman, et al. (2005). "Wnt signaling through Dishevelled, Rac and JNK regulates dendritic development." Nat Neurosci **8**(1): 34-42.

Rust, M. B. (2015). "ADF/cofilin: a crucial regulator of synapse physiology and behavior." Cell Mol Life Sci **72**(18): 3521-3529.

Rust, M. B., C. B. Gurniak, et al. (2010). "Learning, AMPA receptor mobility and synaptic plasticity depend on n-cofilin-mediated actin dynamics." EMBO J **29**(11): 1889-1902.

Rust, M. B. and T. Maritzen (2015). "Relevance of presynaptic actin dynamics for synapse function and mouse behavior." Exp Cell Res **335**(2): 165-171.

Sakaba, T. and E. Neher (2003). "Involvement of actin polymerization in vesicle recruitment at the calyx of Held synapse." J Neurosci **23**(3): 837-846.

Sakai, N., K. Sasaki, et al. (1997). "Modulation of serotonin transporter activity by a Protein kinase C activator and an inhibitor of Type 1 and 2A Serine/Threonine Phosphatases." Journal of Neurochemistry.

Saneyoshi, T., G. Wayman, et al. (2008). "Activity-dependent synaptogenesis: regulation by a CaM-kinase kinase/CaM-kinase I/betaPIX signaling complex." Neuron **57**(1): 94-107.

Sankaranarayanan, S., P. P. Atluri, et al. (2003). "Actin has a molecular scaffolding, not propulsive, role in presynaptic function." Nat Neurosci **6**(2): 127-135.

Sarmiere, P. D. and J. R. Bamburg (2004). "Regulation of the neuronal actin cytoskeleton by ADF/cofilin." J Neurobiol **58**(1): 103-117.

Scott, E. K. and L. Luo (2001). "How do dendrites take their shape?" Nat Neurosci **4**(4): 359-365.

Segal, M. (2005). "Dendritic spines and long-term plasticity." Nat Rev Neurosci **6**(4): 277-284.

Shoop, R. D., N. Yamada, et al. (2000). "Cytoskeletal links of neuronal acetylcholine receptors containing alpha 7 subunits." J Neurosci **20**(11): 4021-4029.

Simonishvili, S., M. R. Jain, et al. (2013). "Identification of Bax-interacting proteins in oligodendrocyte progenitors during glutamate excitotoxicity and perinatal hypoxia-ischemia." ASN Neuro **5**(5): e00131.

Smeets, W. J., O. Marin, et al. (2000). "Evolution of the basal ganglia: new perspectives through a comparative approach." J Anat **196 (Pt 4)**: 501-517.

Sofroniew, M. V. and H. V. Vinters (2010). "Astrocytes: biology and pathology." Acta Neuropathol **119**(1): 7-35.

Spiering, D. and L. Hodgson (2011). "Dynamics of the Rho-family small GTPases in actin regulation and motility." Cell Adh Migr **5**(2): 170-180.

Spruston, N. (2008). "Pyramidal neurons: dendritic structure and synaptic integration." Nat Rev Neurosci **9**(3): 206-221.

Stavoe, A. K. and D. A. Colon-Ramos (2012). "Netrin instructs synaptic vesicle clustering through Rac GTPase, MIG-10, and the actin cytoskeleton." J Cell Biol **197**(1): 75-88.

Sumi, T., K. Matsumoto, et al. (1999). "Cofilin phosphorylation and actin cytoskeletal dynamics regulated by rho- and Cdc42-activated LIM-kinase 2." J Cell Biol **147**(7): 1519-1532.

Sun, Y. and S. X. Bamji (2011). "beta-Pix modulates actin-mediated recruitment of synaptic vesicles to synapses." J Neurosci **31**(47): 17123-17133.

Svitkina, T. M. and G. G. Borisy (1999). "Arp2/3 complex and actin depolymerizing factor/cofilin in dendritic organization and treadmilling of actin filament array in lamellipodia." J Cell Biol **145**(5): 1009-1026.

Tahirovic, S. and F. Bradke (2009). "Neuronal polarity." Cold Spring Harb Perspect Biol **1**(3): a001644.

Takahashi, H., H. Yamazaki, et al. (2009). "Activity of the AMPA receptor regulates drebrin stabilization in dendritic spine morphogenesis." J Cell Sci **122**(Pt 8): 1211-1219.

Takeuchi, Y., T. Matsuura, et al. (1983). "Immunohistochemical observation of serotonin neurons in newborn mouse and rat brainstem cultures." Arch Histol Jpn **46**(1): 79-86.

Tessier-Lavigne, M. and C. S. Goodman (1996). "The molecular biology of axon guidance." Science **274**(5290): 1123-1133.

Tirion, M. M., D. Benavraham, et al. (1995). "Normal-Modes as Refinement Parameters for the F-Actin Model." Biophysical Journal **68**(1): 5-12.

Tronche, F., C. Kellendonk, et al. (1999). "Disruption of the glucocorticoid receptor gene in the nervous system results in reduced anxiety." Nat Genet **23**(1): 99-103.

van Brederode, J. F., M. K. Helliesen, et al. (1991). "Distribution of the calcium-binding proteins parvalbumin and calbindin-D28k in the sensorimotor cortex of the rat." Neuroscience **44**(1): 157-171.

van Groen, T., P. Miettinen, et al. (2003). "The entorhinal cortex of the mouse: organization of the projection to the hippocampal formation." Hippocampus **13**(1): 133-149.

Vartiainen, M. K., T. Mustonen, et al. (2002). "The three mouse actin-depolymerizing factor/cofilins evolved to fulfill cell-type-specific requirements for actin dynamics." Mol Biol Cell **13**(1): 183-194.

Vaughn, J. E. (1989). "Fine structure of synaptogenesis in the vertebrate central nervous system." Synapse **3**(3): 255-285.

Verdoorn, T. A., A. Draguhn, et al. (1990). "Functional properties of recombinant rat GABAA receptors depend upon subunit composition." Neuron **4**(6): 919-928.

Walther, D. J., J. U. Peter, et al. (2003). "Synthesis of serotonin by a second tryptophan hydroxylase isoform." Science **299**(5603): 76.

Wang, D. D. and A. R. Kriegstein (2009). "Defining the role of GABA in cortical development." J Physiol **587**(Pt 9): 1873-1879.

Watanabe, M., K. Nomura, et al. (2005). "Myosin-Va regulates exocytosis through the submicromolar Ca2+-dependent binding of syntaxin-1A." Mol Biol Cell **16**(10): 4519-4530.

Wilhelm, B. G., S. Mandad, et al. (2014). "Composition of isolated synaptic boutons reveals the amounts of vesicle trafficking proteins." Science **344**(6187): 1023-1028.

Winder, S. J. and K. R. Ayscough (2005). "Actin-binding proteins." J Cell Sci **118**(Pt 4): 651-654.

Wisden, W., D. J. Laurie, et al. (1992). "The distribution of 13 GABAA receptor subunit mRNAs in the rat brain. I. Telencephalon, diencephalon, mesencephalon." J Neurosci **12**(3): 1040-1062.

Wolf, M., A. M. Zimmermann, et al. (2015). "ADF/Cofilin Controls Synaptic Actin Dynamics and Regulates Synaptic Vesicle Mobilization and Exocytosis." Cereb Cortex **25**(9): 2863-2875.

Wu, G. Y., D. J. Zou, et al. (1999). "Dendritic dynamics in vivo change during neuronal maturation." J Neurosci **19**(11): 4472-4483.

Xia, J., X. Zhang, et al. (1999). "Clustering of AMPA receptors by the synaptic PDZ domain-containing protein PICK1." Neuron **22**(1): 179-187.

Yao, J., J. Qi, et al. (2006). "Actin-dependent activation of presynaptic silent synapses contributes to long-term synaptic plasticity in developing hippocampal neurons." J Neurosci **26**(31): 8137-8147.

Yonezawa, N., E. Nishida, et al. (1990). "Inhibition of the interactions of cofilin, destrin, and deoxyribonuclease I with actin by phosphoinositides." J Biol Chem **265**(15): 8382-8386.

Zheng, C. Y., R. S. Petralia, et al. (2010). "SAP102 is a highly mobile MAGUK in spines." J Neurosci **30**(13): 4757-4766.

Zhou, Q., K. J. Homma, et al. (2004). "Shrinkage of dendritic spines associated with long-term depression of hippocampal synapses." Neuron **44**(5): 749-757.

Zhou, Q., M. Xiao, et al. (2001). "Contribution of cytoskeleton to the internalization of AMPA receptors." Proc Natl Acad Sci U S A **98**(3): 1261-1266.

Zimmerman, L., B. Parr, et al. (1994). "Independent regulatory elements in the nestin gene direct transgene expression to neural stem cells or muscle precursors." Neuron **12**(1): 11-24.

Zimmermann, A. M., T. Jene, et al. (2015). "Attention-Deficit/Hyperactivity Disorder-like Phenotype in a Mouse Model with Impaired Actin Dynamics." Biol Psychiatry **78**(2): 95-106.